

CANADIAN THESES ON MICROFICHE

THÈSES CANADIENNES SUR MICROFICHE



National Library of Canada
Collections Development Branch

Canadian Theses on
Microfiche Service

Ottawa, Canada
K1A 0N4

Bibliothèque nationale du Canada
Direction du développement des collections

Service des thèses canadiennes
sur microfiche

NOTICE

The quality of this microfiche is heavily dependent upon the quality of the original thesis submitted for microfilming. Every effort has been made to ensure the highest quality of reproduction possible.

If pages are missing, contact the university which granted the degree.

Some pages may have indistinct print especially if the original pages were typed with a poor typewriter ribbon or if the university sent us an inferior photocopy.

Previously copyrighted materials (journal articles, published tests, etc.) are not filmed.

Reproduction in full or in part of this film is governed by the Canadian Copyright Act, R.S.C. 1970, c. C-30. Please read the authorization forms which accompany this thesis.

**THIS DISSERTATION
HAS BEEN MICROFILMED
EXACTLY AS RECEIVED**

AVIS

La qualité de cette microfiche dépend grandement de la qualité de la thèse soumise au microfilmage. Nous avons tout fait pour assurer une qualité supérieure de reproduction.

S'il manque des pages, veuillez communiquer avec l'université qui a conféré le grade.

La qualité d'impression de certaines pages peut laisser à désirer, surtout si les pages originales ont été dactylographiées à l'aide d'un ruban usé ou si l'université nous a fait parvenir une photocopie de qualité inférieure.

Les documents qui font déjà l'objet d'un droit d'auteur (articles de revue, examens publiés, etc.) ne sont pas microfilmés.

La reproduction, même partielle, de ce microfilm est soumise à la Loi canadienne sur le droit d'auteur, SRC 1970, c. C-30. Veuillez prendre connaissance des formules d'autorisation qui accompagnent cette thèse.

**LA THÈSE A ÉTÉ
MICROFILMÉE TELLE QUE
NOUS L'AVONS REÇUE**

Canada



National Library of Canada

Bibliothèque nationale du Canada

Canadian Theses Division

Division des thèses canadiennes

Ottawa, Canada
K1A 0N4

67432

PERMISSION TO MICROFILM — AUTORISATION DE MICROFILMER

• Please print or type — Écrire, en lettres moulées ou dactylographier

Full Name of Author — Nom complet de l'auteur

YVON THÉRIAULT

Date of Birth — Date de naissance

CANADA

Country of Birth — Lieu de naissance

23 11 51

Permanent Address — Résidence fixe

1770 - 37 ST. EDMONTON
T6L 2R2 ALTA

Title of Thesis — Titre de la thèse

¹H NMR STUDIES OF THIOL/DISULFIDE EXCHANGE
Reactions of Penicillamine and Captopril with
Disulfides

UofA

University — Université

Degree for which thesis was presented — Grade pour lequel cette thèse fut présentée

PHD

Year this degree conferred — Année d'obtention de ce grade

1985

Name of Supervisor — Nom du directeur de thèse

Rapenstein

Permission is hereby granted to the NATIONAL LIBRARY OF CANADA to microfilm this thesis and to lend or sell copies of the film.

The author reserves other publication rights, and neither the thesis nor extensive extracts from it may be printed or otherwise reproduced without the author's written permission.

L'autorisation est, par la présente, accordée à la BIBLIOTHÈQUE NATIONALE DU CANADA de microfilmer cette thèse et de prêter ou de vendre des exemplaires du film.

L'auteur se réserve les autres droits de publication; ni la thèse ni de longs extraits de celle-ci ne doivent être imprimés ou autrement reproduits sans l'autorisation écrite de l'auteur.

Date

12/12/84

Signature

Yvon Thériault

THE UNIVERSITY OF ALBERTA

¹H NMR STUDIES OF THIOL/DISULFIDE EXCHANGE REACTIONS
OF PENICILLAMINE AND CAPTOPRIL WITH DISULFIDES

by

YVON THÉRIAULT

A THESIS

SUBMITTED TO THE FACULTY OF GRADUATE STUDIES AND RESEARCH
IN PARTIAL FULFILMENT OF THE REQUIREMENTS FOR THE DEGREE
DOCTOR OF PHILOSOPHY

DEPARTMENT OF CHEMISTRY

EDMONTON, ALBERTA

SPRING 1985

THE UNIVERSITY OF ALBERTA

RELEASE FORM

NAME OF AUTHOR YVON THÉRIAULT

TITLE OF THESIS ^1H NMR STUDIES OF THIOL/DISULFIDE EXCHANGE
REACTIONS OF PENICILLAMINE AND CAPTOPRIL
WITH DISULFIDES

DEGREE FOR WHICH THESIS WAS PRESENTED Ph.D.

YEAR THIS DEGREE GRANTED 1985

Permission is hereby granted to THE UNIVERSITY OF ALBERTA LIBRARY to reproduce single copies of this thesis and to lend or sell such copies for private, scholarly or scientific research purposes only.

The author reserves other publication rights, and neither the thesis nor extensive extracts from it may be printed or otherwise reproduced without the author's written permission.

(Signed) Yvon Thériault,

PERMANENT ADDRESS:


1770-37 street,
EDMONTON, ALTA.

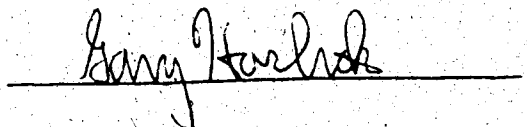
DATED Nov 30

1984

THE UNIVERSITY OF ALBERTA
FACULTY OF GRADUATE STUDIES AND RESEARCH

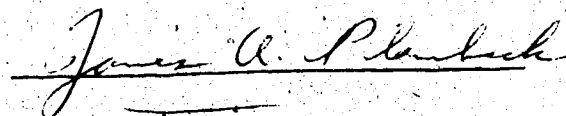
The undersigned certify that they have read, and recommend to the Faculty of Graduate Studies and Research, for acceptance, a thesis entitled ^1H NMR STUDIES OF THIOL/DISULFIDE EXCHANGE REACTIONS OF PENICILLAMINE AND CAPTOPRIL WITH DISULFIDES submitted by YVON THÉRIAULT in partial fulfilment of the requirements for the degree of DOCTOR OF PHILOSOPHY

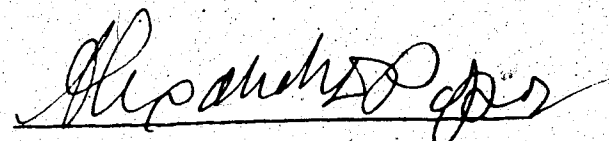

Supervisor







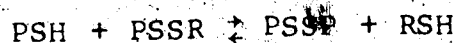
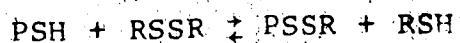



External Examiner

DATE 30 NOV 84

ABSTRACT

The thiol/disulfide exchange reactions of penicillamine (PSH) with oxidized glutathione, cystine and several related disulfides (RSSR) have been studied by ^1H NMR. The reactions take place in two steps:



The kinetics and equilibria of the oxidation of penicillamine by glutathione disulfide to form, in the first step, penicillamine-glutathione mixed disulfide and glutathione and, in the second step, penicillamine disulfide and glutathione have been studied over the pH range 4-9 by ^1H NMR. Similarly, the kinetics and equilibria of the reactions of PSH with cystine were characterized over the pH range 5-8, while the reactions with the disulfides of cysteamine, homocysteine, 2-mercaptoethanol, mercaptoacetic acid, 3-mercaptopropionic acid and mercaptosuccinic acid were studied at neutral pH. The kinetics and equilibria of the oxidation of N-acetylpenicillamine by glutathione disulfide were also studied at neutral pH. Conditional equilibrium and rate

constants for the oxidation of penicillamine by glutathione disulfide and cystine at pH 7.4 are presented and discussed in terms of the metabolism of penicillamine.

For all the disulfides studied, the rate and equilibrium constants for the first step are much larger than those for the second step. The extent to which the first reaction occurs is within a factor of ~3 of that predicted by a random distribution, while the extent to which the second reaction occurs is considerably less than for a random distribution (a factor of ~20). This indicates a small tendency for penicillamine to form its symmetrical disulfide by thiol/disulfide exchange reactions. This and the smaller reducing power of penicillamine as compared to cysteine and glutathione are attributed to steric hindrance from the methyl groups adjacent to the sulfur.

The rates and equilibria of the thiol/disulfide exchange reactions studied are dependent on the protonation states of the species involved. In order to characterize fully the thiol/disulfide exchange reactions of PSH with oxidized glutathione and cystine in terms of the reactive species involved, the acid/base chemistry of the reactants and products were studied using ^1H and ^{13}C chemical shift data. The acid/base chemistry of the ammonium groups of penicillamine-glutathione mixed

disulfide has been characterized by ^{13}C NMR and that of the ammonium groups of penicillamine-cysteine mixed disulfide by ^1H NMR. The mixed disulfides were formed by thiol/disulfide exchange. Chemical shift titration data were obtained simultaneously for the mixed disulfides, the thiols, and the symmetrical disulfides in the mixture. Since the fractional titration of individual ammonium groups can be obtained directly from chemical shift data, it was not necessary to isolate the mixed disulfides. The chemical shift data indicates that the two ammonium groups of each of the mixed disulfides are titrated over the same pH range, with the acidity of the ammonium group of the penicillamine part of the penicillamine-glutathione mixed disulfide 4.4 times as acidic as that of the glutathione part. In the penicillamine-cysteine mixed disulfide, the penicillamine ammonium group is 1.7 times as acidic as that of the cysteine part. Macroscopic and microscopic acid dissociation constants are reported for each of the mixed disulfides. The advantages of NMR as a method for characterizing the acid/base chemistry of mixed disulfides is discussed.

From the above acid/base study, the pH independent equilibrium and rate constants for the thiol/disulfide exchange reactions written in terms of the reactive species present in the pH range used (which includes

physiological pH) were calculated. From the pH dependence of the rate of the reaction of PSH with cystine and oxidized glutathione and the species distribution diagrams versus pH, the reactive species were identified as penicillamine with its amino group protonated and its thiol group deprotonated. The reactive species for the disulfides cystine, oxidized glutathione, penicillamine-cysteine mixed disulfide and penicillamine-glutathione mixed disulfide are the species with the amino groups protonated.

Finally, the oxidation of captopril (CpSH) by glutathione disulfide (GSSG) via thiol/disulfide exchange to form, in the first step, CpSSG and GSH and, in the second step, CpSSCp and GSH, has been studied in aqueous solution by ^1H NMR. Due to slow rotation around the amide bond(s) of CpSH and CpSSCp and of the captopril part of CpSSG, separate resonances are observed for the cis and trans conformations across these bonds. Conformational equilibrium constants were estimated as a function of pH for CpSH, CpSSCp and CpSSG from the intensities of resonances for the cis and trans isomers. These equilibrium constants were used in the determination of equilibrium constants for the two steps in the oxidation of CpSH by GSSG. The results suggest that CpSH has a greater tendency to reduce disulfide bonds by

thiol/disulfide exchange at physiological pH, and thus form mixed disulfides, than do the thiol groups in amino acids. Also, the conformational equilibrium constants indicate that, at physiological pH, approximately two thirds of the captopril, either free or in a disulfide form, has the trans conformation.

ACKNOWLEDGEMENTS

My sincere thanks to Dr. D.L. Rabenstein for his guidance and help during the course of this work. I am also grateful to all my colleagues, past and present, for their discussions and advice.

Financial support from the Alberta Heritage Foundation for Medical Research and the University of Alberta is gratefully acknowledged.

TABLE OF CONTENTS

CHAPTER	PAGE
I. THIOLS, DISULFIDES AND THIOL/DISULFIDE EXCHANGE REACTIONS.....	1
A. Introduction.....	1
B. The Oxidation of Thiol Groups.....	2
C. The Uses of Penicillamine in Medicine.....	7
D. The Use of Captopril in Medicine.....	10
E. Thiol/Disulfide Exchange Reactions: Equilibrium Considerations.....	11
F. Previous Studies of Thiol/Disulfide Exchange Reactions.....	15
G. This Thesis.....	24
II. EXPERIMENTAL.....	28
A. Chemicals.....	28
B. Preparation of Solutions.....	30
C. Electrolysis Cell.....	33
D. pH Measurementss.....	38
E. Nuclear Magnetic Resonance Measurements.....	39
1. Instrumentation and Method.....	39
2. Chemical Shift Measurements.....	41
3. T ₁ Measurements.....	42
4. Area Measurements.....	48

CHAPTER	PAGE
F. Ionic Strength Correction.....	54
G. Non-Linear Least Squares Program.....	56
H. Chemical Shift Titration Experiments.....	57
I. Kinetic Studies.....	59
J. Equilibrium Studies.....	64
K. Air Oxidation of Penicillamine in Aqueous Solution.....	66
1. Rate of Oxidation of PSH versus pH.....	67
2. Rate of PSH Oxidation versus Initial PSH and PSSP Concentrations.....	74
III. ACID/BASE CHEMISTRY OF SELECTED THIOLS AND DISULFIDES IN AQUEOUS SOLUTION.....	78
A. Introduction.....	78
B. Determination of Acid Dissociation Constants by NMR.....	81
1. Monoprotic Acids.....	82
2. Diprotic Acids.....	84
a. Common Resonance Method.....	87
b. Unique Resonance Method.....	89
C. Chemical Shift Data for the Penicillamine/Oxidized Glutathione System....	93
1. Acid Dissociation Constants for Penicillamine.....	106

CHAPTER	PAGE
2. Acid Dissociation Constants for Reduced Glutathione.....	114
3. Acid Dissociation Constants for PSSP.....	121
4. Acid Dissociation Constants for GSSG.....	123
5. Acid Dissociation Constants for PSSG.....	126
D. Chemical Shift Data for the Penicillamine/Cystine System.....	132
1. Acid Dissociation Constants of CSH.....	140
2. Acid Dissociation Constants of CSSC.....	141
3. Acid Dissociation Constants of PSSC.....	144
E. pH Dependence of the Chemical Shifts for the ¹ H Resonances of Imidazole.....	147
IV, EQUILIBRIA AND KINETICS OF PENICILLAMINE- OXIDIZED GLUTATHIONE THIOL/DISULFIDE EXCHANGE REACTIONS.....	154
A. Introduction.....	154
B. Determination of Equilibrium Constants.....	156
1. The Model.....	156
2. Determination of Equilibrium Concentrations.....	160
3. Experimental Data.....	162
4. Calculation of pH Independent Equil- ibrium Constants.....	170

CHAPTER	PAGE
C. Determination of Rate Constants.....	174
1. The Reaction of PSH with GSSG.....	175
a. The Order of the Reaction.....	180
b. The Kinetic Model.....	183
c. Experimental Data.....	188
d. Calculation of pH Independent Rate Constant.....	190
2. The Reaction of Glutathione with Ox- idized Penicillamine.....	196
D. Reaction of N-Acetyl-D,L-Penicillamine with Oxidized Glutathione.....	203
E. Discussion.....	206
V. EQUILIBRIA AND KINETICS OF THIOL/DISULFIDE EXCHANGE REACTIONS OF PENICILLAMINE WITH CYSTINE AND RELATED DISULFIDES.....	213
A. Introduction.....	213
B. Determination of Equilibrium Constants for the PSH/CSSC System.....	215
1. Experimental Data.....	217
2. Determination of the pH Independent Equilibrium Constants.....	220

CHAPTER	PAGE
C. Determination of Rate Constants for the PSH/CSSC System.....	223
1. The Reaction of PSH with CSSC.....	224
2. The Reaction of CSH with PSSP.....	234
D. Reaction of Penicillamine with Other Disulfides.....	239
E. Discussion.....	246
VI. A STUDY OF THE FORMATION AND CONFORMATIONAL EQUILIBRIA OF SYMMETRICAL AND MIXED DISULFIDES OF CAPTOPRIL.....	254
A. Introduction.....	254
B. Conformational Equilibria of Captopril and Captopril-Containing Species.....	257
1. Conformational Equilibria of Captopril..	257
2. Conformational Equilibria of Captopril Disulfide.....	264
3. Conformational Equilibria of the Mixed Disulfide of Captopril with Glutathione.....	270
C. Equilibrium Constants for the Thiol/Di-sulfide Exchange Reactions Between Captopril and Oxidized Glutathione.....	275

CHAPTER	PAGE
D. Discussion:.....	278
1. Cis/trans Conformational Equilibria of CpSH, CpSSCp and CpSSG.....	278
2. CpSH/GSSG Thiol/Disulfide Exchange Reaction.....	281
VII. CONCLUSION.....	286

REFERENCES.....	295

LIST OF TABLES

TABLE	PAGE
1. Oxidation/reduction potentials of some thiols.....	14
2. Thiol/disulfide exchange reaction equilibrium constants.....	17
3. T_1 values of the methyl protons of PSSC in a 0.026 <u>M</u> PSSC solution in aqueous 1 <u>M</u> KCl/0.003 <u>M</u> EDTA, measured at 200 MHz and at 25°C.....	47
4. Assignment of the various resonances of Figure 15.....	94
5. Assignment and chemical shift data (vs DSS) for the various ^{13}C resonances in Figure 20.....	102
6. Chemical shift data (vs DSS) for the various protonated forms of PSH and PSH-containing molecules.....	108
7. Macroscopic acid dissociation constants for thiols, symmetrical disulfides and mixed disulfides.....	109
8. Microscopic acid dissociation constants for thiols, disulfides and mixed disulfides.....	115

9. Assignments of the ^1H resonances of PSH, PSSP, CSH, CSSC and PSSC resonances in Figure 34.....	136
10. Experimental values of the conditional equilibrium constant, K_{1c} , as a function of pD.....	164
11. Experimental values of the conditional equilibrium constant, K_{1c} , as a function of pH.....	165
12. Values obtained as a function of time for the equilibrium constants K_{1c} and K_{2c} , under reduced pressure in sealed NMR tubes.....	167
13. Values obtained as a function of pH for the equilibrium constants K_{1c} and K_{2c} under reduced pressure.....	168
14. Observed and predicted values for K_{2c} in aqueous solution.....	173
15. Determination of the forward rate and order of the reaction of PSH with GSSG.....	182
16. Conditional rate constants for the reaction of PSH with GSSG as a function of pH.....	189
17. Observed and predicted conditional rate constants for the reaction of PSH with GSSG.....	196

TABLE	PAGE
18. Conditional rate constants for the reaction of GSH with PSSP.....	201
19. Conditional equilibrium and rate constants for the PSH/GSSG thiol/disulfide exchange reactions at pH 7.4.....	209
20. Conditional equilibrium constants, K_{1c} and K_{2c} for the penicillamine-cystine thiol/disulfide exchange reaction as a function of pH.....	219
21. Comparison between observed and predicted conditional equilibrium constant, K_{1c}	221
22. Comparison between observed and predicted conditional equilibrium constant, K_{2c}	222
23. Forward conditional rate constants, k_{1c} for the reaction of PSH with CSSC as a function of pH.....	228
24. Comparison between observed and predicted conditional forward rate constants as a function of pH.....	233
25. Conditional equilibrium constants for the reaction of penicillamine with selected disulfides (RSSR) in the pH range 7-8.....	242

TABLE	PAGE
26. Conditional forward rate constants for the reaction of penicillamine with selected disulfides (RSSR).....	244
27. Conditional equilibrium and rate constants for the PSH/CSSC thiol/disulfide exchange reaction at pH 7.4.....	249
28. Conditional equilibrium constants for the reaction of penicillamine with selected disulfides (RSSR) at pH 7.4.....	250
29. Identification of captopril-containing species.....	261
30. The conformational equilibrium constants of CpSSCp at pH* 6.....	269
31. Cis/trans conformational equilibrium constants for proline-containing molecules.....	280

LIST OF FIGURES

FIGURE	PAGE
1. Schematic diagram of the electrolysis cell.....	34
2. 200 MHz ^1H NMR spectra measured during the electrolysis of 10 milliliters of an acidic solution of 0.02 M oxidized mercaptoacetic acid to the reduced form. The electrolysis current was 6.4 milliamperes. Aliquots were removed and quenched at the times indicated.....	37
3. 200 MHz ^1H NMR spectra measured by the inversion-recovery method for determination of T_1 values for 0.01 M PSH at pH 4 in aqueous 1 M KCl/0.003 M EDTA solution and at 25°C. Numbers by spectra indicate τ values (in seconds) in the inversion-recovery pulse sequence and chemical shifts are relative to DSS. The resonances, with increasing chemical shift, are from the two methyl resonances of PSH, a spurious peak, the $\text{CH}_2\text{-CH}_2$ group of EDTA, the CH_α of PSH and the four CH_2 groups of EDTA, respectively.....	43
4. Determination of the 90° pulse width for ^1H NMR at 200 MHz on the Bruker WH-200. The resonances are for the methyl protons of 0.01	

- M PSH at pH 4 in aqueous 1 M KCl solution/0.003 M EDTA at 25°C..... 45
5. T_1 values as a function of pH for the methyl protons of 0.01 M PSH, 0.02-0.04 M PSSG and 0.02 M PSSP in 1 M aqueous KCl solution containing 0.003 M EDTA at 200 MHz and 25°C..... 46
6. 200 MHz spectrum for a mixture of PSH and PSSP showing the amplitudes of the integral for PSH and PSSP resonances..... 50
7. Calibration curve for synthetic mixtures of PSH and PSSP in 1 M KCl/0.003 M EDTA solution at 200 MHz and 25°C. The ratio $[PSSP]/([PSH] + [PSSP])$ found by NMR is plotted versus the ratio calculated from the amounts added..... 52
8. 1H NMR spectra versus time for the oxidation of 0.03 M PSH in aqueous 1 M KCl/0.002 M EDTA solution at pH 8.07 and 25°C. The time course of the reaction was followed by quenching aliquots as a function of time. Spectra are not plotted with the same vertical and horizontal scales. The chemical shifts shown are approximate only for the first four spectra and with respect to DSS..... 68

9. Plot of PSH concentration (millimolar) versus time and as a function of pH for 0.0042 M PSH solutions exposed to atmospheric oxygen..... 70
10. Plot of initial rates for the various time course curves in Figure 9 (in units of millimolar per hour) versus pH showing the effect of pH on the initial rate..... 71
11. Plots of PSH concentrations versus time showing the two distinct rates of reaction at pH > 6. Conditions are the same as those in Figure 8..... 73
12. Plots of PSH concentration versus time for three PSH solutions with different initial concentrations at pH 7.5..... 75
13. Plots of the initial oxidation rate (in units of millimolar per hour) for 0.0039 M PSH between pH 7.4-7.8 and 25°C, versus initial PSSP concentrations. The rate of air oxidation of PSH is independent of PSSP concentrations..... 76
14. Structural formulae of some thiols and disulfides involved in thiol/disulfide exchange reactions..... 79

15. 200 MHz ^1H NMR spectra of A) 0.10 M PSH, B) 0.093 M GSSG, C) mixture prepared from 0.050 M PSH and 0.047 M GSSG, D) 0.050 M GSH and E) 0.020 M PSSP at the ambient NMR probe temperature of 26°C. Each solution was prepared in aqueous 1 M KCl solution containing 0.003 M EDTA and some t-butanol (TBA) for internal reference at pH 7.0..... 95
16. Methyl region of the 200 MHz ^1H NMR spectra of 0.010 M PSH in aqueous 1 M KCl solution containing 0.003 M EDTA and 0.003 M TBA as internal reference at 26°C..... 97
17. Methyl region of the 200 MHz ^1H NMR spectra of 0.020 M PSSP containing some TBA in aqueous 1 M KCl solution containing 0.003 M EDTA..... 98
18. Methyl region of the 200 MHz ^1H NMR spectra of a mixture of PSH, PSSP and GSSG. The original concentrations were 0.02 M PSH, 0.01 M PSSP, 0.01 M GSSG and some TBA in aqueous 1 M KCl, 0.003 M EDTA solution..... 99
19. ^1H chemical shift data for the methyl resonances of PSH, PSSP and PSSG versus DSS in aqueous 1 M KCl, 0.003 M EDTA solution.

- The smooth curves through the chemical shift data of PSH are theoretical curves calculated with Equations 57 and 77 and the constants in Table 7..... 100
20. ^{13}C NMR spectra (90.56 MHz) of A) 0.1 M PSH, B) 0.1 M GSSG, C) 0.064 M PSH, 0.019 M PSSP, 0.101 M PSSG, 0.022 M GSH and 0.014 M GSSG, D) 0.1 M GSH and E) 0.1 M PSSP. Each solution contained 0.03 M dioxane as internal reference. Solutions A, B, D and E were at pH 4.0 in 1 M KCl aqueous solution; solution C was at pH 4.52 in 0.4 M KCl aqueous solution. The thiol and disulfide concentrations in solution C were calculated from resonances 1, 5, 9; 4, 8, 12; 14, 19, 26; 16, 24 and 28. See Table 5 for assignment. The resonance labeled 0 is for the internal reference dioxane which was set at 67.40 ppm..... 105
21. Macroscopic and microscopic acid dissociation schemes for penicillamine and cysteine..... 107
22. Species distribution diagram for penicillamine. Numbers refer to the various protonated forms shown in Figure 21. These

curves were generated with $pK_{A1} = 2.54$, $pK_{A2} = 8.01$ and $pK_{A3} = 10.63$, $pK_{a12} = 8.02$ and $pK_{a13} = 9.43$ 113

23. Macroscopic and microscopic acid dissociation schemes for reduced glutathione..... 117

24. The average number of acidic protons per GSH molecule, \bar{p} , versus pH. The solid line is the theoretical curve calculated with Equation 79 and $pK_{A3} = 8.67$ and $pK_{A4} = 9.44$ 119

25. Species distribution diagram for reduced glutathione. Numbers refer to the various protonated forms shown in Figure 23. These curves were generated with $pK_{A1} = 2.05$, $pK_{A2} = 3.47$, $pK_{A3} = 8.67$, $pK_{A4} = 9.44$, $pK_{a123} = 8.91$ and $pK_{a124} = 9.04$ 120

26. Macroscopic and microscopic acid dissociation schemes for oxidized penicillamine, cystine and PSSC. In the case of PSSC, the ammonium group of the PS part of PSSC is labelled 3 and that of the CS part 4..... 122

27. Species distribution diagram for oxidized penicillamine. The various deprotonated forms associated with the numbers are shown in Figure 26. The fractional concentrations

FIGURE	PAGE
<p>were calculated with $pK_{A1} = 1.40$, $pK_{A2} = 2.05$, $pK_{A3} = 7.76$ and $pK_{A4} = 8.71$.....</p>	124
28. Macroscopic and microscopic deprotonation schemes of oxidized glutathione.....	125
29. Species distribution diagram for oxidized glutathione. The various deprotonated forms associated with the numbers are summarized in Figure 28. The fractional concentrations were calculated with $pK_{A1} = 1.58$, $pK_{A2} = 2.41$, $pK_{A3} = 3.08$, $pK_{A4} = 4.00$, $pK_{A5} = 8.73$ and $pK_{A6} = 9.49$	127
30. Macroscopic and microscopic acid dissociation schemes of the mixed disulfide, PSSG.....	128
31. pH dependence of the ^{13}C chemical shifts of the penicillamine and glutamyl alpha carbons of PSSG (Table 5) versus DSS.....	129
32. The pH dependence of the fractional titration of the penicillamine ($f_{4,d}$) and glutamyl ($f_{5,d}$) ammonium groups of PSSG and the average number of ammonium protons per PSSG molecule (\bar{p}). The smooth curve through the \bar{p} data is the theoretical curve calculated with Equation 79 and the constants in Table 7.....	131

33. Species distribution diagram of the mixed disulfide, PSSG. Numbers refer to the various deprotonated forms in Figure 30; the solid curves were generated with $pK_{a1234} = 8.22$, $pK_{a1235} = 8.86$, $pK_{A4} = 8.13$ and $pK_{A5} = 9.24$ 134
34. 200 MHz 1H NMR spectra in D_2O of A) 0.2 M PSH, B) 0.2 M CSSC, C) 0.1 M PSH + 0.1 M CSSC, D) 0.4 M CSH and E) 0.01 M PSSP at pH 10 and at the ambient probe temperature of $26^\circ C$ 138
35. Chemical shifts of the methine and methyl protons of PSH, PSSP and the PSH part of PSSC as a function of pH..... 139
36. Methyl region of the 200 MHz 1H NMR spectra of a mixture of PSH, PSSP and CSSC. The original concentrations consisted of 0.008 M PSH, 0.001 M PSSP, 0.002 M CSSC and 0.0007 M TBA in 1 M KCl aqueous solution containing 0.003 M EDTA..... 142
37. Species distribution diagram for CSH. Numbers refer to the various protonated forms shown in Figure 21. The fractional concentrations were calculated with $pK_{A1} =$

1.87, $pK_{A2} = 8.19$, $pK_{A3} = 10.29$, $pK_{a12} = 8.48$
 and $pK_{a13} = 8.50$ 143

38. Species distribution diagram for CSSC. The various deprotonated forms associated with the numbers are shown in Figure 26. These curves were generated with $pK_{A1} = 1.51$, $pK_{A2} = 2.21$, $pK_{A3} = 7.88$ and $pK_{A4} = 9.30$.

39. The pH dependence of the fractional titration of the penicillamine ($f_{3,d}$) and cysteine ($f_{4,d}$) ammonium groups of PSSC and the average number of ammonium groups per molecule (\bar{p}). The smooth curve through the \bar{p} data is the theoretical curve calculated with Equation 79 for the values of K_{A3} and K_{A4} listed in Table 7..... 146

40. Species distribution diagram for PSSC. See Figure 26 for the protonated forms associated with the numbers. The fractional concentrations were calculated with $pK_{A1} = 1.80$, $pK_{A2} = 2.24$, $pK_{A3} = 8.04$ and $pK_{A4} = 8.93$ 148

41. 1H NMR spectra at 200 MHz of 0.05 M imidazole in 1 M aqueous KCl, 0.003 M EDTA solution..... 151

42. ^1H chemical shift data of the C2-H and C4,5-H resonances of imidazole. Conditions are the same as in Figure 41..... 152
43. The model used to evaluate equilibrium and kinetic data for the PSH/GSSG exchange reaction in the pH range 4-10..... 158
44. Plot of the conditional equilibrium constant K_{1c} for the reaction of PSH with GSSG, versus the solution pH or pD. The solid line through the points is the theoretical dependence of K_{1c} on pH predicted by equation 115 with $K_1 = 34.8$ and the constants in Table 7..... 171
45. 200 MHz ^1H NMR time course spectra for the reaction of PSH with GSSG. (Left) Initial concentrations of PSH and GSSG, 0.0160 M, pH 3.96. (Right) Initial concentrations of PSH and GSSG, 0.00400 M, pH 6.61. Solutions prepared in 1 M aqueous KCl solution containing 0.003 M EDTA. Temperature, 25°C..... 176
46. Kinetic data for the formation of PSSG by reaction of PSH with GSSG at pH 3.96 and 9.01. The initial concentrations of PSH and GSSG were 0.0160 M at pH 3.96. At pH 9.01,

- the initial concentrations were 0.00143 M PSH and 0.00137 M GSSG. The extent of reaction was followed in situ (pH 3.96) and by quenching the reaction (pH 9.01) as a function of time..... 178
47. Concentration jump experiment showing the effect of adding GSH to an equilibrium mixture obtained by reaction of PSH with GSSG in D₂O at pD 7.5 with initial concentrations of 0.0013 M PSH and GSSG. The equilibrium mixture is 0.0003 M PSH, 0.0001 M PSSP and 0.0008 M PSSG. At t = 355 minutes, GSH concentration was increased by 0.0013 M..... 184
48. Plot of the natural logarithm of B versus time; B is given by Equation 133. The initial concentrations of PSH and GSSG were 0.00200 M in 1 M aqueous KCl solution containing 0.003 M EDTA; pH 6.97..... 187
49. Plots of the logarithm of the fractional concentration, α , for the species PSH⁰, PS⁻, and PS²⁻, and of the conditional rate constant k_{1c} as a function of pH. The solid curve through the experimental points is the theoretical curve predicted by Equation 140

- and the value $k_1 = 190 \text{ M}^{-1}\text{min}^{-1}$ 191
50. 200 MHz ^1H NMR time course spectra for the reaction of GSH with PSSP at pH 8.03. The initial concentrations were 0.108 M GSH and 0.100 M PSSP in 1 M KCl solution containing 0.003 M EDTA. Temperature of the water bath, 25°C. The extent of the reaction was monitored by quenching aliquots of the reaction mixture. The pH of the quenched aliquot was ~0.5. Prior to the NMR measurement, each aliquot was adjusted to pH ~4 for better resolution of the methyl resonances..... 198
51. The concentrations of PSH, PSSG and PSSP obtained from the time course spectra in Figure 50..... 199
52. 200 MHz ^1H NMR time course spectra for the reaction of N-PSH with GSSG. The resonances are from the methyl groups on N-PSH. Initial concentrations were 0.00365 M and 0.0348 M for N-PSH and GSSG respectively. [TBA] = 0.004 M, pH 6.58 in 1 M KCl aqueous solution.... 204
53. 200 MHz time course spectra for the reaction of PSH with CSSC. Solution pH, 5.94.

- Initial concentration, 0.00504 M PSH and 0.00297 M CSSC. Reaction was carried out at 24°C in situ, inside a 5 mm NMR tube in 1 M aqueous KCl solution containing 0.003 M EDTA.... 225
54. The concentrations of PSH and PSSC as a function of time for the experiment described in Figure 53. The solid lines are theoretical for a second order reaction with $k_{1c} = 8.35 \text{ M}^{-1}\text{min}^{-1}$ and $X_e = 0.00214 \text{ M}$ in Equation 136..... 227
55. The logarithm of the fractional concentration α of PSH in the amino-protonated, thiol-deprotonated (PS^-) and amino-deprotonated, thiol-deprotonated (PS^{2-}) forms and of the forward rate constant k_{1c} for the reaction of PSH with CSSC versus pH. The solid curve through the experimental points is the theoretical curve predicted by Equation 140 and $k_1 = 1091 \text{ M}^{-1}\text{min}^{-1}$ 230
56. 200 MHz ^1H NMR time course spectra of the methyl and methine groups of PSH, PSSP and PSSC in a solution containing initially 0.102 M CSH and 0.100 M PSSP. The reaction was carried out at pH 12.44, aliquots were

- quenched as a function of time by lowering the pH to ~0.5, and then the pH was raised to pH 9 when NMR spectra were run so that resolved resonances would be obtained for the various species. The pH was not identical for each aliquot..... 236
57. Progress curves for PSH, PSSC and PSSP as obtained from data of the type shown in Figure 56..... 238
58. Structural formulae of selected disulfides..... 240
59. 200 MHz ^1H spectra of the methyl groups in a solution which contained initially 0.0328 M PSH and 0.0331 M SuSSSu as a function of time. 1 M KCl, 0.003 M EDTA, pH 7.61, 25°C..... 245
60. 360 MHz ^1H NMR spectra of 0.062 M captopril (pH* = 6.0) and 0.042 M captopril disulfide (pH* = 6.0). In the 1-1.5 ppm region, the gain was reduced by a factor of 2..... 258
61. Expansion of the methyl resonances in Figure 60 (1.11-1.21 ppm). Resolution was enhanced by doing a Gaussian multiplication with the Bruker Aspect 2000 software. Resonance assignments are given in Table 29..... 260

62. The fractional concentrations of the cis and trans forms of captopril as a function of pH*..... 263
63. ^1H NMR spectrum of the methyl region of a pH* 7.0 solution containing captopril-glutathione mixed disulfide and captopril disulfide. Details of the preparation of the mixed disulfide are given in the text. Gaussian multiplication was used to enhance the resolution..... 271
64. The fractional concentrations of the cis and trans forms of captopril-glutathione mixed disulfide as a function of pH*..... 274
65. The methyl region of the ^1H NMR spectrum of a solution prepared by reacting 0.045 M CpSH with 0.041 M GSSG at pH* 6.0 for 341 hours in a degassed, sealed NMR tube. Resolution was enhanced by Gaussian multiplication. Resonance assignments are given in Table 29..... 276
66. The thiol/disulfide exchange equilibria and CpSH, CpSSCp, and CpSSG conformational equilibria occurring in a solution prepared by reacting CpSH and GSSG. The subscripts t and c indicate trans and cis conformations

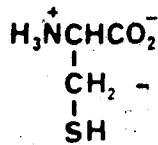
across the amide bond(s) of the captopril in
CpSH and CpSSCp or the captopril part of
CpSSG..... 282

CHAPTER I

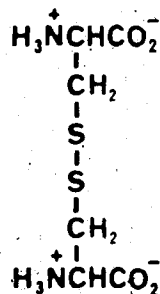
THIOLS, DISULFIDES AND THIOL/DISULFIDE EXCHANGE REACTIONS

A. Introduction

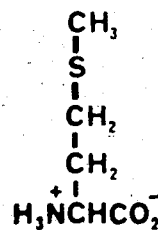
Sulfur is an essential element for living organisms, being a constituent of several amino acids, many peptides and proteins and numerous other biological molecules. In peptides and proteins, sulfur is commonly present in the thiol (sulfhydryl) group of cysteine (I), the disulfide group of cystine (II) and the thioether group of methionine (III).



I



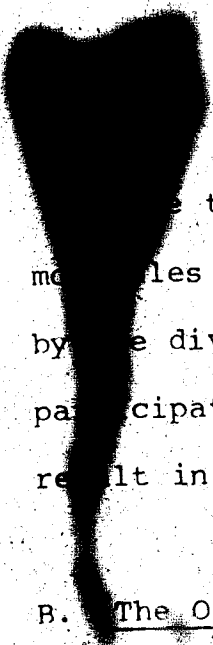
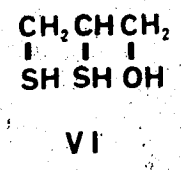
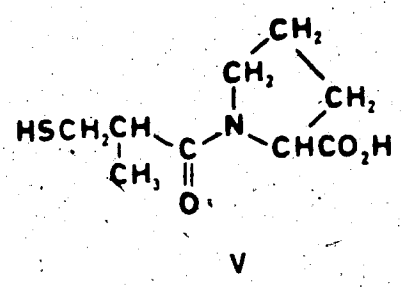
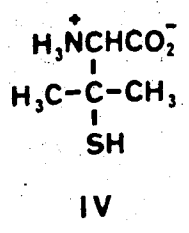
II



III

The roles of the thiol, disulfide and thioether groups in peptides and proteins are varied, including the maintenance of oxidation/reduction equilibria, the

activity of numerous enzymes and stabilization of macromolecular structure of proteins [1,2]. The thiol group is also present in several drug molecules, including penicillamine (β,β -dimethyl cysteine, IV), captopril (1-[2(S)-3-mercapto-2-methyl-1-oxopropyl]-L-proline, V) and British anti-Lewisite (2,3-dimercaptopropanol, VI).



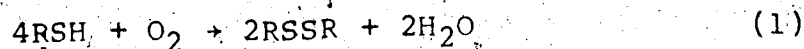
Thiol groups in peptides, proteins and drug molecules are characterized by their high reactivity and by the diverse chemical reactions in which they participate. Among the most important are reactions which result in the oxidation of thiols to disulfides.

B. The Oxidation of Thiol Groups

The metabolism and biological function of thiols depends to a large extent upon the ease with which they

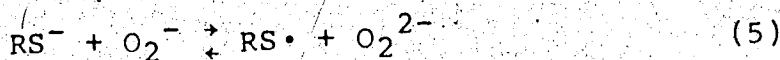
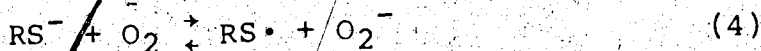
are oxidized. Under the mild oxidizing conditions of biological systems, disulfides are the products of the oxidation reactions. There are several different pathways by which this oxidation occurs in biological systems, including autoxidation and oxidation by disulfides.

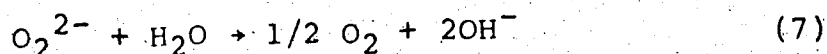
Autoxidation refers to oxidation by dissolved oxygen. The disulfide product can be a symmetrical disulfide or a mixed disulfide, as shown by Equations 1 and 2.



The rate of oxidation depends on several factors, including pH, temperature, thiol concentration, the nature of the thiol and the presence of metal impurities [3].

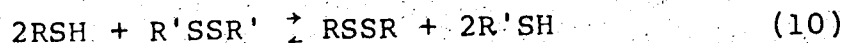
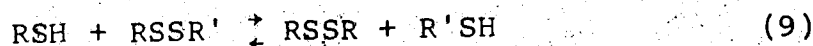
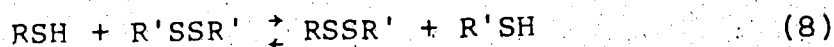
The rate of oxidation increases with pH, which suggests that the active species is the deprotonated thiolate anion, RS^- . The overall oxidation reaction is thought to occur by the following steps [3,4]:





Step 4 is proposed to be the rate determining step. Autoxidation of thiols is catalyzed by traces of metal ions, particularly Cu(II) and Fe(III) [5].

Oxidation of thiols by disulfides proceeds according to the 2-step reaction sequence represented by Equations 8 and 9:

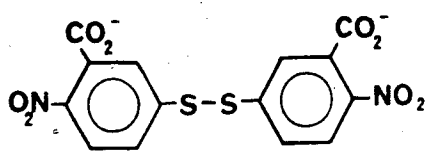


These reactions are generally referred to as thiol/disulfide exchange reactions.

The overall oxidation occurs in two steps, with the mixed disulfide $RSSR'$ formed as a stable intermediate in the first step. Numerous mixed disulfides have been identified in biological systems, including cysteine-homocysteine mixed disulfide in human plasma [6-8], cysteine-penicillamine mixed disulfide in human urine [9], cysteine-glutathione mixed disulfide in liver homogenate

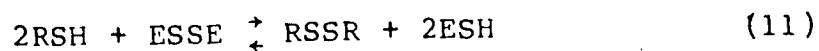
[10] and calf lens [11], and glutathione-coenzyme A mixed disulfide in rat [12] and bovine [13] liver. Protein-small molecule mixed disulfides also occur in biological fluids. Among the most well characterized is that formed between the thiol group of bovine serum albumin (BSA) and cysteine; the thiol group of approximately 40% of naturally-occurring BSA exists in the form of a mixed disulfide with cysteine. It is for this reason that nonintegral values (typically 0.6-0.7) are obtained for the number of thiol groups in BSA [14].

Among oxidants for thiols, disulfides are of particular importance because they react with thiols to form only disulfides, and they show little reactivity with other functional groups in biological molecules. This highly specific nature of the reaction of disulfides with thiols forms the basis for the most widely used methods for determining the levels of thiol-containing molecules in biological fluids. Among the disulfide reagents for thiols, 5,5'-dithiobis-(2-nitrobenzoic acid) (Ellman's reagent, DTNB, VII) [15] is the most popular.



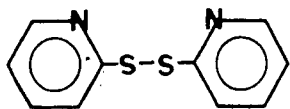
VII

Ellman's reagent reacts with thiols according to the overall reaction

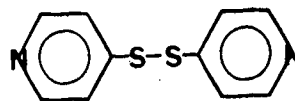


where ESSE represents Ellman's reagent and ESH, 2-nitro-5-thiobenzoic acid. Because the equilibrium for Equation 11 lies far to the right, RSH is quantitatively oxidized to RSSR by an excess of Ellman's reagent. The amount of RSH oxidized is determined from the absorbance at 412 nm, the λ_{max} for the anion of ESH; Ellman's reagent itself does not absorb significantly at this wavelength.

The disulfides 2,2'-dithiodipyridine (VIII) and 4,4'-dithiodipyridine (IX) are also widely used as reagents for thiols [16,17].



VIII



IX

The thiopyridones formed by reaction with thiols absorb strongly at 340 and 324 nm, respectively.

Thiol/disulfide exchange reactions are of considerable importance in living systems. In cells and in biological fluids, they provide the reaction pathway by which the various thiols and disulfides present are maintained in a state of dynamic equilibrium. They also are important in the metabolism of thiol-containing drug molecules, and in some cases they form the chemical basis for their pharmacological and therapeutic activity. The thiol/disulfide exchange reactions of the drugs penicillamine and captopril with relatively low molecular weight disulfides are the subject of this thesis.

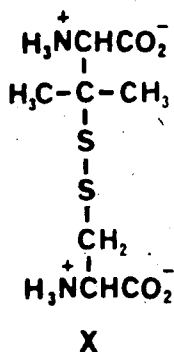
C. The Uses of Penicillamine in Medicine

Penicillamine (IV) is a structural analog of the naturally-occurring amino acid cysteine (I), in which the two hydrogens on the β -carbon of cysteine are replaced by methyl groups. PSH can be obtained by acid hydrolysis of penicillin, and was first found in vivo in 1953 by Walshe in the urine of patients being treated with penicillin [18]. Subsequently, penicillamine itself has been found to be of use in medicine.

The first use of penicillamine in medicine was for the treatment of Wilson's disease, an inherited metabolic disorder in which Cu^{2+} is accumulated in various tissues

of the body. Because of its chemical structure, Walshe deduced that it should chelate divalent metal ions, including Cu^{2+} , and thereby promote its excretion from patients with Wilson's disease. This proved to be correct, and today penicillamine is the drug of choice for the treatment of Wilson's disease [19]. It also is used for the treatment of intoxication by other heavy metals, including Pb^{2+} and Hg^{2+} [20].

Penicillamine also is used for the treatment of cystinuria, a metabolic disorder in which precipitates of the relatively insoluble disulfide cystine (solubility of 7.8×10^{-4} M in pH 6.95 phosphate buffer [21]) form in the renal tract [22]. Its use for the treatment of cystinuria was based on the observation that penicillamine reacts with cystine to form the penicillamine-cysteine mixed disulfide (PSSC, X) [23].



Because PSSC is considerably more soluble than CSSC, treatment with penicillamine results in decreased formation of cystine precipitate as well as dissolution of the deposits formed prior to treatment with penicillamine. Thus, the molecular basis for this therapeutic use of penicillamine is the thiol/disulfide exchange reaction involving PSH and CSSC. Although all the pathways by which PSH is metabolized have not yet been identified, this is considered to be the major pathway in all patients treated with penicillamine, regardless of the disease being treated [9]. Less than half of an injected dose of penicillamine is recovered in the urine, and of that, the majority is the PSSC mixed disulfide, with a small amount of PSSP and a trace of PSH [9,24].

The most recent, and currently the most widespread, use of penicillamine in medicine is for the treatment of rheumatoid arthritis [25,26]. The rationale which led to the study of penicillamine in rheumatoid arthritis was based on a possible reaction of the thiol group of penicillamine with the disulfide bonds of rheumatoid factor [27]. Penicillamine is effective for the treatment of rheumatoid arthritis, and is considered by some to be the drug of choice for treatment of severe rheumatoid arthritis. Although the mechanism of action at the molecular level has not been elucidated, thiol/disulfide

exchange reactions involving penicillamine are undoubtedly involved [28].

D. The Use of Captopril in Medicine

Captopril (V) is a recently developed drug for the treatment of high blood pressure. High blood pressure can result from the over production of the octapeptide angiotensin II, which causes the constriction of blood vessels, from the inactive decapeptide angiotensin I, the conversion being catalyzed by angiotensin-converting enzyme [29-31]. Captopril was designed to inhibit angiotensin-converting enzyme by interacting with the enzyme at its active site. The design of the molecule was based on the assumption that the active site of this carboxypeptidase-like enzyme is similar to that of carboxypeptidase-A, whose active site has been characterized by crystallography [32]. Both angiotensin-converting enzyme and carboxypeptidase A contain a Zn^{2+} ion at their active sites, and a key feature in the design of captopril was the assumption that its thiol group would bind to the Zn^{2+} of angiotensin-converting enzyme [29-31].

The metabolism of captopril has yet to be elucidated, however by analogy with penicillamine, it seems likely that thiol/disulfide exchange reactions involving

disulfides such as cystine and oxidized glutathione will be important metabolic pathways.

F. Thiol/Disulfide Exchange Reactions: Equilibrium Considerations

Because of their importance, thiol/disulfide exchange reactions involving thiol-containing biological molecules have been the subject of a large amount of research. This research has included studies of both their kinetic and their equilibrium properties. In this section, some relationships which are used to characterize thiol/disulfide exchange equilibria are presented and then previous studies of thiol/disulfide exchange reactions which are particularly relevant to this thesis are discussed.

The overall oxidation of a thiol to its disulfide occurs via two consecutive, reversible equilibria, Equations 8 and 9. The equilibrium constants for the reactions are defined as:

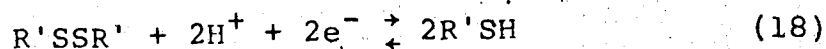
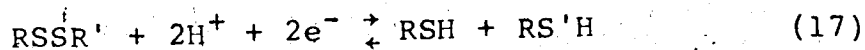
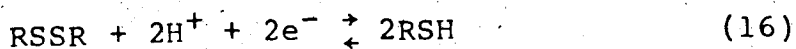
$$K_{1c} = \frac{[RSSR'] [R'SH]}{[RSH] [R'SSR']} \quad (12)$$

$$K_{2c} = \frac{[RSSR] [R'SH]}{[RSH] [RSSR']} \quad (13)$$

$$K_{3c} = \frac{[RSSR](R'SH)^2}{[RSH]^2[R'SSR']} \quad (14)$$

$$K_{3c} = K_{1c}K_{2c} \quad (15)$$

If the distribution of R and R' among the various thiol and disulfide species is determined by probability, K_{1c} will equal 2, K_{2c} will equal 0.5 and K_{3c} will equal 1. This random distribution was first observed by McAllan and coworkers during synthesis of symmetrical and unsymmetrical disulfides from various mixtures of two thiols [33]. Equilibrium constants K_{1c} - K_{3c} are related to the differences in the oxidation-reduction potentials of the three couples, defined by Equations 16-18, according to Equations 19-21.

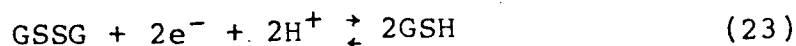
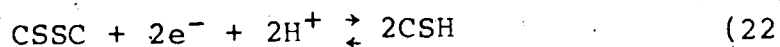


$$E^\circ_{RSSR'/RSH, R'SH} - E^\circ_{R'SSR'/R'SH} = \frac{-2.303 RT}{nF} \log K_{1c} \quad (19)$$

$$E^\circ_{RSSR/RSH} - E^\circ_{RSSR'/RSH, R'SH} = \frac{-2.303 RT}{nF} \log K_{2c} \quad (20)$$

$$E^\circ_{RSSR/RSH} - E^\circ_{R'SSR'/R'SH} = \frac{-2.303 RT}{nF} \log K_{3c} \quad (21)$$

Due to the affinity of sulfur for metals, it has not been possible to measure the standard oxidation-reduction potentials for thiols directly. Rather, their standard potentials have been determined indirectly by measuring equilibrium constants for their oxidation by oxidizing agents of known standard potential. Standard potentials obtained in this way for the cystine (CSSC)/cysteine (CSH) (Equation 22) and oxidized glutathione (GSSG)/glutathione (GSH) (Equation 23) couples, are summarized in Table 1.



GSSG and GSH have the structural formulae XI and XII.

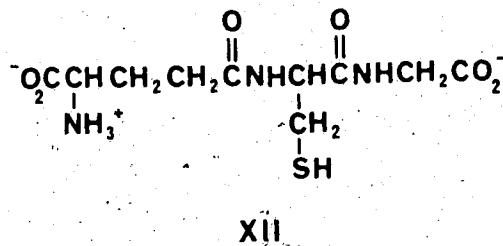
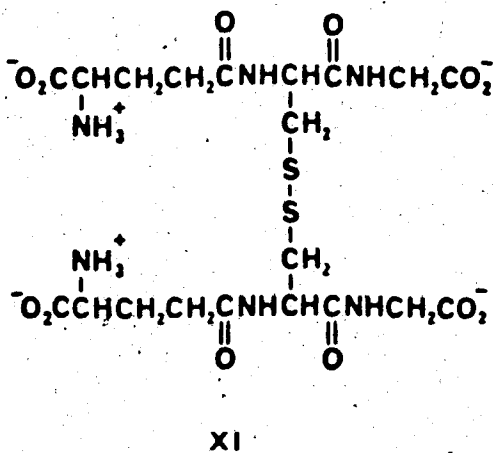


Table 1. Oxidation/reduction potentials of some thiols.

Couple	Condition	E_0 (V)	Reference
$\text{CSSC} + 2e^- + 2\text{H}^+ \rightleftharpoons 2\text{CSH}$	pH 7	-0.21 - -0.23	34
	pH 7	-0.22	37
$\text{GSSG} + 2e^- + 2\text{H}^+ \rightleftharpoons 2\text{GSH}$	pH 7.0, 40°C	-0.24	55
	pH 7.0	-0.25	56

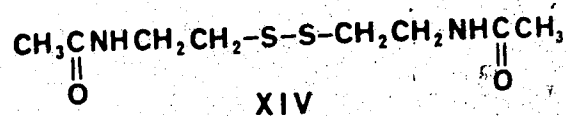
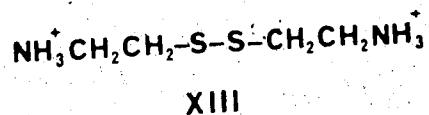
F. Previous Studies of Thiol/Disulfide Exchange Reactions

The kinetics and equilibria of thiol/disulfide exchange reactions of a variety of thiols with the CSSC/CSH and GSSG/GSH systems, as well as with related small molecules, and thiol/disulfide containing proteins, have been studied. Because both the reactants and products are thiols and disulfides, an essential part of this research has been the development of methods with which reactants and/or products could be monitored selectively. The methods which have been developed are generally based upon a physical or chemical property of one of the reactants and/or products, and thus are limited to specific systems.

Among the earliest studies of thiol/disulfide exchange reactions involving biological molecules are those of Kolthoff, Stricks and Kapoor [21], who, in 1955, reported equilibrium constants for the reactions of GSH and mercaptoacetic acid ($\text{HSCH}_2\text{CO}_2\text{H}$) with CSSC. The equilibrium constants were calculated from the increased solubility of CSSC, which is only slightly soluble over the pH range 5-7 (the solubility of CSSC in pH 6.95 phosphate buffer is 7.8×10^{-4} M), in solutions containing GSH or MSH. The solubility is increased by the reaction of GSH and MSH with CSSC to form the more soluble mixed

disulfide, CSSG and CSSM and the thiol CSH. The equilibrium constants obtained in this study for the GSSG/GSH exchange reaction are listed in Table 2. From these equilibrium constants, the standard electrode potential for the GSSG/GSH couple was calculated to be 0.07 V relative to that for the CSSC/CSH couple. Hoff et al. also made the important observation that the active species in these reactions are the thiolate anions, GS^- , MS^- and CS^- , and not the undissociated thiols GSH, MSH and CSH. This has since been found to be true in numerous other studies of thiol/disulfide exchange reactions [34-38].

In 1957 and 1958, Eldjarn and Pihl [34-36] reported equilibrium constants at pH 7.4 and 37°C for thiol/disulfide exchange reactions involving CSH and GSH and the related disulfides cystamine (C'SSC', XIII), N,N'-diacetylcystamine (AC'SSC'A, XIV) and several derivatives



of cystamine. The method used by Eldjarn and Pihl to

Table 2. Thiol/disulfide exchange reaction equilibrium constants^a

R'SSR'	RSH	K _{1c}	K _{2c}	K _{3c}	Reference
CSSC	GSH	2.8	1.0	2.8	21
CSSC	C'SH	4.76	0.75	3.6	34
CSSC	AC'SH	5.00	0.62	3.1	34
GSSG	C'SH	5.00	0.34	1.7	34
GSSG	AC'SH	2.86	0.28	0.8	34
CSSC	GSH	3.2	1.2	3.9	37
CSSC	GSH	3.74	0.791	4.72	38
CSSC	PSH	0.13	~0.01	-	9

^aDefined by Equations 8-10 and 12-15.

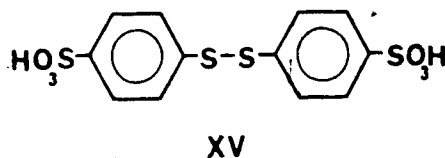
measure the equilibrium constants was based on the reaction of thiols with disulfides which were labelled with the radioactive isotope ^{35}S . Reaction products were separated by paper electrophoresis at pH 2. With this method, the concentrations of three of the five species present in the thiol/disulfide exchange reaction (e.g. C'SSC', C'SSC and C'SH when CSH exchanges with C'SSC') could be determined. Some of the results obtained in these studies are listed in Table 2. From the magnitudes of the thiol/disulfide equilibrium constants, Eldjarn and Pihl calculated the reduction potential for the CSSC/CSH, C'SSC'/C'SH and AC'SSC'A/AC'SH couples to be +0.0101, -0.0071 and +0.0030 V respectively, relative to that of the GSSG/GSH couple at pH 7.4 and 37°C. Eldjarn and Hambræus used the ^{35}S isotope method to estimate the kinetic and equilibrium properties of the reaction of penicillamine with cystine at pH 7.4 [9]. The equilibrium constants are listed in Table 2. The equilibrium constant K_2 for the formation of PSSP was reported to be practically zero.

Jocelyn studied the direct reaction of GSH with CSSC as well as the reverse reaction of CSH with GSSG. The method used to obtain the equilibrium constants for the stepwise exchange reactions (Equations 8 and 9) and the overall exchange reaction involved determining (i) the GSH

concentration in equilibrium reaction mixtures by measuring the absorbance which develops at 265 nm when concentrated HCl is added to GSH solution, (ii) the total thiol concentration, and thus the CSH concentration by difference with the GSH concentration from (i), by measuring the absorbance at 412 nm after reaction with DTNB, and (iii) the GSSG concentration by first selectively reducing GSSG by an enzyme catalyzed reaction, then determining total thiol as in (ii), and finally, calculating the GSSG by difference knowing total thiol before reduction of GSSG from (ii). The equilibrium constants for the exchange reaction of GSH with CSSC are given in Table 2. The standard potential of the GSSG/GSH and CSSC/CSH couples determined at pH 7 in this work are given in Table 1. The method used in this study is limited to exchange reactions involving glutathione, since determinations (i) and (iii) are based on specific reactivities of GSH and GSSG respectively. However, it has not been applied to the study of other exchange reactions of glutathione, perhaps because of the uncertainties introduced by determining all the concentrations except that of GSH by difference.

At about the same time, Gorin and coworkers [38] also reported equilibrium constants for the exchange reaction of GSH with CSSC, as well as the reaction of GSH and CSH

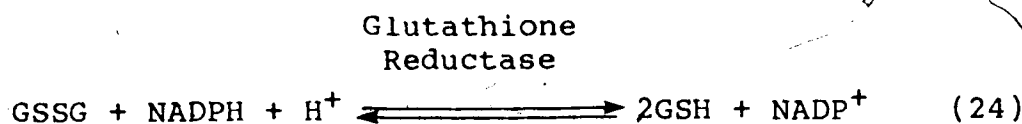
with 4,4'-dithiobisbenzene sulfonate (XV) [39-41]. Their



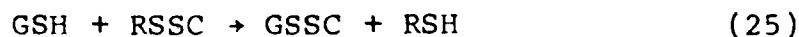
values for the equilibrium constants for the GSH/CSSC exchange reaction at pH 6.6 and 25°C are given in Table 2. These values were obtained by analyzing the equilibrium mixture for the concentrations of all five species using an amino acid analyzer. The equilibrium constants are, in general, in good agreement with those reported by Jocelyn and by Kolthoff, Stricks and Kapoor. From this value for the equilibrium constant, Gorin and Doughty [38] calculated the standard potential for the GSSG/GSH couple to be -0.017 V relative to that for the CSSC/GSH couple. It is clear from the works of Kolthoff and coworkers, Jocelyn, and Gorin and coworkers that the standard potentials for the GSSG/GSH and CSSC/CSH couples are similar.

The kinetics of the reaction of GSH with cystine and with a series of alkylmercaptan-cysteine mixed disulfides (RSSC) were studied by Weber, Hartter and Flohé [42]. Reaction rates were determined by measuring the rate of production of GSSG, using the coupled enzymatic reduction

of GSSG (Equation 24) as the indicator reaction.



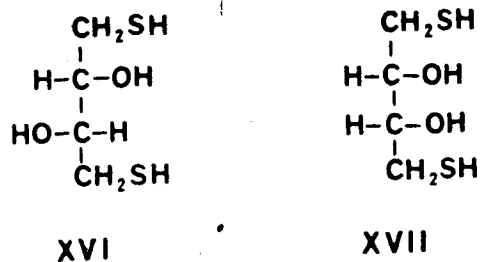
The reduction of GSSG was followed by measuring the absorbance due to NADPH at 360 nm. The initial rate of the exchange reaction is bimolecular, with the second order rate constant for the reaction:



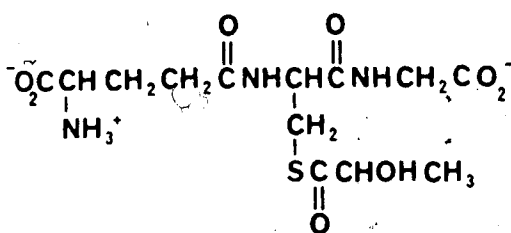
having the values $R =$ cysteine, 0.2190; methyl, 0.06040; benzyl, 0.05040; ethyl, 0.03460; propyl, 0.03130; isopropyl, 0.01870; and t-butyl, 0.00799 $\text{M}^{-1}\text{sec}^{-1}$ at pH 7. Of particular interest to the present study is the relatively small rate constant observed when R is t-butyl. This was attributed to steric effects due to the bulkiness of the t-butyl group.

In the most detailed studies of the mechanistic aspects of thiol/disulfide exchange reactions involving biological disulfides to date, Szajewski and Whitesides [43] examined the dependence of the rate and equilibrium constants for the reaction of a series of thiols with GSSG

on thiol structure. Thiols studied included both mono and dithiols, with particular emphasis on those that are used to reverse or prevent autoxidation of thiol groups in proteins, e.g. dithiothreitol (XVI), dithioerythritol (XVII),



mercaptoethanol ($\text{HSCH}_2\text{CH}_2\text{OH}$), and mercaptoacetic acid ($\text{HSCH}_2\text{CO}_2\text{H}$). The rate of release of GSH from GSSG was determined at pH 7.0 and 30°C by using a fast enzymatic following reaction in which GSH is converted to S-lactoyl glutathione (XVIII) by reaction with methylglyoxal in the



XVIII

presence of the enzyme glyoxalase-I. The concentration of XVIII was monitored spectrophotometrically by measuring its absorbance at 240 nm. Although this method appears to be convenient for measuring both the kinetic and equilibrium properties of exchange reactions involving

GSSG, it cannot be used with the aminothiols cysteine and $\text{H}_2\text{NCH}_2\text{CH}_2\text{SH}$, and presumably the related aminothiol penicillamine, because they also react with methylglyoxal to form species which strongly absorb at 240 nm. The results of this study were interpreted to indicate that thiol/disulfide exchange is a mechanistically simple $\text{S}_{\text{N}}2$ displacement reaction which follows the Brönsted relation:

$$\log k = c + \beta_{\text{nuc}} \text{pK}_{\text{A}}^{\text{nuc}} + \beta_{\text{c}} \text{pK}_{\text{A}}^{\text{c}} + \beta_{\text{lg}} \text{pK}_{\text{A}}^{\text{lg}} \quad (26)$$

where nuc is nucleophile, c is central and lg is leaving group sulfur. A correlation was found between the $\text{pK}_{\text{A}}^{\ddagger}$ of the thiolate nucleophile and the rate of its attack on a sterically unencumbered disulfide bond, with the rate constant increasing as the pK_{A} increases. β_{nuc} , β_{c} and β_{lg} are Brönsted coefficients and c is a constant necessary for the equation to fit the observed data.

In addition to these studies, there have been several studies of thiol/disulfide exchange reactions involving thiols such as GSH and CSH with aromatic disulfides such as DTNB (VII), 2,2'- and 4,4'-dithiodipyridine (VIII and IX), and 4,4'-dithiobisbenzene sulfonate (XV), [39-41,44-54]. It has not been possible to measure equilibrium constants for these reactions because the equilibrium lies

far to the right due to the weak disulfide bonds formed by aromatic disulfides and the low pK_A values of the aromatic thiols. However, their kinetics have been studied in detail by using the absorbance of the aromatic thiolate anions. The studies of Hupe and coworkers [45-47] have provided a detailed picture of the mechanism of the exchange reaction with DTNB. Their results indicate that displacement occurs by an S_N2 pathway involving no kinetically distinguishable metastable intermediate, which agrees with the conclusions of Whitesides and coworkers for alkyl disulfides [43].

G. This Thesis

As described above, the molecular basis for the medical use of penicillamine and captopril, as well as their metabolism, depends largely on the chemistry of their thiol groups. Among the several reactions possible for thiol groups in living systems, thiol/disulfide exchange reactions are of particular importance. Thiol/disulfide exchange reactions of penicillamine and captopril are the subject of this thesis.

The main technique used to study these exchange reactions is 1H NMR, with some results also obtained by ^{13}C NMR. NMR was used for these studies because it

provides information at the molecular level. Thus, it might be possible to characterize directly thiol/disulfide exchange reactions by observation of resonances from some or all of the species involved.

As discussed previously, the rates and equilibria of thiol/disulfide exchange reactions are dependent on the protonation states of the species involved. Although the acid/base chemistry of most of the thiols and symmetrical disulfides studied in this thesis have been reported previously, there are no reports in the literature on the acid/base chemistry of mixed disulfides. In order to be able to characterize fully the exchange reactions of PSH with oxidized glutathione and cystine, the acid/base chemistry of the mixed disulfides PSSG and PSSC has been studied, along with the acid/base chemistry of several of the other thiols and disulfides involved. The acid/base chemistry of the mixed disulfides was characterized using chemical shift data obtained for solutions in which the mixed disulfide was formed in situ by reaction of PSH with the appropriate disulfide. Simultaneously, data were obtained on the acid/base chemistry of the thiols and disulfides in equilibrium with the mixed disulfide. This detailed information which can be obtained at the molecular level for thiol/disulfide exchange reactions at equilibrium illustrates one of the main advantages of NMR

for these studies. The results obtained for the acid/base chemistry of thiols, disulfides and mixed disulfides are presented in Chapter III.

A study of the equilibrium and kinetic properties of the penicillamine/oxidized glutathione exchange reaction is presented in Chapter IV. This reaction was studied for several reasons: (i) Glutathione, both in its reduced and oxidized forms, is thought to be a natural constituent of every living cell. For example, GSH is present at the 2 mM level in human erythrocytes. Thus, reactions of PSH with oxidized GSH are likely to be important in the metabolism of PSH. Also, because of the importance of GSH in biological systems, information about its reactions with thiols is of general interest. (ii) To a first approximation, GSSG might serve as a model for disulfide groups in proteins, since the cystinyl group is bonded at both its amino and carboxyl groups to other amino acids via peptide bonds. (iii) The results of studies of the exchange reactions of other thiols with GSSG are available for comparison. This is of interest because it is thought that steric hindrance due to the two methyl groups on the carbon bearing the thiol group makes PSH somewhat different from other thiol compounds [28].

In Chapter V, the results of a study of the equilibria and kinetics of the reaction of PSH with

cystine are presented. This reaction was chosen for study because of its importance (i) as the molecular basis for the use of PSH in the treatment of cystinuria and (ii) as a pathway for the metabolism of PSH. This reaction has been studied previously, however these studies have only provided estimates of the equilibrium and kinetic properties of the reaction at pH 7. In Chapter V, the kinetics and equilibria of the reaction have been studied over a wide range of solution pH so as to characterize their pH dependence. Similar results are also presented in Chapter V for the reaction of PSH with several other disulfides.

The results of studies of thiol/disulfide exchange reactions of captopril are presented in Chapter VI. The most detailed study involves the reaction of captopril with GSSG. The thiol/disulfide exchange reactions of captopril are found to be considerably more complicated than those of PSH since captopril exists in two different conformations which are in equilibrium.

CHAPTER II

EXPERIMENTAL

A. Chemicals

D-penicillamine, PSH, reduced and oxidized glutathione, GSH and GSSG, respectively, N-acetyl-D,L-penicillamine, D,L-cysteine and 5,5'-dithiobis-(2-nitrobenzoic acid) (DTNB), all from Sigma Chemical Company, were used as received unless stated otherwise. On several occasions, PSH was first electrolyzed to reduce traces (<1%) of oxidized penicillamine. On one occasion, stock solutions of PSH and GSSG were passed through a cation exchange column (as described below) for removal of possible metal ion impurities. D-penicillamine disulfide, D,L-PSH, 2-hydroxyethyl disulfide (98%), cystamine, cysteamine (2-aminoethanethiol) and imidazole (99%), were obtained from Aldrich Chemical Company, Inc. Mercaptosuccinic acid was from Aldrich or Eastman Organic Chemicals. D,L-cystine, dithiodiglycolic acid and D,L-homocystine were from ICN Pharmaceuticals, Inc. D,L-homocysteine was from Nutritional Biochemicals Corporation. 3-Mercaptopropionic acid and the oxidized form of both mercaptosuccinic acid and D,L-2-

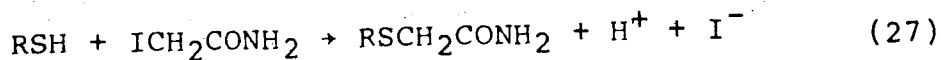
mercaptopropanoic acid were synthesized by Dr. A. Arnold of this laboratory. Reduced and oxidized captopril were generously provided by E.R. Squibb and Son, Inc. Tert-butyl alcohol (TBA, BDH Chemicals), sodium 2,2-dimethyl-2-silapentane-5-sulfonate (DSS, Merck Sharp and Dohme of Canada Limited) and 1,4 dioxane (BDH Chemicals) were used as chemical shift internal references. The salt bridge for the electrolysis cell was made with agar from Baker and Adamson. All other chemicals were reagent grade and were used without purification unless otherwise stated.

Potassium chloride (American Scientific and Chemical or Fisher Scientific Company Ltd.) was purified by passing through a column packed with Dowex 50W-X8 cation exchange resin (J.T. Baker Chemical Co.). The resin was first prepared by washing with 6 M HCl (Fisher Scientific Company Ltd.), 2 M NaOH (American Scientific and Chemical or BDH Chemicals), and then methanol (Anachemia Ltd.). Doubly distilled water was used to rinse the resin between the various steps. Usually, the washing/rinsing cycle was repeated one more time. The resin was then poured into a 1.5 x 16 cm column fitted at the bottom with a cotton plug. Approximately one liter of 1 M KCl solution was eluted at ~2 milliliters per minute. The first 50 milliliters were discarded. After passing through the column, EDTA was added to the KCl solution (0.003 M EDTA) to complex trace metal ion impurities.

B. Preparation of Solutions

The required amounts of thiols and disulfides were weighed and dissolved in ~5 milliliters of acidified 1 M KCl solution containing 0.003 M EDTA. The KCl solution used was previously purified by passing through a Dowex-50X ion exchange column to remove divalent metal ions which catalyze the oxidation of thiols [57]. The resulting acidic solutions were then diluted to the required volume and kept tightly stoppered at 4°C. Unless otherwise stated, all solutions are in 1 M aqueous KCl solution containing 0.002-0.003 M EDTA.

The concentrations of the thiol and disulfide stock solutions, usually 0.1 M, were calculated on the basis of weights of solid used. The purity of several of the disulfides used was determined by titrating their carboxylic acid groups with NaOH, using the indicators m-cresol purple or bromothymol blue. These two indicators were chosen on the basis of literature pK_A values for the carboxylic acid groups. For the titration of GSSG, the indicator was chosen on the basis of a published titration curve [58]. The purity of PSH and GSH was checked by titrating their thiol groups by the method of Benesch and Benesch [59]. In this method, the thiol group is reacted with iodoacetamide according to the reaction:



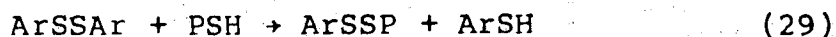
The protons liberated are then titrated with carbonate-free NaOH [60]. The NaOH solution used was standardized by titration of potassium hydrogen phthalate (Analar, dried for >2 hours at a temperature of 120°C) with phenolphthalein as indicator.

The procedure used for the reaction of thiol groups with iodoacetamide is as follows: first the pH of the RSH solution is adjusted to the methyl red indicator end-point (~ pH 5.75). Excess iodoacetamide is added and then the solution is titrated with base to the phenolphthalein end point. The pH is increased to increase the rate of the alkylation reaction. The protons liberated as reaction 27 proceeds lower the pH, and more base is added to return the pH to the phenolphthalein end point. After the reaction is over (< 5 minutes), the solution is titrated back to the methyl red indicator end point.

The amount of RSH present is calculated from:

$$\text{moles RSH present} = \text{moles base} - \text{moles acid} \quad (28)$$

Occasionally, the concentration of the PSH stock solution was determined by the DTNB method [15,61]. In the presence of excess DTNB, the stoichiometric ratio between PSH and the aromatic thiol anion TNB is 1:1.



ArSSAr, ArSSP and ArSH represent DTNB, the mixed disulfide of PSH with DTNB and TNB anion, respectively. The concentration of ArSH was determined by measuring the absorbance, A , at 412 nm on a Cary 118 spectrometer at 25°C. Using Beer's law, the concentration of PSH was calculated as

$$[\text{PSH}] = A/ab \quad (30)$$

where a is the molar absorptivity coefficient of TNB ($14100 \pm 300 \text{ M}^{-1}\text{cm}^{-1}$ at pH 7 and 25°C, in 0.05 M phosphate buffer) and b is the cell path length (1.00 cm). The molar absorptivity coefficient was determined in the same buffer containing known amounts of mercaptoacetic or 3-mercaptopropanoic acid which had been standardized by pH titration or by the method of Benesch and Benesch [59].

The thiols and disulfides used were found to have a purity >98%, except for GSH and $(-SCH_2CH_2COOH)_2$ which were found to be 96% each. The presence of water and/or oxidized GSSG is probably responsible for the purities of less than 100%. The proper correction was applied to solutions of these two compounds in order to give the correct concentrations as calculated from the weights.

At pH less than 4, thiol oxidation is slow (as will be shown later), thus acid was added to lower the pH and solutions were stored at 4°C to minimize air oxidation.

All solutions containing thiols and disulfides were manipulated in such a way as to minimize air oxidation. This included degassing the solutions with N_2 or argon, covering the solutions with a N_2 or argon atmosphere during pH adjustments and time course studies, and by flushing the NMR tubes with N_2 or argon before adding the sample solution.

C. Electrolysis Cell

The PSH stock solutions were generally electrolyzed at a Hg pool electrode (Figure 1), using a constant current of 6.4 mA, to reduce trace amounts of oxidized PSH. The electrolysis cell [62] consisted of an inverted U-shaped tube of ~1 mm i.d., one arm of which was placed

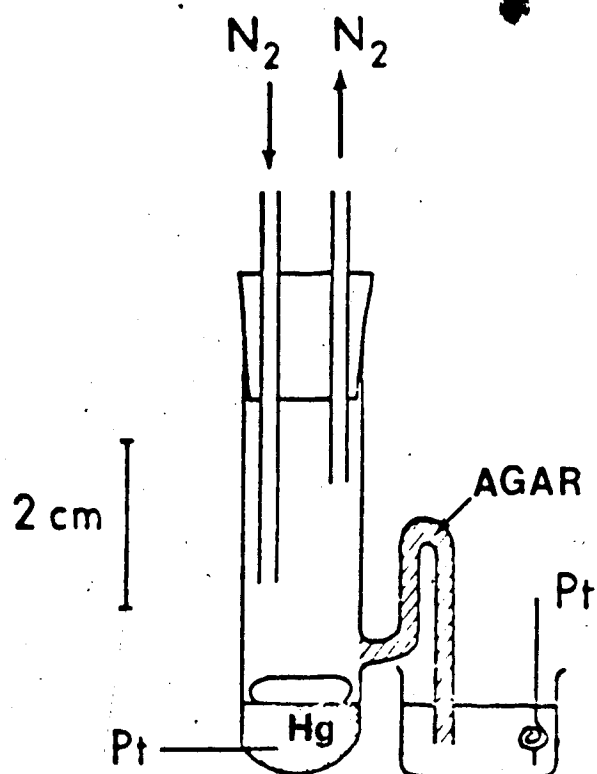
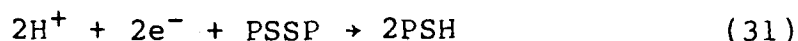


Figure 1. Schematic diagram of the electrolysis cell.

1 cm from the bottom of a 1.5 x 5-10 cm tube which contained a pool of Hg ~0.5 cm in depth. The Hg pool was connected to the negative lead of a Leeds & Northrup constant current coulometer via a platinum wire which was sealed into the bottom of the tube. The other arm was dipped into a small beaker containing a saturated solution of NaCl. The positive lead of the coulometer was connected to a platinum or copper wire counter electrode which was dipped into this solution. To provide contact between the salt solution and the solution in the Hg-containing tube, the U-shaped tube was filled with saturated NaCl/2% Agar.

During electrolysis, the sample solution (>2 mL) was stirred under an argon or N₂ atmosphere with a magnetic stirring bar placed on top of the Hg pool.

The reduction of PSSP is represented by Equation 31.



Since two moles of protons are needed for each mole of PSSP reduced, the pH of the solution was adjusted to pH ~2 by the addition of concentrated HCl. Periodically, the pH of the solution was checked with a combination pH electrode dipped directly into the electrolysis cell and

HCL was added if the solution pH was greater than pH 3.

To test the efficiency of the electrolysis system, a solution containing 90% PSH (4 millimolar) and 10% PSSP (0.4 millimolar) was reduced. A ^1H NMR spectrum taken 5 minutes after the start of electrolysis showed no PSSP resonances indicating that within 5 minutes, the PSSP had been completely reduced. In the course of this experiment, the pH had increased by 0.5 pH unit, as predicted by Equation 31. In another experiment, 0.02 M oxidized mercaptoacetic acid (MSSM) was electrolyzed. Figure 2 shows NMR spectra taken at various times during the electrolysis. As expected, this solution, which is 50 times more concentrated, had no detectable amount of MSSM left after 153 minutes (top spectrum in Figure 2).

D. pH Measurements

pH measurements were made at 25°C, using a water bath and a jacketed cell, or at ambient temperature if the temperature was $25 \pm 1^\circ\text{C}$. The pH readings were taken with standard Fisher Accumet or Orion pH meters. Either a standard glass electrode with a fiber tip, saturated calomel reference electrode or a microcombination electrode were used. The pH meters were calibrated with potassium biphthalate, phosphate-NaOH and potassium

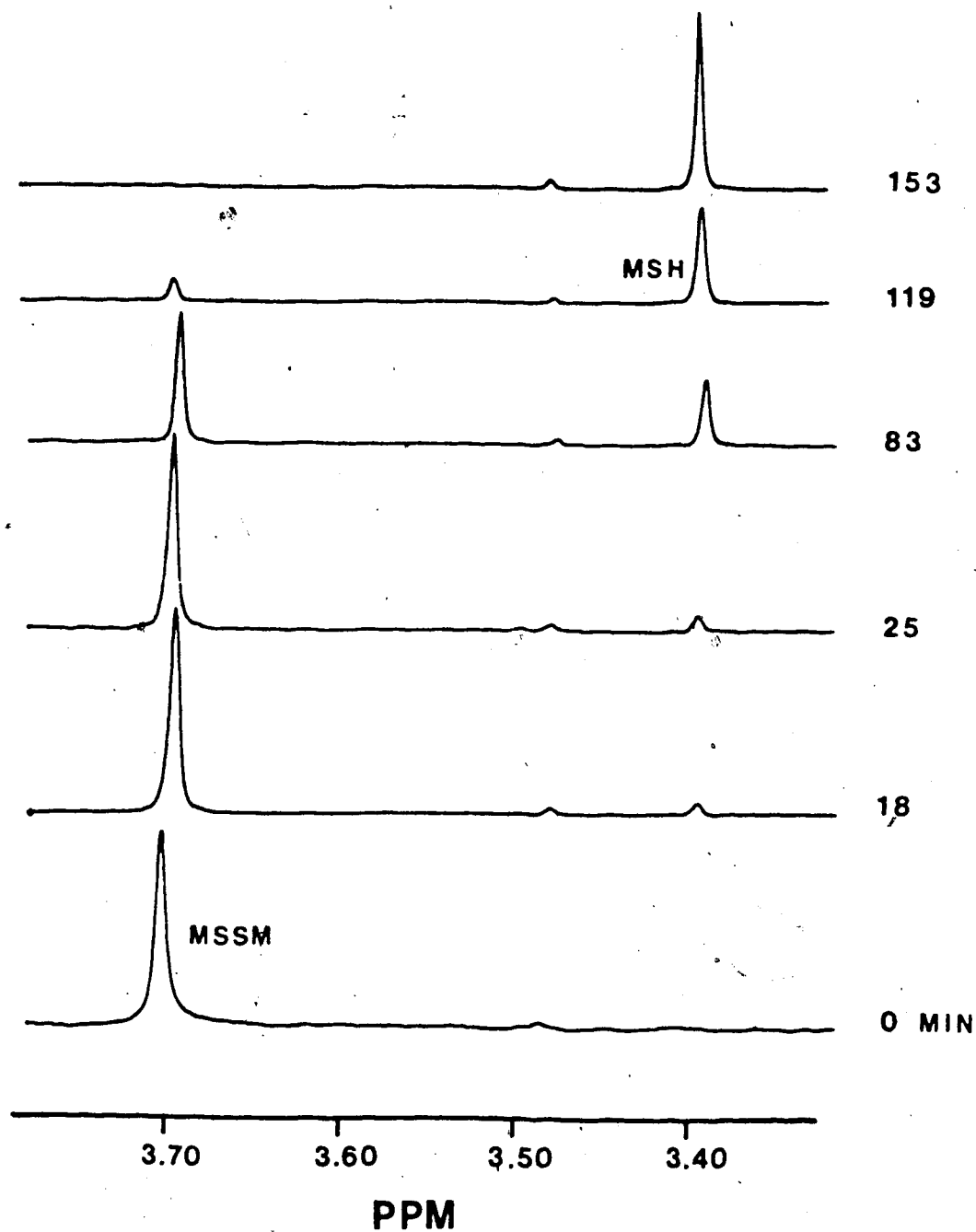


Figure 2. 200 MHz ^1H NMR spectra measured during the electrolysis of 10 milliliters of an acidic solution of 0.02 M oxidized mercaptoacetic acid to the reduced form. The electrolysis current was 6.4 milliamperes. Aliquots were removed and quenched at the times indicated.

carbonate-borate-KOH standards of 0.05 M each and nominal pH values of 4.00, 7.00 and 10.00, respectively.

pH measurements for solutions prepared in D₂O were converted to pD values as follows [63]:

$$\text{pD} = \text{pH meter reading} + 0.4 \quad (32)$$

The pH values of solutions in several of the kinetic runs were determined indirectly from the chemical shifts of imidazole in the solution. This is discussed further in Chapter III. The procedure involved adjusting quickly the pH of the solution to the approximate pH value desired, and then the solution was degassed. The imidazole indicator in the solution provided a convenient way of monitoring the pH of solutions in sealed NMR tubes during long time course studies. The use of imidazole as an internal pH indicator is restricted to the pH region 6.3-8. More details can be found in Chapter III.

E. Nuclear Magnetic Resonance Measurements

1. Instrumentation and Method

NMR spectra were obtained on Bruker WH-200, WH-400 or WM-360 spectrometers. All spectra were measured by the pulse/Fourier transform (P/FT) method. The probe

temperature was occasionally adjusted to 25°C (WH-200) with a variable temperature unit but most experiments were carried out at the ambient probe temperature which was $25 \pm 2^\circ\text{C}$. For the ^{13}C experiments, air was blown over the sample tube in the probe to minimize sample heating which accompanies the use of broadband ^1H decoupling. In this way, the temperature was maintained close to 25°C.

Spectrometer operation was under the control of an Aspect 2000 computer system. Processing of free induction decays (FIDs) was also done on the Aspect 2000 system using standard Bruker software.

Most of the studies of thiol/disulfide exchange equilibria and kinetics were done in aqueous solution. The presence of the large water resonance (H_2O proton concentration $\sim 110 \text{ M}$) causes a dynamic range problem for measurement of ^1H NMR spectra by the P/FT method. To avoid the dynamic range problem, the water resonance was partially removed by the technique of solvent suppression. In this experiment, the water resonance is saturated by applying via the decoupling channel a strong radio frequency pulse at its resonance frequency for about 2 seconds duration [64]. The decoupler is then gated off, the normal observation pulse is applied, and the FID is collected.

Most ^1H NMR spectra were obtained with the WH-200 NMR

spectrometer. Because the magnet in this spectrometer is very stable (e.g. no detectable drift over a period of an hour), it was possible to run the aqueous samples without the use of a field/frequency lock. To lock the spectrometer would have required the addition of a deuterated compound to the sample solution, which would have increased the possibility of contamination. One result of not having a lock signal is that it is more difficult to shim the magnet, and thus resonances are broader than would normally be obtained with optimum shimming.

So that concentrations could be obtained from signal intensities, the delay time between successive pulses was set to at least 5 times the longest spin-lattice relaxation time (T_1) of the resonances of interest. The delay is the sum of the decoupling time plus the time required for the acquisition of the FID. The spectral sweep width and the number of points in the final frequency domain spectrum were such that there were at least 5 points above the half height of each resonance so that accurate resonance intensities could be obtained for quantitative analysis [65].

Another potential source of error in making quantitative measurements from NMR spectra obtained by the P/FT method is that excitation by the pulse may not be

uniform across the entire spectral width [66]. By using resonances that are close together, the effect of this source of error is minimized. In an experiment involving mercaptoacetic acid and GSSG, the RF carrier frequency was progressively shifted and the intensities of the resonances of interest were measured as a function of the distance between the signal and the carrier frequency to see whether the intensities of various signals decrease in magnitude. No significant changes in the NMR intensities were detected.

2. Chemical Shift Measurements.

Proton chemical shifts were measured relative to the internal reference tert-butyl alcohol (TBA) but are reported relative to the methyl resonances of DSS. The methyl resonance of tert-butyl alcohol in 1 M aqueous KCl solution containing 0.003 M EDTA was found to be 1.2397 ppm to high frequency from DSS at pH 4.02, 7.40 and 10.07.

¹³C chemical shifts were measured relative to 1-4 dioxane but are reported relative to TMS. The chemical shift of dioxane was set at 67.40 ppm [67] with respect to TMS.

In the acid-base chemistry studies, it was found that the TBA chemical shift varied with respect to dioxane at pH 0.5. Therefore, the chemical shift studies were carried out at pH > ~0.5.

3. T₁ Measurements

The determination of concentration from the intensity of resonances in spectra measured by P/FT NMR requires that the nuclear magnetization return to equilibrium before the pulse is applied. To ensure that this is so, a repetition time (the time between successive pulses) greater than 5 times the longest spin-lattice relaxation time (T₁) of the resonances of interest was used.

To set the repetition time to the appropriate value, T₁ values need to be known. T₁ values were determined on selected samples by the inversion-recovery method [68], which consists of the pulse sequence 180°-τ-90°-acquisition-delay. The 180° pulse inverts the magnetization which then is allowed to recover by spin-lattice relaxation for time τ. The 90° pulse samples the magnetization to determine the amount of recovery. The repetition time, i.e. the time between successive experiments, is set to greater than 5 times the estimated T₁ values. The experiment is repeated at different τ values, giving a series of spectra of the type shown in Figure 3.

The relaxation times were obtained by fitting the intensity versus τ data to Equation 33 using Hanssum's method [69] and the non-linear least squares program KINET [70].

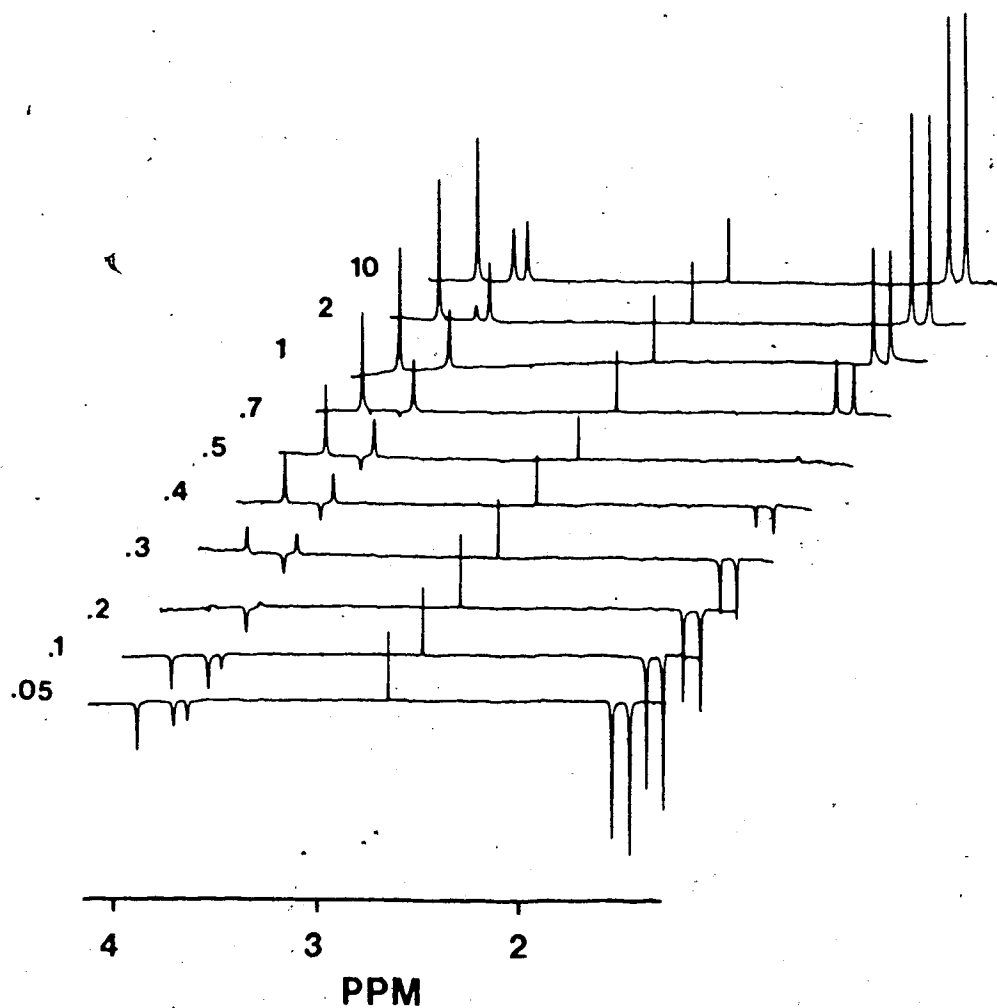


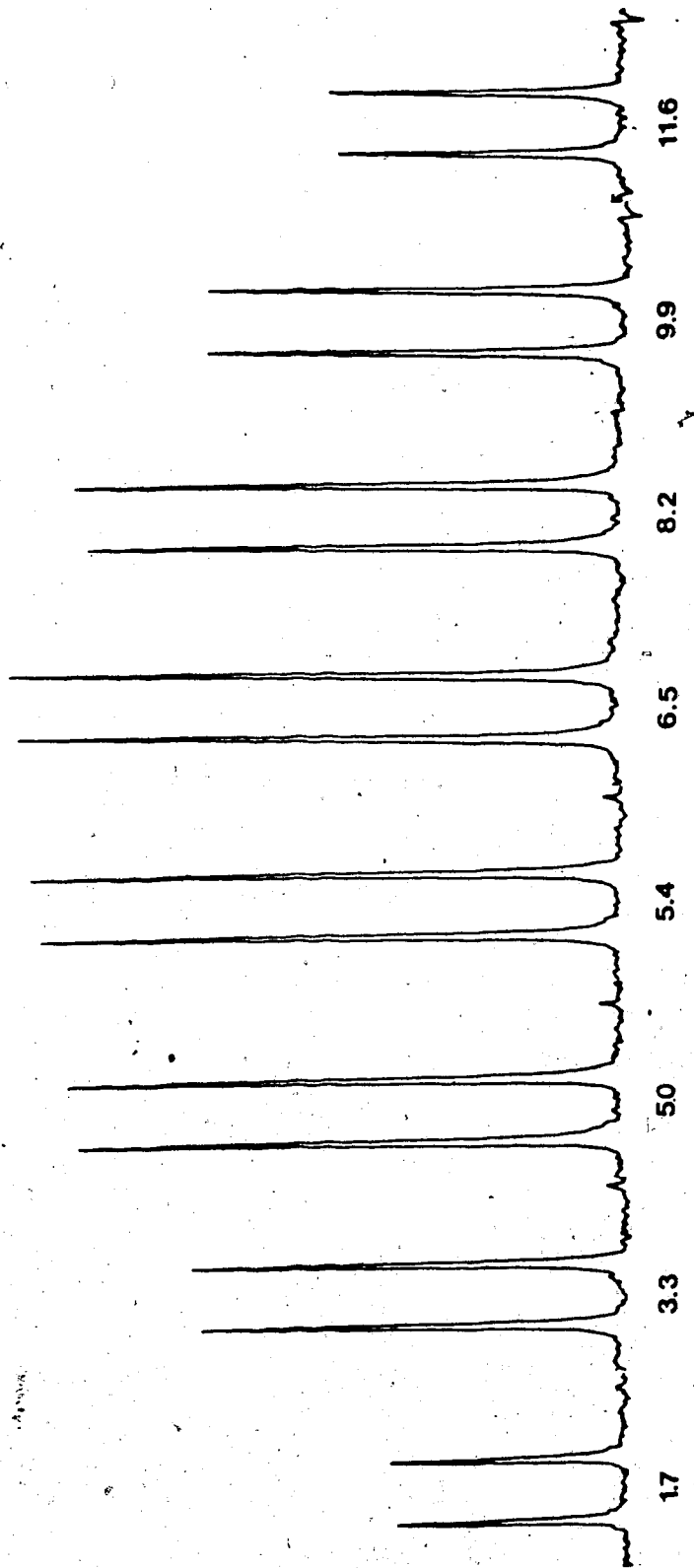
Figure 3. 200 MHz ^1H NMR spectra measured by the inversion-recovery method for determination of T_1 values for 0.01 M PSH at pH 4 in aqueous 1 M KCl/0.003 M EDTA solution and at 25°C. Numbers by spectra indicate τ values (in seconds) in the inversion-recovery pulse sequence and chemical shifts are relative to DSS. The resonances, with increasing chemical shift, are from the two methyl resonances of PSH, a spurious peak, the $\text{CH}_2\text{-CH}_2$ group of EDTA, the CH_α of PSH and the four CH_2 groups of EDTA, respectively.

$$M_t = M_0 (1 + k(1 - \exp(\frac{T}{T_1}))) \exp(\frac{\tau}{T_1}) \quad (33)$$

where M_t and M_0 are resonance intensities at $t = \tau$ and at equilibrium, respectively. M_0 is obtained from the resonance intensity at $\tau > 5T_1$. k is an unknown inhomogeneity parameter and T is the repetition time.

To measure spin-lattice relaxation times, it is necessary to use pulses which give flip angles close to 180° and 90° . The pulse length for a 90° flip angle on the WH-200 spectrometer was determined using a sample consisting of 0.01 M PSH in 1 M aqueous KCl solution containing 0.003 M EDTA. The procedure consisted of measuring signal intensity as a function of pulse length. The results are shown in Figure 4. From a comparison of resonance intensities, a value of 6.2 μsec was selected for a 90° pulse. A value of 12.4 μsec was used for a 180° pulse.

The values of T_1 as a function of pH are summarized in Figure 5 for the methyl resonances of PSH, PSSP and PSSG and in Table 3 for PSSC. The results in Figure 5 show that the T_1 values are fairly independent of pH except for those of PSH. The T_1 values in Table 3 for PSSC show a slight general increase with pH.



PULSE WIDTH (μ SEC)

Figure 4. Determination of the 90° pulse width for ^1H NMR at 200 MHz on the Bruker WH-200. The resonances are for the methyl protons of 0.01 M PSH at pH 4 in aqueous 1 M KCl solution/0.003 M EDTA at 25°C .

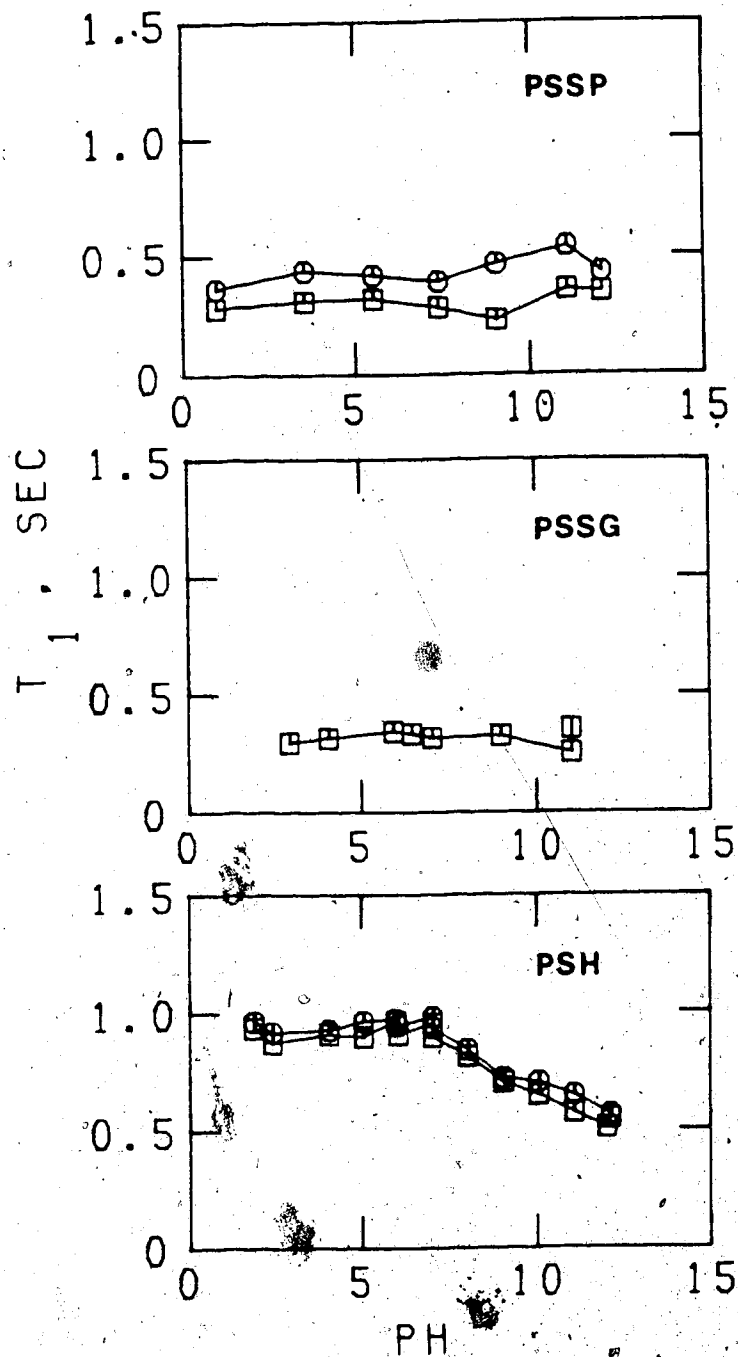


Figure 5. T_1 values as a function of pH for the methyl protons of 0.01 M PSH, 0.02-0.04 M PSSG and 0.02 M PSSP in 1 M aqueous KCl solution containing 0.003 M EDTA at 200 MHz and 25°C.

Table 3. T_1 values of the methyl protons of PSSC in a 0.026 M PSSC solution in aqueous 1 M KCl/0.003 M EDTA, measured at 200 MHz and at 25°C.

pH	T_1 (sec) ^a	
	Downfield	Upfield
1.01	0.28	0.35
4.03	0.36	0.44
5.50	0.33	0.43
10.05	0.39	0.55

^aUncertainty is ±5%.

From the results in Figure 5 and Table 3, a repetition time of 5 seconds was selected for most experiments.

4. Area Measurements

The areas under resonances in NMR spectra measured by the P/FT method are directly related to the concentration of nuclei giving the resonance if repetition times of greater than $5T_1$ are used. Under optimum conditions, an overall precision of 2% is possible [71]. In this thesis, spectra were measured with repetition times of greater than $5T_1$, and the areas of the resonances were used to determine concentrations from which equilibrium constants and rate constants were obtained.

The relative areas under the resonances of interest were measured by three methods: (i) planimeter, (ii) triangulation, and (iii) integration subroutine in the Aspect 2000 software. Most of the areas were measured by method (iii). However, methods (i) and (ii) were used when resonances were small and partially overlapping with other resonances and/or the baseline was poor. This was usually the case, for example, when it was necessary to use millimolar concentrations to slow down reaction rates so that the initial stage of the kinetics could be observed.

Thiol/disulfide exchange reactions with bulky reactants and thiol oxidations are totally defined by measuring the concentration of one thiol or one disulfide. For example, for the thiol oxidation of PSH to PSSP, both species concentrations are calculated from the relative areas I_x and I_y in Figure 6. Figure 6 shows a typical spectrum with the integral trace from which areas were obtained. The figure shows the resonance for the methyl groups of PSH and PSSP in a mixture of the two. As discussed in Chapter III, the two methyl groups of PSH have different chemical shifts, as do the two methyl groups of PSSP. The two resonances from PSH and the two from PSSP are identified in the figure. The concentrations of PSSP and PSH were calculated from the areas under the resonances x and y, which are given by the vertical displacement of the integral trace I_x and I_y . The fractional concentrations (f) of the total PSH as PSH and PSSP are given by Equations 34 and 35:

$$f(\text{PSH}) = \frac{I_y}{I_x + I_y} \quad (34)$$

$$f(\text{PSSP}) = \frac{I_x}{I_x + I_y} \quad (35)$$

The concentrations of PSH and PSSP are given by Equations 36 and 37:

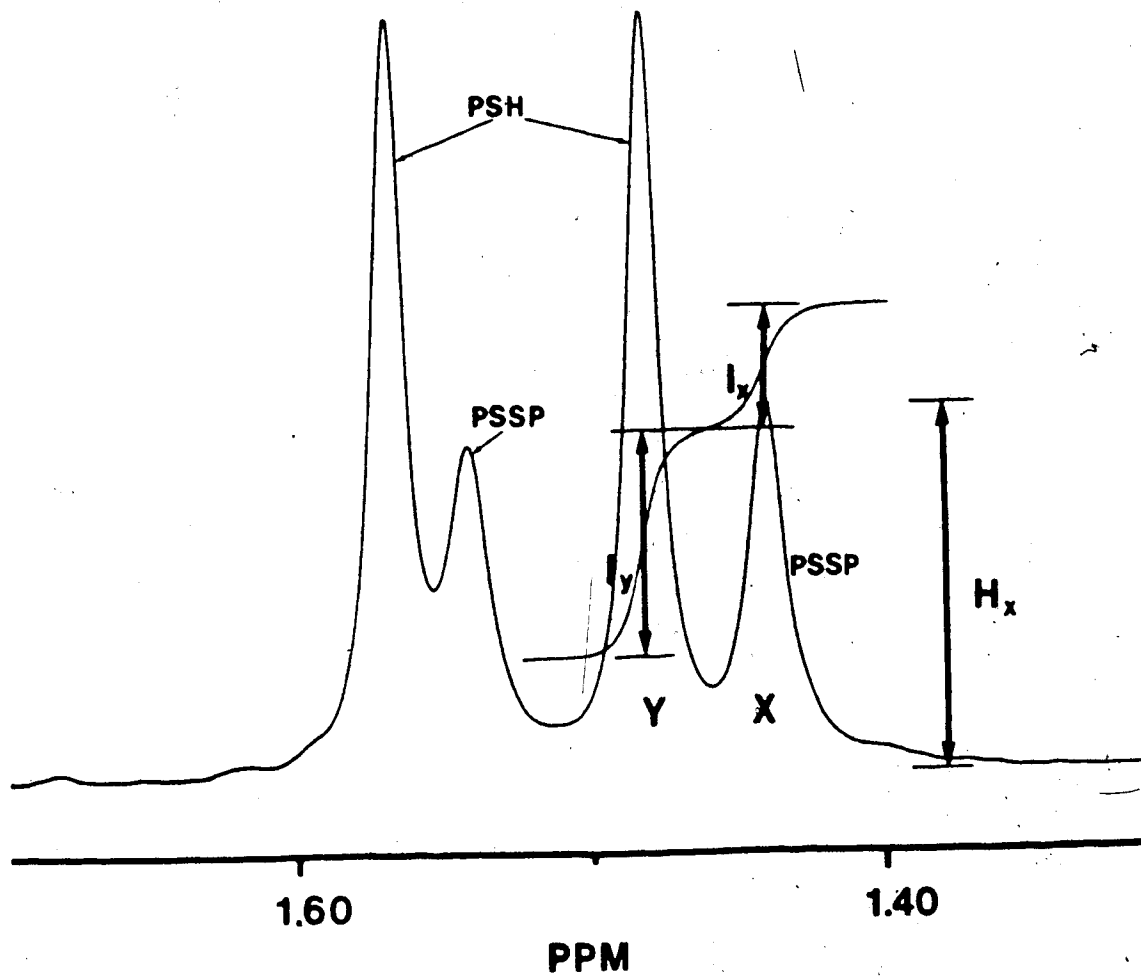


Figure 6. 200 MHz spectrum for a mixture of PSH and PSSP showing the amplitudes of the integral for PSH and PSSP resonances.

$$[\text{PSH}] = f(\text{PSH}) \cdot [\text{PSH}]_0 \quad (36)$$

$$[\text{PSSP}] = \frac{f(\text{PSSP})}{2} \cdot [\text{PSH}]_0 \quad (37)$$

$[\text{PSH}]_0$ is the initial concentration of PSH. The factor 2 accounts for the two methyl groups giving each resonance of PSSP.

For thiol/disulfide exchange reactions involving a bulky reactant such as PSH, a single kinetic equilibrium step is observed, as will be shown in Chapter IV. The species concentrations are given by equations similar to Equations 34 and 36.

To determine the accuracy of concentrations determined for the various components of a mixture from areas measured by the integration software, a series of solutions containing PSH and PSSP in varying ratios was prepared. Figure 7 shows the ratio of $[\text{PSSP}]/([\text{PSSP}] + [\text{PSH}])$ obtained from the integral trace plotted versus that calculated from the concentrations of PSH and PSSP in the mixtures. The average deviation between the theoretical and observed ratios is 0.02. This indicates that the relative errors in measurement of concentrations from the integral traces are largest when there is a low concentration of one component. Whenever possible, conditions

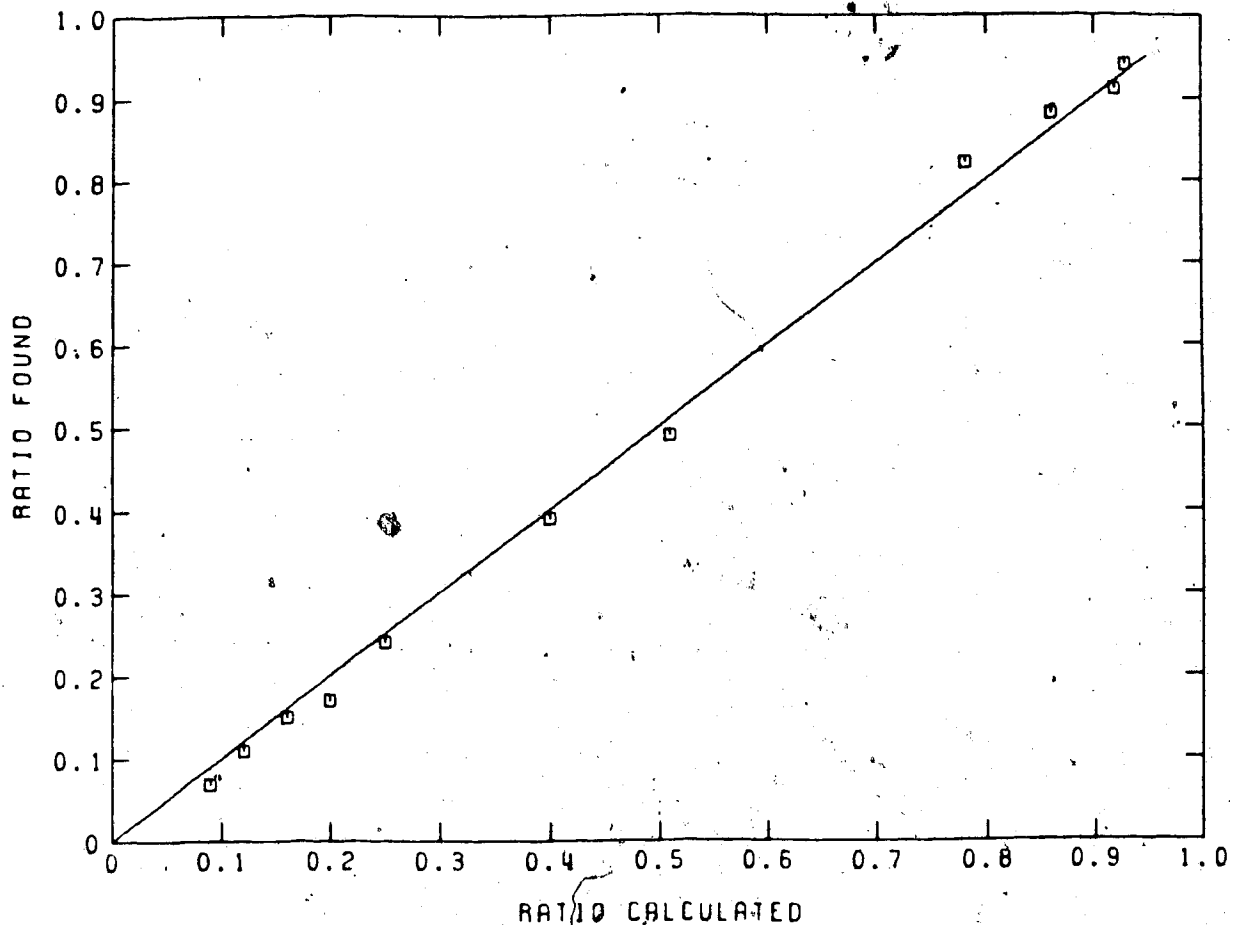


Figure 7. Calibration curve for synthetic mixtures of PSH and PSSP in 1 M KCl/0.003 M EDTA solution at 200 MHz and 25°C. The ratio $[PSSP]/([PSH] + [PSSP])$ found by NMR is plotted versus the ratio calculated from the amounts added.

were adjusted in order to minimize this uncertainty.

When a series of spectra were measured with the same spectrometer settings and conditions, e.g. in time course studies, the fractional concentrations were determined from peak heights rather than areas. The procedure used involved first calculating a factor which relates peak height to fractional concentration; this factor was then used to calculate fractional concentrations from peak heights. The method used will be illustrated with the spectrum in Figure 6. In the first step, the data in Figure 6 is used to calculate the height resonance X would have for these experimental conditions if all the penicillamine in the solution were PSSP, H_{100} :

$$H_{100} = H_x \frac{(I_x + I_y)}{I_x} \quad (38)$$

In analyzing data from a time course study, H_{100} is calculated from several spectra taken near the end of the time course run. Then, the fractional concentration of PSSP in the other spectra taken with these same measurement conditions is calculated with Equation 39:

$$f(\text{PSSP}) = \frac{H_x}{H_{100}} \quad (39)$$

F. Ionic Strength Correction

The literature values for acid dissociation constants of compounds studied in this research were generally obtained under conditions different from those used here. The literature values were usually obtained by pH titration experiments at 25°C but at a variety of different ionic strengths. Literature values were converted to the ionic strength used in this work ($I = 1$ M) so that comparisons could be made with acid dissociation constants determined in Chapter III. Also, literature values are needed for the evaluation of some of the thiol/disulfide exchange kinetic data.

The ionic strength dependence of the acid dissociation constants can be accounted for by using activity coefficients calculated with the Davies equation [72-74]:

$$-\log \gamma_i = \frac{A z^2 I^{1/2}}{1 + I^{1/2}} - 0.1 z^2 I \quad (40)$$

where $A = 0.5115$ (l/mole)^{1/2} and γ_i is the activity coefficient for a species of charge Z .

Generally, acid dissociation constants in the literature are mixed concentration-activity acid dissociation constants. For example, the mixed constant

for the acid-base equilibrium:



is given by

$$K_A = \frac{a_{\text{H}} [\text{A}]}{[\text{HA}]} \quad (42)$$

where a_{H} is calculated from the pH meter reading. The thermodynamic acid dissociation constant, K_A^{T} , which is independent of the ionic strength of the solution, is given by

$$K_A^{\text{T}} = \frac{a_{\text{H}} a_{\text{A}}}{a_{\text{HA}}} \quad (43)$$

In terms of concentrations, K_A^{T} is given by

$$K_A^{\text{T}} = \frac{\gamma_{\text{A}} [\text{A}] a_{\text{H}}}{\gamma_{\text{HA}} [\text{HA}]} \quad (44)$$

where γ_{A} and γ_{HA} are activity coefficients. Substituting Equation 42 into Equation 44, Equation 45 is obtained.

$$K_A^{\text{T}} = \frac{\gamma_{\text{A}}}{\gamma_{\text{HA}}} K_A \quad (45)$$

From Equation 45, the relationship between the literature

K_A values, $K_A(\text{lit})$, and K_A at $I = 1 \text{ M}$ is given by Equation 46.

$$K_A = \frac{\gamma_A(\text{lit}) \gamma_{HA}}{\gamma_{HA}(\text{lit}) \gamma_A} K_A(\text{lit}) \quad (46)$$

γ_{HA} and γ_A are the activity coefficients at $I = 1 \text{ M}$ as calculated from Equation 40 and $\gamma_A(\text{lit})$ and $\gamma_{HA}(\text{lit})$ are the activity coefficients for the literature ionic strength.

Even though "the proper method of calculating the activity coefficient of hybrid ions is still not completely clear" [75], such expressions containing two empirical constants are satisfactory for a 1:1 electrolyte up to an ionic strength of $I = 1 \text{ M}$ [60].

G. Non-Linear Least Squares Program

The values of several constants were obtained by fitting experimental data to a model using the non-linear least squares program KINET [70]. These constants include acid dissociation constants, chemical shifts of various species not observed directly, and rate and equilibrium constants. The variables in the experimental data included pH, chemical shift and time. The estimates of the unknown parameters, which are required by KINET, were

obtained by inspection of the experimental data. Values obtained for constants by KINET are usually reported with a linear standard deviation which indicates the quality of the fit.

H. Chemical Shift Titration Experiments

To illustrate how chemical shift titration data, i.e. the variation in chemical shift with pH, were obtained, a detailed description of the procedure used for PSH will be given here. These data were used in Chapter III for the calculation of the macroscopic acid dissociation constants of PSH. Chemical shift titration data for other molecules were obtained by similar procedures.

A 100 milliliter solution containing 0.010 M PSH, 0.002 M TBA, 1 M KCl and 0.003 M EDTA was prepared in deionized doubly distilled water. Argon gas was then bubbled through the solution for ~8 minutes. A 50 milliliter portion was taken for the preparation of samples covering the pH range 0.5-4. The pH was adjusted by adding small amounts of concentrated HCl or NaOH as necessary. The HCl or NaOH was added on a platinum wire so that very small amounts could be added to cause small changes in pH. One minute after the addition of base or acid, a pH reading was taken. The solution was diluted by

<10% by the total amount of HCl and NaOH added. At selected pH values, 0.5 milliliter aliquots were transferred to 5 mm NMR tubes. In this particular example, 18 samples were taken to define the pH region 0.5 to 4. At the end of the titration, the solution was discarded and the pH meter calibration checked.

The second 50 milliliter portion of the PSH solution was titrated from pH 4 to 12 by the same procedure. Forty NMR samples were taken over this pH region. The 58 NMR tubes were kept at 4°C until they were used.

Proton NMR measurements were made on the Bruker WH-200 without a field/frequency lock as described earlier. To obtain good signal-to-noise, 50 scans were averaged for each spectrum. The samples were run at the ambient probe temperature of 24°C. A sweep width of 1500 Hz was used. The FID was collected in 16K data points, which results in a digital resolution of 0.18 Hz/point in the frequency domain spectrum obtained by Fourier transformation. The repetition time was 5.4 seconds. The water resonance was suppressed by gating on the decoupler at the water resonance frequency for 2 seconds, as described in section E. The chemical shifts of the two methyl resonances of PSH were measured with respect to TBA. The uncertainty in the chemical shift was 0.001 ppm or 0.2 Hz.


I. Kinetic Studies

Two methods were used to obtain time course kinetic data for the thiol/disulfide exchange reactions. In the first method, the time course was followed in situ by measuring NMR spectra as a function of time with the sample continuously in the spectrometer. In the second method, aliquots were removed from the reaction mixture as a function of time, the reaction was quenched, and then NMR spectra were measured for all the aliquots taken once the reaction was over. One representative experiment of each type will be described.

The reaction mixtures, which consisted of a thiol and a disulfide as initial reactants, were usually prepared from 0.1 M stock solutions of the thiol and disulfide. Typically, 1-2 milliliters of each stock solution were used. The aliquots of the stock solutions were brought to the desired volume with 1 M aqueous KCl/0.003 M EDTA solution. Then the pH of each solution was adjusted to the appropriate value. If a long delay was necessary before the start of the kinetic experiment, these two freshly prepared solutions were frozen solid by placing them momentarily in contact with dry ice and then they were stored at -2°C . Prior to the beginning of the time course study, these samples were thawed and equilibrated.

to 25°C or room temperature. At time = 0, the two reactants were quickly mixed together. In those studies by method one, a 0.5 milliliter aliquot was transferred to a 5 mm NMR tube which had been previously flushed with argon gas. The NMR tube was put in the spectrometer and equilibrated to the probe temperature for ~3 minutes. During that time, the frequency of the decoupler was set to the water resonance frequency. Then time course data were obtained by running the spectrometer in an automated mode. Spectra were obtained at preselected times, with successive spectra stored on disk for processing later. Approximately ten spectra were generally collected at times appropriate to cover the complete time course. The spectra were then analyzed to obtain areas and thus fractional concentrations by one of the techniques described earlier.

The pH of the solution was taken, at some later time, from the remaining solution which was stored in the freezer until pH measurement.

In those studies by method two, 0.5 milliliter aliquots were withdrawn from the reaction vessel, placed in a 1-dram vial, and then ed in ~2 seconds by lowering the pH with a few drops of concentrated HCl or 0.1-0.5 milliliter concentrated phosphoric acid. The resulting 0.6 to 1 milliliter solution had a final pH

value of 0.5-2. At the start of the reaction, aliquots were taken every 20 seconds or so, and then the time interval was increased to minutes, etc. After quenching, the sample was transferred to an NMR tube and stored at 4°C until measurement of the spectrum.

The rate of thiol/disulfide exchange is pH dependent. To bring the rate for the various reactions to time scales at which they could be measured, different concentrations were used in different pH regions. For reactions carried out in the pH range 4-5, reactants in the concentration range 0.010-0.024 M were used. At pH 4, ~8 days were needed for the system to reach equilibrium whereas at pH 5, most of the data were collected overnight. If the system had not yet come to equilibrium, the sample was left in a water bath at 25°C and data collected again the next day or later in order to complete the time course curve. In this pH range, both thiol/disulfide exchange and air oxidation reactions were slow.

At pH values greater than 6, the rates were faster and thus smaller concentrations were used. However, the minimum concentrations which could be used were dictated by the sensitivity of the NMR spectrometer. Concentrations of 0.001 to 0.002 M were needed to obtain spectra with reasonable signal-to-noise and in a

sufficiently short time that enough successive spectra could be collected by method one to define the kinetic curve.

To illustrate method one, an experiment in which kinetic data for the reaction of PSH with GSSG were obtained will be described. The pH of the reaction mixture was 6.97, and the reactants were both present at a concentration of 0.002 M. Equilibrium was reached in ~80 minutes. During that interval, 12 spectra were collected, each resulting from the averaging of 18 scans. An acquisition time of 1.6 seconds was used, and an additional delay of 6 seconds was used between scans to ensure complete spin-lattice relaxation. The total time for acquisition of each spectrum was 137 seconds ($t_{1/2}$, the midpoint is 68.5 sec). This is ~3% of the time required for the reaction to reach the equilibrium position. A larger collection time would result in the data not accurately representing the fractional concentration at a given point of the kinetic curve. Each kinetic point on the time course curve represents the time elapsed since the mixing of the initial reactants plus the value of $t_{1/2}$. The S/N of the first kinetic point, for the reactant PSH is 50 and decreases to 20 at equilibrium. Correspondingly, the S/N for the product PSSG increases continuously to a final value of 50. The S/N ratio used

is defined by Equation 47 [76].

$$S/N = \frac{S \times 2.5}{X_{pp}} \quad (47)$$

S and X_{pp} are the signal intensity and peak to peak intensity of the noise in the baseline, respectively.

For each spectrum, the area was determined using methods described in Section E, and then the fractional concentrations of PSH and PSSG were calculated. These values, together with the times at which the spectra were measured, were fitted using KINET to an equation for a second order reaction to obtain the rate constant for the reaction.

The measurement of reaction rates at high pH by method one was accompanied by air oxidation of PSH. As will be seen later, PSH oxidizes readily at these pH values. For example, at pH 7, some 5% of the total area after 30 minutes will be due to oxidized PSH for a solution containing originally 0.002 M PSH. In order to minimize air oxidation in the high pH studies, method two was used. To illustrate, at pH 8.45 and with both reactants present at a concentration of 0.002 M, equilibrium was reached in ~10 minutes. At these low concentrations, ~20 minutes of signal averaging was needed

to obtain a spectrum with an adequate S/N ratio.

The solution pH was monitored in the time course studies because the rate depends on pH. For reaction mixtures of 0.001-0.003 M in initial reactant concentrations for PSH and GSSG, the pH was observed to decrease by ~0.02 unit during the complete course. This change is so small that it will have a negligible effect on the rate constants calculated from the time course data.

J. Equilibrium Studies

Because of the autoxidation of thiols, it was necessary in the equilibrium studies to degas samples which took a long time to come to equilibrium. Two methods of degassing the sample were used: degassing under vacuum and bubbling inert gas through the sample.

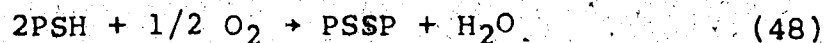
The bubbling technique consisted of passing nitrogen or argon gas via a Pasteur pipet or microsintered tube through the entire volume of the sample. Then during sample preparation, e.g. adjustment of pH, the delivery tube was removed from the solution and placed a few centimeters above the solution surface to produce a continuous blanket of inert gas over the solution. NMR tubes were also flushed with the gas before they were used.

However, this approach could not be used to study systems which required more than a few hours to come to equilibrium due to oxidation by residual air. To study systems which required longer periods of time to come to equilibrium, e.g. days, the sample was degassed on a vacuum line.

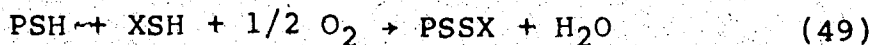
The vacuum line consisted of a trap containing liquid nitrogen or a dry ice-glycol slurry, a Pirani gauge and a series of valves connecting the vacuum portion of the line to a rotary pump. For connection to the vacuum line, a male ground glass joint was attached to the top of the NMR tube. When attaching the ground glass joint to the NMR tube, a slight constriction was made near the top of the NMR tube for easy sealing of the tube. The degassing procedure was as follows. A freeze-pump-thaw cycle was begun by solidifying the sample in the NMR tube and then opening the proper valve to the sample in the NMR tube when the pressure had decreased to 0.05-0.1 mm Hg. After a few minutes, the valve was closed and the sample allowed to reach room temperature. The cycle was repeated at least 3 times. The NMR tube was then sealed at the constriction by heating with a gas torch.

K. Air Oxidation of Penicillamine in Aqueous Solution

Thiols are easily oxidized to the disulfide form in the presence of air [3,4,17,77-83]. Penicillamine samples which were degassed showed little or no sign of oxidation confirming that the reactions that take place in the presence of air probably involve oxygen:



or, in the presence of two thiols



Since oxidation by either of these reactions would lead to errors in the equilibrium and kinetic constants determined in this thesis, the oxidation of PSH by oxygen was studied. This involved measuring time courses for the oxidation of PSH as a function of pH and initial reactant and product concentrations. The time course data were obtained by NMR. Oxidation reactions involving two thiols as in Equation 49, were not studied but the formation of PSSX was observed in some experiments described later in this thesis.

1. Rate of Oxidation of PSH versus pH

^1H NMR spectra measured as a function of time for a 0.03 M solution of PSH at pH 8.07 are shown in Figure 8. These spectra show the methyl region. As described previously, the two methyl groups of PSH give two separate resonances in this region, as do the two methyl groups of PSSP. The spectrum at the bottom of the figure indicates that little oxidation takes place during the first 5 hours. The two smaller resonances at 1.44 and 1.54 ppm increase with time and were assigned to the reaction product, PSSP. These chemical shifts are similar to those measured separately for a solution of PSSP. The reaction was followed for 192 hours. The extent of reaction was calculated from the relative areas of the PSH and PSSP resonances. A plot of fraction reacted versus time indicates that the reaction will be complete in ~200 hours.

A detailed study of the pH dependence of the oxidation of PSH by air was carried out. Ten milliliter portions of 0.0042 M PSH were placed in 15 milliliter vials (hypo-vial from Pierce, Chemical Company). The pH of the solutions were then adjusted to selected values in the range 4-10. The vials were loosely stoppered with a septum; however, the metal seal was not crimped. The vials were then stored at 25°C.

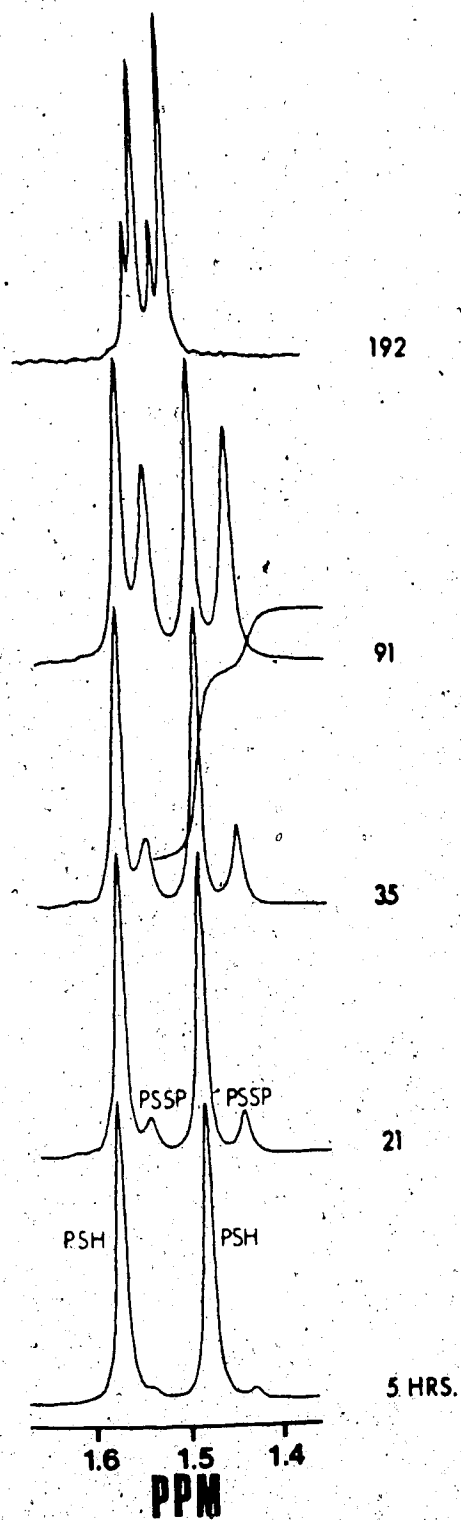


Figure 8. ¹H NMR spectra versus time for the oxidation of 0.03 M PSH in aqueous 1 M KCl/0.002 M EDTA solution at pH 8.07 and 25°C. The time course of the reaction was followed by quenching aliquots as a function of time. Spectra are not plotted with the same vertical and horizontal scales. The chemical shifts shown are approximate only for the first four spectra and with respect to DSS.

Time course data were collected over a period of 2 to 6 days by quenching 0.5 milliliter aliquots of reaction mixture and then measuring the NMR spectrum for the aliquot. The results are summarized in Figure 9. The linearity of the plots is characteristic of zero order reactions, i.e. reactions in which the rates are independent of both PSH and PSSP concentrations. The change in the oxidation rate at pH 10.24, indicated by the dotted line in Figure 9, is probably due to a sudden agitation of the reaction vessel during the sampling step at 60 hours which increases O_2 concentration in solution and therefore the rate of oxidation. After a while, the O_2 concentration returns to the same level as before and consequently to the same oxidation rate.

The initial rates of oxidation, defined by Equation 50

$$-\text{rate initial} = \frac{\Delta [\text{PSH}]}{\Delta \text{time}} \quad (50)$$

were calculated from the slopes of the concentration versus time plots of Figure 9 at $t = 0$. Figure 10 shows the initial rates plotted as a function of pH. At pH 4, the rate of oxidation is slow. As the pH is increased, the rate of oxidation increases, reaching a maximum rate

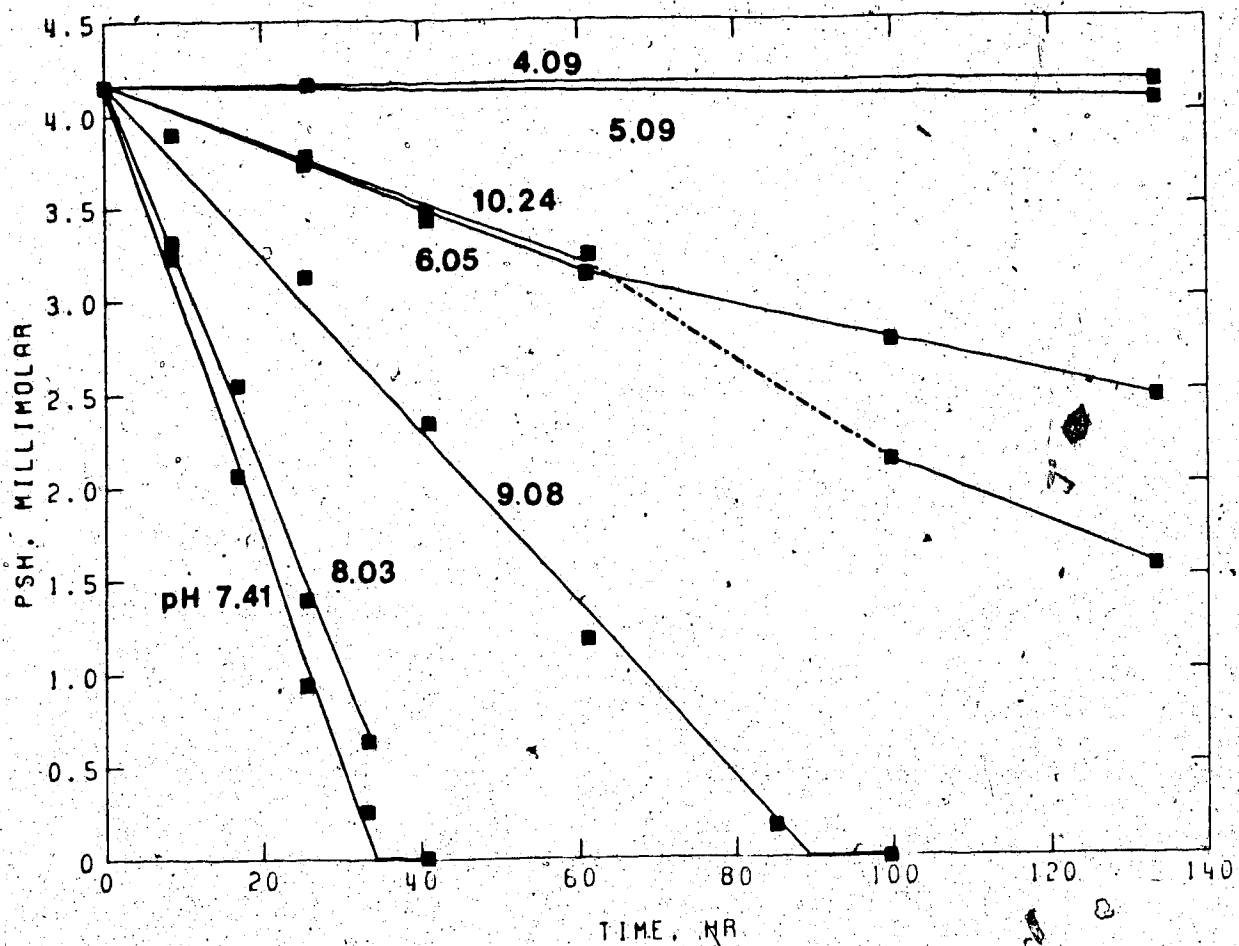


Figure 9. Plot of PSH concentration (millimolar) versus time and as a function of pH for 0.0042 M PSH solutions exposed to atmospheric oxygen.

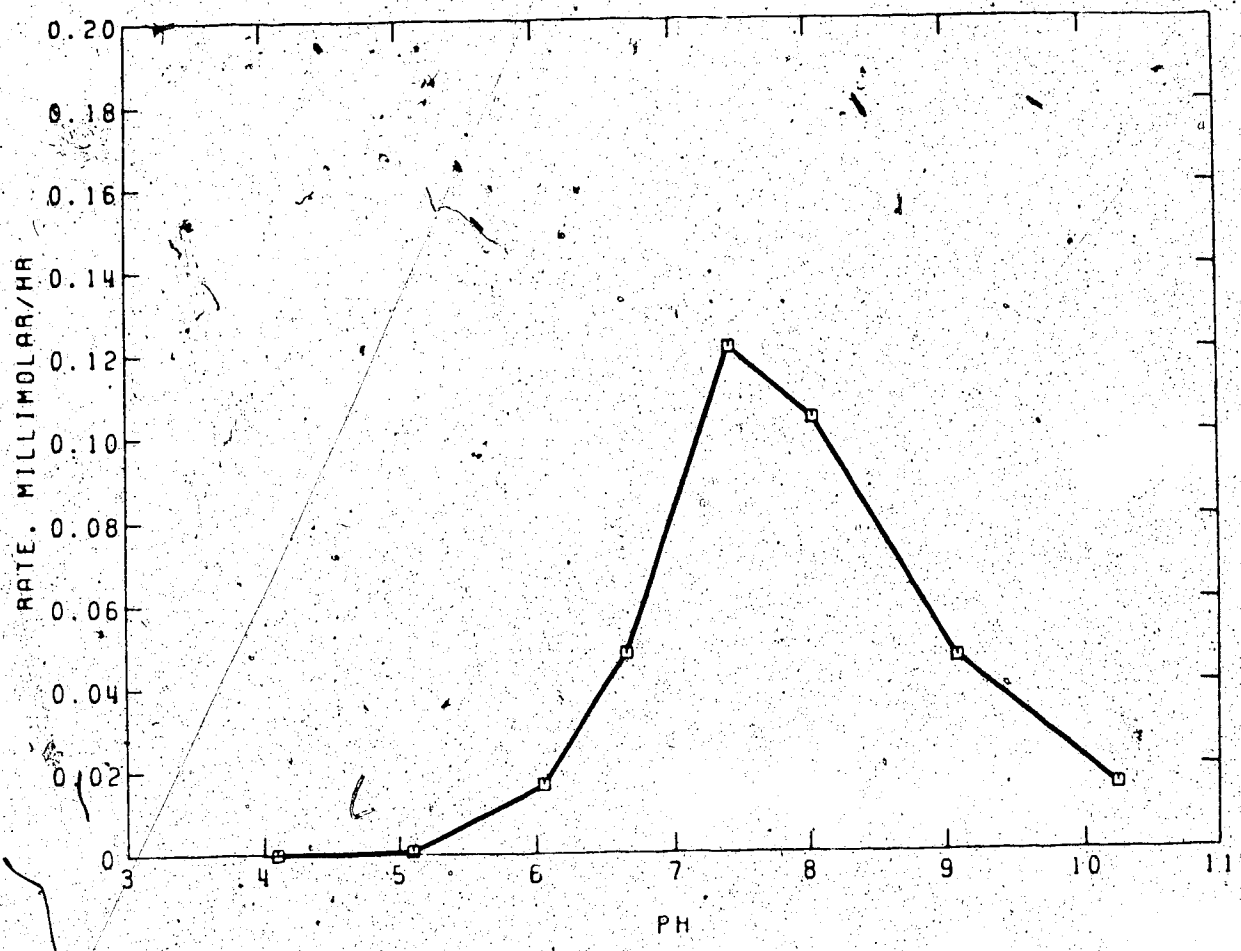


Figure 10. Plot of initial rates for the various time course curves in Figure 9 (in units of millimolar per hour) versus pH showing the effect of pH on the initial rate.

somewhere around pH 7.5. At higher pH, the rate decreases again.

The pH-rate profile shown in Figure 10 is similar to that observed for the oxidation of GSH to GSSG [79] and cysteine to cystine [81]. Since this type of pH rate profile is not observed for mercaptoacetic acid [79] and, since it was observed in this research that captopril and mercaptosuccinic acid undergo little oxidation, it would seem that this type of dependence of the rate of thiol oxidation on pH cannot be a characteristic property of the thiol group alone but rather, it must depend in some way upon the acid-base characteristics of the amino group as well [79].

Plots of PSH concentration versus time for solutions in the pH range 6-7 were found to be characterized by regions having two distinct rates of reaction, as shown in Figure 11. The time at which the transition from the initial rate to the final rate occurred decreases as the pH is increased from 6 to 7. At pH 7-9, no transition is observed, apparently because the PSH is oxidized completely before the transition could occur. In any case, this change, if present at $\text{pH} > 9$ or $\text{pH} < 6$, is difficult to detect because the reactions are so slow that measuring time becomes so long as to be impractical. At these long times, it was difficult to obtain reproducible results.

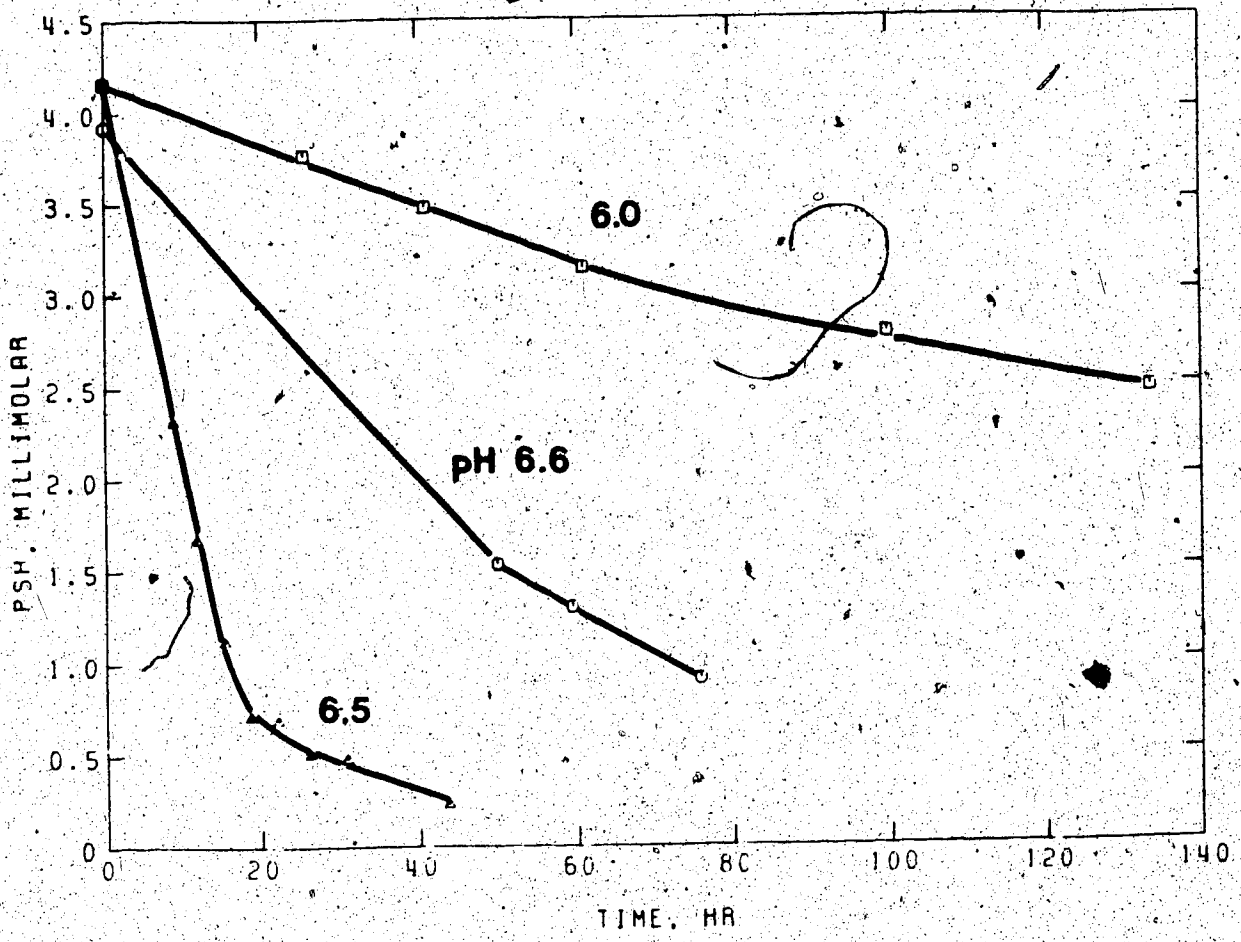


Figure 11. Plots of PSH concentrations versus time showing the two distinct rates of reaction at pH > 6. Conditions are the same as those in Figure 8.

The two distinct rates of reaction observed above for PSH seem to indicate the titration of some catalyst by the product PSSP. When no free catalyst remains, a second oxidation pathway which occurs at a much slower rate, takes over. This type of behaviour has been observed for other thiols [82,83] and depends on the initial concentration of thiol used and its relative concentration with respect to O_2 concentration in solution [82].

2. Rate of PSH Oxidation versus Initial PSH and PSSP Concentrations

Further studies were carried out to verify that the oxidation of PSH is zero order with respect to PSH and PSSP concentrations. A wide range of concentrations, typical of those used in the research described later in this thesis, were studied.

The time courses obtained for three solutions containing PSH at concentrations of 0.0039, 0.0076 and 0.012 M are presented in Figure 12. The initial rates of oxidation are 0.10, 0.071 and 0.099 millimolar per hour, respectively, i.e. within experimental error they are independent of the initial PSH concentrations. In another series of experiments, the rate of oxidation of 0.0039 M PSH was measured as a function of the concentration of PSSP added to the solution. The results presented in Figure 13 show that the rate of oxidation of PSH is

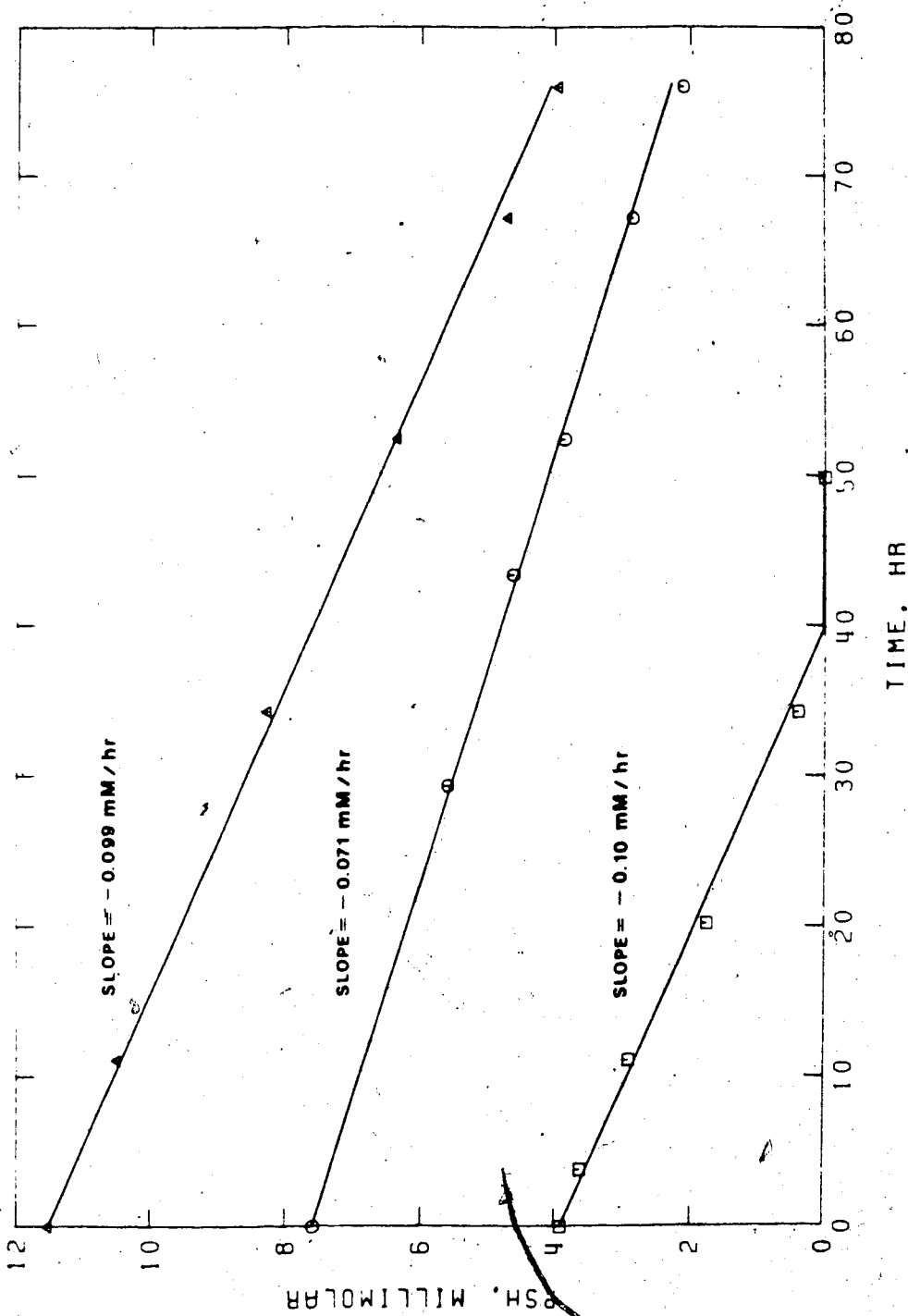


Figure 12. Plots of PSH concentration versus time for three PSH solutions with different initial concentrations at pH 7.5.

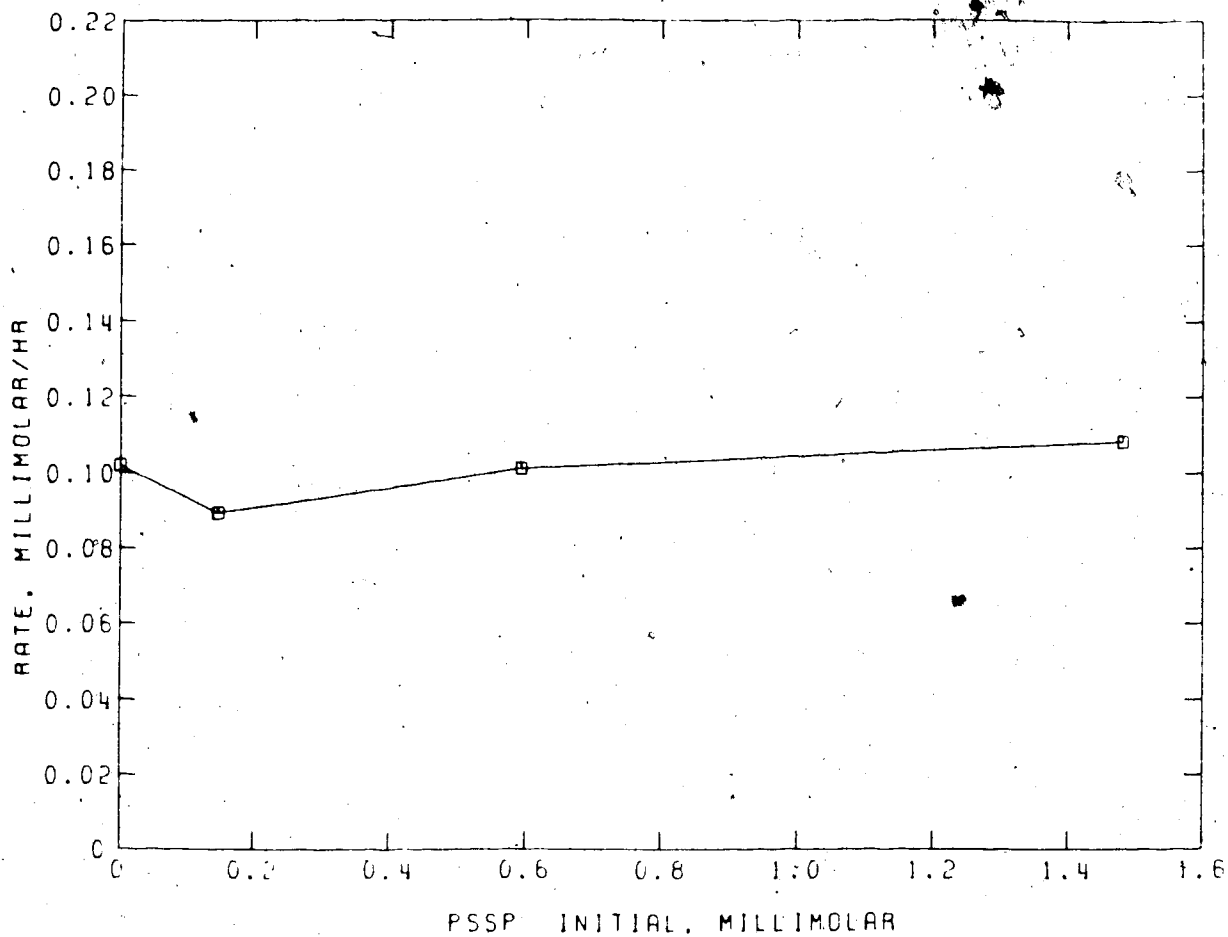


Figure 13. Plots of the initial oxidation rate (in units of millimolar per hour) for 0.0039 M PSH between pH 7.4-7.8 and 25°C, versus initial PSSP concentrations. The rate of air oxidation of PSH is independent of PSSP concentrations.

independent of PSSP concentration.

Examination of oxidation reaction curves reveals that the kinetic behaviour of the PSH oxidation is not subject to the initial PSH or PSSP concentrations under the present experimental conditions used. The oxidation of PSH via Equation 49 was not measured but evidence presented later in the thesis shows that these are faster than those of Equation 48 probably because of less overall steric hindrance.

As mentioned earlier, reactions that were slow were studied under reduced pressure and in sealed NMR tubes. In order to test the efficiency of the freeze-pump-thaw cycle in removing oxygen from the sample, a 0.06 M PSH solution at pH 8 (near the maximum rate of oxidation in Figure 10) was prepared accordingly and sealed in a 5 mm NMR tube as described earlier. After 10 days, no sign of PSSP was detected in the ^1H NMR spectrum. However, the ^1H NMR spectrum shows that ~3% of PSH had been oxidized after 33 days probably by the very small amount of residual air.

CHAPTER III

ACID/BASE CHEMISTRY OF SELECTED THIOLS AND DISULFIDES IN AQUEOUS SOLUTION

A. Introduction

In Chapters IV and V, the kinetics and equilibria of thiol/disulfide exchange reactions involving penicillamine with oxidized glutathione and penicillamine with cystine are investigated. Both systems are studied over a wide range of pH values. Complete analysis of the data requires a prior knowledge of the acid dissociation constants of the thiols and disulfides (Figure 14) including the penicillamine-glutathione and penicillamine-cystine mixed disulfides 3 and 8 in Figure 14. Literature values are available for the acid dissociation constants of the thiols and symmetrical disulfides, but not for the mixed-disulfides. In this chapter, their acid dissociation constants are determined by ^1H and ^{13}C NMR spectroscopy.

The NMR method for determining acid dissociation constants is ideally suited to the present work because it does not require a pure sample of the acid. Rather, the fractional titration of acidic groups, from which acid

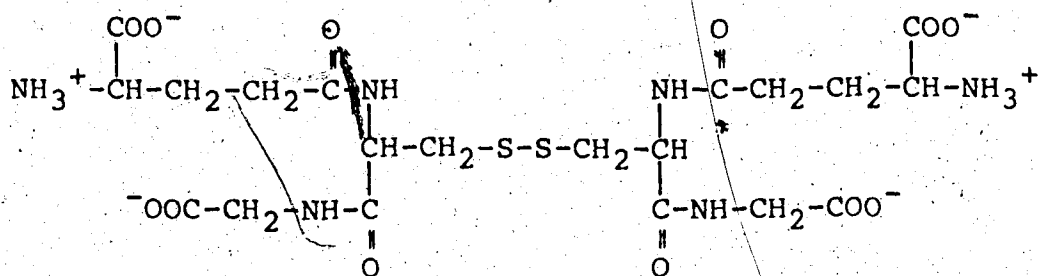
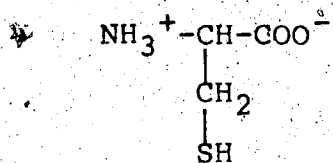
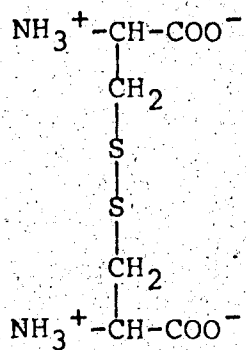
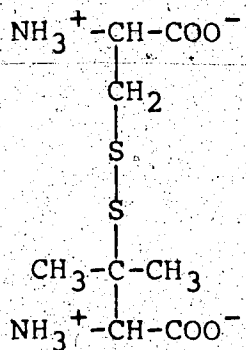
5. Oxidized Glutathione (GSSG)6. Cysteine (CSH)7. Cystine (CSSC)8. Penicillamine-Cysteine Mixed Disulfide (PSSC)

Figure 14. (Continued)

dissociation constants can be calculated, can be determined directly from NMR chemical shifts. Thus, with the NMR method, it is not necessary to prepare a pure sample of the mixed disulfide. The procedure used in this work involved reacting penicillamine with oxidized glutathione and with cystine to form an equilibrium mixture containing the desired mixed disulfide as well as the thiols and the symmetrical disulfides. Chemical shift data were obtained for the mixture as a function of pH. With the high resolution of the spectrometer used in this work, it was possible to resolve resonances not only for the mixed disulfide, but also for the thiols and symmetrical disulfides, making it possible to determine simultaneously the acid dissociation constants for all the thiols and disulfides in the equilibrium mixture.

Also, in this chapter, the pH dependence of the (chemical shifts of the ^1H resonances of imidazole are characterized for the purpose of using imidazole as an internal pH indicator in the thiol/disulfide exchange studies.

B. Determination of Acid Dissociation Constants by NMR

In general, proton transfer reactions are fast on the NMR time scale so that, as the acidic groups of a molecule

are titrated, the observed chemical shifts are the population weighted averages of those with the groups in their protonated and deprotonated forms. The method used to extract acid dissociation constants from the chemical shift data depends on whether the acid is monoprotic or polyprotic and, in the latter case, on whether the chemical shifts are affected by the protonation state of a single acidic group or by several groups. In the first situation, the resonance will be referred to as a unique resonance and, in the second case, as a common resonance.

1. Monoprotic Acids

For a monoprotic acid, HA, the observed chemical shift, δ_{obsd} , for a resonance from nuclei located near enough to the acidic group to be affected by its state of protonation is the population weighted average of its chemical shifts [84] when the molecule is protonated, δ_{HA} , and deprotonated, δ_{A} .

$$\delta_{\text{obsd}} = \alpha_{\text{HA}} \delta_{\text{HA}} + \alpha_{\text{A}} \delta_{\text{A}} \quad (51)$$

where α_{HA} and α_{A} are the fractional concentrations of the molecule in the protonated and deprotonated forms ($\alpha_{\text{HA}} + \alpha_{\text{A}} = 1$). In terms of the species present, α_{HA} and α_{A} are defined as

$$\alpha_{HA} = \frac{[HA]}{[HA] + [A]} \quad (52)$$

$$\alpha_A = \frac{[A]}{[HA] + [A]} \quad (53)$$

By appropriate substitution using the acid dissociation constant,

$$K_A = \frac{a_H [A]}{[HA]} \quad (54)$$

Equations 55 and 56 are obtained.



$$\alpha_{HA} = \frac{a_H}{a_H + K_A} \quad (55)$$

$$\alpha_A = \frac{K_A}{a_H + K_A} \quad (56)$$

where a_H represents the activity of hydrogen ion as determined directly from the pH meter reading (10-pH meter reading). In the above expressions and in those to come, the charge of the proton and of the various species has been omitted for brevity.

Substitution of these equations into Equation 51 yields:

$$\delta_{\text{obsd}} = \frac{a_{\text{H}} \delta_{\text{HA}} + K_{\text{A}} \delta_{\text{A}}}{a_{\text{H}} + K_{\text{A}}} \quad (57)$$

This equation expresses the observed chemical shift in terms of the experimental variable, pH and the three constants, δ_{HA} , δ_{A} and K_{A} . For many acids, δ_{HA} and δ_{A} can be obtained directly as the limiting chemical shifts at low and high pH, respectively, in which case K_{A} is the only unknown in Equation 57. K_{A} can be extracted from the chemical shift data with Equation 57 by several procedures; the procedure used in this thesis involves fitting the chemical shift data to Equation 57 by means of the non-linear least squares method. The non-linear least squares calculations were done with the computer program KINET, written by Dye and Nicely [70]. If δ_{HA} and/or δ_{A} cannot be determined directly from experimental data, e.g. due to overlap with another resonance, these can be treated as unknowns along with K_{A} in the non-linear least squares curve fitting.

2. Diprotic Acids

The procedure used to evaluate the acid dissociation constants for diprotic acids depends on whether the

spectrum contains only common resonances, i.e. resonances whose chemical shift depends on the state of protonation of both acidic groups or unique resonances for each acidic group, i.e. resonances whose chemical shift depends only on the state of protonation of one of the two acidic groups.

Before discussing the specific methods, the macroscopic and microscopic acid-base chemistry of diprotic acids will be considered. The discussion will consider only the case in which the two acidic groups are of similar acidity and thus are titrated over the same pH range [85]. At the macroscopic level, the acid dissociation is described by:

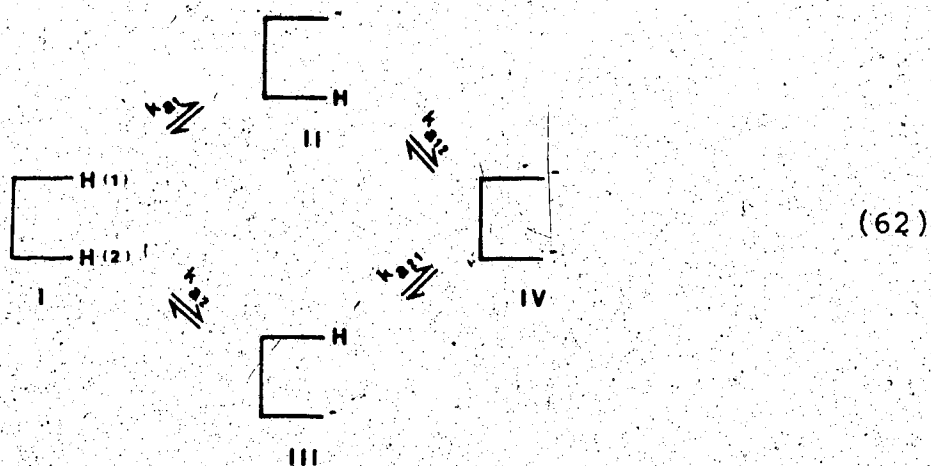


$$K_{\text{H}_2\text{A}} = \frac{a_{\text{H}}[\text{HA}]}{[\text{H}_2\text{A}]} \quad (59)$$



$$K_{\text{HA}} = \frac{a_{\text{H}}[\text{A}]}{[\text{HA}]} \quad (61)$$

At the molecular level, the proton in the monoprotated form, HA, will be distributed between the two acidic groups (II and III in Equation 62) depending on their relative acidities. The acid dissociation at the microscopic level is described by the following scheme:



where k_{a1} , k_{a2} , k_{a12} and k_{a21} are the microscopic acid dissociation constants. The last number of the subscript identifies the acidic group being deprotonated in that step; a preceding number identifies the group deprotonated in a previous step. These microscopic acid dissociation constants are defined by Equations 63-66.

$$k_{a1} = \frac{a_H[\text{II}]}{[\text{I}]} \quad (63)$$

$$k_{a2} = \frac{a_H[\text{III}]}{[\text{I}]} \quad (64)$$

$$k_{a12} = \frac{a_H[\text{IV}]}{[\text{II}]}, \quad (65)$$

$$k_{a21} = \frac{a_H[\text{IV}]}{[\text{III}]} \quad (66)$$

The macroscopic constants are related to the microscopic constants by:

$$K_{\text{H}_2\text{A}} = k_{a1} + k_{a2} \quad (67)$$

$$K_{\text{HA}} = \frac{k_{a12}k_{a21}}{k_{a12} + k_{a21}} \quad (68)$$

$$K_{\text{H}_2\text{A}} K_{\text{HA}} = k_{a1}k_{a12} = k_{a2}k_{a21} \quad (69)$$

a. Common Resonance Method [86]

The chemical shift observed for a common resonance, δ_{obsd} , is given by:

$$\delta_{\text{obsd}} = \alpha_{\text{H}_2\text{A}} \delta_{\text{H}_2\text{A}} + \alpha_{\text{HA}} \delta_{\text{HA}} + \alpha_{\text{A}} \delta_{\text{A}} \quad (70)$$

where α_{H_2A} , α_{HA} and α_A are the fractional concentrations and δ_{H_2A} , δ_{HA} and δ_A , the chemical shifts of the common resonance for the H_2A , HA and A forms ($\alpha_{H_2A} + \alpha_{HA} + \alpha_A = 1$). The fractional concentrations are defined as:

$$\alpha_{H_2A} = \frac{[H_2A]}{[H_2A] + [HA] + [A]} \quad (71)$$

$$\alpha_{HA} = \frac{[HA]}{[H_2A] + [HA] + [A]} \quad (72)$$

$$\alpha_A = \frac{[A]}{[H_2A] + [HA] + [A]} \quad (73)$$

Substitution of Equations 59 and 61 for K_{H_2A} and K_{HA} into Equations 71, 72 and 73 leads to

$$\alpha_{H_2A} = \frac{a_H^2}{a_H^2 + a_H K_{H_2A} + K_{H_2A} K_{HA}} \quad (74)$$

$$\alpha_{HA} = \frac{a_H K_{H_2A}}{a_H^2 + a_H K_{H_2A} + K_{H_2A} K_{HA}} \quad (75)$$

$$\alpha_A = \frac{K_{H_2A} K_{HA}}{a_H^2 + a_H K_{H_2A} + K_{H_2A} K_{HA}} \quad (76)$$

Substitution of Equations 74, 75 and 76 into Equation 70 yields

$$\delta_{\text{obsd}} = \frac{a_{\text{H}}^2 \delta_{\text{H}_2\text{A}} + a_{\text{H}} K_{\text{H}_2\text{A}} \delta_{\text{HA}} + K_{\text{H}_2\text{A}} K_{\text{HA}} \delta_{\text{A}}}{a_{\text{H}}^2 + a_{\text{H}} K_{\text{H}_2\text{A}} + K_{\text{H}_2\text{A}} K_{\text{HA}}} \quad (77)$$

Equation 77 expresses the observed chemical shift in terms of a_{H} , the experimental variable and the five constants, $\delta_{\text{H}_2\text{A}}$, δ_{HA} , δ_{A} , $K_{\text{H}_2\text{A}}$ and K_{HA} . $\delta_{\text{H}_2\text{A}}$ and δ_{A} can often be obtained directly as the limiting chemical shifts at low and high pH, respectively. However, δ_{HA} cannot generally be obtained directly because, if the two groups are of similar acidity, there is no pH at which HA is the only species present. $K_{\text{H}_2\text{A}}$, K_{HA} and δ_{HA} can be obtained simultaneously by fitting the common resonance chemical shift data to Equation 77 with the non-linear least squares program KINET.

b. Unique Resonance Method [86]

The procedure used to evaluate the macroscopic pK_{A} 's when there was a unique resonance for each acidic group involved determining the average number of protons per molecule, \bar{p} , from the chemical shift data and then fitting the \bar{p} vs pH data to obtain the pK_{A} 's. For a diprotic acid, \bar{p} is defined as:

$$\bar{p} = \frac{2[H_2A] + [HA]}{[H_2A] + [HA] + [A]} \quad (78)$$

Substitution of Equations 74 and 75 into Equation 78 yields:

$$\bar{p} = \frac{2a_H^2 + a_H K_{H_2A}}{a_H^2 + a_H K_{H_2A} + K_{H_2A} K_{HA}} \quad (79)$$

\bar{p} was obtained from the chemical shift data as follows.

Since each resonance is unique, its chemical shift is the weighted average of the chemical shifts when the particular acidic group is protonated and deprotonated. For example, the observed chemical shift for the unique resonance for acidic group 1, $\delta_{\text{obsd},1}$, is given by:

$$\delta_{\text{obsd},1} = f_{1,p} \delta_{1,p} + f_{1,d} \delta_{1,d} \quad (80)$$

where $f_{1,p}$ and $f_{1,d}$ are the fractional concentrations, and $\delta_{1,p}$ and $\delta_{1,d}$ the chemical shifts of the unique resonance when the acidic group 1 is protonated and deprotonated.

The fractional concentrations are given by:

$$f_{1,p} = \frac{[I] + [III]}{[I] + [II] + [III] + [IV]} \quad (81)$$

$$f_{1,d} = \frac{[\text{III}] + [\text{IV}]}{[\text{I}] + [\text{II}] + [\text{III}] + [\text{IV}]} \quad (82)$$

where the species are defined by Equation 62. For group 2, the fractional concentrations are given by:

$$f_{2,p} = \frac{[\text{I}] + [\text{II}]}{[\text{I}] + [\text{II}] + [\text{III}] + [\text{IV}]} \quad (83)$$

$$f_{2,d} = \frac{[\text{III}] + [\text{IV}]}{[\text{I}] + [\text{II}] + [\text{III}] + [\text{IV}]} \quad (84)$$

Substitution of the relationship $f_{1,p} + f_{1,d} = 1$ into Equation 80 leads to

$$f_{1,d} = \frac{\delta_{\text{obsd},1} - \delta_{1,p}}{\delta_{1,d} - \delta_{1,p}} \quad (85)$$

$\delta_{1,p}$ and $\delta_{1,d}$ are the limiting shifts at low and high pH, respectively. With Equation 85, the fractional deprotonation of group 1 can be calculated from the chemical shift data for unique resonance 1. The fractional deprotonation of group 2, $f_{2,d}$ can be calculated from the chemical shift data for the unique resonance for group 2 using a similar equation. \bar{p} is then calculated with Equation 86.

$$\bar{p} = 2 - f_{1,d} - f_{2,d} \quad (86)$$

The macroscopic constants K_{H_2A} and K_{HA} are obtained by fitting the \bar{p} vs pH data to Equation 79 using the non-linear least squares program KINET.

The procedure used to evaluate the microscopic acid dissociation constants k_{a1} , k_{a2} , k_{a12} and k_{a21} involves calculating the ratio of the concentrations of the species II and III (Equation 62). From Equations 63 to 66, this ratio is given by Equation 87.

$$\frac{[II]}{[III]} = \frac{k_{a1}}{k_{a2}} = \frac{k_{a21}}{k_{a12}} \quad (87)$$

From Equations 82 and 84, this ratio is also given by:

$$\frac{[II]}{[III]} = \frac{f_{1,d} - \alpha_A}{f_{2,d} - \alpha_A} \quad (88)$$

α_A is the fractional concentration of species IV (Equation 76). The microconstants can be determined from the average ratio, II/III calculated from the chemical shift data of the two unique resonances at several pH values, (Equation 88) and Equations 67, 68 and 87. For example, k_{a2} can be calculated using Equations 67 and 87:

$$k_{a2} = \frac{K_{H_2A}}{\left(1 + \frac{[III]}{[III]}\right)} \quad (89)$$

k_{a1} can be determined from the value of k_{a2} and Equation 67. Similarly k_{a12} and k_{a21} are evaluated from Equations 68 and 87.

C. Chemical Shift Data for the Penicillamine/Oxidized Glutathione System

A, B, D and E in Figure 15 are 1H NMR spectra of pH 7.0 solutions of PSH, GSSG, GSH and PSSP, respectively. Their structural formulae are shown in Figure 14. Spectrum C is for a solution prepared by mixing PSH and GSSG. The spectrum was obtained within a few hours after mixing. As will be shown in Chapter IV, PSH reacts with GSSG on this time scale to produce PSSG, however, the further reaction of PSH with PSSG to form PSSP is so slow that there is no detectable PSSP in the mixture. Each solution also contains t-butyl alcohol for an internal reference, and 0.003 M EDTA. Resonance assignments are given in Table 4.

The extra resonances in Figure 15C are assigned to those of PSSG, based on general stoichiometry of the thiol/disulfide reaction and on results from a reduction experiment with dithiothreitol (DTT). The proton time

Table 4. Assignment of the various resonances of Figure 15.

Molecule	Chemical Shift versus DSS, ppm	Group Assignment
TBA	1.2397	CH ₃
EDTA	3.24	CH ₂ -CH ₂
	3.63	CH ₂ -COOH
PSH	1.47	CH ₃
	1.57	CH ₃
	3.68	CH _α
GSSG	2.15	Glu-C _β
	2.54	Glu-C _γ
	2.9-3.3	Cys-C _β (AB) ^a
	3.79	Gly-C _α (AB)
	3.80	Glu-C _α
	~4.8	Cys-C _α (X) ^b
GSH	2.16	Glu-C _β
	2.55	Glu-C _γ
	2.96	Cys-C _β (AB) ^a
	3.78	Gly-C _α (AB)
	3.80	Glu-C _α
PSSP	~4.8	Cys-C _α (X) ^b
	1.43	CH ₃
	1.53	CH ₃
PSSG	3.70	CH _α
	1.39	CH ₃
	1.53	CH ₃
	2.15	Glu-C _β
	2.54	Glu-C _γ
	2.9-3.3	Cys-C _β (AB) ^a
	3.8	CH _α
	3.8	Gly-C _α (AB)
	3.8	Glu-C _α
~4.8	Cys-C _α (X) ^b	

^a AB part of an ABX pattern.

^b X part of an ABX pattern.

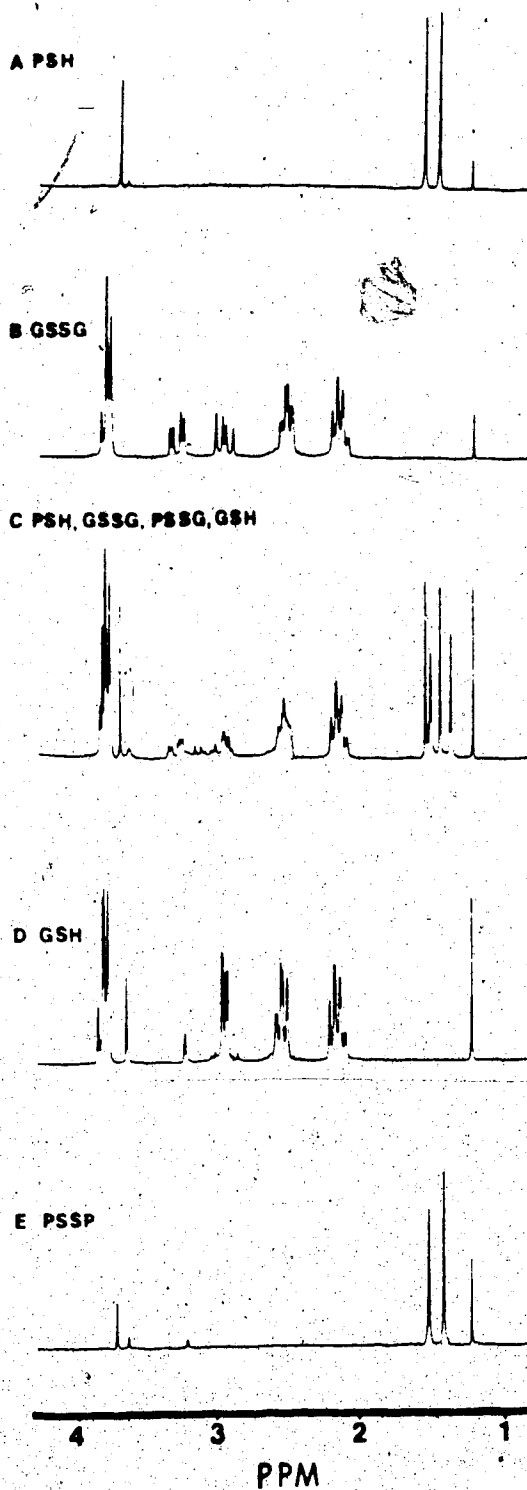


Figure 15. 200 MHz ^1H NMR spectra of A) 0.10 M PSH, B) 0.093 M GSSG, C) mixture prepared from 0.050 M PSH and 0.047 M GSSG, D) 0.050 M GSH and E) 0.020 M PSSP at the ambient NMR probe temperature of 26°C. Each solution was prepared in aqueous 1 M KCl solution containing 0.003 M EDTA and some t-butanol (TBA) for internal reference at pH 7.0.

course spectra show that these extra resonances decrease in intensity upon reacting with DTT and confirm the presence of a disulfide bond in PSSG. The ^1H nuclei of the two methyl groups of PSH, PSSG and PSSP give separate resonances because of the asymmetric center at the α -carbon [87]. As shown in spectra A and E, each α proton resonance is a singlet. However, because of the extensive overlap of resonances in the 2-4 ppm region in spectrum C, the methyl resonances were used to study the reaction of PSH with GSSG. Also, the methyl resonances are further from the strong water signal (~ 4.8 ppm) than the other resonances, making their detection easier at low concentration. In addition, they are three times as intense as the resonance for the methine proton of PSH, the only other ^1H resonance for PSH and PSSP, and for the PSH part of PSSG. Spectra for the methyl protons of PSH and PSSP are shown at several pH values in Figure 16 and 17, respectively. In Figure 18 are shown spectra for the methyl protons in a mixture containing originally PSH, PSSP and GSSG. This mixture produces PSSG. Assignments in Figure 18 were made by comparison with spectra in Figures 16 and 17. The extra methyl resonances in Figure 18 were assigned to those of PSSG. The chemical shifts of the two methyl resonances for PSH, PSSP and PSSG are plotted versus pH in Figure 19.

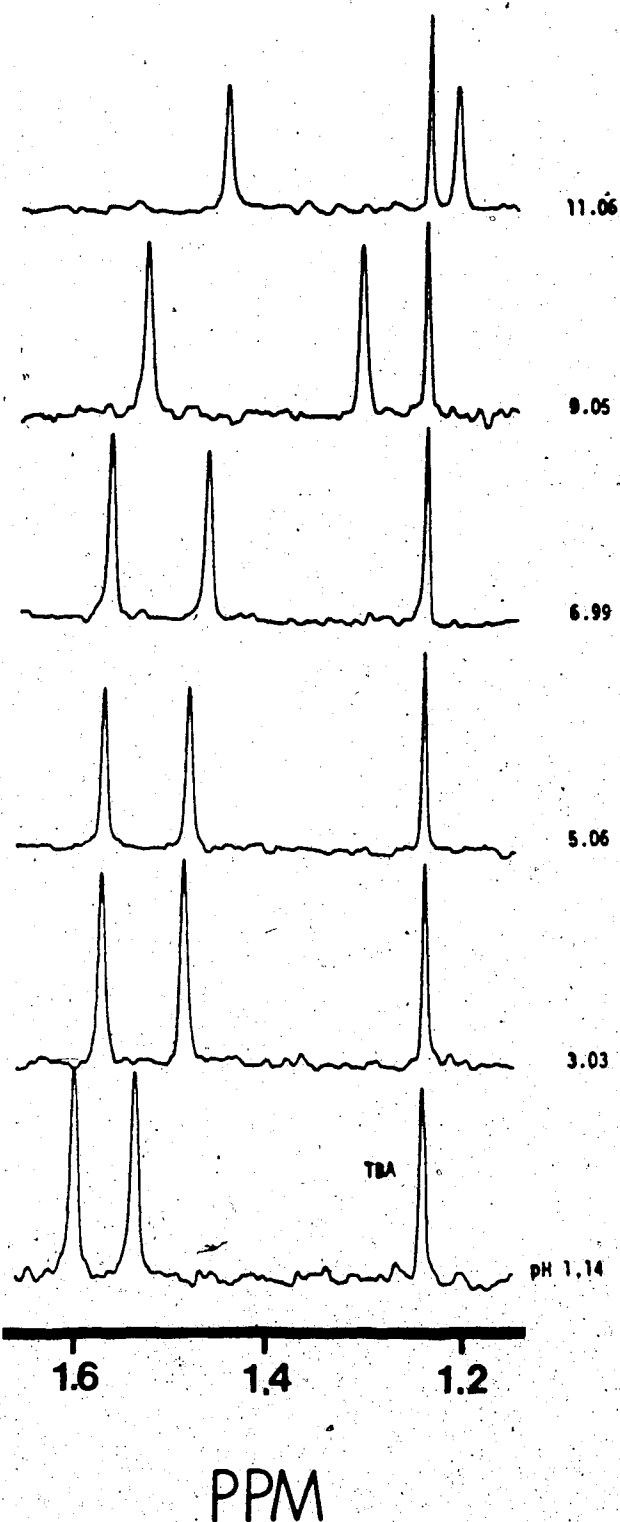


Figure 16. Methyl region of the 200 MHz ^1H NMR spectra of 0.010 M PSH in aqueous 1 M KCl solution containing 0.003 M EDTA and 0.003 M TBA as internal reference at 26°C.

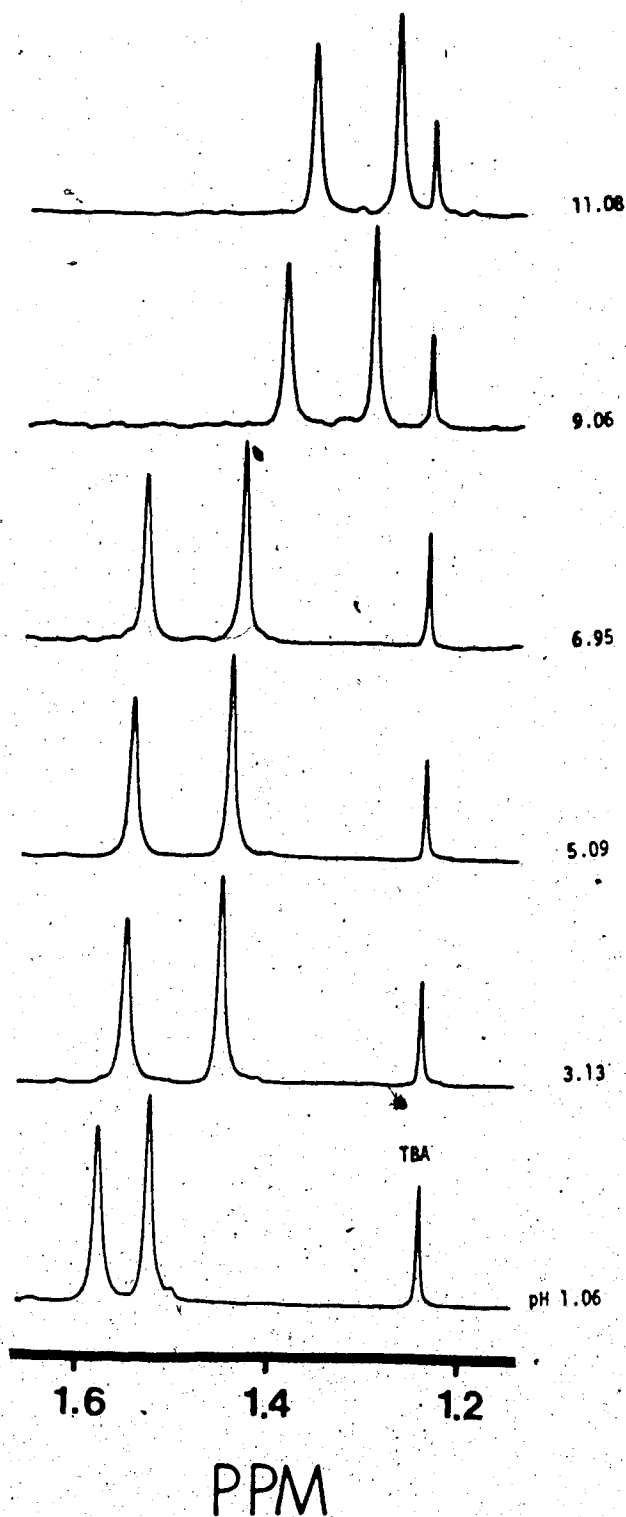


Figure 17. Methyl region of the 200 MHz ^1H NMR spectra of 0.020 M PSSP containing some TBA in aqueous 1 M KCl solution containing 0.003 M EDTA.

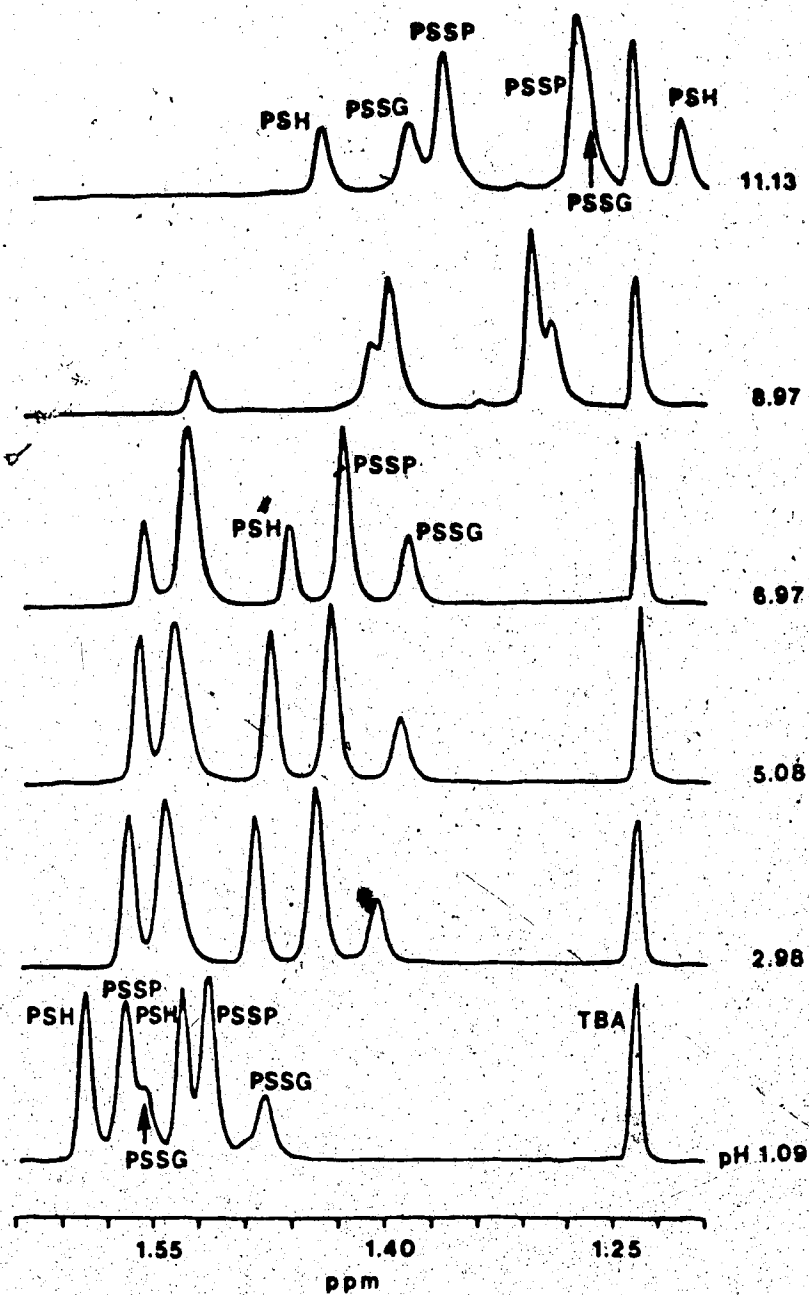


Figure 18. Methyl region of the 200 MHz ^1H NMR spectra of a mixture of PSH, PSSP and GSSG. The original concentrations were 0.02 M PSH, 0.01 M PSSP, 0.01 M GSSG and some TBA in aqueous 1 M KCl, 0.003 M EDTA solution.

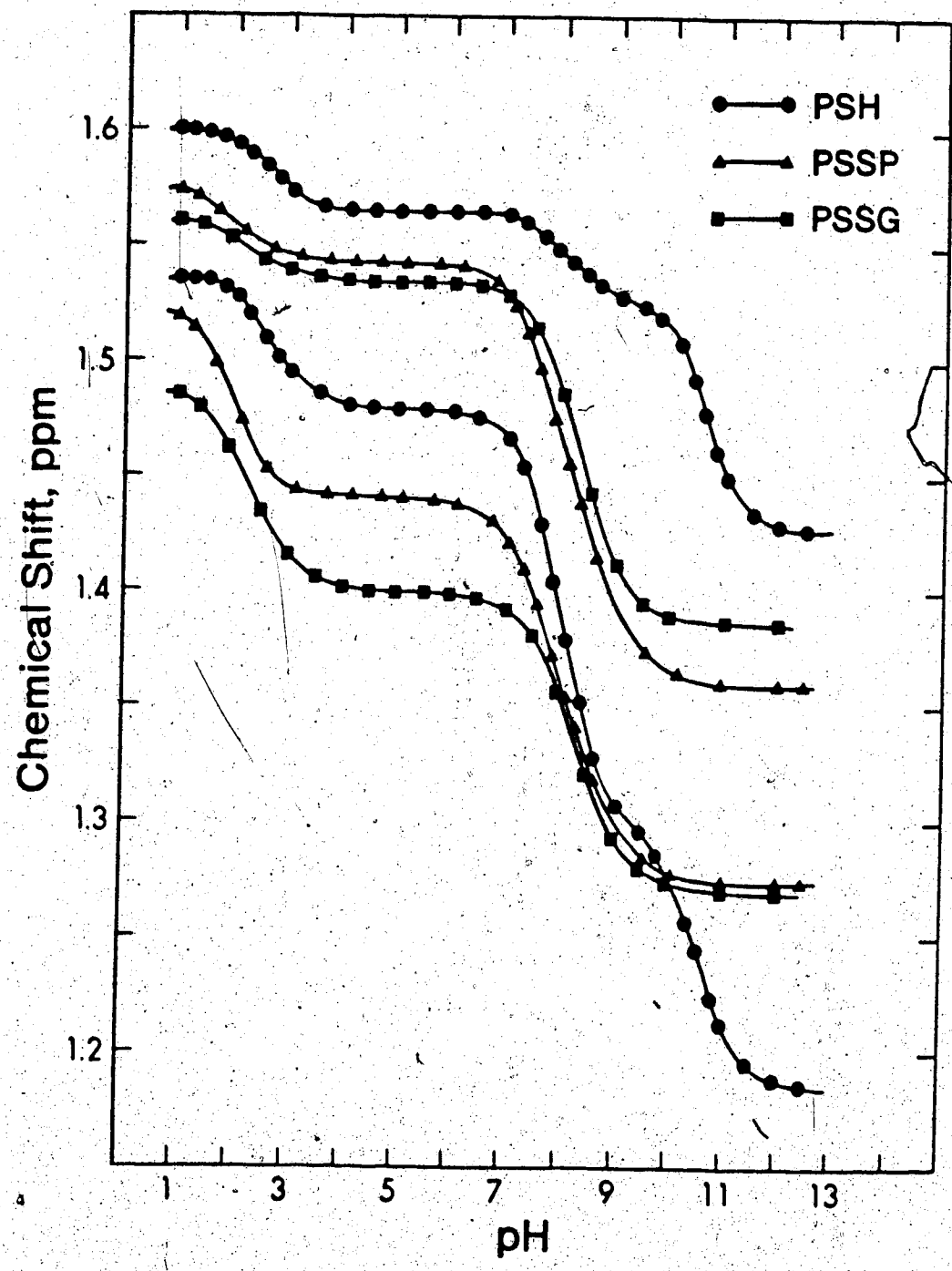


Figure 19. ¹H chemical shift data for the two methyl resonances (Figure 18) of PSH, PSSP and PSSG versus DSS in aqueous 1 M KCl, 0.003 M EDTA solution. The smooth curves through the chemical shift data of PSH are theoretical curves calculated with Equations 57 and 77 and the constants in Table 7.

A, B, D and E in Figure 20 are ^{13}C NMR spectra of pH 4 solutions of PSH, GSSG, GSH and PSSP, respectively. Spectrum C is for a solution prepared by mixing 0.20 M PSH and 0.078 M GSSG. The solution was bubbled with air after equilibrium was reached to oxidize PSH to PSSP and GSH to GSSG. Then more PSH was added and the procedure repeated. This resulted in a solution containing more PSSG than would be present if the total amounts of PSH (0.20 M) and GSSG added had been mixed directly. Also, the solution contains some PSSP. Resonance assignments are given in Table 5. Assignments were done using published chemical shift data [88] and standard procedures such as the effect of pH on the chemical shift of resonances for nuclei near to acidic groups. As in the ^1H NMR spectra of PSH, PSSG and PSSP, the two methyl groups give chemically-shifted ^{13}C resonances.

^{13}C spectra were measured as a function of pH for the solution used to obtain spectrum C in Figure 20. The results are tabulated in Table 5. Because some resonances cross over as the pH is changed, e.g. resonances 6 and 26 cross over as the pH is increased from 4.5 to 12.3, ^{13}C spectra were obtained, for assignment purposes, at pH 4, 9 and 13 for individual solutions of PSH, PSSP, GSH and GSSG.

Table 5. Assignment and chemical shift data (vs DSS) for the various ^{13}C resonances in Figure 20.

pH	PSH				PSSP			
	C_α 1 ^a	C_β 2	CH_3 3	CH_3 4	C_α 5	C_β 6	CH_3 7	CH_3 8
4.52	65.69	44.95	31.21	28.76	63.01	50.96	27.70	23.69
5.47	65.71	44.95	31.22	28.76	63.03	50.98	27.69	23.69
6.06	65.72	44.96	31.24	28.78	63.04	51.00	27.70	23.68
6.53	65.75	44.98	31.28	28.80	63.05	51.04	27.70	23.66
6.98	65.83	45.04	31.38	28.85	63.13	51.19	27.71	23.64
7.38	65.99	45.16	31.58	28.99	63.29	51.43	27.72	23.62
7.95	66.41	45.50	32.10	29.29	63.61	52.16	27.73	23.46
8.48	66.88	45.87	32.56	29.63	64.00	52.96	27.73	23.30
8.99	67.21	46.08	33.10	29.83	64.33	53.56	27.69	23.17
9.44	67.40	46.2	33.19	29.89	64.50	54.1	27.66	23.11
9.80	67.59	-	33.37	29.88	64.55	54.1	27.63	23.11
10.02	67.77	46.53	33.52	29.84	64.60	54.20	27.63	23.10
10.46	68.34	46.79	33.97	29.73	64.61	54.27	27.64	23.10
10.97	69.10	47.19	34.62	29.53	64.62	54.23	27.63	23.10
11.52	69.60	47.32	35.01	29.44	64.63	54.29	27.62	23.10
12.27	69.94	47.49	35.29	29.37	64.66	54.31	27.65	23.14

Continued

Table 5 (Cont'd.)

pH	PSSG									
	PSH-C α 9	PSH-C β 10	CH ₃ 11	CH ₃ 12	Glu-C α 13	Cys-C α 14	GLY-C α 15	Cys-C β 16	Glu-C γ 17	Glu-C β 18
4.52	62.08	51.83	27.31	22.79	55.18	54.16	44.29	41.69	32.39	27.12
5.47	62.08	51.84	27.30	22.78	55.19	54.16	44.44	41.69	32.41	27.13
6.06	62.09	51.86	27.31	22.77	55.19	54.17	44.46	41.69	32.40	27.14
6.53	62.09	51.89	27.30	22.76	55.19	54.17	44.47	41.67	32.39	27.15
6.98	62.18	52.01	27.29	22.76	55.20	54.17	44.47	41.68	32.41	27.17
7.38	62.31	52.28	27.25	22.78	55.24	54.18	44.48	41.70	32.44	27.25
7.95	62.66	53.00	27.20	22.73	55.30	54.17	44.48	41.65	32.46	27.46
8.48	63.12	53.96	27.11	22.65	55.46	54.15	44.48	41.60	32.56	28.02
8.99	63.47	54.71	27.04	22.58	55.76	54.12	44.47	41.57	32.73	29.07
9.44	63.63	55.05	27.02	22.55	56.09	54.09	44.47	41.58	32.94	30.18
9.80	63.71	55.20	26.99	22.55	56.30	54.06	44.46	41.53	33.06	30.92
10.02	63.74	55.25	27.00	22.53	56.38	54.06	44.47	41.57	33.12	31.18
10.46	63.75	55.31	27.00	22.53	56.49	54.05	44.47	41.59	33.17	31.52
10.97	63.76	55.32	27.00	22.53	56.52	54.05	44.48	41.58	33.20	31.66
11.52	63.77	55.33	26.99	22.53	56.53	54.04	44.48	41.60	33.21	31.70
12.27	63.81	55.36	27.02	22.54	56.56	54.07	44.47	41.62	33.22	31.74

Continued

Table 5 (Cont'd.)

pH	GSH										GSSG									
	Cys-C _α 19	Glu-C _α 20	Gly-C _α 21	Glu-C _α 22	Glu-C _γ 23	Glu-C _β 24	Cys-C _β 25	Glu-C _α 26	Cys-C _α 27	Gly-C _α 28	Cys-C _β 29	Glu-C _γ 30	Glu-C _β 31	Cys-C _α 32	Gly-C _α 33	Cys-C _β 34	Glu-C _γ 35	Glu-C _β 36		
4.52	56.52	55.18 ^a	44.3	32.4	27.1	26.49	55.18	53.60	44.3	39.79	32.4	27.1	55.19	53.59	44.4	39.79	32.4	27.1		
5.47	56.51	55.19	44.4	32.4	27.1	26.49	55.19	53.59	44.4	39.79	32.4	27.1	55.19	53.59	44.5	39.78	32.4	27.1		
6.06	56.52	55.19	44.5	32.4	27.1	26.51	55.19	53.59	44.5	39.76	32.4	27.2	55.19	53.59	44.5	39.76	32.4	27.2		
6.53	56.53	55.19	44.5	32.4	27.2	26.51	55.20	53.58	44.5	39.79	32.4	27.2	55.20	53.58	44.5	39.79	32.4	27.2		
6.98	56.55	55.20	44.5	32.4	27.2	26.55	55.24	53.62	44.5	39.80	32.4	27.2	55.24	53.62	44.5	39.80	32.4	27.2		
7.38	56.60	55.24	44.5	32.4	27.2	26.63	55.30	53.60	44.5	39.80	32.5	27.5	55.30	53.60	44.5	39.80	32.5	27.5		
7.95	56.76	55.30	44.5	32.5	27.5	26.86	55.46	53.58	44.5	39.76	32.6	28.0	55.46	53.58	44.5	39.76	32.6	28.0		
8.48	57.17	55.46	44.5	32.6	28.0	27.18	55.76	53.56	44.5	39.69	32.7	29.1	55.76	53.56	44.5	39.69	32.7	29.1		
8.99	57.81	55.76	44.5	32.7	29.1	27.52	56.09	53.50	44.5	39.70	32.9	30.2	56.09	53.50	44.5	39.70	32.9	30.2		
9.44	58.37	56.09	44.5	32.9	30.2	27.63	56.30	-	44.5	-	33.1	30.9	56.30	-	44.5	-	33.1	30.9		
9.80	58.75	56.30	44.5	33.1	30.9	27.80	56.38	53.49	44.5	39.54	33.1	31.2	56.38	53.49	44.5	39.54	33.1	31.2		
10.02	58.88	56.38	44.5	33.1	31.2	27.90	56.49	53.47	44.5	39.62	33.2	31.5	56.49	53.47	44.5	39.62	33.2	31.5		
10.46	59.07	56.49	44.5	33.2	31.5	27.94	56.52	53.49	44.5	-	33.2	31.7	56.52	53.49	44.5	-	33.2	31.7		
10.97	59.14	56.52	44.5	33.2	31.7	27.95	56.53	-	44.5	-	33.2	31.7	56.53	-	44.5	-	33.2	31.7		
11.52	59.15	56.53	44.5	33.2	31.7	27.99	56.56	-	44.5	-	33.2	31.7	56.56	-	44.5	-	33.2	31.7		
12.27	59.18	56.56	44.5	33.2	31.7	27.99	56.56	-	44.5	-	33.2	31.7	56.56	-	44.5	-	33.2	31.7		

^aNumber refers to resonances in Figure 20. The resonance labeled O refers to the internal reference dioxane which was set at 67.40 ppm (vs DSS). The temperature was maintained at 25°C.

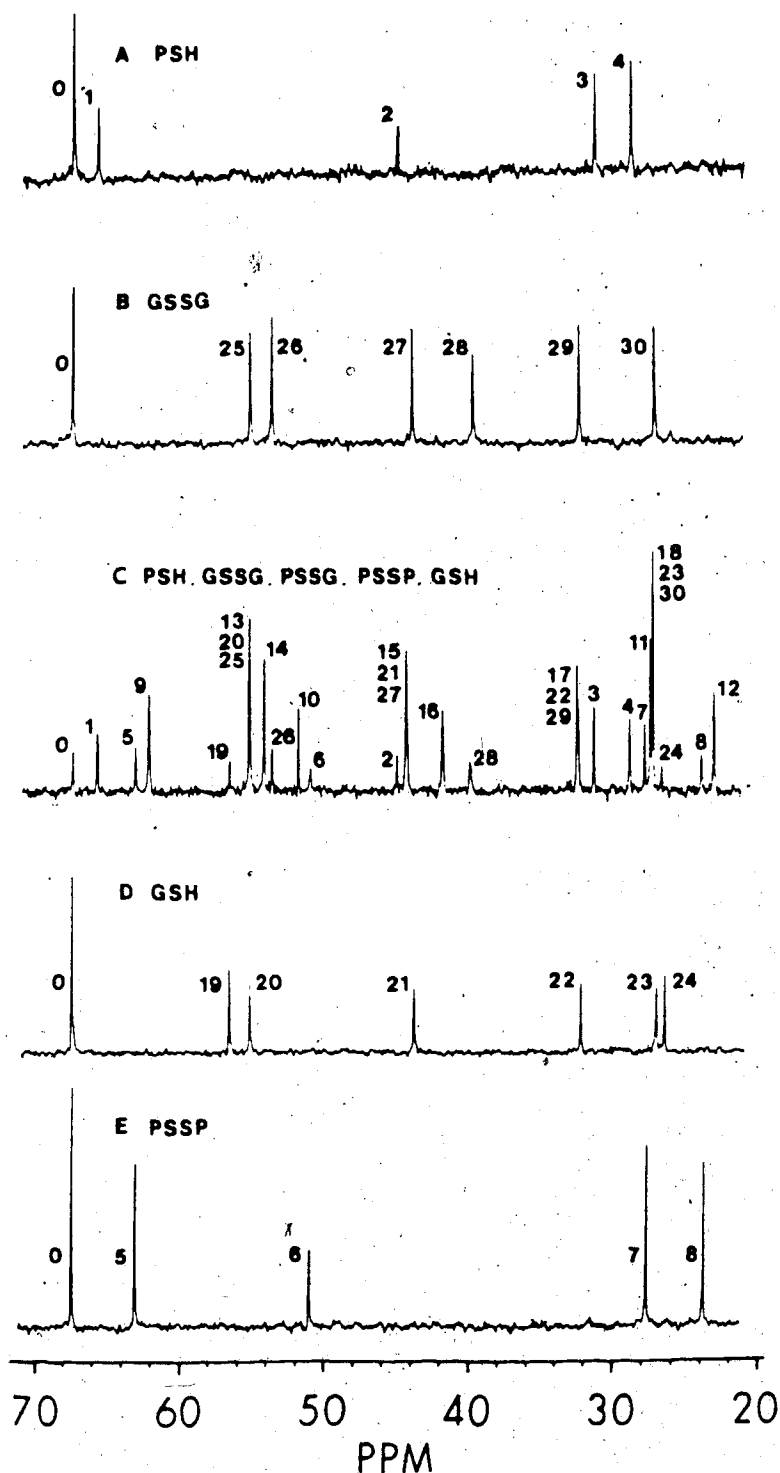


Figure 20. ^{13}C NMR spectra (90.56 MHz) of A) 0.1 M PSH, B) 0.1 M GSSG, C) 0.064 M PSH, 0.019 M PSSP, 0.101 M PSSG, 0.022 M GSH and 0.014 M GSSG, D) 0.1 M GSH and E) 0.1 M PSSP. Each solution contained 0.03 M dioxane as internal reference. Solutions A, B, D and E were at pH 4.0 in 1 M KCl aqueous solution; solution C was at pH 4.52 in 0.4 M KCl aqueous solution. The thiol and disulfide concentrations in solution C were calculated from resonances 1, 5, 9; 4, 8, 12; 14, 19, 26; 16, 24 and 28. See Table 5 for assignment. The resonance labeled 0 is for the internal reference dioxane which was set at 67.40 ppm.

1. Acid Dissociation Constants for Penicillamine

The deprotonation scheme for PSH is shown in Figure 21. At low pH, PSH is a triprotic acid. However, since the carboxylic acid group titrates completely before the ammonium and thiol groups are titrated, the dissociation of the carboxylic acid group can be treated as the dissociation of a monoprotic acid. The ammonium and thiol groups are similar in acidity and thus their titration ranges overlap. With reference to the general discussion of diprotic acids presented earlier, K_{A2} and K_{A3} in Figure 21 are equivalent to K_{H_2A} and K_{HA} , respectively (Equations 59 and 61). K_{A1} for PSH was evaluated from the 1H chemical shift data shown in Figure 16 and 19 over the pH range 1-5. The two sets of chemical shift data for the two separate methyl resonances were evaluated independently to yield two values for K_{A1} by fitting the data to Equation 57 as described above for the monoprotic acid. The chemical shifts for the H_3A and H_2A forms of PSH are summarized in Table 6 and the two values for pK_{A1} are listed in Table 7. These tables also contain the 1H chemical shift values, literature pK_A values and pK_A values determined later in this chapter for the other thiols and disulfides.

Two sets of values for the macroscopic acid dissociation constants K_{A2} and K_{A3} were obtained from the

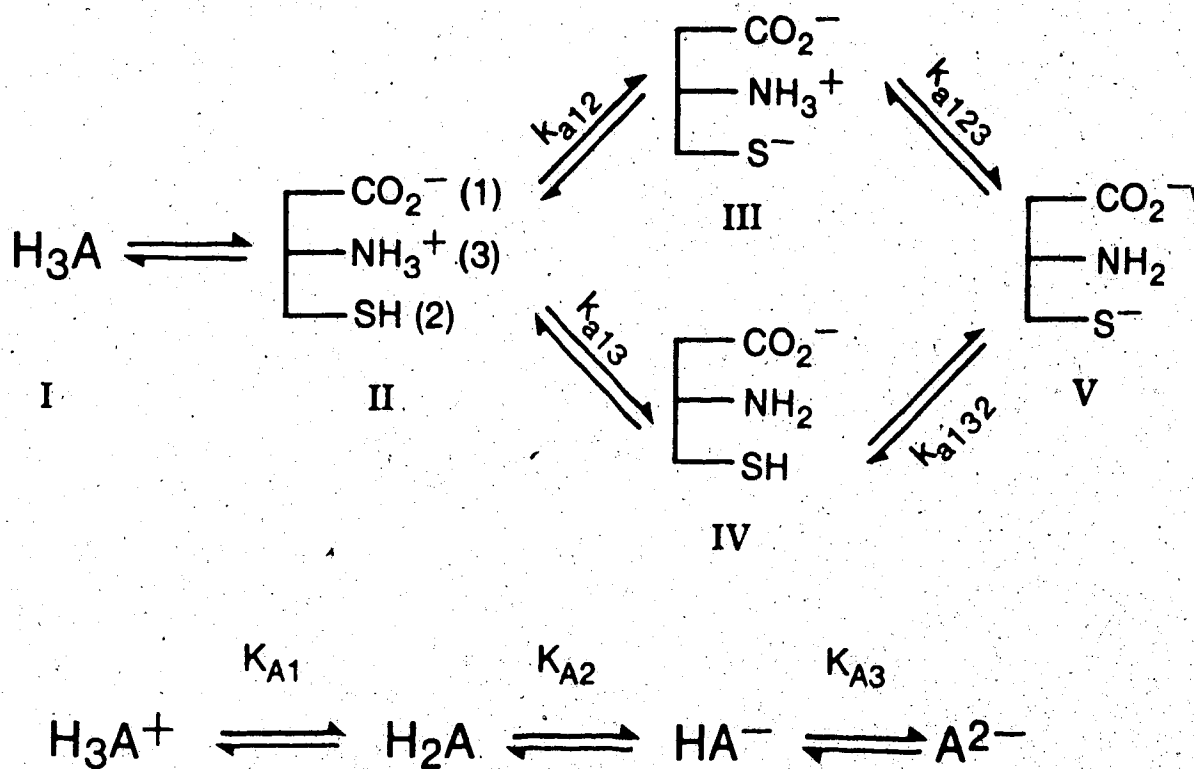


Figure 21. Macroscopic and microscopic acid dissociation schemes for penicillamine and cysteine.

Table 6. Chemical shift data (vs DSS) for the various protonated forms of PSH and PSH-containing molecules.

Molecule	¹ H Chemical Shift						Group
	H _{5A}	H _{4A}	H _{3A}	H _{2A}	HA	A	
PSH			1.5428	1.4828	1.2994	1.1867	CH ₃
			1.6054	1.5694	1.5322	1.4274	CH ₃
			4.1583	3.7180	--	3.0430	CH _α
PSSP		1.5248	--	1.4439	--	1.2772	CH ₃
		1.5773	--	1.5465	--	1.3670	CH ₃
		4.1023	--	3.7253	--	3.2582	CH _α
PSSG	1.4897	--	--	1.4009	--	1.2736	CH ₃
	1.5639	--	--	1.5364	--	1.3908	CH ₃
	--	--	--	3.84	--	3.34	CH _α
PSSC		1.5117	--	1.4364	--	1.2633	CH ₃
		1.6074	--	1.5563	--	1.3984	CH ₃
		3.4694	--	3.3421	--	3.0128	CSH-CH ₂
		4.2391	--	3.8458	--	3.3554	PSH-CH _α
	4.5048	--	4.0677	--	3.5308	CSH-CH _α	

^aChemical shift data vs DSS were obtained either directly from the limiting chemical shift in the chemical shift versus pH data or indirectly from the non-linear least squares program.

Table 7. Macroscopic acid dissociation constants for thiols, symmetrical disulfides and mixed disulfides.

Molecule	Ionic Strength, M	Acid Dissociation Constants						Source
		pK _{A1}	pK _{A2}	pK _{A3}	pK _{A4}	pK _{A5}	pK _{A6}	
PSH	1	2.55±0.03	8.03±0.02	10.62±0.02				This Work: ¹ H
	1	2.52±0.03	7.99±0.04	10.64±0.02				This Work: ¹ H
	0.4	-	8.04±0.04	10.64±0.03				This Work: ¹³ C
	0.8	-	8.02	10.63				88
	0.15	2.44	7.97	10.46				103
	0.10	-	7.88	10.43				104
0.1	-	8.04	10.68				105	
1 ^a	2.47	7.93±0.08	10.41±0.13					
PSSP	0.4	-	-	7.76±0.02	8.71±0.02			This Work: ¹³ C
	0.1	-	-	7.76	8.72			95
	0.15	1.32	2.02	7.44	8.59			96
	1 ^a	1.40	2.05	7.52±0.15	8.55±0.06			
	0.4	-	-	8.67±0.03	9.44±0.03			This Work: ¹³ C
GSH	0.35	2.05	3.40	8.72	9.49			91
	0.16	-	-	8.74	9.62			92
	0.15	-	3.59	8.75	9.65			93
	0.30	-	3.46	8.64	9.50			94
	1 ^a	2.05	3.47±0.08	8.67±0.04	9.49±0.01			

Continued

Table 7 (Cont'd.)

Molecule	Ionic Strength, $\frac{M}{M}$	Acid Dissociation Constants						Source
		pK_{A1}	pK_{A2}	pK_{A3}	pK_{A4}	pK_{A5}	pK_{A6}	
GSSG	0.4	-	-	-	-	8.73±0.05	9.49±0.04	This Work: ¹³ C
	0.15	-	-	3.15	4.03	8.57	9.54	93
	0.7	1.60	2.42	3.03	4.04	8.97	9.70	94
^{1a}	1.58	2.41	3.08±0.06	4.00±0.08	8.72±0.41	9.55±0.29		
pSSG	0.4	-	-	-	8.13±0.02	9.24±0.01		This Work: ¹³ C
	0.8	-	8.15	10.33				88
	0.8	-	8.26	10.38				88
0.10	-	8.13	10.11				104	
0.15	-	8.30	10.40				97	
0	1.71	8.33	10.78				106	
0	-	8.39	10.76				98	
^{1a}	1.87	8.19±0.07	10.29±0.14					
CSSC	0.1	-	-	7.95	8.95			107
	0	1.04	2.05	8.00	10.25			106
	^{1a}	1.51	2.21	7.88±0.04	9.30±0.68			
PSSC	^{1a}	1.80±0.03	2.24±0.03	8.04±0.01	8.93±0.01			This Work: ¹ H

^aLiterature pK_A values were corrected to the ionic strength (I) of 1 M as described in the experimental section and the average calculated.

pH 4-12 ^1H chemical shift data (Figure 19) of the two methyl resonances of Figure 16. Because of the proximity of the methyl protons to the ammonium and thiol groups, each methyl resonance is affected by the protonation state of each acidic group. K_{A2} and K_{A3} were obtained by fitting each set of chemical shift data to the equation presented above for the common resonance method (Equation 77). The chemical shifts obtained for the three protonated forms of PSH in the pH range 4-12 and the values obtained for $\text{p}K_{A2}$ and $\text{p}K_{A3}$ are given in Tables 6 and 7, respectively.

Values for K_{A2} and K_{A3} were also determined from the ^{13}C chemical shift data in Table 5 using the chemical shift of the C_α carbon of PSH. The resonance for this carbon is well resolved from the other resonances over the entire pH range. It also is closer to the ammonium group than are the methyl carbons, and thus its chemical shift is more sensitive to deprotonation of the ammonium group. The C_α resonance is more intense than the C_β resonance since C_β is a quaternary carbon and thus its intensity is not significantly enhanced by the nuclear Overhauser effect [89]. Values for K_{A2} and K_{A3} were obtained using the common resonance method by fitting the ^{13}C chemical shift vs pH data to Equation 77. The limiting chemical shifts at low and high pH in Table 5

were used for the chemical shifts of the H_2A and A species. The values obtained for K_{A2} and K_{A3} are given in Table 7; the value obtained for δ_{HA} is 67.31 ppm.

It is shown in Chapter IV that the reactive thiol species in the thiol/disulfide exchange reactions are the thiol deprotonated forms. For PSH, these are species III and V in Figure 21. The fractional concentration, α , of the various protonated forms of PSH is shown as a function of pH in Figure 22. These curves were calculated using the values determined in this work for pK_{A1} , pK_{A2} and pK_{A3} . For example, the species distribution (curve I in Figure 22) of the fully protonated form of PSH, H_3A^+ in Figure 21, was calculated as follows:

$$\alpha_{H_3A^+} = \alpha_I = \frac{a_H^3}{a_H^3 + a_H^2 K_{A1} + a_H K_{A1} K_{A2} + K_{A1} K_{A2} K_{A3}} \quad (90)$$

The others were calculated similarly using different terms in the numerator. The distribution of HA (curve (III + IV) in Figure 22) between species III and IV (curves III and IV in Figure 22) was calculated using microconstants k_{a12} and k_{a13} and α_{II} calculated using the macroscopic constants determined in this work. α_{III} and α_{IV} were calculated with Equations 91 and 92.

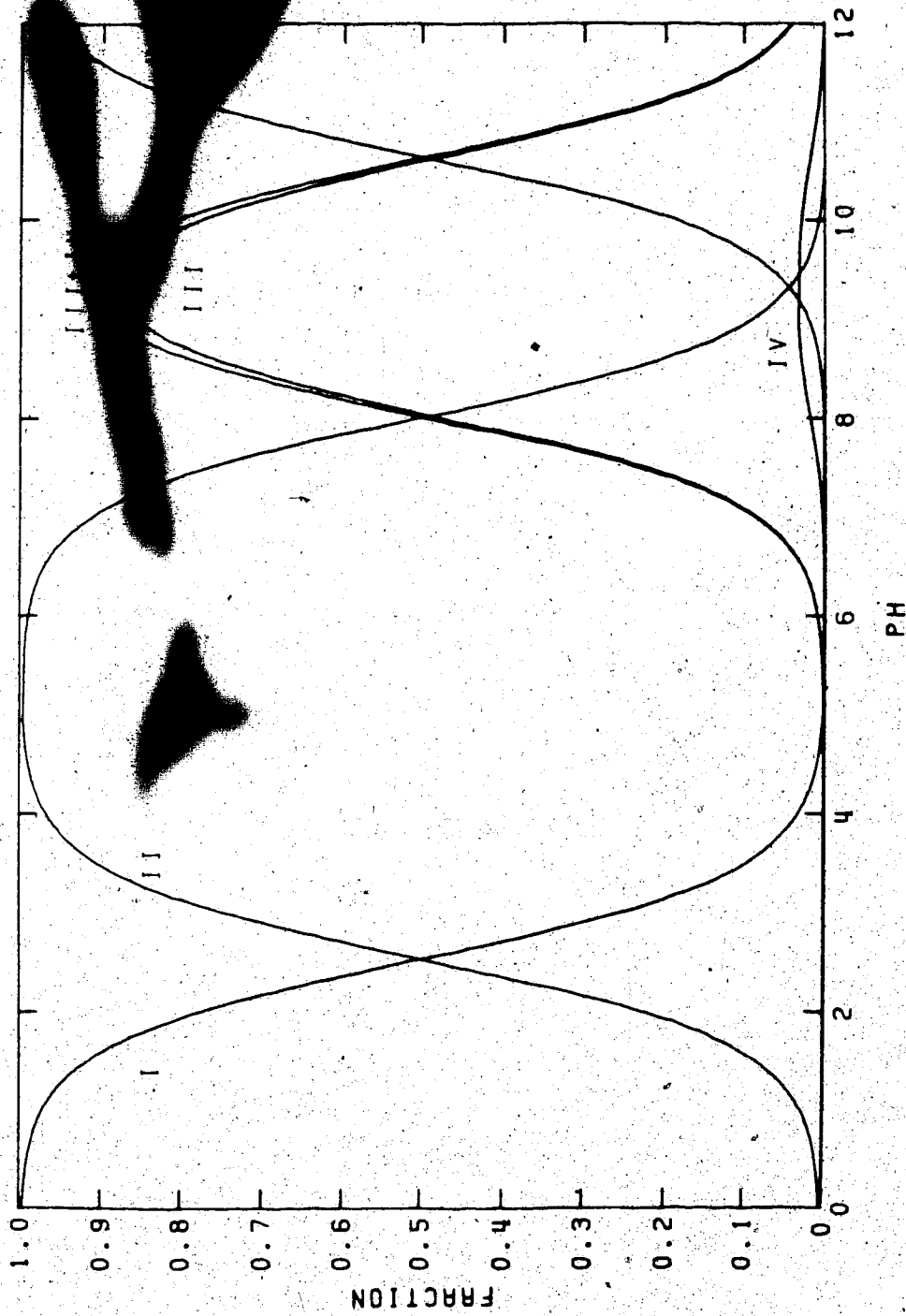


Figure 22. Species distribution diagram for penicillamine. Numbers refer to the various protonated forms shown in Figure 21. These curves were generated with $pK_{A1} = 2.54$, $pK_{A2} = 8.01$ and $pK_{A3} = 10.63$, $pK_{A2} = 8.02$ and $pK_{A3} = 9.43$.

$$\alpha_{III} = \frac{k_{a12}}{a_H} \alpha_{II} \quad (91)$$

$$\alpha_{IV} = \frac{k_{a13}}{a_H} \alpha_{II} \quad (92)$$

The literature value for pK_{a12} [90] corrected to the ionic strength conditions of this work is 8.02. The microconstant pK_{a13} was calculated from the values of pK_{a12} and pK_{A2} with an equation analogous to Equation 67. The values of the microscopic acid dissociation constants, pK_{a13} , pK_{a123} and pK_{a132} of PSH (Figure 21) together with various microconstants of other molecules are listed in Table 8. In calculating pK_{a123} and pK_{a132} , equations similar to Equation 69 were used.

2. Acid Dissociation Constants for Reduced Glutathione

The deprotonation scheme for GSH is shown in Figure 23. Macroconstants K_{A1} and K_{A2} were taken from the literature; K_{A3} and K_{A4} were calculated from the ^{13}C chemical shift data for GSH listed in Table 5.

The acid dissociation constants were evaluated by the unique resonance method described above. Since the $Glu-C_\alpha$ carbon is seven bonds removed from the thiol group but only one bond removed from the ammonium group, changes in its chemical shift in the pH region 5-12 are considered to be due only to the titration of the ammonium group, i.e.

Table 8. Microscopic acid dissociation constants for thiols, disulfides and mixed disulfides.

Molecule	Acid Group	Acid Dissociation Constant	pk _a	Source
PSH	NH ₃ ⁺	K _{a13}	9.43	b
	NH ₃ ⁺	K _{a123}	10.61	b
	SH	K _{a12}	8.02	90
	SH	K _{a132}	9.20	b
CSH	NH ₃ ⁺	K _{a13}	8.50	b
	NH ₃ ⁺	K _{a123}	10.00	b
	SH	K _{a12}	8.48 ± 0.10	97-100
	SH	K _{a132}	9.98	b
GSH	NH ₃ ⁺	K _{a124}	9.04	b
	NH ₃ ⁺	K _{a1234}	9.20	b
	SH	K _{a123}	8.91 ± 0.09	91,92
	SH	K _{a1243}	9.07	b
PSSP	NH ₃ ⁺	K _{a123} , K _{a124}	8.06 ± 0.02	This Work: 13C
	NH ₃ ⁺	K _{a1234} , K _{a1243}	8.41 ± 0.02	This Work: 13C
GSSG	NH ₃ ⁺	K _{a12345} , K _{a12346}	9.03 ± 0.05	This Work: 13C
	NH ₃ ⁺	K _{a123456} , K _{a123465}	9.19 ± 0.04	This Work: 13C

Table 8 (Cont'd.)

Molecule	Acid Group	Acid Dissociation Constant	pK_a^a	Source
PSSG	NH_3^+ (PS)	Ka1234	8.22 ± 0.06	This Work: ^{13}C
	NH_3^+ (GS)	Ka1235	8.86 ± 0.06	"
	NH_3^+ (GS)	Ka12345	9.15 ± 0.06	"
	NH_3^+ (PS)	Ka12354	8.51 ± 0.06	"
PSSC	NH_3^+ (PS)	Ka123	8.24 ± 0.02	This Work: 1H
	NH_3^+ (CS)	Ka124	8.47 ± 0.02	"
	NH_3^+ (CS)	Ka1234	8.73 ± 0.02	"
	NH_3^+ (PS)	Ka1243	8.50 ± 0.02	"

^aLiterature values were corrected to an ionic strength of 1 M.

^bMicroscopic constants were calculated from a given microscopic constant (average obtained from literature values) and the various macroscopic constants listed in Table 7. See text for details.

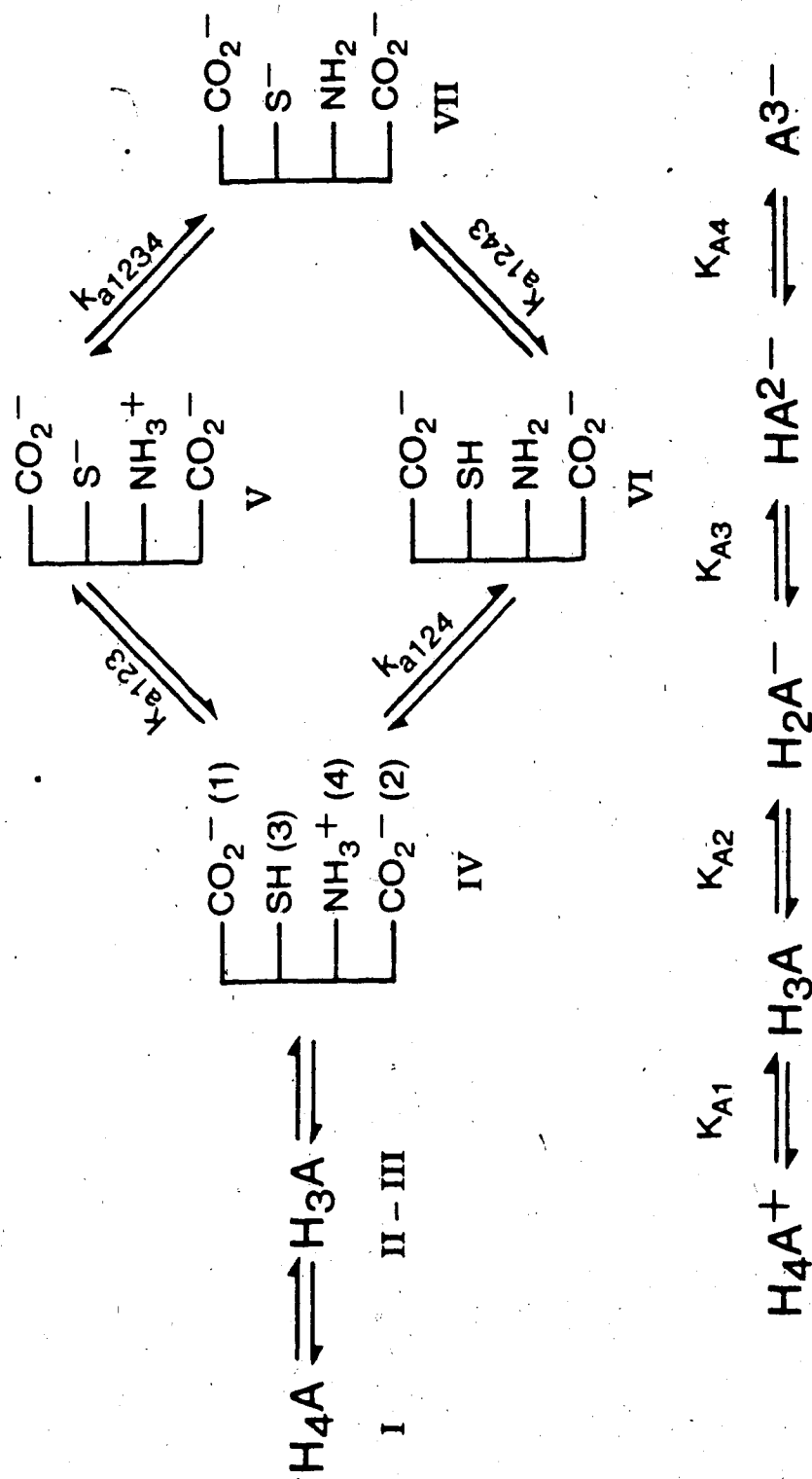


Figure 23. Macroscopic and microscopic acid dissociation schemes for reduced glutathione.

the Glu-C $_{\alpha}$ resonance is treated as a unique resonance for the ammonium group. Similarly, the Cys-C $_{\alpha}$ resonance is treated as a unique resonance for the thiol group. The fractional titration of the ammonium and the thiol groups ($f_{1,d}$ and $f_{2,d}$ respectively) as a function of pH was calculated from the Glu-C $_{\alpha}$ and Cys-C $_{\alpha}$ chemical shift data using Equation 85. From the fractional titration values, \bar{p} , the average number of acidic protons per GSH molecule, was calculated with Equation 86. The results are plotted in Figure 24. K_{A3} and K_{A4} were obtained by fitting the \bar{p} data in Figure 24 to Equation 79; K_{A3} and K_{A4} are equivalent to K_{H_2A} and K_{HA} in Equation 79. The results are given in Table 7. Also given in Table 7 are literature values for K_{A3} and K_{A4} , as well as for K_{A1} and K_{A2} [91-94].

The fractional concentrations of the various protonated forms of GSH are shown as a function of pH in Figure 25. The curves were calculated using macroscopic constants listed in Table 7. Since the thiol deprotonated species are the reactive species in the thiol/disulfide exchange reactions, the distribution of the species HA $^{2-}$ (V + VI in Figure 23) between species V and VI was calculated using the values for the microconstants pk_{a123} and pk_{a124} (identified in Figure 23) listed in Table 8. The average literature value for pk_{a123} , corrected to the

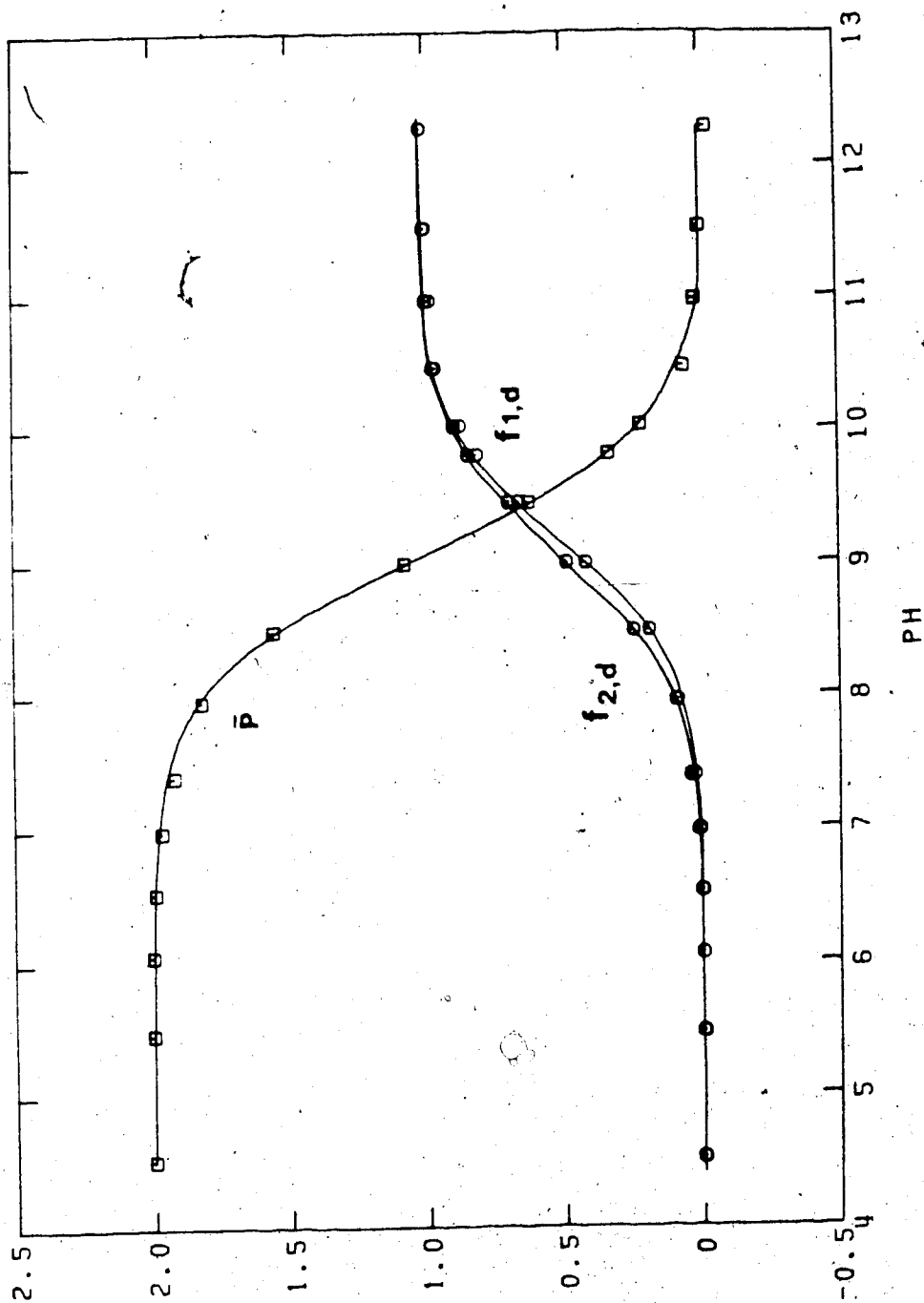


Figure 24. The average number of acidic protons per GSH molecule, \bar{p} , versus pH. The solid line is the theoretical curve calculated with Equation 79 and $pK_{A3} = 8.67$ and $pK_{A4} = 9.44$.

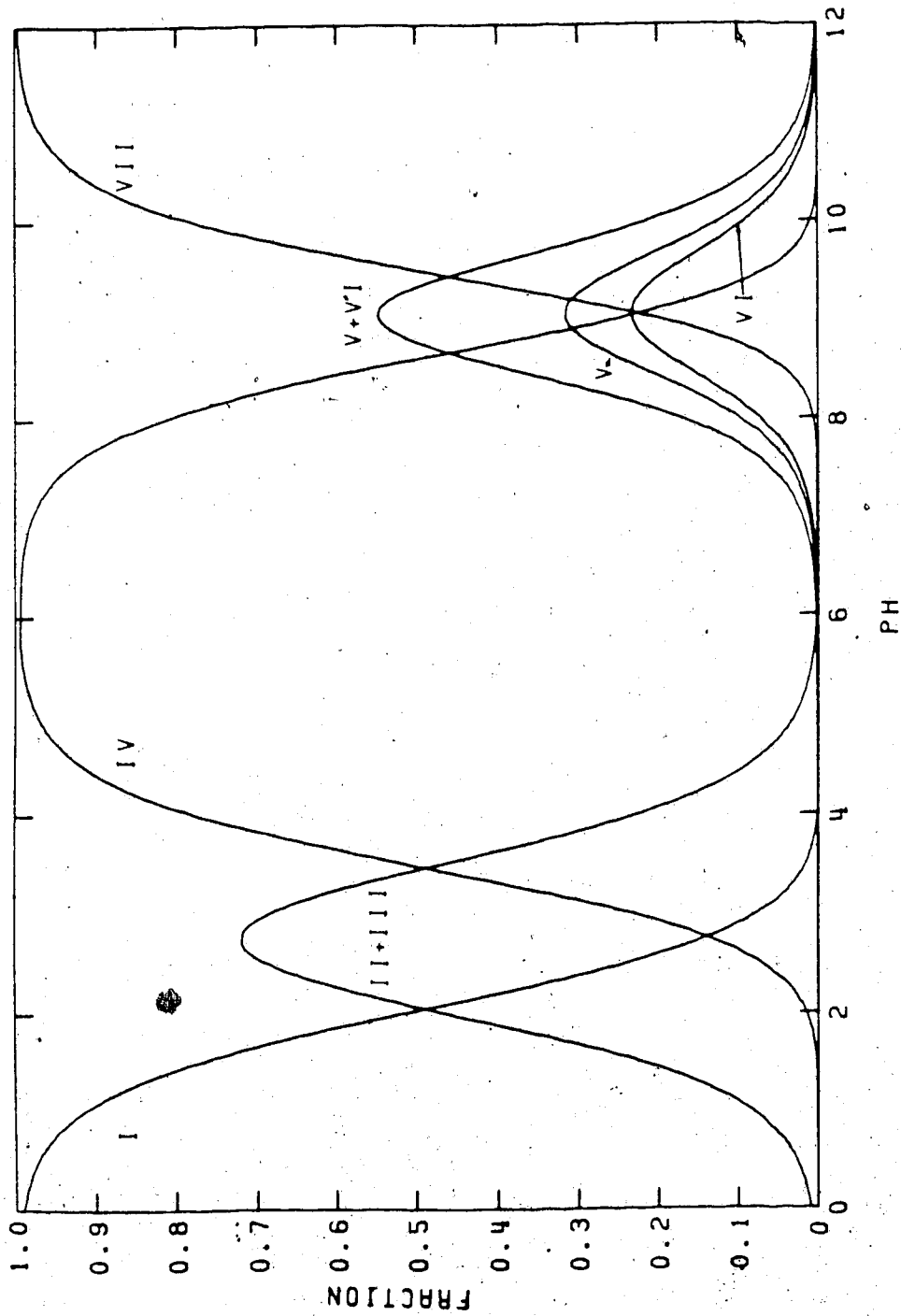


Figure 25. Species distribution diagram for reduced glutathione. Numbers refer to the various protonated forms shown in Figure 23. These curves were generated with $pK_{A1} = 2.05$, $pK_{A2} = 3.47$, $pK_{A3} = 8.67$, $pK_{A4} = 9.44$, $pK_{A123} = 8.91$ and $pK_{A124} = 9.04$.

ionic strength conditions of this work is 8.91 ± 0.09 [91,92]. The values of pK_{a124} , pK_{a1234} and pK_{a1243} were calculated from the values of pK_{a123} and other macroconstants in a manner similar to those of PSH above.

3. Acid Dissociation Constants for PSSP

The deprotonation scheme for PSSP is shown in Figure 26. Because PSSP is a symmetrical disulfide, $k_{a123} = k_{a124} = K_{A3}/2$; and $k_{a1234} = k_{a1243} = 2K_{A4}$. The various values are listed in Table 8. Literature values for $K_{A1} - K_{A4}$ are listed in Table 7 [95,96]. Values for K_{A3} and K_{A4} were determined from the ^{13}C chemical shift data in Table 5 for the C_α carbon of PSSP. The data were treated using the unique resonance method since the C_α carbon is one bond removed from one ammonium group and six bonds removed from the other. However, proton exchange is rapid on the NMR time scale and a single averaged resonance is observed for C_α . Thus, the chemical shift corresponds to the H_2A form at pH 5 and to the A^{2-} form at pH 12. Correspondingly, the fractional change in the chemical shift at a given pH from that at pH 5 to that at pH 12 gives the fractional titration of the two ammonium groups. \bar{p} is given by the equation

$$\bar{p} = 2 - 2f_d \quad (93)$$

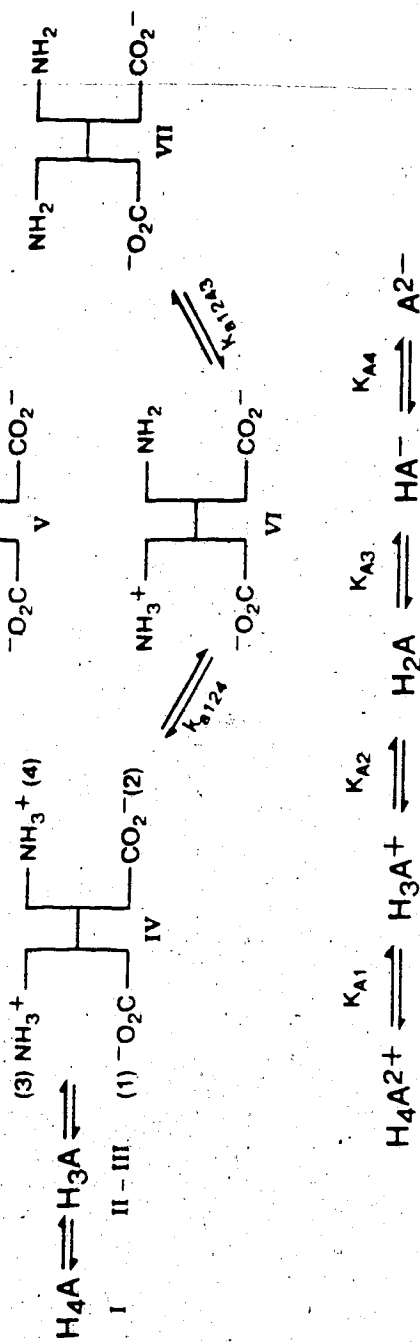


Figure 26. Macroscopic and microscopic acid dissociation schemes for oxidized penicillamine, cysteine and PSSC. In the case of PSSC, the ammonium group of the PS part of PSSC is labelled 3 and that of the CS part 4.

where f_d ($f_{1,d} = f_{2,d} = f_d$) varies from 0 to 1 and was calculated with Equation 85. The values obtained for K_{A3} and K_{A4} by fitting the \bar{p} versus pH data to Equation 79 are listed in Table 7.

Fractional concentrations calculated from the macroconstants are plotted in Figure 27. Because of the symmetrical nature of the molecule, the H_3A^+ form is equally distributed between species II and III and the HA form between species V and VI.

4. Acid Dissociation Constants for GSSG

The deprotonation scheme for GSSG is shown in Figure 28. Literature values are not available for the microconstants for the carboxylic acid group, and no attempt was made to determine them in this work since it is the deprotonation at the ammonium group which is important in the thiol/disulfide exchange studies.

Literature values for the macroscopic constants for the carboxylic acid groups, $K_{A1} - K_{A4}$, are given in Table 7 [93,94]. As with PSSP, the microscopic constants for the ammonium groups are simply related to their macroscopic constants by the equations $k_{a12345} = k_{a12346} = K_{A5}/2$ and $k_{a123456} = k_{a123465} = 2K_{A6}$. These are listed in Table 8. Macroconstants K_{A5} and K_{A6} were evaluated from the

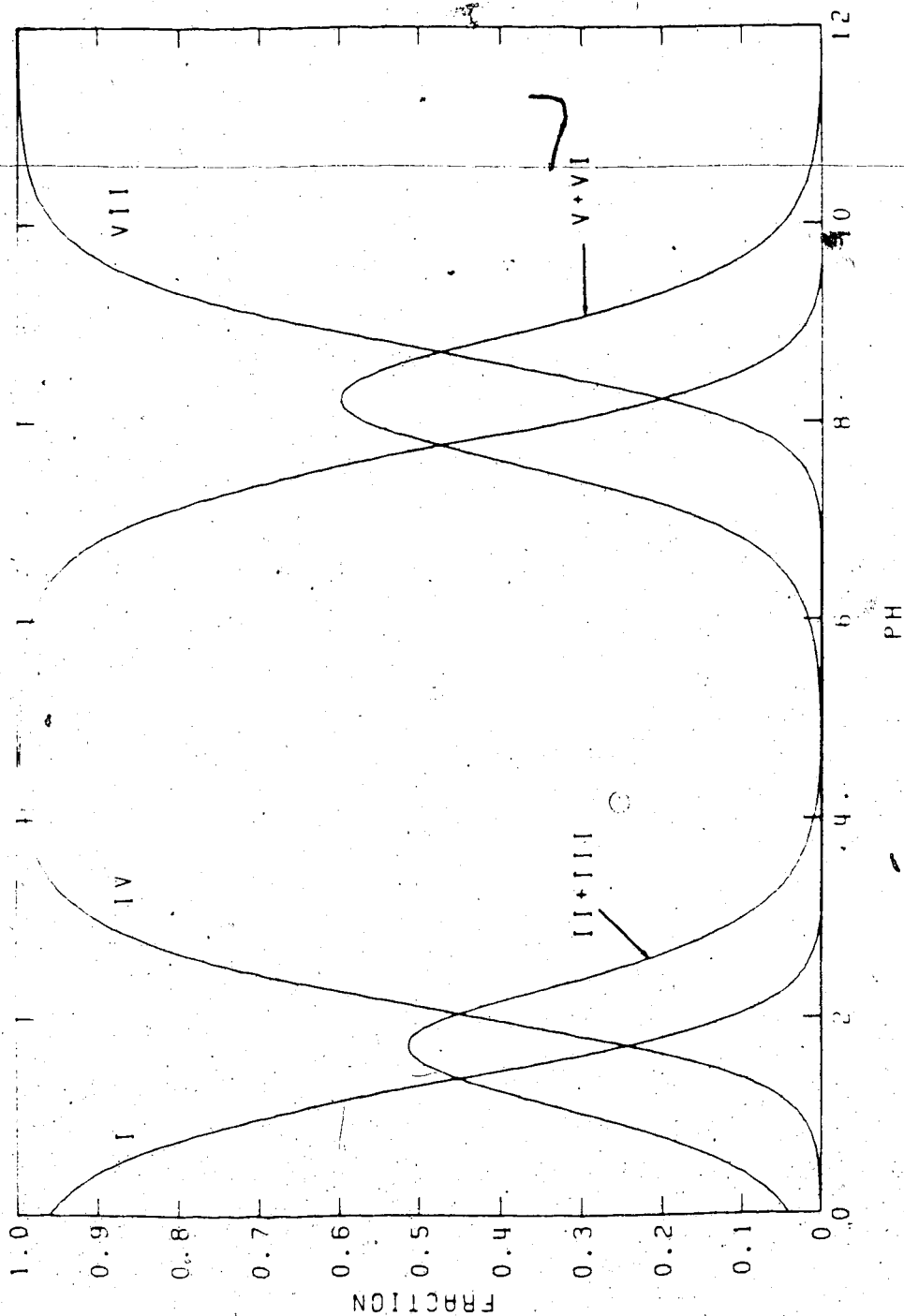


Figure 27. Species distribution diagram for oxidized penicillamine. The various deprotonated forms associated with the numbers are shown in Figure 26. The fractional concentrations were calculated with $pK_{A1} = 1.40$, $pK_{A2} = 2.05$, $pK_{A3} = 7.76$ and $pK_{A4} = 8.71$.

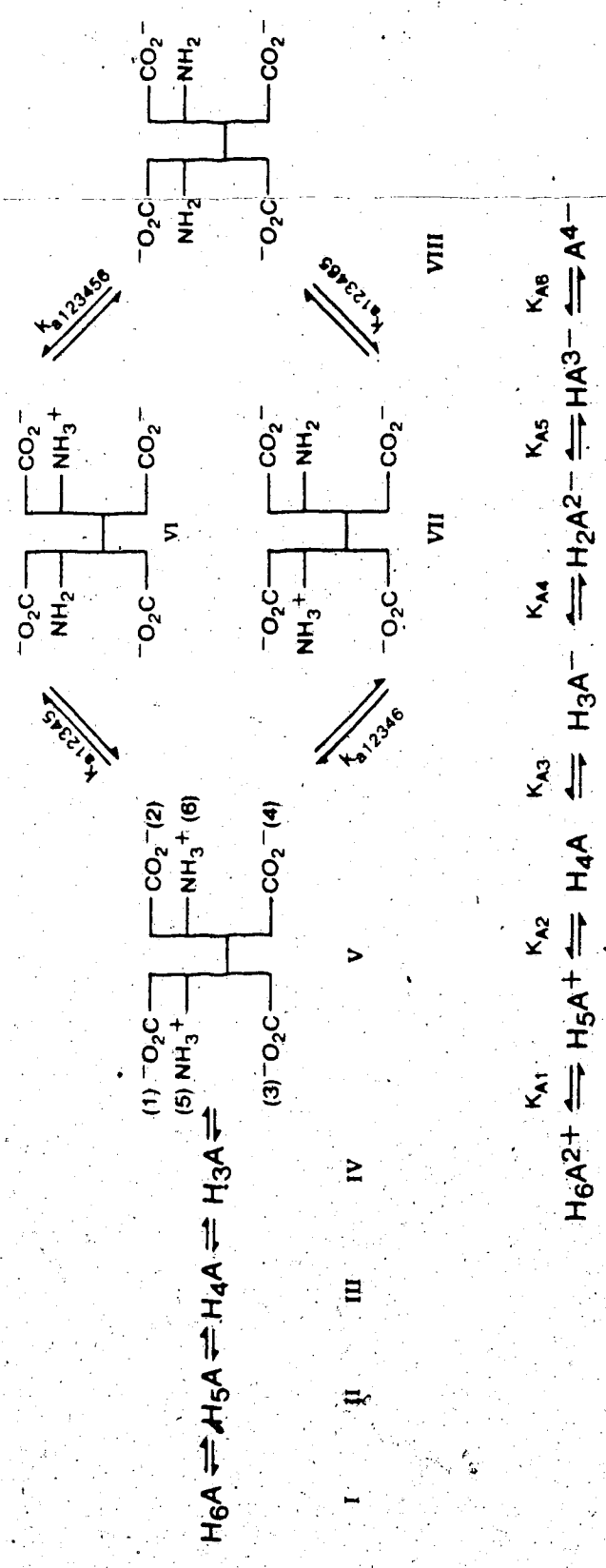


Figure 28. Macroscopic and microscopic deprotonation schemes of oxidized glutathione.

chemical shift data in Table 5 for Glu-C $_{\alpha}$. The data were treated by the unique resonance method since each Glu-C $_{\alpha}$ carbon is one bond removed from one ammonium group and sixteen bonds removed from the other. The treatment was identical to that described above for PSSP. The values obtained for K $_{A5}$ and K $_{A6}$ are given in Table 7. The species distribution calculated for GSSG from the macroconstants is given in Figure 29. Because of the symmetry, HA $^{3-}$ is equally distributed between VI and VII.

5. Acid Dissociation Constants for PSSG

The deprotonation scheme for PSSG is shown in Figure 30. There are no literature values for any of the acid dissociation constants of PSSG. No attempt was made to determine the macroconstants for the carboxylic acid groups since it is the deprotonation at the amino groups which is of interest in the thiol/disulfide exchange studies. Macroscopic constants K $_{A4}$ and K $_{A5}$ and microscopic constants k $_{a1234}$, k $_{a1235}$, etc. in Figure 30 were calculated from ^{13}C data.

Macroscopic constants K $_{A4}$ and K $_{A5}$ were calculated from the ^{13}C chemical shift data in Table 5 for the Glu-C $_{\alpha}$ and PSH-C $_{\alpha}$ carbons of PSSG. ^{13}C chemical shift titration data for the PSH-C $_{\alpha}$ and Glu-C $_{\alpha}$ carbons of PSSG are presented in Figure 31. Since 11 bonds separate the

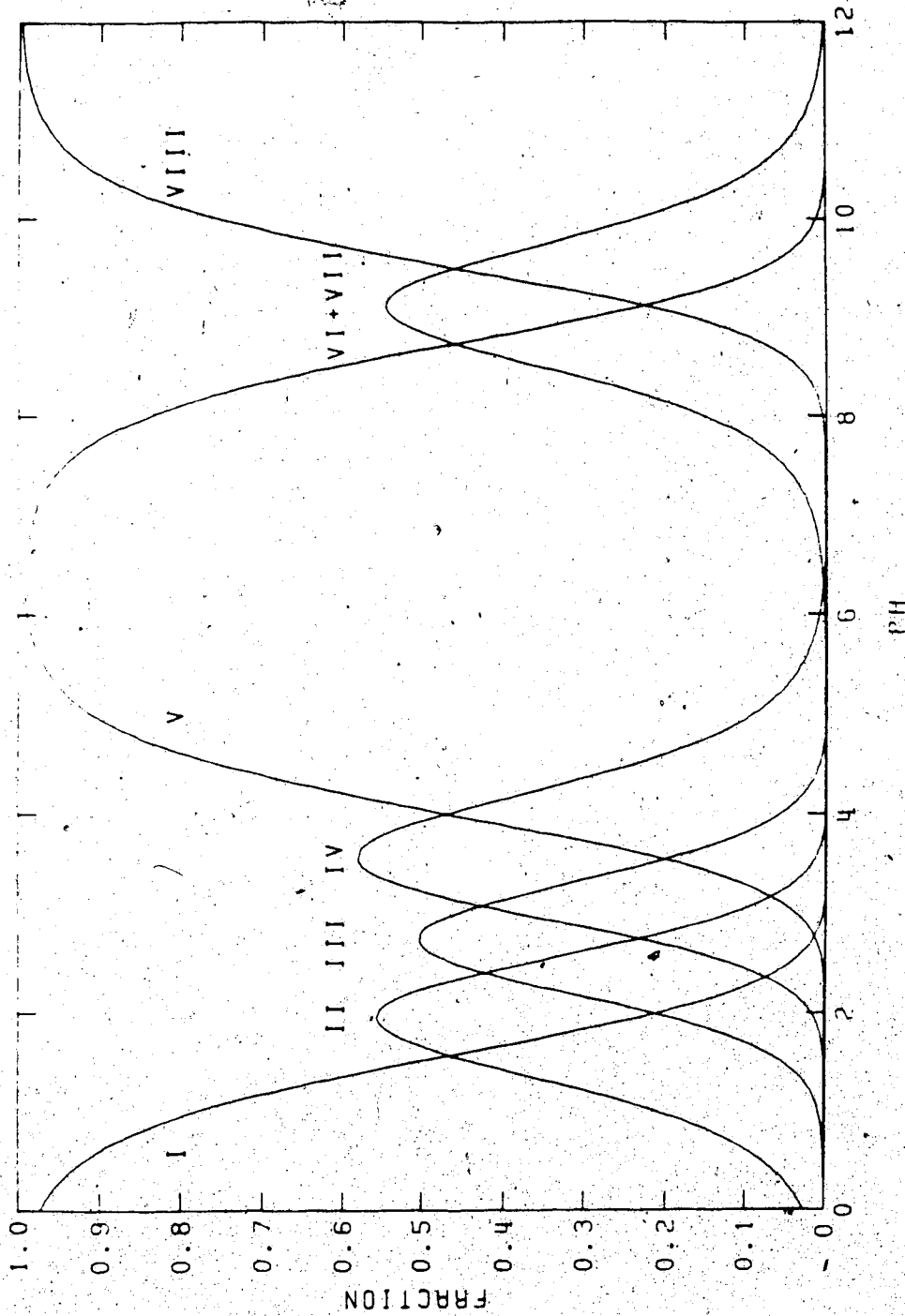


Figure 29. Species distribution diagram for oxidized glutathione. The various deprotonated forms associated with the numbers are summarized in Figure 28. The fractional concentrations were calculated with $pK_{A1} = 1.58$, $pK_{A2} = 2.41$, $pK_{A3} = 3.08$, $pK_{A4} = 4.00$, $pK_{A5} = 8.73$ and $pK_{A6} = 9.49$.

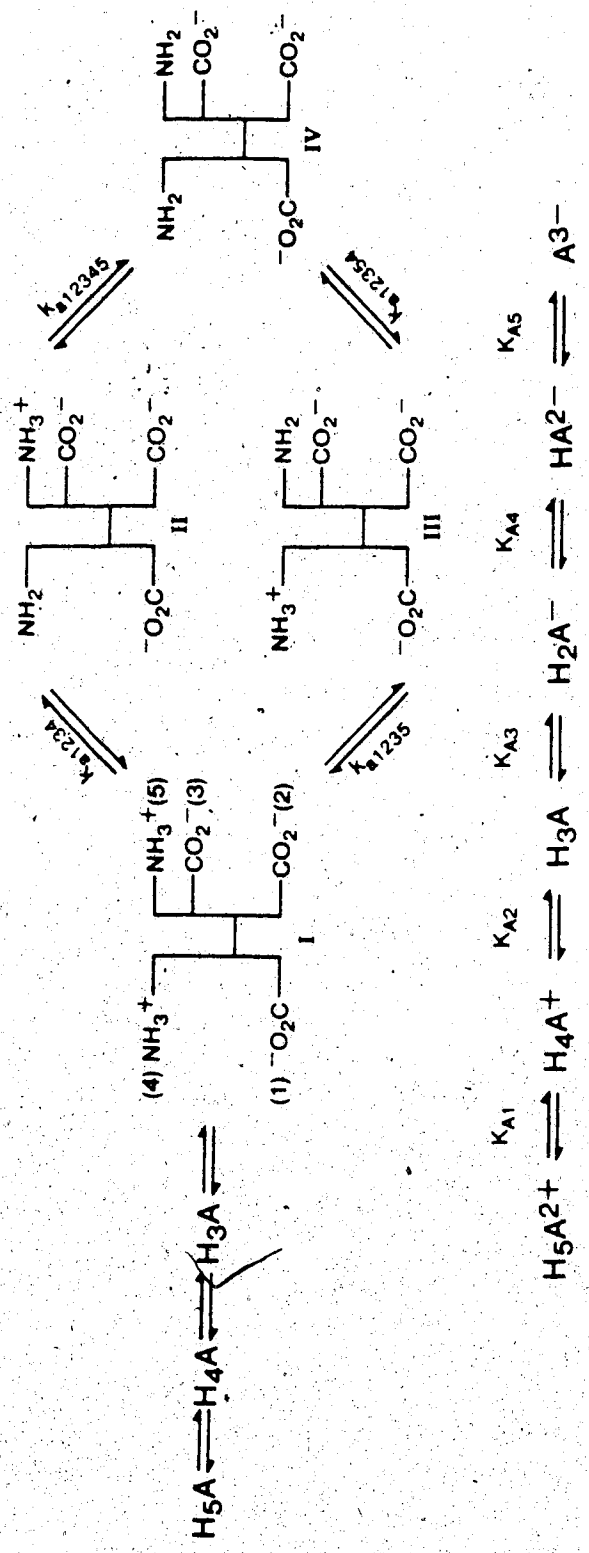


Figure 30. Macroscopic and microscopic acid dissociation schemes of the mixed disulfide, PSSG.

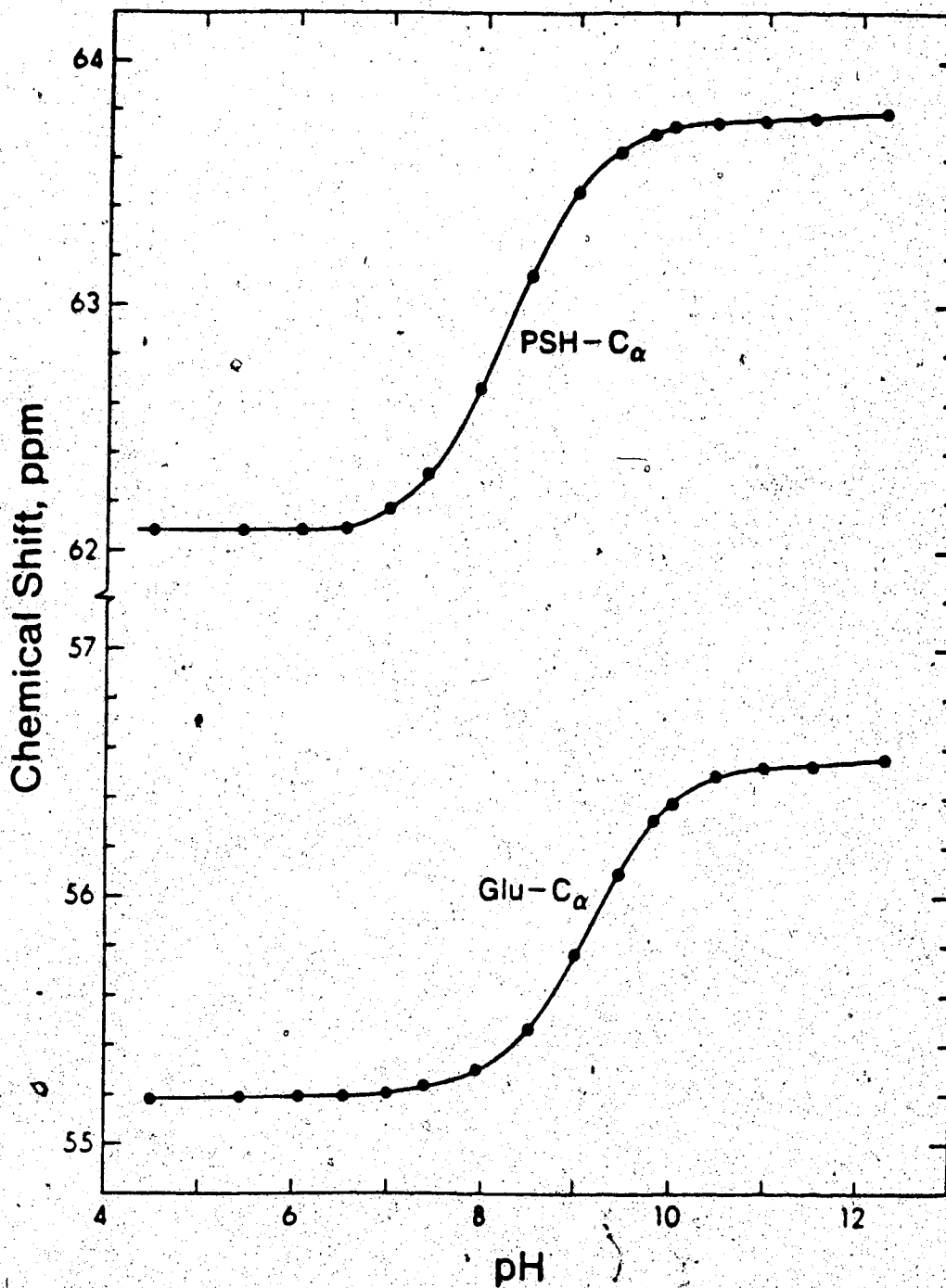


Figure 31. pH dependence of the ^{13}C chemical shifts of the penicillamine and glutamyl alpha carbons of PSSG (Table 5) versus DSS.

PSH-C_α carbon from the glutamyl ammonium group in PSSG, changes in the chemical shift of the PSH-C_α resonance can be assumed to be due only to changes in the protonation state of the penicillamine ammonium group. The fractional titration of each of the two ammonium groups (f_{4,d} and f_{5,d}) was calculated from the ¹³C chemical shift data using an equation analogous to Equation 85. The fractional deprotonation curves for groups 4 and 5 are shown in Figure 32. The average number of titratable ammonium protons per molecule, \bar{p} , was then calculated as a function of pH from the fractional titration data using Equation 86. The \bar{p} versus pH data are also shown in Figure 32.

The values for the macroconstants K_{A4} and K_{A5} were obtained by curve fitting the \bar{p} versus pH data in Figure 32 to Equation 79. The results are given in Table 7. The solid curve through the \bar{p} vs pH data in Figure 32 is theoretical for Equation 79 using the values listed in Table 7.

Microconstants for PSSG were calculated from the macroconstants by calculating the average ratio of the concentrations of species II and III (Figure 30) using Equation 88. This ratio is equal to the ratios k_{a1234}/k_{a1235} and k_{a12354}/k_{a12345} . The average value obtained for the ratio from data at 8 pH values (data

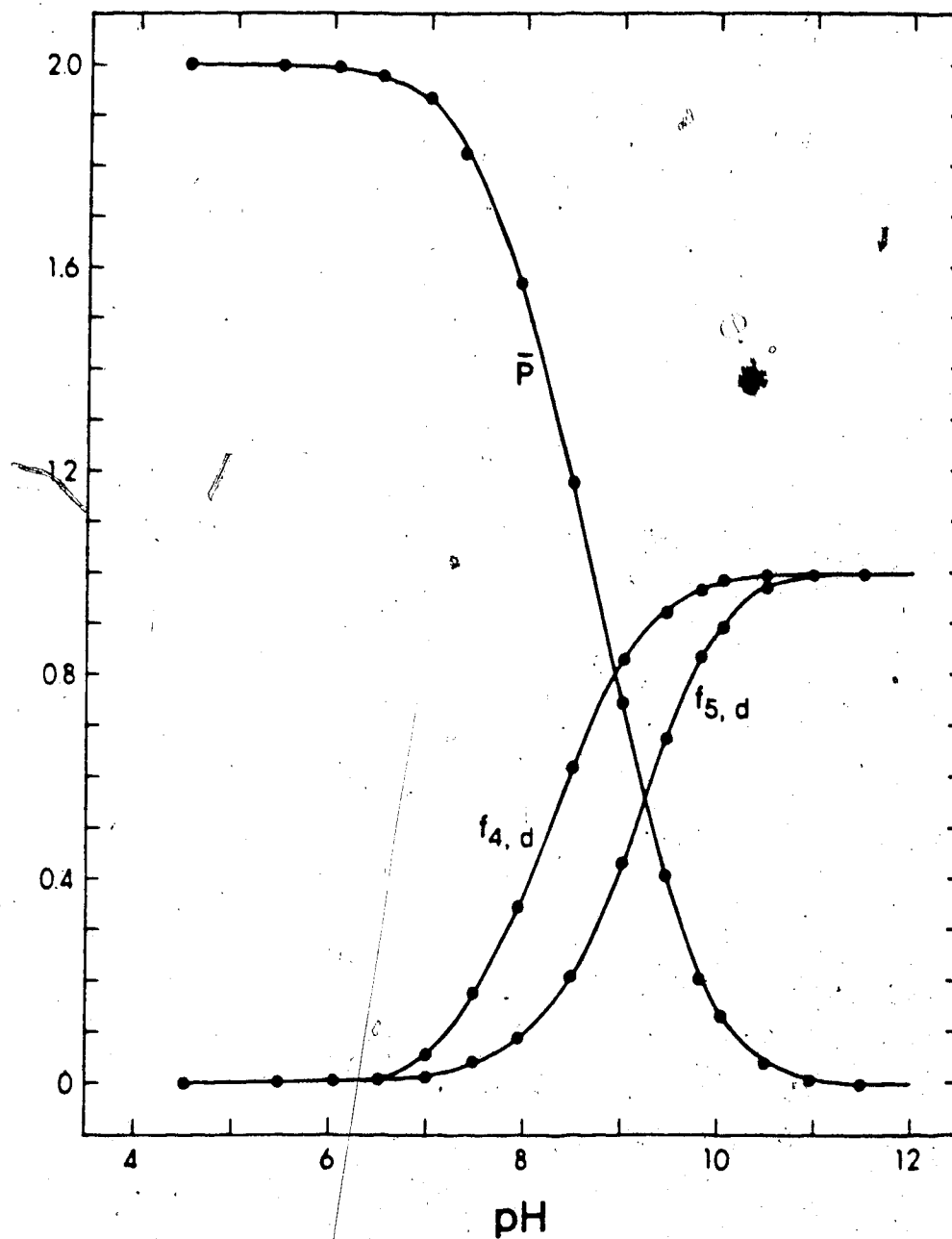


Figure 32. The pH dependence of the fractional titration of the penicillamine ($f_{4,d}$) and glutamyl ($f_{5,d}$) ammonium groups of PSSG and the average number of ammonium protons per PSSG molecule (\bar{p}). The smooth curve through the \bar{p} data is the theoretical curve calculated with Equation 79 and the constants in Table 7.

between pH 7.5 and 10.5 in Figure 31) is 4.38 with a standard deviation of 0.53. The microconstants listed in Table 8 for PSSG were calculated from this average ratio and the macroconstants using Equations 67, 68, 87 and 88 as shown earlier.

Figure 33 shows the pH dependence of the distribution of PSSG among its various ammonium protonated forms using the macroconstants and microconstants listed in Table 7 and 8 respectively. The pH dependence of the distribution of PSSG among species II and III was calculated using equations similar to Equations 91 and 92.

D. Chemical Shift Data for the Penicillamine/Cystine System

Spectra A, B, D and E in Figure 34 are ^1H NMR spectra of 0.2 M PSH, 0.2 M CSSC, 0.4 M CSH and 0.01 M PSSP solutions, respectively at pH 10 in D_2O . Spectrum C is for a solution containing a mixture of 0.1 M PSH and 0.1 M CSSC. The spectrum was obtained a few hours after mixing. The structural formulae of these thiols and disulfides are shown in Figure 14.

The ^1H spectra of PSH and PSSP were discussed previously. The ^1H NMR spectrum of CSH (Figure 34D) consists of an ABX pattern. The AB part is centered at

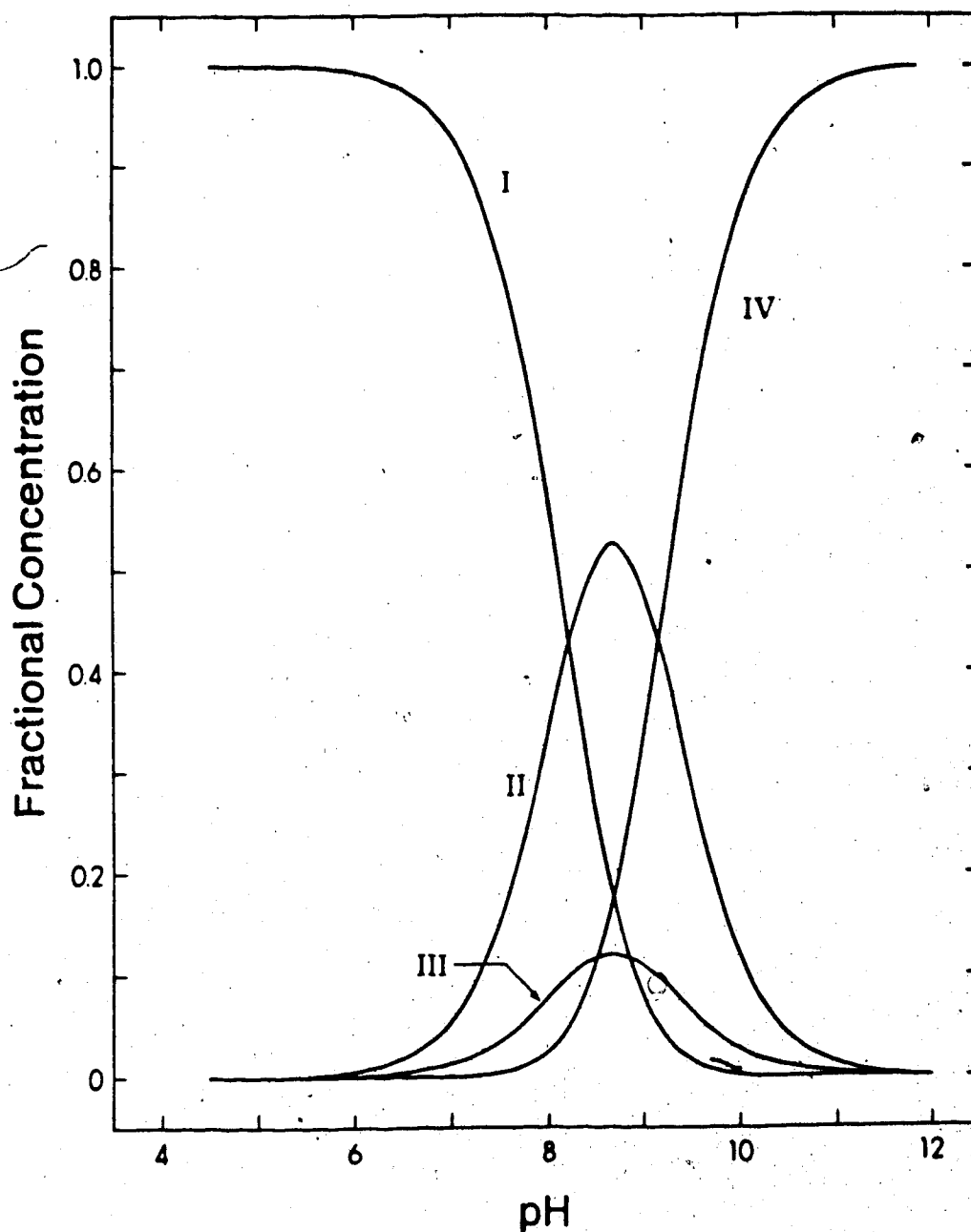


Figure 33. Species distribution diagram of the mixed disulfide, PSSG. Numbers refer to the various deprotonated forms in Figure 30; the solid curves were generated with $pK_{a1234} = 8.22$, $pK_{a1235} = 8.86$, $pK_{A4} = 8.13$ and $pK_{A5} = 9.24$.

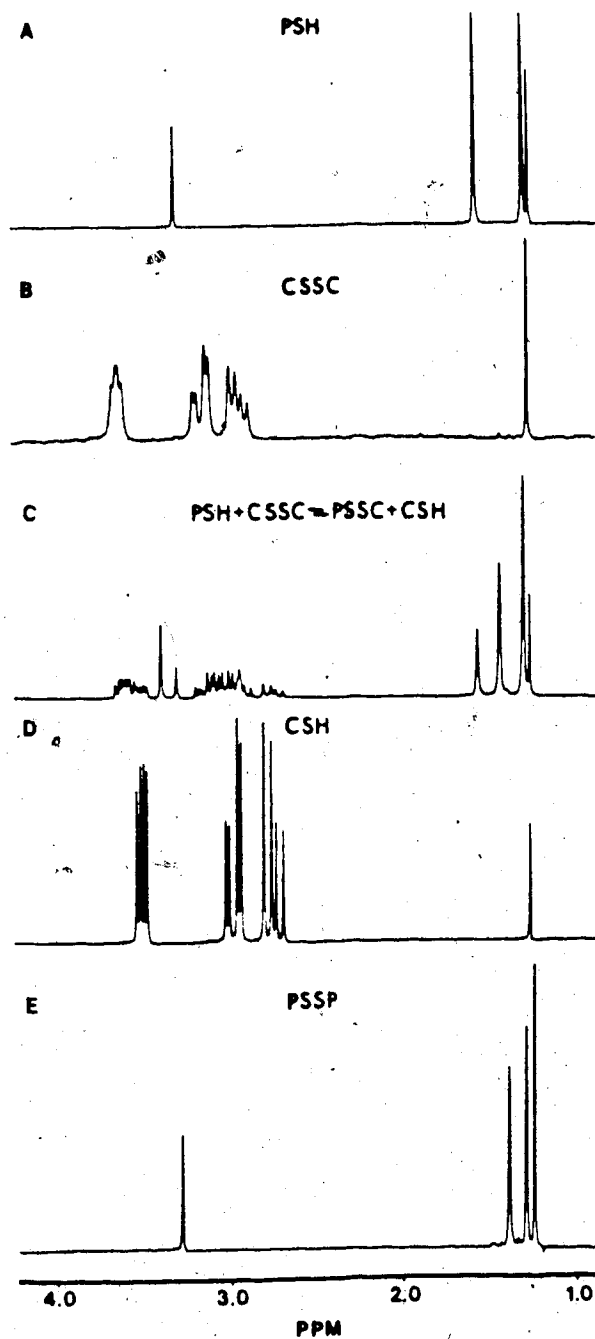


Figure 34. 200 MHz ^1H NMR spectra in D_2O of A) 0.2 M PSH, B) 0.2 M CSSC, C) 0.1 M PSH + 0.1 M CSSC, D) 0.4 M CSH, and E) 0.01 M PSSP at pH 10 and at the ambient probe temperature of 26°C .

2.83 ppm and is from the two nonequivalent methylene protons on C_β , while the X part, centered at 3.48 ppm, is from the methine proton on C_α . Figure 34B shows the spectrum of CSSC which also consists of an ABX pattern with the same assignment. In spectrum C, the spectrum shows additional resonances besides those from PSH and CSSC. These are assigned to PSSC and CSH. As will be shown later in Chapter V, PSH reacts readily with CSSC, on this time scale, to produce both PSSC and CSH. However, the rate of reaction of the mixed-disulfide, PSSC with a second PSH molecule to form PSSP and CSH is much slower, so that no detectable amount of PSSP is observed as shown in Figure 34C. Table 9 gives the resonance assignments for the spectra of PSH, CSSC, CSH, PSSP and PSSC in Figure 34.

The ^1H NMR spectrum of PSSC consists of a singlet at 3.37 ppm from the methine proton on the C_α part of PSH and a multiplet at 3.5 ppm due to the X part from the methine proton on C_α of the cysteine part of the molecule. The AB part is centered at 2.9 ppm and is from the two nonequivalent methylene protons on C_β of the cysteine part of the molecule. The CH_α resonance of the PSH part of PSSC is well resolved from that of PSH, PSSP and PSSC (CSH part) and from the CH_2 resonances of the cysteine moiety of the three CSH-containing molecules over a wide pH

Table 9. Assignments of the ^1H resonances of PSH, PSSP, CSH, CSSC and PSSC resonances in Figure 34.

Molecule	Chemical Shift, ppm vs DSS	Group Assignment
TBA	1.2397	CH_3
PSH	1.27	CH_3
	1.55	CH_3
	3.29	CH_α
CSSC	2.8-3.2	$\text{CH}_2\beta(\text{AB})$
	3.5-3.6	$\text{CH}_\alpha(\text{X})$
CSH	2.6-2.8	$\text{CH}_2\beta(\text{AB})$
	3.4-3.5	$\text{CH}_\alpha(\text{X})$
PSSP	1.29	CH_3
	1.39	CH_3
	3.28	CH_α
PSSC	1.28	CH_3
	1.41	CH_3
	2.6-3.2	$\text{CH}_2\beta(\text{AB})$
	3.37	$\text{CH}_\alpha(\text{PSH part})$
	3.4-3.6	$\text{CH}_\alpha(\text{X})$

range, as shown by the chemical shift data plotted in Figure 35. The equilibria and kinetics of the thiol/disulfide exchange reactions were characterized using the methine as well as the methyl resonances described next.

The ^1H nuclei of the two methyl groups of PSSC give two separate resonances at 1.28 and 1.41 ppm due to the asymmetric center at the α -carbon as in PSH, PSSP and PSSG.

To illustrate the resolution between methyl resonances for the various species, spectra for the methyl protons of PSSC in a mixture containing PSH, PSSP and PSSC are shown in Figure 36. Assignments in Figure 36 were made by comparison with spectra A, B, D and E in Figure 34. Figure 35 shows the chemical shift of the two methyl resonances of PSSC together with those of PSH and PSSP for comparison. The chemical shift data plotted in Figure 35 for PSH and PSSP are those described earlier in Figure 19. The figure shows that the high field methyl resonance of PSSC is well resolved from the PSH and PSSP resonances, whereas those of PSH and PSSP overlapped at $\text{pH} < 1$. However, as will be shown in Chapter V, there is little PSSP formed in the reaction of PSH with CSSC and thus the overlap of PSH and PSSP resonances is not a problem. In the intermediate pH range 3-8, the overlap between the

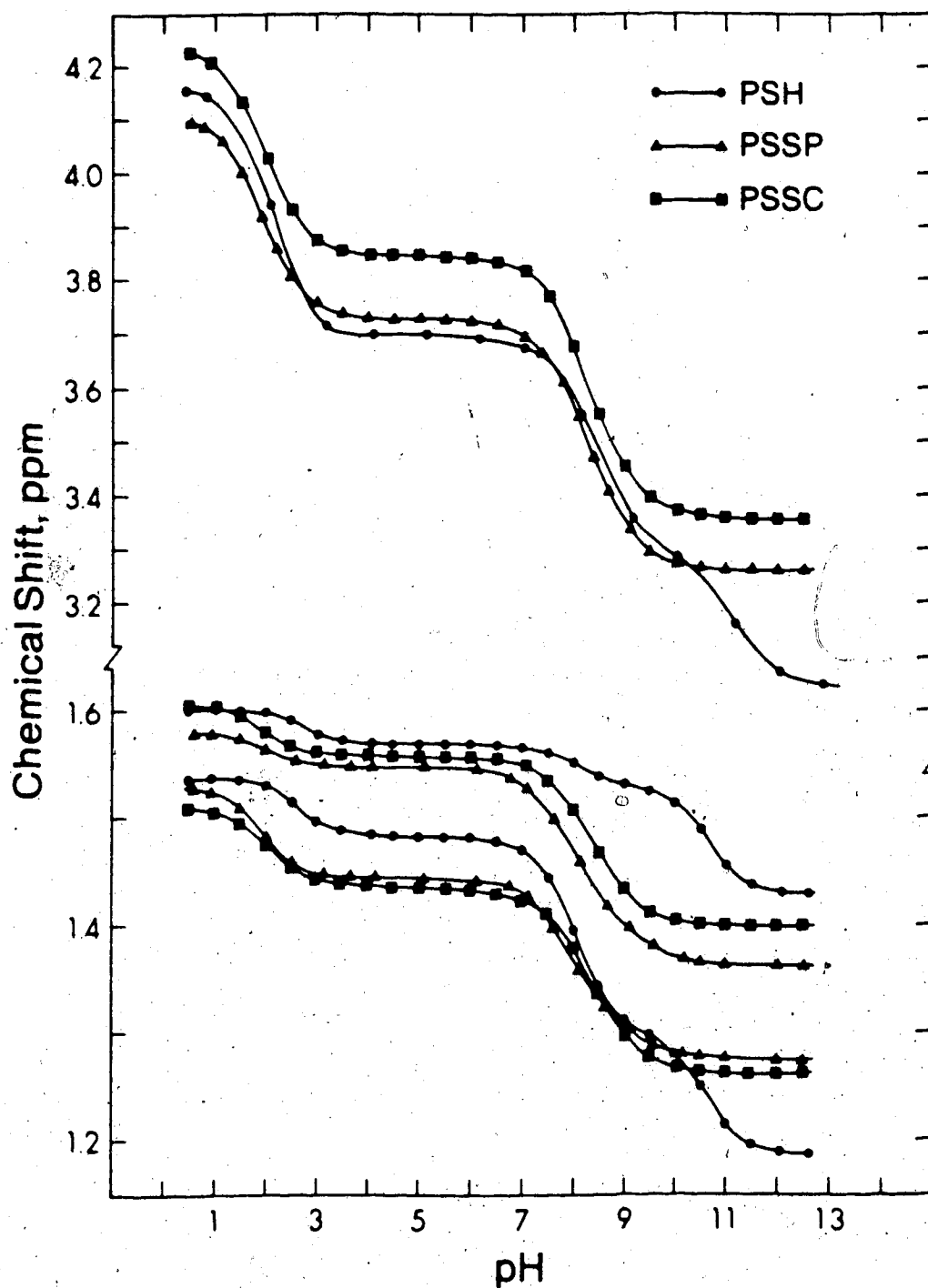


Figure 35. Chemical shifts of the methine and methyl protons of PSH, PSSP and the PSH part of PSSC as a function of pH.

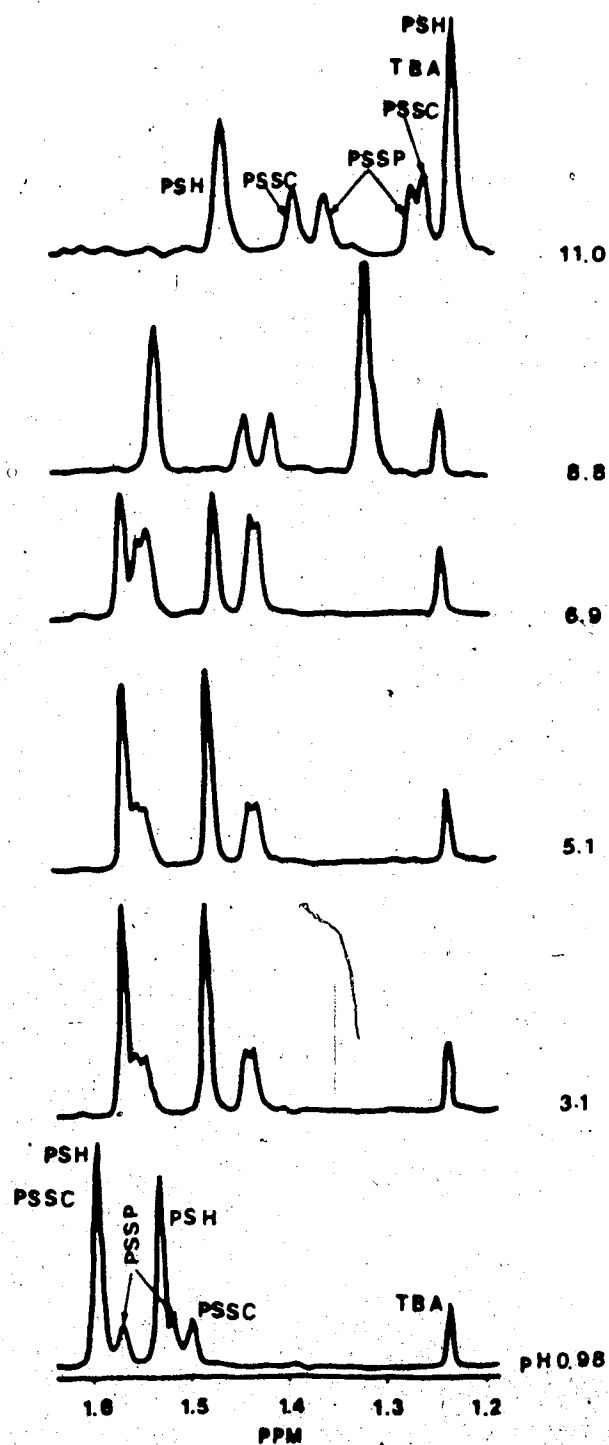


Figure 36. Methyl region of the 200 MHz ^1H NMR spectra of a mixture of PSH, PSSP and CSSC. The original concentrations consisted of 0.008 M PSH, 0.001 M PSSP, 0.002 M CSSC and 0.0007 M TBA in 1 M KCl aqueous solution containing 0.003 M EDTA.

PSSC and PSSP methyl resonances is quite extensive. In order to detect small amounts of PSSP unambiguously in these cases, i.e. during equilibrium and time course studies of the reaction, the pH of the reaction solution was adjusted to either a low or high pH value in order to achieve an increase in resolution. This will be discussed in greater detail in Chapter V.

The ^1H chemical shift data for PSSC in Figure 35 were for a solution prepared by mixing 0.03 M PSH and 0.09 M cystine at pH 8.8. After reaction for 15 minutes, the solution was bubbled with air for 3 days to oxidize the CSH and PSH to CSSC and PSSP. The final concentrations of PSSP and PSSC were 0.003 M and 0.03 M respectively as determined from the relative areas of the various methyl resonances. Due to its low solubility, CSSC precipitates from the solution. The concentration of CSSC remaining in solution was small enough that it did not interfere with the chemical shift measurements of other resonances such as the CH and CH_2 resonances of the cysteine part of PSSC.

1. Acid Dissociation Constants of CSH

CSH contains the same acidic groups as PSH, and thus its acid/base chemistry is described by the deprotonation scheme shown in Figure 21 for PSH.

Literature values for K_{A1} , K_{A2} and K_{A3} are listed in Table 7. The fractional concentrations of the various protonated forms of CSH calculated from the three macroconstants are shown in Figure 37 as a function of pH. The species distribution of HA between CSH species III and IV in Figure 21 was calculated using literature values for the microconstants k_{a12} and k_{a13} . α_{III} and α_{IV} were calculated using Equations 91 and 92. The literature value for pK_{a12} [97-100] corrected to the ionic strength conditions used in this work is 8.48. Other microconstants were calculated from this value and macroconstants in Table 7 and the results are listed in Table 8. As shown in Figure 37, the species distributions of III and IV of CSH, in the pH region 6-12, are almost equal. This contrasts with the distribution of species III and IV of PSH in Figure 22 where the fractional concentration of III is much greater than that of IV.

2. Acid Dissociation Constants of CSSC

The deprotonation scheme of cystine is shown in Figure 26. Literature values for K_{A1} , K_{A2} , K_{A3} and K_{A4} are listed in Table 7. Fractional concentrations calculated from the four macroconstants are plotted in Figure 38. As with PSSP and GSSG, the microscopic constants for the ammonium groups are simply related to

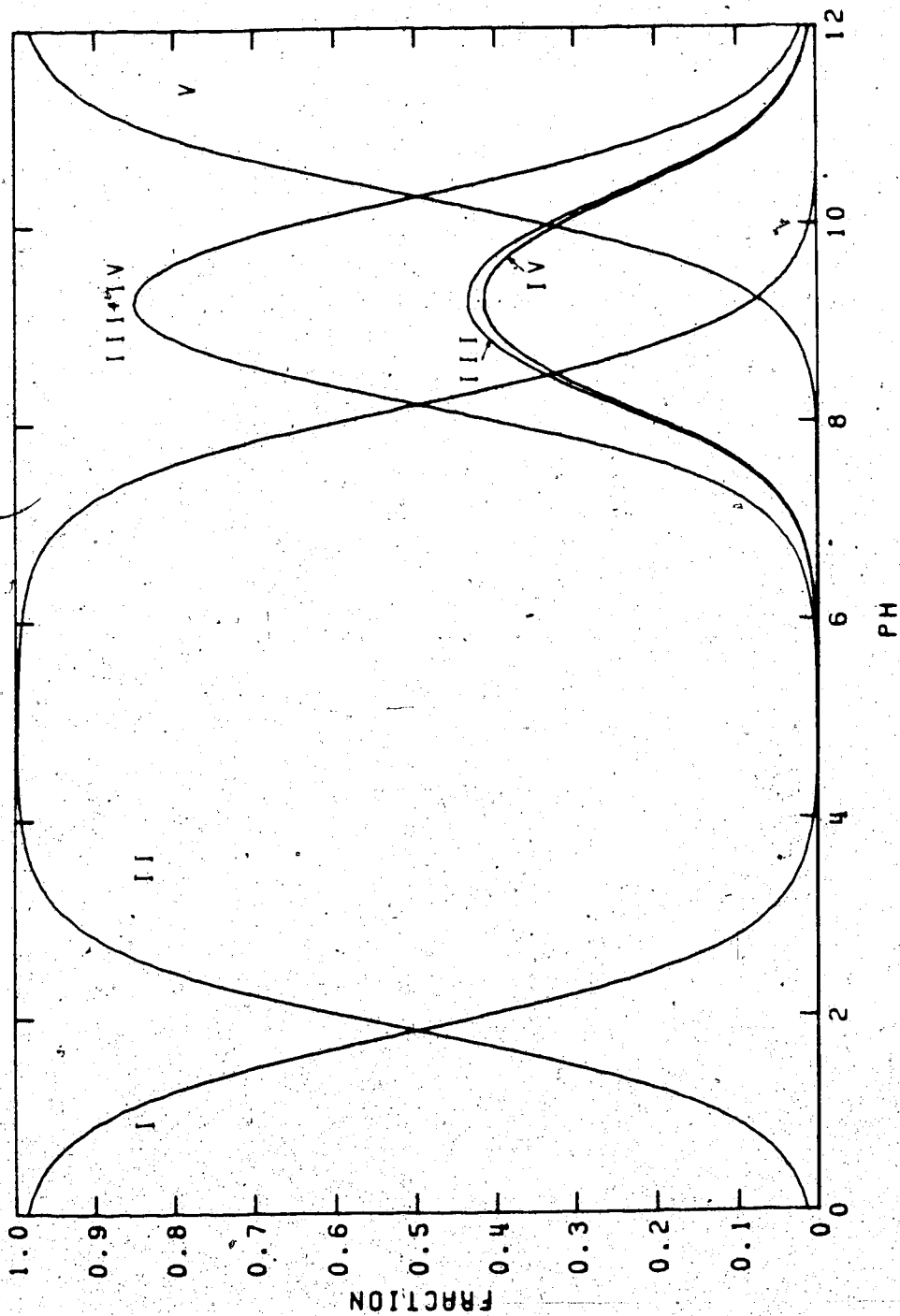


Figure 37. Species distribution diagram for CSH. Numbers refer to the various protonated forms shown in Figure 21. The fractional concentrations were calculated with $pK_{A1} = 1.87$, $pK_{A2} = 8.19$, $pK_{A3} = 10.29$, $pK_{A2} = 8.48$ and $pK_{A3} = 8.50$.

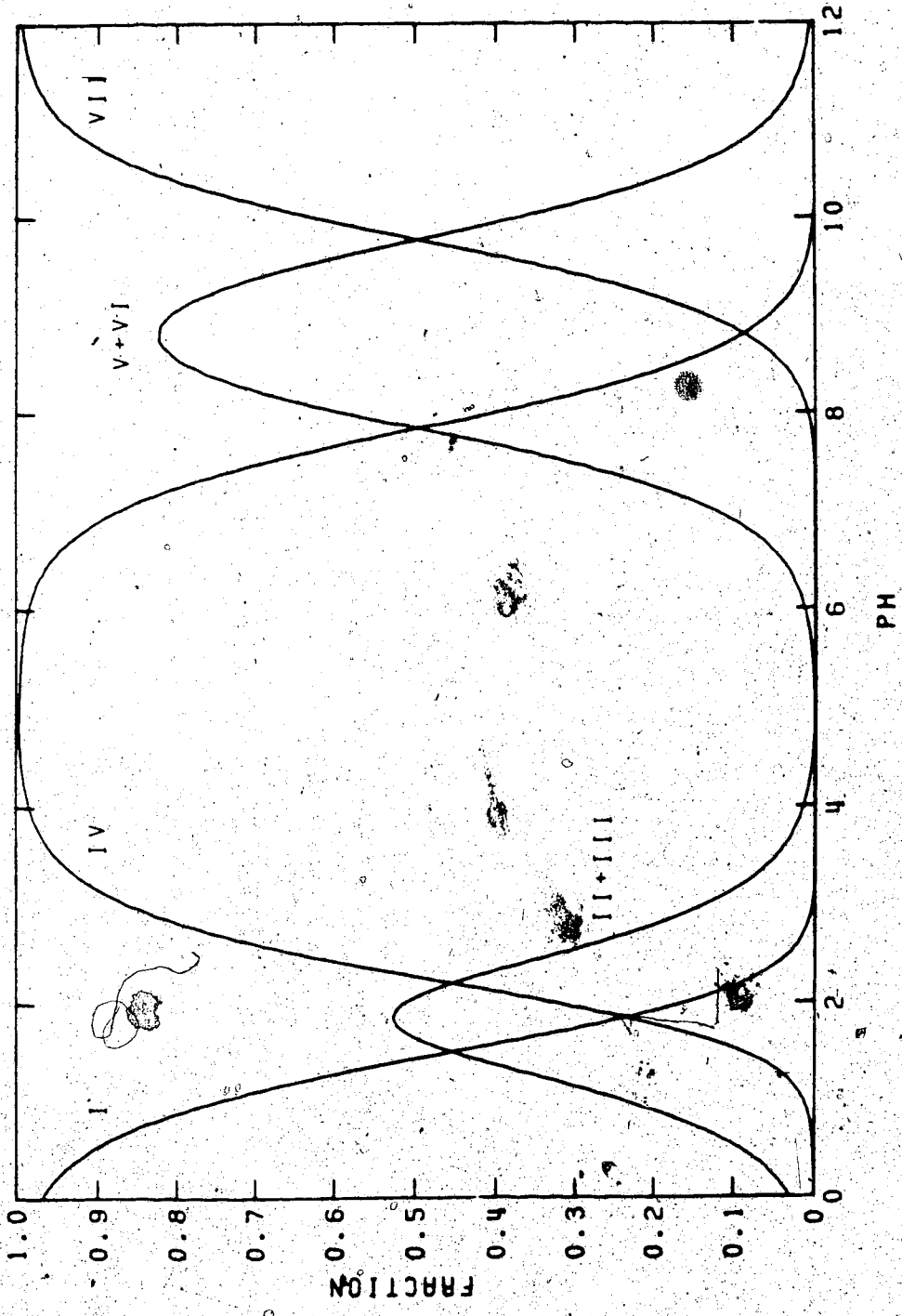


Figure 38. Species distribution diagram for CSSC. The various deprotonated forms associated with the numbers are shown in Figure 26. These curves were generated with $pK_{A1} = 1.51$, $pK_{A2} = 2.21$, $pK_{A3} = 7.88$ and $pK_{A4} = 9.30$.

their macroscopic constants by the equations, $k_{a123} = k_{a124} = K_{A3}/2$ and $k_{a1234} = k_{a1243} = 2K_{A4}$.

3. Acid Dissociation Constants of PSSC

The deprotonation scheme for PSSC is shown in Figure 26. There are no literature values for the four macroconstants of PSSC, $K_{A1} - K_{A4}$. These four values were determined by ^1H NMR using the methine chemical shift data of Figure 35.

The ^1H chemical shift data (Figure 35) for the CH_α resonances of the penicillamine in and cysteine moieties of PSSC were used to calculate the fractional titration of the two carboxylic groups of PSSC ($f_{1,d}$ and $f_{2,d}$) over the pH range 1-5 using Equation 85.

Since the proton on the C_α carbon of the penicillamine part of the molecule is seven bonds removed from the carboxylic acid group of the cysteine part, changes in the chemical shift of the proton on the penicillamine C_α carbon over the pH range 1-5 are assumed to be due only to titration of the penicillamine carboxylic acid group. Likewise, changes in the chemical shift of the cysteine C_α proton are assumed to be due to titration of the cysteine carboxylic acid group. Hence, the chemical shift data were treated by the unique resonance method using Equation 86 to calculate \bar{p} . The

macroscopic constants, K_{A1} and K_{A2} , were obtained by fitting \bar{p} versus pH data to Equation 79 as described earlier. The values obtained are listed in Table 7.

Macroscopic constants K_{A3} and K_{A4} were also calculated from the chemical shift data for the two α protons over the pH range 4-12. Again, the data were treated by the unique resonance method. Fractional titration of each of the two ammonium groups ($f_{3,d}$ and $f_{4,d}$) was calculated as a function of pH from the chemical shift data in the pH range 4-12. The ammonium groups of the PSH and CSH parts are labelled 3 and 4 respectively. Figure 39 shows the two fractional titrations as a function of pH. \bar{p} was then calculated and the results used to obtain K_{A3} and K_{A4} . \bar{p} data are shown as a function of pH in Figure 39.

Microconstants were calculated from the macroconstants by calculating the average ratio of the concentrations of species V and VI (Figure 26), which is equal to the ratios k_{a123}/k_{a124} and k_{a1243}/k_{a1234} . The average value obtained for the ratio using Equation 88 is 1.70 ± 0.05 from data at 21 pH values. The microconstants were calculated using this value and Equations 67, 68 and 87 as described earlier. The results are listed in Table 8.

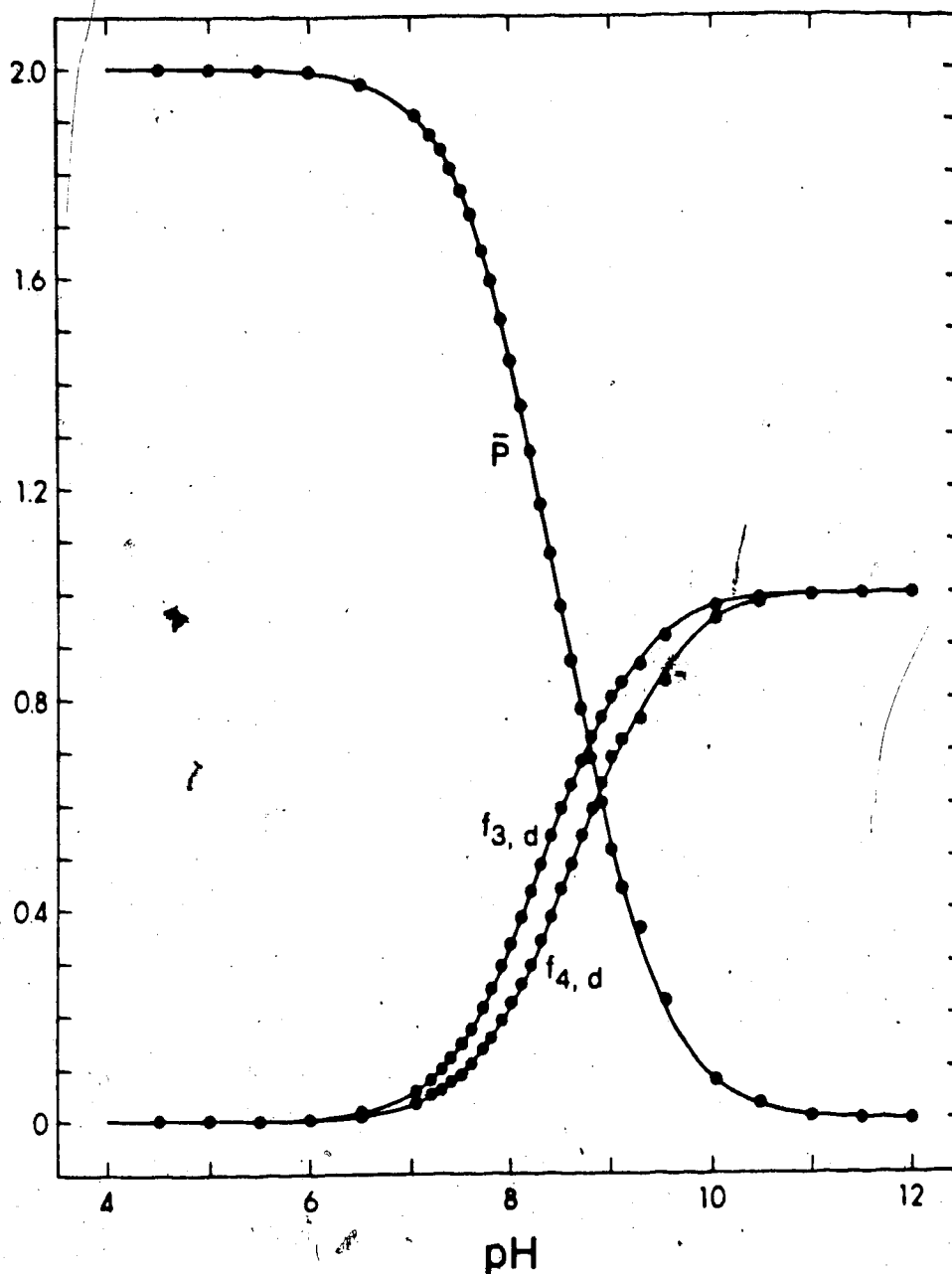


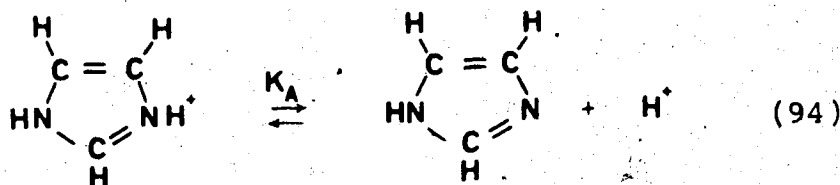
Figure 39. The pH dependence of the fractional titration of the penicillamine ($f_{3,d}$) and cysteine ($f_{4,d}$) ammonium groups of PSSC and the average number of ammonium groups per molecule (\bar{p}). The smooth curve through the \bar{p} data is the theoretical curve calculated with Equation 79 for the values of K_{A3} and K_{A4} listed in Table 7.

The species distribution diagram for PSSC is shown in Figure 40.

E. pH Dependence of the Chemical Shifts for the ^1H Resonances of Imidazole

Because it was not convenient to measure the pH of some solutions in the thiol/disulfide exchange experiments, imidazole was used as an internal pH indicator. The basis of the method is that the chemical shifts of the ^1H NMR resonances for imidazole are pH dependent. This pH dependence is characterized in this section for use in the later studies.

The acid dissociation equilibrium for imidazole is:



The acid dissociation equilibrium for imidazole can be expressed as:

$$\text{pH} = \text{p}K_A + \log \frac{[\text{A}]}{[\text{HA}]} \quad (95)$$

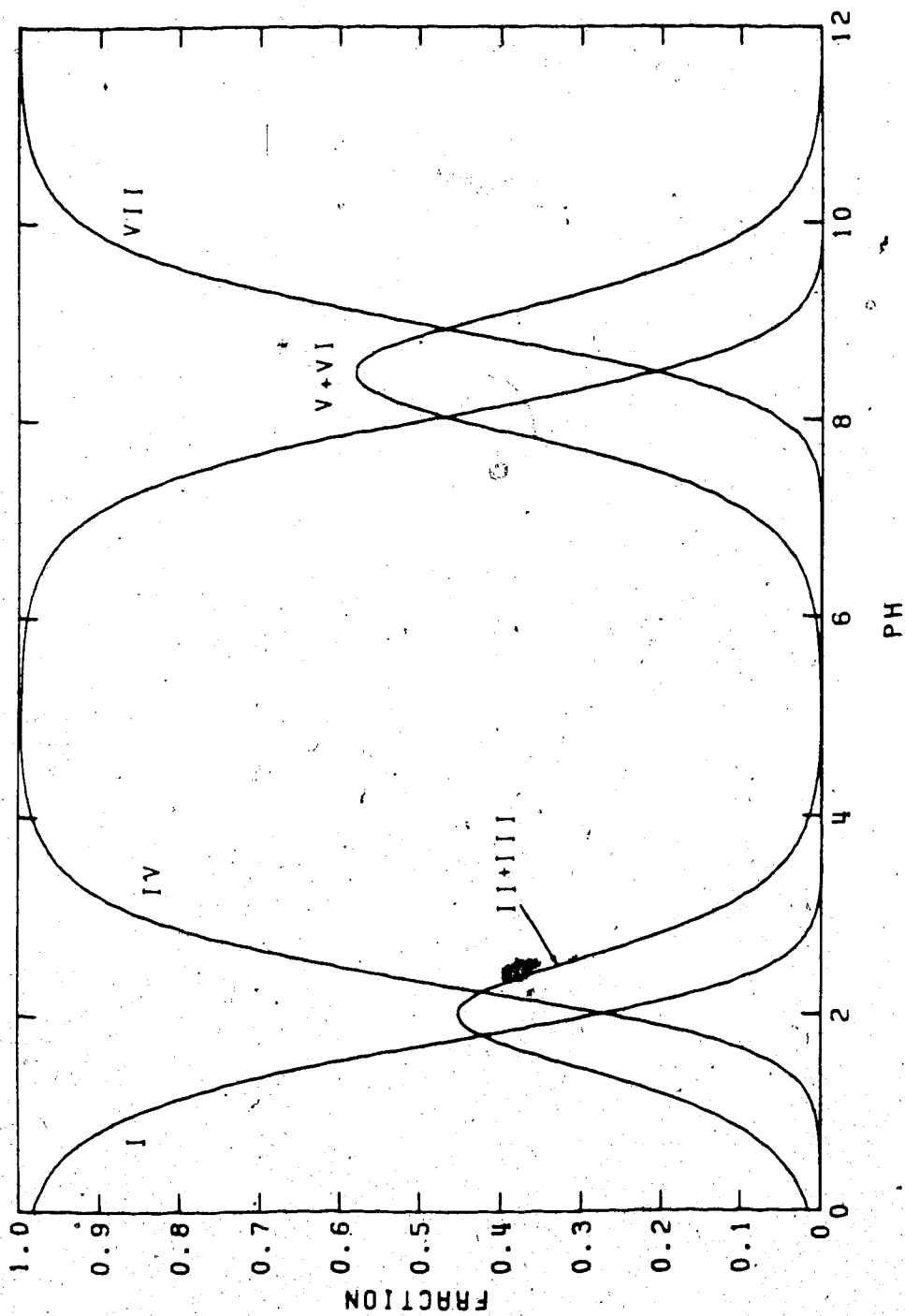


Figure 40. Species distribution diagram for PSSC. See Figure 26 for the protonated forms associated with the numbers. The fractional concentrations were calculated with $pK_{A1} = 1.80$, $pK_{A2} = 2.24$, $pK_{A3} = 8.04$ and $pK_{A4} = 8.93$.

In the NMR experiment, the fractions in the protonated (f_{HA}) and deprotonated (f_A) forms are obtained from the chemical shift data, rather than the concentrations.

Since $[A] = f_A([HA] + [A])$ and $[HA] = f_{HA}([HA] + [A])$, Equation 95 can be rewritten as

$$pH = pK_A - \log \frac{f_A}{f_{HA}} \quad (96)$$

f_A and f_{HA} can be expressed in terms of the observed chemical shift as:

$$f_A = \frac{\delta_{obsd} - \delta_{HA}}{\delta_A - \delta_{HA}} \quad (97)$$

$$f_{HA} = \frac{\delta_A - \delta_{obsd}}{\delta_A - \delta_{HA}} \quad (98)$$

Substitution of these equations into Equation 96 yields

$$pH = pK_A + \log \left(\frac{\delta_{obsd} - \delta_{HA}}{\delta_A - \delta_{obsd}} \right) \quad (99)$$

If δ_A , δ_{HA} and pK_A are known, the pH can be calculated from δ_{obsd} .

^1H NMR spectra for imidazole are shown as a function of pH in Figure 41. Each spectrum consists of two singlets of relative intensity approximately 1:2, corresponding to the protons C2-H and C4,5-H respectively. Chemical shift data are presented as a function of pH in Figure 42. These data were treated by the method described at the beginning of this chapter for a monoprotic acid. Values of 7.28 ± 0.01 and 7.27 ± 0.01 were obtained for the pK_A from the C2-H and C4,5-H data, respectively. These are in good agreement with the literature values of 7.11 [101] and 7.15 [102] adjusted to the present ionic strength conditions. Although good estimates of the chemical shifts for the HA and A forms of imidazole could be obtained from the low and high pH chemical shift data, δ_{HA} and δ_{A} were also treated as unknowns in the non-linear least squares curve fitting calculations. The values obtained for δ_{HA} and δ_{A} are: 8.7000 ± 0.0007 ppm and 7.7820 ± 0.0008 ppm for C2-H and 7.4892 ± 0.0005 ppm and 7.1380 ± 0.0006 ppm for C4,5-H. The equations which relate the observed chemical shift to pH are, for the C2-H and C4,5-H resonances, respectively:

$$\text{pH} = 7.28 + \log \left(\frac{\delta_{\text{obsd}} - 8.7000}{7.7820 - \delta_{\text{obsd}}} \right) \quad (100)$$

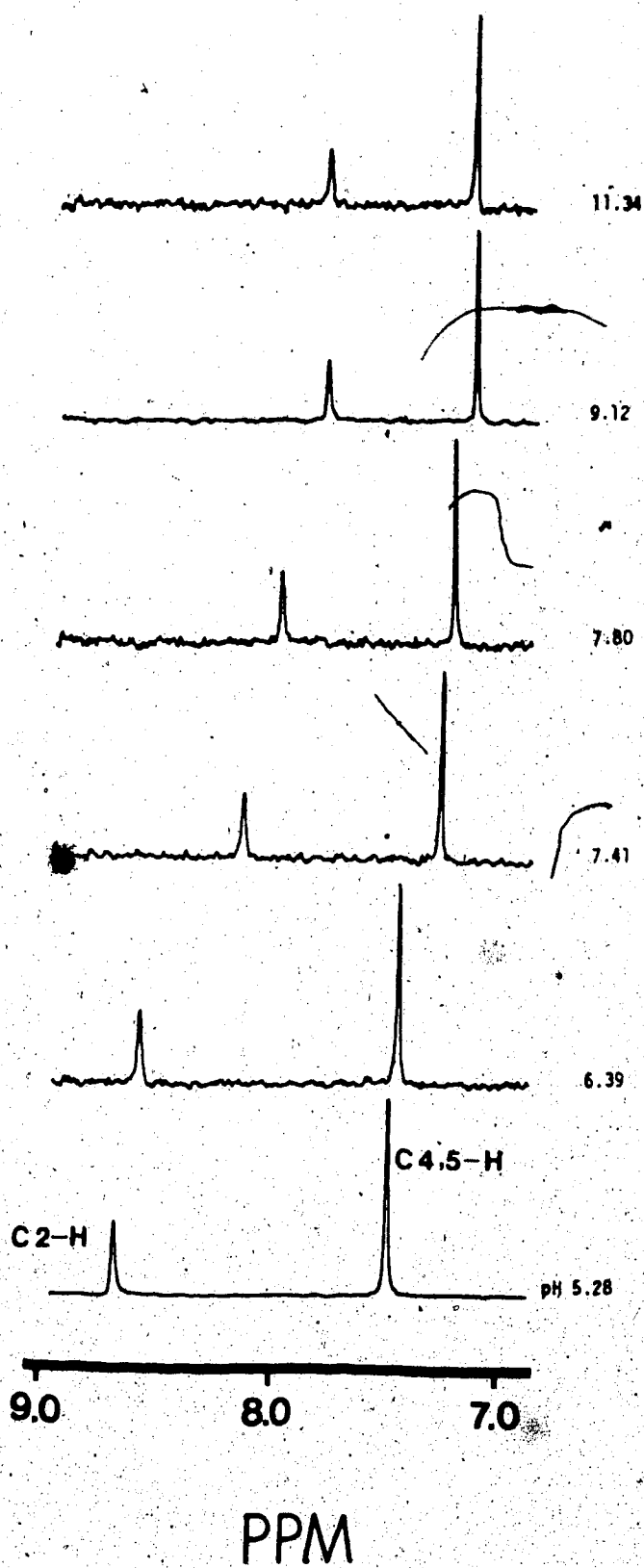


Figure 41. ^1H NMR spectra at 200 MHz of 0.05 M imidazole in 1 M aqueous KCl, 0.003 M EDTA solution.

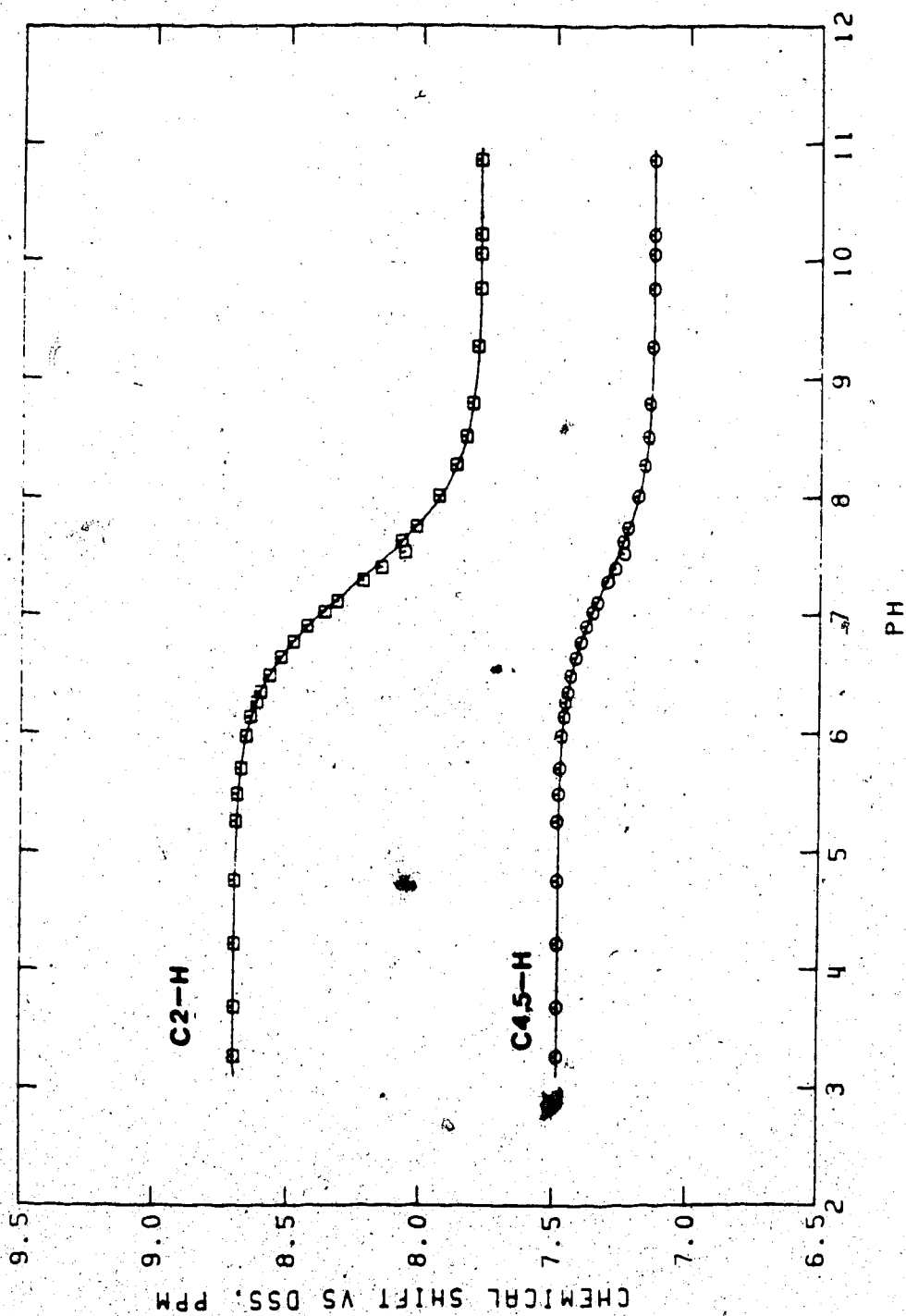


Figure 42.

^1H chemical shift data of the C2-H and C4,5-H resonances of imidazole.

Solution conditions are as in Figure 41. The smooth curves through the experimental points are theoretical curves calculated with Equations 100 and 101.

$$\text{pH} = 7.27 + \log \left(\frac{\delta_{\text{obsd}} - 7.4892}{7.1380 - \delta_{\text{obsd}}} \right) \quad (101)$$

The most accurate values of pH can be obtained from imidazole chemical shifts over the pH range 6.3-8.3.

(Outside this range, the chemical shifts approach those of the HA and A species, and small errors in chemical shift measurement result in relatively large errors in pH.

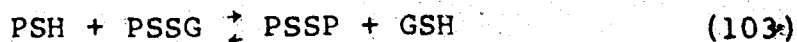
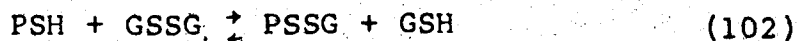
CHAPTER IV

EQUILIBRIA AND KINETICS OF PENICILLAMINE/OXIDIZED GLUTATHIONE THIOL/DISULFIDE EXCHANGE REACTIONS

A. Introduction

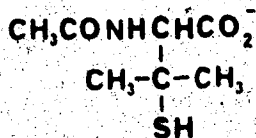
As discussed in Chapter I, thiol/disulfide exchange reactions involving penicillamine (1 in Figure 14) are of importance for the understanding of penicillamine metabolism. In this chapter, the equilibria and kinetics of the thiol/disulfide exchange reactions for the penicillamine/glutathione system are characterized over a range of solution conditions. Glutathione is generally the most abundant non-protein thiol in cellular systems, e.g. it is present at the 0.002 M level in human erythrocytes [108,109]. The reduced form, GSH (4 in Figure 14), is in equilibrium with its oxidized form, GSSG (5 in Figure 14), and the equilibrium favors the GSH form. For example, in healthy human erythrocytes, greater than 99% of the glutathione is in the GSH form [110]. However in blood plasma, the extracellular fluid contains a small amount of GSSG and no measurable amount of GSH [111].

The thiol/disulfide exchange reactions for the PSH/GSSG system are described by



As shown in Chapter III, the five species involved in these two reactions exist in various protonated forms, depending on the solution pH, and thus, the equilibria and kinetics of these two reactions are expected to be pH dependent. In this chapter, these reactions have been studied over the pH range 4-10. First, the equilibria and then the kinetics of the reactions are described.

The equilibria and kinetics for the oxidation of N-acetyl-D,L-penicillamine (N-PSH, XIX) by glutathione disulfide at neutral pH are also reported.



XIX

In the above studies, glutathione disulfide was chosen because of its natural occurrence in biological systems [111,112], because it is involved in the

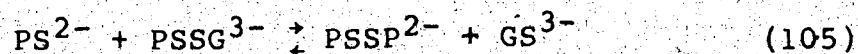
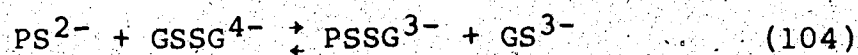
metabolism of PSH [28] and, because, to a first approximation, it serves as a model for disulfide bonds in proteins since its cystine is placed between two amino acid residues.

B. Determination of Equilibrium Constants

As mentioned above, the equilibrium constants for reactions 102 and 103 are expected to be pH dependent because of the acid/base reactions involving amino, thiol and carboxylic acid groups over the pH range studied. These pH dependent equilibrium constants can be expressed in terms of the acid dissociation constants of the reactants and products and the equilibrium constants for the equilibria written in terms of the fully deprotonated species according to the model shown below.

1. The Model

The thiol/disulfide exchange reactions, written in terms of all species in their fully deprotonated forms are:



where the various species are defined in Figures 21, 23, 26, 28 and 30 in Chapter III. The exchange equilibrium constants for these reactions are

$$K_1 = \frac{[\text{PSSG}^{3-}][\text{GS}^{3-}]}{[\text{PS}^{2-}][\text{GSSG}^{4-}]} \quad (106)$$

$$K_2 = \frac{[\text{PSSP}^{2-}][\text{GS}^{3-}]}{[\text{PS}^{2-}][\text{PSSG}^{3-}]} \quad (107)$$

Experimentally, equilibrium constants for reactions 102 and 103 were measured over a range of pH values. Since their magnitude depends on pH, due to protonation reactions occurring simultaneously, these equilibrium constants are conditional equilibrium constants and will be referred to as K_{1c} and K_{2c} .

$$K_{1c} = \frac{[\text{PSSG}]_t [\text{GSH}]_t}{[\text{PSH}]_t [\text{GSSG}]_t} \quad (108)$$

$$K_{2c} = \frac{[\text{PSSP}]_t [\text{GSH}]_t}{[\text{PSSG}]_t [\text{PSH}]_t} \quad (109)$$

where $[\text{PSH}]_t$ is the sum of the various protonated forms of PSH, etc. K_1 is related to K_{1c} as follows. The reaction scheme, including protonation reactions of importance over the pH range studied, is given in Figure 43. The acid

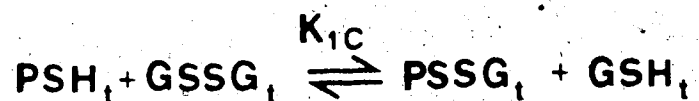
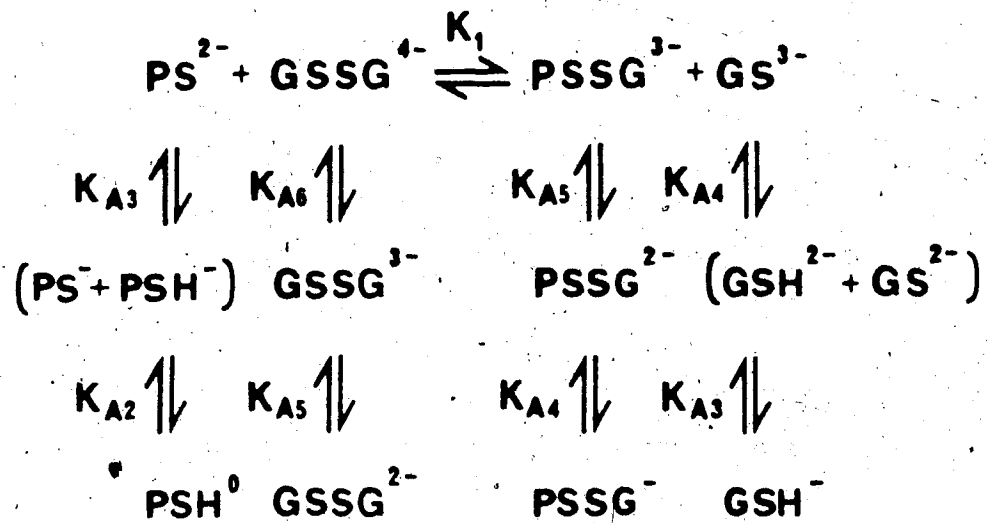


Figure 43. The model used to evaluate equilibrium and kinetic data for the PSH/GSSG exchange reaction in the pH range 4-10.

dissociation constants are defined and their values given in Chapter III. At a given pH, the fractional concentrations of PSSG^{3-} , GS^{3-} , PS^{2-} and GSSG^{4-} are given by $\alpha_1 - \alpha_4$ respectively.

$$\alpha_1 = \frac{[\text{PSSG}^{3-}]}{[\text{PSSG}]_t} = \frac{K_{A4} K_{A5}}{a_H^2 + a_H K_{A4} + K_{A4} K_{A5}} \quad (110)$$

$$\alpha_2 = \frac{[\text{GS}^{3-}]}{[\text{GSH}]_t} = \frac{K_{A3} K_{A4}}{a_H^2 + a_H K_{A3} + K_{A3} K_{A4}} \quad (111)$$

$$\alpha_3 = \frac{[\text{PS}^{2-}]}{[\text{PSH}]_t} = \frac{K_{A2} K_{A3}}{a_H^2 + a_H K_{A2} + K_{A2} K_{A3}} \quad (112)$$

$$\alpha_4 = \frac{[\text{GSSG}^{4-}]}{[\text{GSSG}]_t} = \frac{K_{A5} K_{A6}}{a_H^2 + a_H K_{A5} + K_{A5} K_{A6}} \quad (113)$$

Rearrangement of these equations and substitution into Equation 108 yields:

$$K_{1c} = \frac{[\text{PSSG}^{3-}][\text{GS}^{3-}]}{[\text{PS}^{2-}][\text{GSSG}^{4-}]} \left(\frac{\alpha_3 \alpha_4}{\alpha_1 \alpha_2} \right) \quad (114)$$

from which the equation

$$K_{1c} = K_1 \left(\frac{\alpha_3 \alpha_4}{\alpha_1 \alpha_2} \right) \quad (115)$$

is obtained. According to Equation 115, K_1 can be calculated from K_{1C} , using values for $\alpha_1 - \alpha_4$ which can be calculated for the pH at which K_{1C} is measured.

K_2 can be related to K_{2C} by the same approach. The result is:

$$K_{2C} = K_2 \left(\frac{\alpha_1 \alpha_3}{\alpha_2 \alpha_5} \right) \quad (116)$$

where $\alpha_1 - \alpha_3$ are defined by Equations 110-112 and

$$\alpha_5 = \frac{[\text{PSSP}^{2-}]}{[\text{PSSP}]_t} = \frac{K_{A3} K_{A4}}{a_H^2 + a_H K_{A3} + K_{A3} K_{A4}} \quad (117)$$

2. Determination of Equilibrium Concentrations

^1H NMR spectra of reaction mixtures containing the various species involved in reactions 102 and 103 were characterized in Chapter III. As described in Chapter III, well-resolved methyl resonances are observed for the three different forms of penicillamine (PSH, PSSG and PSSP). The equilibrium constants, K_{1C} and K_{2C} were determined using equilibrium concentrations calculated from the intensities of the methyl resonances for different solution conditions by the following procedures. First, the areas of well resolved resonances

for PSH, PSSG, and in some cases, PSSP, were determined as described in Chapter II. The fraction (f) of the total penicillamine in each of these three forms was then calculated from the relative areas using Equations 118-120.

$$f_{\text{PSH}} = \frac{\text{area PSH resonance}}{\text{total area}} \quad (118)$$

$$f_{\text{PSSG}} = \frac{\text{area PSSG resonance}}{\text{total area}} \quad (119)$$

$$f_{\text{PSSP}} = \frac{\text{area PSSP resonance}}{\text{total area}} \quad (120)$$

where total area equals the sum of the areas for the PSH, PSSG and PSSP resonances. Concentrations of the three penicillamine species were then calculated from these fractions and the initial PSH concentrations, $[\text{PSH}]_0$, with Equations 121-123.

$$[\text{PSH}]_t = f_{\text{PSH}} [\text{PSH}]_0 \quad (121)$$

$$[\text{PSSG}]_t = f_{\text{PSSG}} [\text{PSH}]_0 \quad (122)$$

$$[\text{PSSP}]_t = f_{\text{PSSP}} [\text{PSH}]_0 / 2 \quad (123)$$

The factor 2 in Equation 123 accounts for the fact that for each methyl resonance of PSSP, 6 methyl hydrogens are involved versus 3 for each of the methyl resonances of PSH and PSSG. The equilibrium concentrations of GSH and GSSG were then calculated from these concentrations and $[GSSG]_0$ and $[PSH]_0$ with Equations 124 and 125.

$$[GSH]_t = [PSH]_0 - [PSH]_t \quad (124)$$

$$[GSSG]_t = [GSSG]_0 + \frac{[PSH]_t - [PSH]_0 - [PSSG]_t}{2} \quad (125)$$

K_{1c} and K_{2c} were then calculated by substitution of these concentrations into Equations 108 and 109.

3. Experimental Data

Equilibrium data were collected for three different sets of experimental conditions: (i) in D_2O , under an argon atmosphere; (ii) in H_2O , under an argon atmosphere and (iii) in H_2O , under reduced pressure, i.e. the NMR tubes were degassed under vacuum and then sealed. The latter technique was found to be necessary for the measurement of K_{2c} , since the kinetics of this reaction are slow and, at the long reaction times required, aerial oxidation of PSH and GSH lead to irreproducible results with experimental conditions (i) and (ii).

The results obtained in D_2O and H_2O under an argon atmosphere are presented in Tables 10 and 11, respectively. The areas measured for the PSH and PSSG methyl resonances were obtained less than 24 hours after mixing the reactants for the data in Tables 10 and 11. Beyond this time, PSSP and PSSG resonances increase due to air oxidation of PSH and GSH to PSSP and PSSG. When an increase in the PSSP or PSSG resonances was detected (due to air oxidation), area measurements were stopped. As shown later in this chapter, the kinetics of reaction 103 at these concentrations and pH values are sufficiently slow that reaction 102 has reached equilibrium before oxidation to form PSSP begins. This was also confirmed by a constant value obtained for the relative areas when measurements were made hourly from the time of mixing. Thus, these solutions are at equilibrium with respect to reaction 102 but not reaction 103. Under these conditions, the amount of PSSP present is insignificant and the fractional concentrations of PSH and PSSG in Tables 10 and 11 can be determined by Equations 118 and 119. The total area is taken as the sum of the areas of PSH and PSSG resonances. The relative areas of PSH and PSSG in Table 10 are insensitive to the solution pH up to pH ~ 8. At greater pH values, the areas of PSH resonances decrease and correspondingly those of PSSG increase,

△

Table 10. Experimental values of the conditional equilibrium constant, K_{1c} , as a function of pD.

pD	[PSH] ₀ ^a mM	[GSSG] ₀ mM	area PSH	area PSSG	K_{1c} ^b
3.80	60.0	60.0	45.0	55.0	1.49
4.51	60.1	60.0	45.6	54.4	1.43
4.53	60.0	60.0	46.6	53.4	1.31
4.94	60.0	60.0	44.0	56.0	1.62
5.48	60.1	60.0	45.2	54.8	1.48
5.62	60.0	60.0	45.8	54.2	1.40
6.25	60.0	60.0	45.0	55.0	1.50
6.42	60.1	60.0	47.0	53.0	1.27
6.75	60.0	60.0	44.9	55.1	1.55
7.23	60.0	60.0	49.3	50.7	1.06
7.36	60.1	60.0	45.8	54.2	1.41
8.36	60.1	60.0	45.6	54.4	1.42
8.44	60.0	60.0	43.7	56.3	1.66
9.38	60.0	60.0	38.8	61.2	2.49
9.60	60.1	60.0	39.0	61.0	2.45
10.53	60.1	60.0	22.0	78.0	12.7

^aSolutions prepared in 2 M NaClO₄, 0.0005 M EDTA in D₂O under a blanket of argon gas. The equilibrium constants were measured in situ at 25°C and within 24 hours.

^bUncertainty in K_{1c} value is ~15%.

Table 11. Experimental values of the conditional equilibrium constant, K_{1c} , as a function of pH.

pH	[PSH] ₀ ^a mM	[GSSG] ₀ mM	K_{1c}
7.24	26.1	21.9	0.95
7.46	102	132	1.14
7.46	102	120	1.13
7.46	8.58	8.03	1.11
8.01	8.58	8.03	1.59
8.04	26.1	21.9	1.05
9.13	26.1	21.9	1.26
9.16	8.58	8.03	2.01
9.47	8.58	8.03	3.90
10.01	8.58	8.03	5.54

^aSolutions were prepared in aqueous 1 M KCl containing 0.003 M EDTA. Equilibrium constants were calculated from spectra for quenched aliquots. Aliquots were taken within 5 hours after mixing of the reactants. Temperature was 25°C.

indicating a shift in the equilibrium position of Equation 102 to the right. This corresponds to an increase in the value of K_{1c} at $\text{pH} > 8$.

The results obtained in H_2O under reduced pressure in sealed NMR tubes are given in Tables 12 and 13. The purpose of these experiments was to evaluate K_{2c} as well as K_{1c} , under conditions where aerial oxidation to form PSSG and PSSP is minimized. For this, it was necessary to establish when the second reaction had come to equilibrium. The extent of the reaction in the sealed tubes was generally monitored by measuring ^1H NMR spectra every few days for a period up to approximately one month. Typical data obtained over a 17 day period for a pH 6.9 sample are shown in Table 12. These data demonstrate that the first reaction reaches equilibrium rapidly, within the time of the first measurement, and then, the second reaction reaches equilibrium somewhat more slowly. After 27 hours, the area of PSSP shows that the second reaction (Equation 103) has not yet reached equilibrium. From these data, the forward rate constant for the second reaction is estimated to be $0.0004 \text{ M}^{-1}\text{min}^{-1}$, which is in good agreement with kinetic results presented later in this chapter. Because of the slowness of the second reaction, data for this reaction (Table 13) were obtained over a long period of time to ensure the

Table 12. Values obtained as a function of time for the equilibrium constants K_{1c} and K_{2c} , under reduced pressure in sealed NMR tubes. a,b

Time Hrs	Chemical Shift (Imidazole)	pH ^c	area PSH	area PSSG	area PSSP	K_{1c} ^e	K_{2c} ^e
27	8.4239, 7.3829	6.91	52.3	46.5	1.2	1.53	d
58	-	-	51.6	46.5	1.9	1.61	0.0193
77	8.4272, 7.3842	6.90	52.9	45.5	1.6	1.44	0.0163
130	8.4275, 7.3846	6.90	52.6	44.9	2.5	1.43	0.0245
280	8.4340, 7.3872	6.89	52.6	45.5	1.9	1.46	0.0198
410	8.4355, 7.3880	6.88	52.0	45.5	2.5	1.52	0.0258

^aSolutions prepared in 1 M aqueous KCl solution containing 0.003 M EDTA. Initial concentration, 0.0412 M PSH, 0.0308 M GSSG, 0.04 M imidazole and 0.01 M TBA. Temperature, 25°C.

^bValues for K_{1c} and K_{2c} are the average values from several samples of the same solution monitored simultaneously under identical conditions.

^cpH calculated using imidazole chemical shift and Equations 100-101.

^dReaction 103 has probably not yet reached equilibrium.

^eThe average values are $K_{1c} = 1.48 \pm 0.12$ and $K_{2c} = 0.022 \pm 0.005$.

Table 13. Values obtained as a function of pH for the equilibrium constants K_{1c} and K_{2c} under reduced pressure.^a

pH	[PSH] _o mM	[GSSG] _o mM	K_{1c}	K_{2c}
4.20	25.3	25.0	1.78	b
5.11	43.4	24.9	1.53	b
5.14	48.3	48.7	1.26	b
5.96	25.3	25.0	1.64	b
6.00	43.4	24.9	1.71	b
6.91	41.2	30.8	1.48	0.0220
7.01	48.3	48.8	1.18	0.0306
7.35	41.2	30.8	1.46	0.0385
8.06	48.4	48.8	1.39	0.0336
9.10	48.4	48.8	1.42	0.0435
9.97	41.2	30.8	8.79	0.244 ^c
9.99	48.4	48.8	8.36	b

^aPrepared in aqueous 1 M KCl solutions containing 0.003 M EDTA. Temperature, 25°C. Sealed NMR tubes.

^bReaction 103 is not yet at equilibrium.

^cReaction followed for 27 days. Relative heights were used.

second reaction had come to equilibrium. Due to the relatively small amount of PSSP which forms, it was difficult to measure K_{2c} with a high degree of precision.

Imidazole was added as an internal pH indicator for some samples in the pH range 6.5 - 8. The pH dependence of its chemical shifts, as characterized in Chapter III, was used to monitor the pH. As shown in Table 12, the pH of the solution is relatively stable, changing by only 0.03 pH unit over 17 days. At pH 8, this change is twice as much. The cause of this small change is unknown and no peaks due to penicillamine-containing species produced by side reactions were detected at pH 6.9. However, at pH > 7, as many as three unidentified penicillamine resonances were observed, presumably formed by side reactions. Their chemical shifts are 1.46, 1.32 and 1.13 ppm with respect to DDS at pH 10. Their rates of appearance depend on the solution pH, increasing as the pH increases. At pH 10, their rate constants were estimated to be $\sim 10^6$ times smaller than the forward rate for reaction 102. At the concentrations used in these experiments, these additional resonances were first noticed at 21 days, 8 days and 30 hours after mixing at pH 8; 9 and 10, respectively. No additional resonances were observed at pH 7 for as long as 30 days.

4. Calculation of pH Independent Equilibrium Constants

The equilibrium constant, K_1 , defined by Equation 106, was calculated from the K_{1C} values given in Tables 10-13 using Equation 115. Two procedures to calculate K_1 were used. In the first, a value was calculated for K_1 from each of the K_{1C} values listed in Tables 10-13. The term $\alpha_1\alpha_2/\alpha_3\alpha_4$ was calculated at each particular pH using values given in Chapter III for the acid dissociation constants, and the K_1 value calculated with Equation 115. For example, at pH 3.80, the ratio $\alpha_1\alpha_2/\alpha_3\alpha_4$ equals 24.7 from which a K_1 value of 36.8 is calculated; at pH 8.06, the ratio is 37.1 and K_1 is 26.7, etc. The average K_1 value of the 38 values obtained from data in Tables 10-13 is $K_1 = 34.0$ with a standard deviation of 6.4. In the second method of calculating K_1 , a value of $K_1 = 34.8$ was obtained from a non-linear squares fit of the K_{1C} versus pH data to Equation 115 using the program KINET. The linear standard deviation was 0.9. The values predicted for K_{1C} (K_{1C} predicted) using the value of 34.8 for K_1 and the $\alpha_1\alpha_2/\alpha_3\alpha_4$ values at pH 3.03 and 8.06 (see above example), are 1.41 and 1.31 respectively. To further show the agreement between the experimental data and the model, the experimental K_{1C} values are plotted versus pH or pD in Figure 44. Also plotted as the solid curve is the theoretical pH dependence of K_{1C} as predicted by Equation

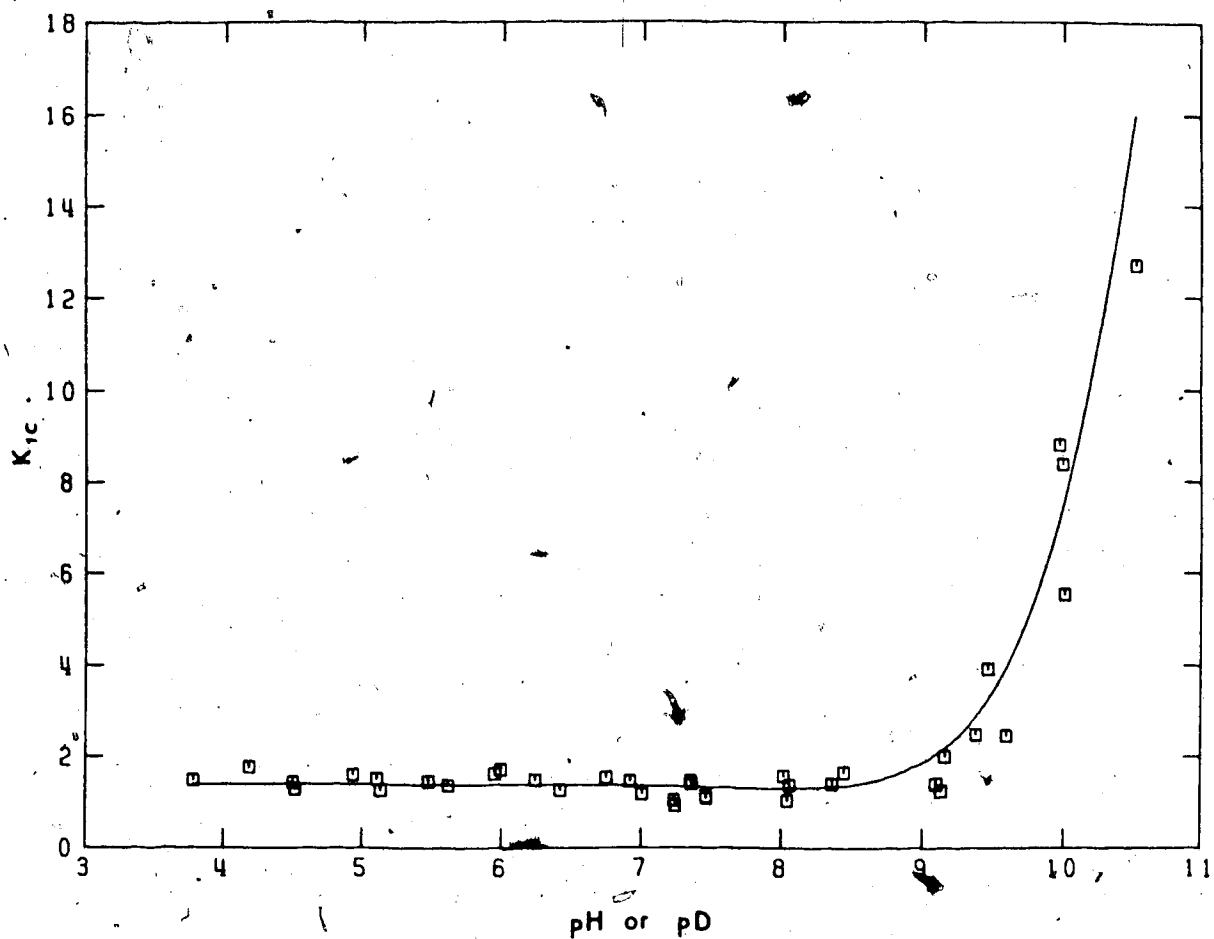


Figure 44. Plot of the conditional equilibrium constant K_{1c} for the reaction of PSH with GSSG, versus the solution pH or pD. The solid line through the points is the theoretical dependence of K_{1c} on pH predicted by equation 115 with $K_1 = 34.8$ and the constants in Table 7.

115. Agreement between the theoretical curve and the experimental data is excellent, particularly at $\text{pH} < 8$. At $\text{pH} > 8$, there is more scatter in the data due to the problem of air oxidation described above and to the increased sensitivity of K_{1C} to the error in the solution pH , however, there is general agreement between the experimental and predicted behavior.

The equilibrium constant K_2 , defined by Equation 107, was calculated from the six values listed for K_{2C} in Table 13 using Equation 116. The data at $\text{pH} < 6$ were not used, even though PSSP was present, because reaction 103 had not yet reached equilibrium. The behavior of K_{2C} as a function of pH is similar to that observed for K_{1C} . The same two procedures described above for the calculation of K_1 from K_{1C} were also used for K_2 . The individual value obtained by multiplying each K_{2C} value by the value for $a_2 a_5 / a_1 a_3$ at that pH are listed in column 4 of Table 14. The average of these six values is $K_2 = 0.85 \pm 0.21$ (standard deviation). The value obtained by fitting the data to Equation 116 with KINET is 0.994 ± 0.098 , (linear standard deviation). The predicted values for K_{2C} as a function of pH are listed in column 5 of Table 14. Considering the uncertainty in the measurement of the equilibrium concentration of PSSP as discussed earlier in this chapter, there is reasonable agreement between the experimental predicted values of K_{2C} .

Table 14. Observed and predicted values for K_{2c} in aqueous solution.^a

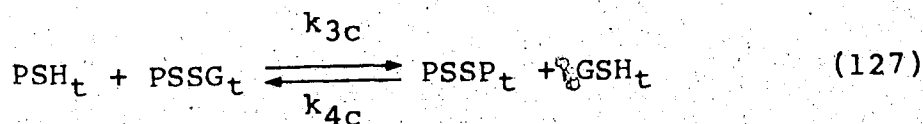
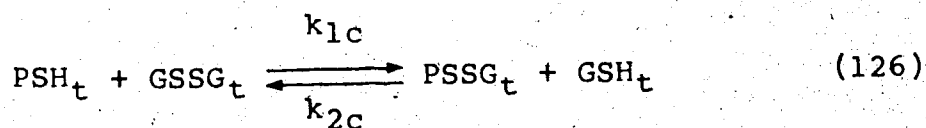
pH	$\frac{\alpha_2 \alpha_5}{\alpha_1 \alpha_3}$	K_{2c}	K_2	K_{2c} predicted
6.91	26.0	0.0220	0.573	0.0382
7.01	26.0	0.0306	0.794	0.0383
7.35	25.6	0.0385	0.986	0.0388
8.06	25.0	0.0336	0.840	0.0397
9.10	16.7	0.0435	0.726	0.0596
9.97	4.84	0.244	1.18	0.205

^aData are those of Table 13.

^bCalculated using $K_2 = 0.994$ and Equation 116.

C. Determination of Rate Constants

In this section, the kinetics of the thiol/disulfide reactions for the penicillamine/glutathione system are characterized for a range of solution conditions. As with the equilibrium constants, the magnitudes of the rate constants depend on pH because of protonation of the thiol, amino and carboxylic acid groups. The kinetics of the thiol/disulfide exchange reactions are characterized by the four pH dependent conditional rate constants, k_{1c} , k_{2c} , k_{3c} and k_{4c} , as defined in Equations 126 and 127.



where PSH_t is the sum of the concentrations of the various protonated forms of PSH at the particular pH, etc.

As discussed in the previous section, the rate of the second reaction is much slower than the first and thus the kinetics of these two reactions can be characterized

separately. The kinetics of the first reaction were characterized by measuring k_{1c} as a function of pH over the pH range 4 to 9. The reverse rate constant, k_{2c} , can then be calculated from k_{1c} and K_{1c} , the conditional equilibrium constant for reaction 102 at the particular pH. The kinetics of the second reaction were characterized by measuring k_{4c} over a range of pH values. The rate constant, k_{3c} can then be calculated from k_{4c} and K_{2c} , the conditional equilibrium constant for the second reaction at the particular pH.

1. The Reaction of PSH with GSSG

The kinetics of the reaction of PSH with GSSG were studied over the pH range 4 to 9 with concentrations of reactants ranging from 0.0015 M to 0.024 M. Altogether, twenty-two kinetic time course runs were successfully carried out, either in situ in a 5 mm NMR tube, or in a reaction vessel. In the latter case, aliquots were withdrawn as a function of time and quenched by lowering the pH. Experimental details are described in Chapter II. Typical time course spectra are shown in Figure 45. Solutions of PSH and GSSG at pH 4 (left spectra in Figure 45) were mixed together at time zero and a 0.5 mL aliquot transferred to a NMR tube. The reaction was followed in situ by measuring NMR spectra as a function of time. The

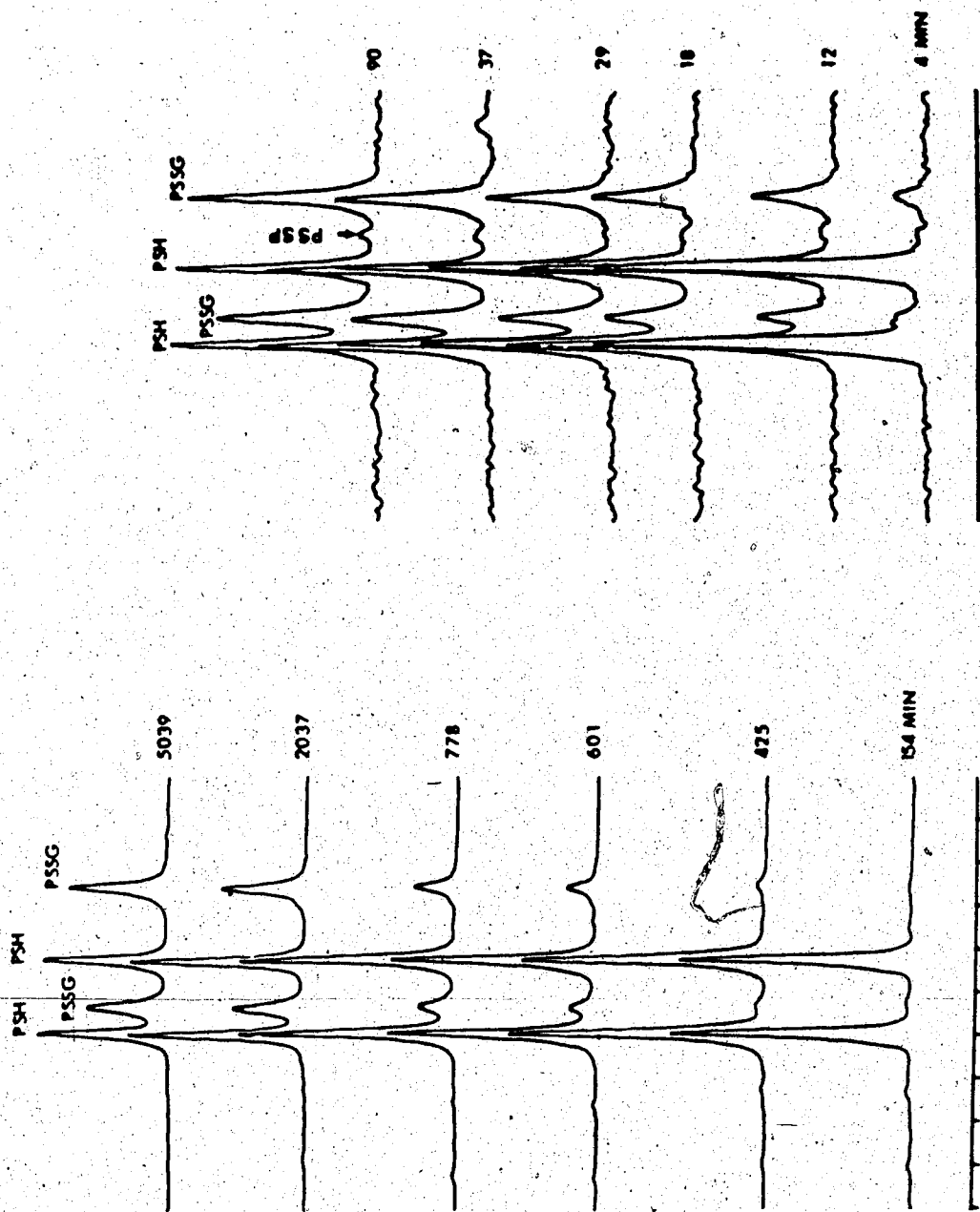


Figure 45. 200 MHz ^1H NMR time course spectra for the reaction of PSH with GSSG. (Left) Initial concentrations of PSH and GSSG, 0.0160 M, pH 3.96. (Right) Initial concentrations of PSH and GSSG, 0.00400 M, pH 6.61. Solutions prepared in 1 M aqueous KCl solution containing 0.003 M EDTA. Temperature, 25°C.

bottom spectrum, taken 154 minutes after mixing shows only the two resonances of PSH, indicating a slow reaction at this pH. However, two new resonances become visible after 425 minutes and progressively increase in intensity thereafter. These are due to the product PSSG. No PSSP resonances were detected after 83 hours (top spectrum), nor after 8 days. Concentrations were calculated as a function of time from relative areas as described earlier in Chapter II. These results are plotted as a function of time in Figure 46 (top figure).

At pH 6.61, the reaction is faster as shown by the series of spectra on the right of Figure 45. A small amount of PSSP is detected at 37 minutes after mixing the reactants. The area measurements of the PSH and PSSG resonances were stopped after 29 minutes and the progress curves calculated from these spectra.

Generally, it was observed that PSSP concentrations reach no more than a few percent of the total PSH concentration at the end of the time course.

Insignificant amounts of PSSP were detected at pH 4 and at pH > 7.5 and 1-2% was detected in the pH range 5-6.7. At pH 7, ~8% of the total PSH concentration (0.002 M) was oxidized to PSSP at the end of two kinetic runs. The overall trend observed is consistent with the results found in Chapter II (Figure 10) for the dependence of the

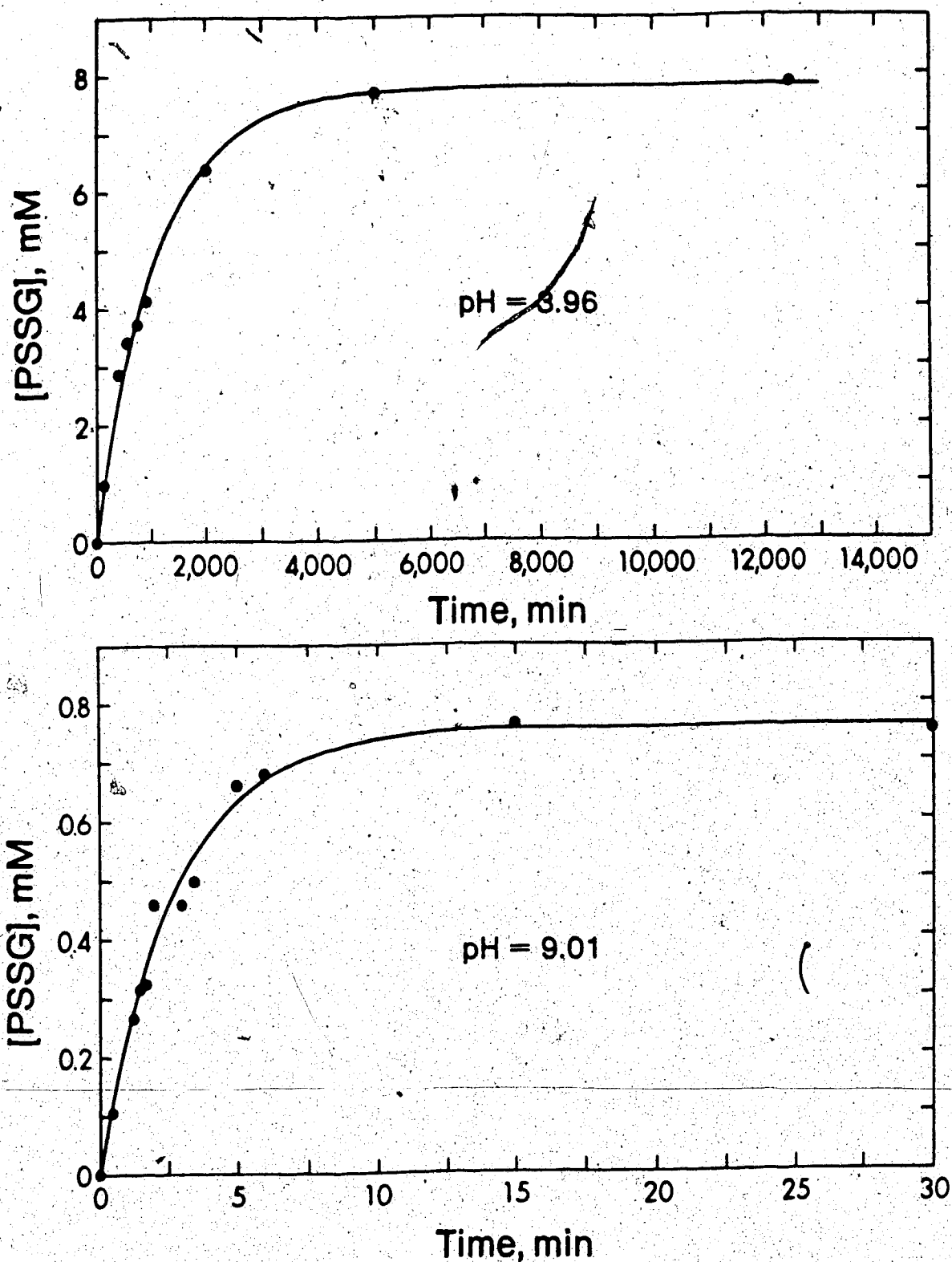


Figure 46. Kinetic data for the formation of PSSG by reaction of PSH with GSSG at pH 3.96 and 9.01. The initial concentrations of PSH and GSSG were 0.0160 M at pH 3.96. At pH 9.01, the initial concentrations were 0.00143 M PSH and 0.00137 M GSSG. The extent of reaction was followed in situ (pH 3.96) and by quenching the reaction (pH 9.01) as a function of time.

rate of oxidation of PSH on the solution pH. This small amount of PSSP at pH 7 did not affect the value of k_{1c} significantly. This was substantiated by the agreement between k_{1c} values obtained by curve fitting and those obtained from the initial slope. For example, the lower limit of the rate constant at pH 6.97, with 7% PSSP present at the end of the time course is $10.0 \text{ M}^{-1}\text{min}^{-1}$ from the initial slope whereas k_{1c} , from the curve fitting of the entire time course data is $11.4 \text{ M}^{-1}\text{min}^{-1}$. The presence of PSSP at the end of the reaction affects mainly the determination of the equilibrium concentration and not k_{1c} , which is determined mainly by the data near the beginning of the experiment. This 10% difference is typical of the uncertainty associated with kinetic studies [113].

In order to minimize errors in the determination of the forward rate constants due to air oxidation at high pH, the initial reactant concentrations were adjusted so that sufficient reaction of PSH with GSSG to form PSSG had occurred to characterize the kinetics of the reaction before significant oxidation of PSH had taken place. For example, according to Figure 10, Chapter II, less than 1% of the PSH in a 0.0025 M solution at pH 9 will be oxidized to PSSP during a 30 minute period. Using this calculation as a rough guideline, the reaction of PSH with GSSG at pH

9.01 was studied by preparing a reaction mixture having PSH and GSSG concentrations of 0.0014 M. The time course was followed by the quenching method described in Chapter II. The reaction was completed within 15 minutes (Figure 46, bottom). No significant amount of PSSP was detected at the end of the time course.

a. The Order of the Reaction

Although other thiol/disulfide exchange reactions have been shown to be second order overall and first order in thiol and disulfide i.e. simple S_N2 displacement reactions [43,45], and to proceed via the thiolate anion [21,34-38,43,45,49], the first kinetic experiments done on the PSH/GSSG system were designed to verify that this is also the order of this reaction. The rate of the forward reaction [113] is given by:

$$\text{rate} = \frac{d[\text{PSSG}]}{dt} = \frac{-d[\text{PSH}]}{dt} \quad (128)$$

$$\text{rate} = k_{1c} [\text{PSH}]^a [\text{GSSG}]^b - k_{2c} [\text{PSSG}]^c [\text{GSH}]^d \quad (129)$$

where a, b, c and d indicate the order with respect to PSH, GSSG, PSSG and GSH respectively. If the reaction is performed by mixing solutions of PSH and GSSG, Equation 129 simplifies, at time = 0, to:

$$\text{rate}(t=0) = k_1 c [\text{PSH}]_0^a [\text{GSSG}]_0^b \quad (130)$$

where $\text{rate}(t=0)$ is the initial rate of the reaction and $[\text{PSH}]_0$ and $[\text{GSSG}]_0$ are the initial concentrations of PSH and GSSG. The initial rate of the reaction is given by the slope of time course curves for PSH and PSSG.

$$\text{rate}(t=0) = \left(\frac{\Delta \text{concentration}}{\Delta t} \right)_{(t=0)} \quad (131)$$

The values of a and b were determined at pH 6.6 using initial rates obtained from the time courses for the formation of PSSG. A pH of 6.6 was selected for this experiment because, at this pH, the rates of the reaction are convenient for continuous monitoring in situ in the NMR spectrometer.

The time course data were obtained from three kinetic runs and plotted as a function of time as in Figure 46. The initial forward rates were obtained from the initial slopes of the PSSG curves, as determined by drawing a straight line through the origin and the first few points. The initial forward rates are presented in Table 15. When both PSH and GSSG concentrations are 0.004 M, an initial rate of 0.78 M/min is observed. The initial rate

Table 15. Determination of the forward rate and order of the reaction of PSH with GSSG.^a

[PSH] ₀ mM	[GSSG] ₀ mM	pH	Rate (t=0) M/min	k _{1c} ^b M ⁻¹ min ⁻¹
4.00	4.00	6.61	0.78	4.9
4.00	8.00	6.59	1.8	5.6
8.00	4.00	6.67	1.8	5.6
average k _{1c}				5.4
STD				± 0.4

^aSolutions were prepared in aqueous 1 M KCl solution containing 0.003 M EDTA. The extent of the reaction was monitored in situ at 25°C in a 5 mm NMR tube which had been flushed with argon gas.

^bCalculated from the initial rate using Equation 132.

increases to 1.8 M/min when the GSSG concentration is doubled, indicating that $b = 1$. Likewise, the initial rate increases to 1.8 M/min when the PSH concentration is doubled, indicating that a is also 1. Thus, these data confirm that the rate equation for the reaction of PSH with GSSG is second order overall, and first order in both PSH and GSSG.

$$\text{rate}_{(t=0)} = k_{1c} [\text{PSH}]_0 [\text{GSSG}]_0 \quad (132)$$

Forward rate constants were also estimated from the initial rate data in Table 15 by dividing the initial rate by the initial concentrations of the reactants. The results are listed in column 5 of Table 15. The average of these values is $5.4 \pm 0.4 \text{ M}^{-1}\text{min}^{-1}$. Because of the initial rate method used, this is a lower limit for k_{1c} at pH 6.6.

b. The Kinetic Model

To characterize the kinetics in more detail, the conditional rate constant, k_{1c} was evaluated over a range of pH values by fitting time course data to a second order reversible kinetic model. The time course data in Figure 47 for a concentration jump experiment show that the second order reversible kinetic model is appropriate for

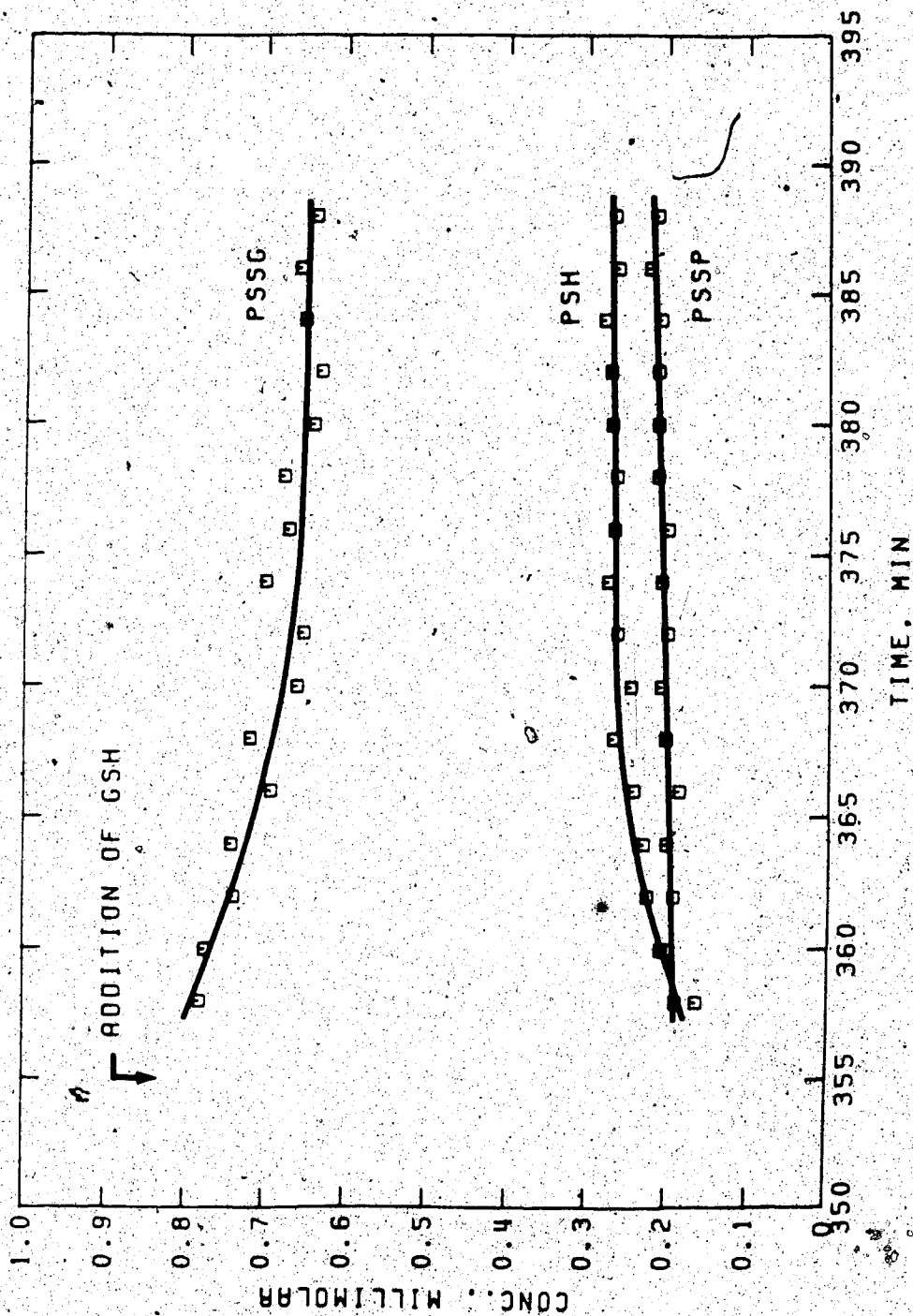


Figure 47. Concentration jump experiment showing the effect of adding GSH to an equilibrium mixture obtained by reaction of PSH with GSSG in D_2O at pD 7.5 with initial concentrations of 0.0013 M PSH and GSSG. The equilibrium mixture is 0.0003 M PSH, 0.0001 M PSSP and 0.0008 M PSSG. At $t = 355$ minutes, GSH concentration was increased by 0.0013 M.

the thiol/disulfide exchange reaction. An aliquot of GSH was added to a reaction vial containing an equilibrium mixture of 0.0003 M PSH, 0.0001 M PSSP and 0.0008 M PSSG. The equilibrium concentrations of GSH and GSSG were 0.001 M and 0.0005 M respectively (assuming no GSH had been oxidized to GSSG). The concentration of GSH was increased by 0.0013 M at $t = 355$ minutes and then a 0.5 mL aliquot of this solution was transferred to a NMR tube. The reaction was monitored in situ by NMR. The concentration of PSSG is seen to decrease with time and the concentration of PSH to increase, as predicted by Le Chatelier's principle for the reaction presented by Equation 126. It is of interest to note the increased concentration of PSSP in Figure 47 with respect to the original equilibrium concentration of PSSP and the slight increase during the time course study. This is due to air oxidation of PSH in the vial while it sat on the laboratory bench and in the NMR tube. From the initial slopes of the time courses of PSH and PSSG in Figure 47, the rate constant, k_{2c} is estimated to be $\sim 10 \text{ M}^{-1}\text{min}^{-1}$ which is in good agreement with values calculated from k_{1c} and K_{1c} . These results indicate that the reaction described by Equation 126 is a second order reversible reaction. The integrated form of a second order reversible rate expression is given by Equation 133 [114].

$$\ln(B) = \left(\frac{k_{1c}}{A}\right)t \quad (133)$$

where t = time after mixing of reactants and

$$A = \frac{X_e}{2A_0 B_0 - X_e (A_0 + B_0)} \quad (134)$$

$$B = \frac{A_0 B_0 (X_e + X) - X_e X (A_0 + B_0)}{A_0 B_0 (X_e - X)} \quad (135)$$

and X = concentration of a product molecule at time t , X_e = its concentration at equilibrium, and A_0 and B_0 are the initial concentrations of the two reactants. For the reaction described by Equation 126, A_0 and B_0 are $[\text{PSH}]_0$ and $[\text{GSSG}]_0$. X and X_e are the sums of all the various protonated forms of PSSG at time t and at equilibrium, respectively. The validity of this model for the PSH/GSSG exchange reaction is further demonstrated by the linearity of the plot of $\ln B$ versus time for a typical data set in Figure 48. Similar plots for data at several pH values over the pH range studied showed similar linearity. Rate constant k_{1c} could be obtained by multiplying the slope by the value of A . However, rather than evaluating k_{1c} by this method, the time course data were fitted to a

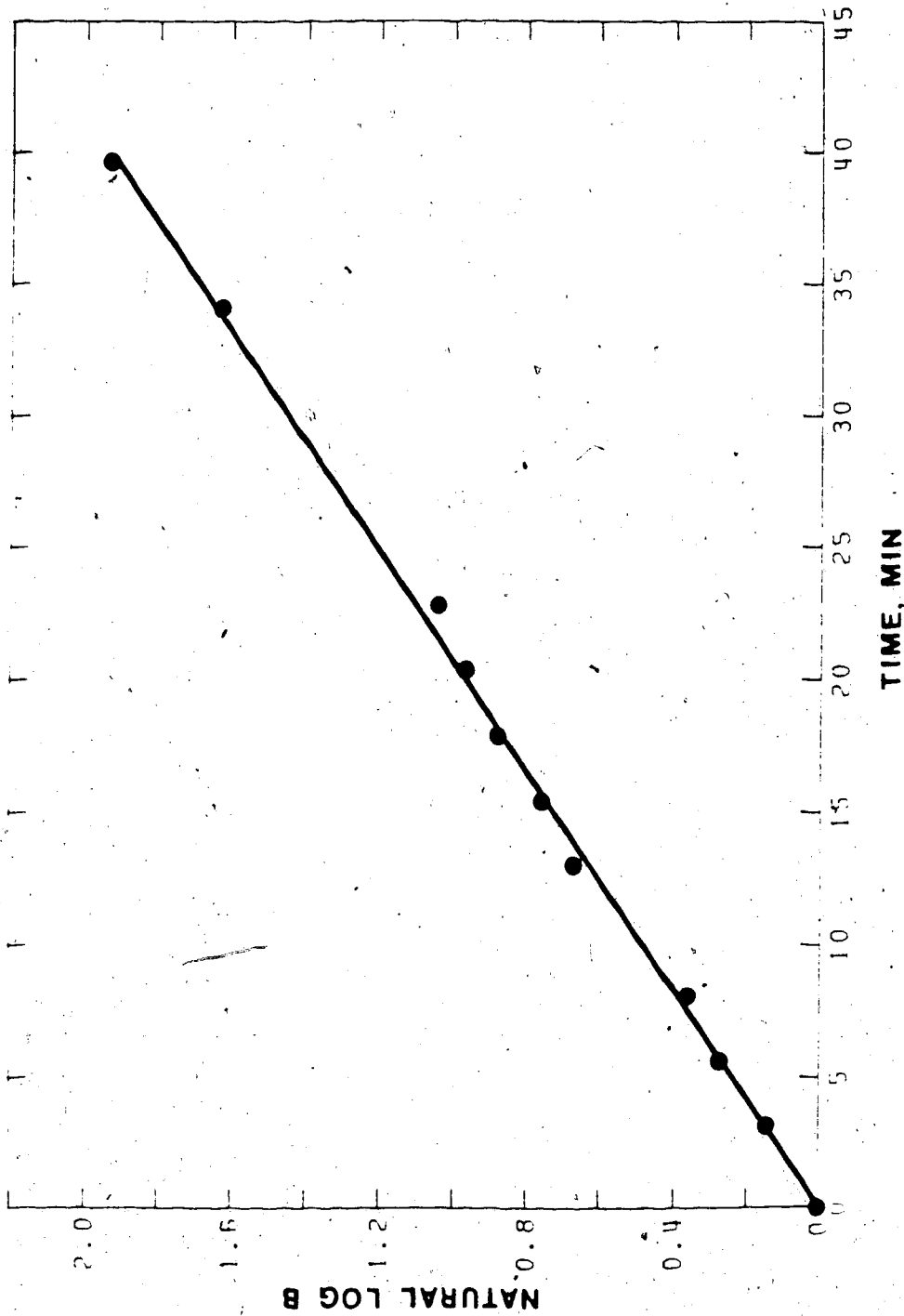


Figure 48. Plot of the natural logarithm of B versus time; B is given by Equation 133. The initial concentrations of PSH and GSSG were 0.00200 M in 1 M aqueous KCl solution containing 0.003 M EDTA; pH 6.97.

modified form of the rate equation (Equation 136) using the non-linear least squares program KINET.

$$X = \frac{A_0 B_0 X_e (1 - \exp(-k_{1c} t))}{X_e (A_0 + B_0) - \frac{A_0 B_0 (1 + \exp(-k_{1c} t))}{A}} \quad (136)$$

This equation is more convenient to use in the non-linear least squares curve fitting calculation. X_e and k_{1c} were both treated as unknowns. The program adjusts the initial estimates given for X_e and k_{1c} to obtain the best fit of the model to the experimental data.

c. Experimental Data

Typical time course data for the formation of PSSG at pH values 4 and 9, along with the theoretical time course curves predicted by the values obtained for k_{1c} and X_e from the fit of the data to Equation 136 are shown in Figure 46.

Time course data from twenty two experiments, covering the pH range 4-9, were treated in this way to obtain values for k_{1c} and X_e . The values obtained for k_{1c} are listed in Table 16. A range of concentrations, from 0.001 M to 0.020 M was used in these studies. The values for k_{1c} vary from 0.026 M⁻¹min⁻¹ at pH 4 to 158 M⁻¹min⁻¹ at pH 9. The values calculated for the equilibrium constant, K_{1c} from the values for X_e , averaged 1.1 ± 0.3

Table 16. Conditional rate constants for the reaction of PSH with GSSG as a function of pH.^a

[PSH] ₀ mM	[GSSG] ₀ mM	pH	k _{1c} ^b M ⁻¹ min ⁻¹	STD DEV ^c M ⁻¹ min ⁻¹
13.3	6.67	3.96	0.0381	0.0077
16.0	16.0	3.96	0.0263	0.0013
24.0	16.0	3.96	0.0339	0.0040
8.00	16.0	3.97	0.0313	0.0056
9.52	16.1	3.97	0.0269	0.0012
20.0	20.0	4.99	0.186	0.0041
20.0	10.0	5.00	0.191	0.0077
10.0	20.0	5.01	0.225	0.0045
4.00	8.00	5.85	1.475	0.054
8.00	8.00	5.96	1.809	0.033
4.00	8.00	6.59	7.03	0.23
4.12	4.04	6.61	6.45	0.43
4.00	4.00	6.61	5.92	0.24
8.00	4.00	6.67	7.51	0.30
8.00	2.00	6.73	8.46	0.54
2.00	1.00	6.93	15.00	0.96
2.00	2.00	6.97	11.39	0.23
3.22	3.13	7.48	60.0	5.2
3.02	2.97	8.04	80.4	7.2
2.06	2.01	8.45	135.4	6.8
2.02	1.98	8.89	158	13
1.43	1.37	9.01	146	12

^aPrepared in 1 M aqueous solution containing 0.003 M EDTA. Temperature, 25°C.

^bCalculated from Equation 136. Reactions followed in situ or by the quenching method.

^cLinear standard deviation given by KINET.

over the pH range 4-8, as compared to the average value of 1.4 ± 0.2 calculated for the same pH range using the data in Tables 10-13. The agreement between these two values is reasonably good, considering that more oxidation of PSH to PSSP occurred in the kinetic experiments and the signal-to-noise ratio was lower in the time course spectra.

d. Calculation of pH Independent Rate Constant

The logarithm of the k_{1c} values listed in Table 16 increases linearly with pH up to pH ~ 7 as shown in Figure 49. The slope of the plot up to this pH is 1. Above pH 7, the slope is less and, as the pH increases, the plot levels off at pH ~ 9 . This pH dependent behaviour is consistent with a model in which the reactive thiol species is in the thiol-deprotonated form. There are two such penicillamine species possible, PS^- (species III in Figure 21) in which the thiol group is deprotonated and the amino group protonated, and PS^{2-} (species V) in which both groups are deprotonated. Both of these species are present at low concentration over the pH range 4 to 7, as indicated by the species distribution of III and V in Figure 22. The pH dependence of the concentrations of the actual reacting forms of penicillamine over the pH range studied should parallel the pH dependence observed for k_{1c} . The logarithm of the fractional concentration of PS^-

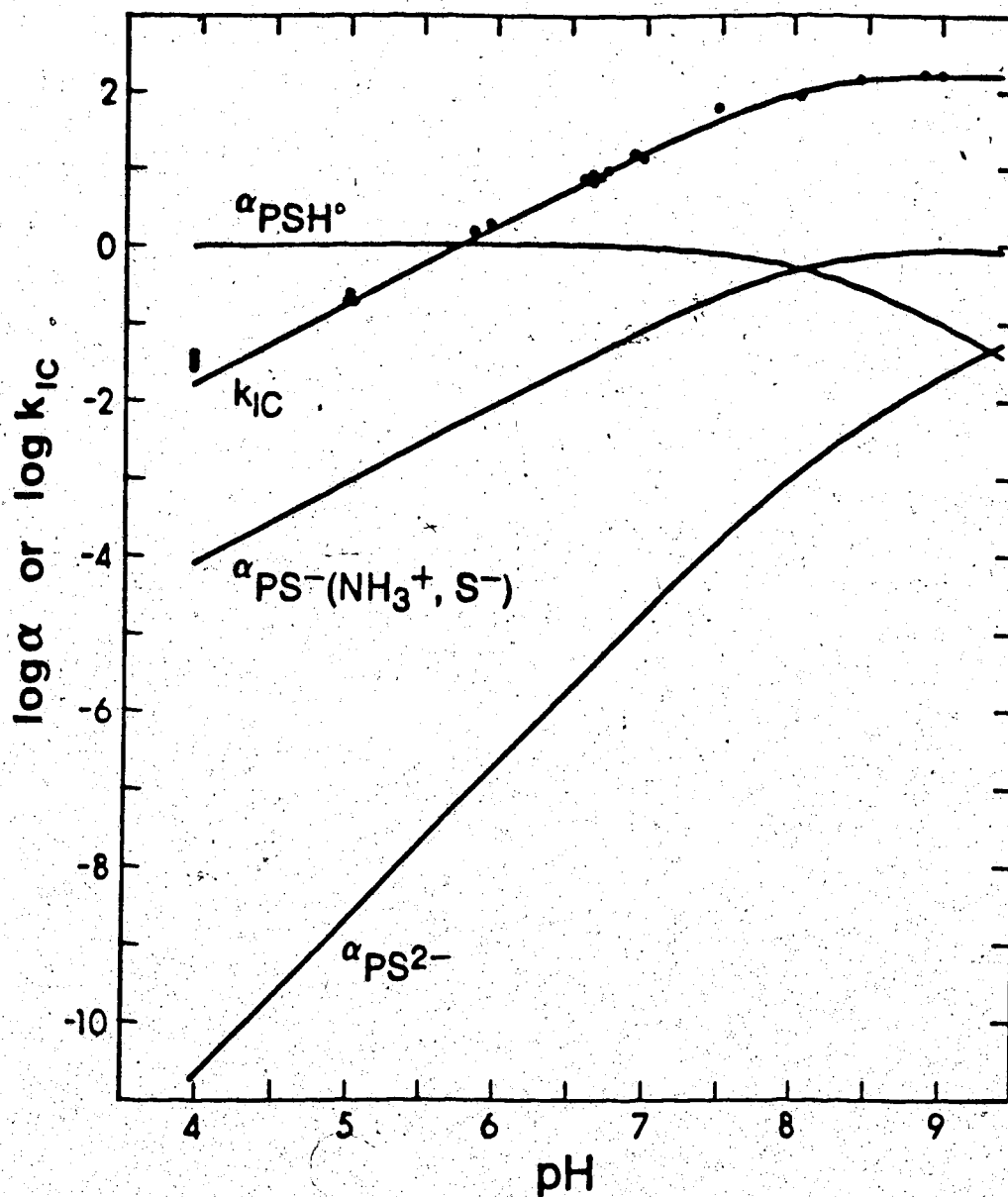


Figure 49. Plots of the logarithm of the fractional concentration, α , for the species PSH^0 , PS^- , and PS^{2-} , and of the conditional rate constant k_{1c} as a function of pH. The solid curve through the experimental points is the theoretical curve predicted by Equation 140 and the value $k_1 = 190 \text{ M}^{-1}\text{min}^{-1}$.

and PS^{2-} are plotted over this pH range in Figure 49. The slope of the plot for PS^- is 1 over the pH range 5 to 7, whereas that for PS^{2-} is 2, indicating the reactive species to be the amino protonated, thiol deprotonated form, i.e. PS^- .

There is also the possibility that the rate constant depends on the protonation state of GSSG. However, the curves in Figure 29 indicate the predominant species to be $GSSG^{2-}$, i.e. the species in which the four carboxylic acid groups are deprotonated and the two amino groups protonated. At the low end of the pH range studied, the species $GSSG^-$ becomes important whereas at the high pH end, $GSSG^{3-}$ becomes important. The pH independent rate constant k_1 was evaluated from data over the pH range 5 to 9. As discussed below, the rate at pH 4 appears to be faster, which may be due to the presence of $GSSG^-$, whereas at pH 9, the rate seems to be unaffected by the presence of some $GSSG^{3-}$, i.e. PS^- apparently reacts with $GSSG^{2-}$ and $GSSG^{3-}$ at a similar rate.

The rate equation for the forward reaction, in terms of the pH independent rate constant k_1 , is:

$$\text{rate} = k_1 [PS^-][GSSG^{2-}] \quad (137)$$

The relationship between k_1 and k_{1c} is given by Equation 138.

$$k_{1c} [\text{PSH}]_t [\text{GSSG}]_t = k_1 [\text{PS}^-] [\text{GSSG}^{2-}] \quad (138)$$

where $[\text{GSSG}]_t \doteq [\text{GSSG}^{2-}]$.

Rearranging this Equation leads to

$$k_{1c} = k_1 \frac{[\text{PS}^-]}{[\text{PSH}]_t} \quad (139)$$

$[\text{PS}^-]/[\text{PSH}]_t$ is the fraction of penicillamine in the PS^- form, which can be calculated from microscopic and macroscopic acid dissociation constants.

$$k_{1c} = k_1 \left(\frac{k_{a12} K_{A1} a_H}{a_H^3 + K_{A1} a_H^2 + K_{A1} K_{A2} a_H + K_{A1} K_{A2} K_{A3}} \right) \quad (140)$$

where k_{a12} , K_{A1} , K_{A2} and K_{A3} are the acid dissociation constants for penicillamine, as defined in Chapter III. Representing the fractional concentration of PS^- by α yields

$$k_{1c} = k_1 \alpha \quad (141)$$

The behaviour of k_{1c} as a function of pH predicted by this model can be qualitatively compared with the results in Figure 49. In the pH range 4-6, $K_{A1}a_H^2 > a_H^3$, $a_H K_{A1} K_{A2}$, $K_{A1} K_{A2} K_{A3}$ and Equation 140 simplifies to

$$k_{1c} = \frac{k_1 k_{a12}}{a_H} \quad (142)$$

Taking the logarithm of both sides:

$$\log k_{1c} = \text{pH} + \log (k_1 k_{a12}) \quad (143)$$

which predicts that, in the pH range 4-6, the plot of the logarithm of k_{1c} versus pH will be linear with a slope of 1. At pH 9, $K_{A1} K_{A2} a_H > a_H^3$, etc. and

$$\log k_{1c} = \log \frac{k_1 k_{a12}}{K_{A2}} = \text{constant} \quad (144)$$

This equation predicts that the plot should level off to a constant value at pH ~ 9. Both trends are observed in the experimental data, where $\log k_{1c}$ increases with pH with a slope of 1 up to pH 7 and then approaches a constant value of ~2.3 at pH 9. This corresponds to $k_1 \sim 200 \text{ M}^{-1} \text{ min}^{-1}$. A value for the rate constant k_1 was obtained from the 17 k_{1c} values over the pH range 5 to 9 by fitting them to

Equation 140 with the non-linear least squares program KINET. The value obtained is $k_1 = 190 \text{ M}^{-1}\text{min}^{-1}$ with a linear standard deviation of $7 \text{ M}^{-1}\text{min}^{-1}$. The fit of the data to the model can be seen by comparison of the solid curve in Figure 49, which is predicted by this value for k_1 , and the experimental values. Even though data at $\text{pH} > 5$ were used to evaluate k_1 , the theoretical curve is extended to $\text{pH} 4$ to show that the model does not satisfactorily fit the data at this pH , presumably because the reactivity of GSSG^{2-} and GSSG^- are different. The rate constant k_1 was also obtained by calculating a value from each k_{1c} and the value for α at that pH , using Equation 141. The results are listed in Table 17. The average of the 17 values listed in column 4 is 193 ± 31 (STD) $\text{M}^{-1}\text{min}^{-1}$.

Calculations were also attempted with a second model which included the species PS^{2-} as a reactant. However, no satisfactory rate constant could be obtained because, as indicated by the plots in Figure 22, the concentration of PS^{2-} is very low over the entire pH range studied.

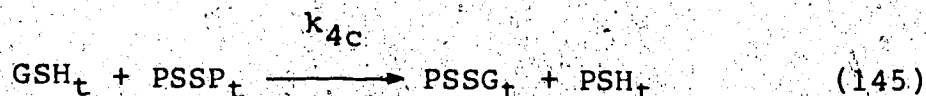
2. The Reaction of Glutathione with Oxidized Penicillamine

The kinetics of the reaction of GSH with PSSP,

Table 17. Observed and predicted conditional rate constants for the reaction of PSH with GSSG.

pH	α	k_{1c} $M^{-1}min^{-1}$	k_1 $M^{-1}min^{-1}$	k_{1c}^a predicted $M^{-1}min^{-1}$
4.99	1086	0.186	202	0.175
5.00	1061	0.191	203	0.179
5.01	1037	0.225	233	0.183
5.85	150.4	1.48	222	1.26
5.96	117.0	1.81	212	1.62
6.59	28.21	7.03	198	6.74
6.61	26.98	6.45	174	7.04
6.61	26.98	5.92	160	7.04
6.67	23.64	7.51	178	8.04
	20.72	8.46	175	9.17
	13.46	15.0	202	14.1
	12.36	11.4	141	15.4
	4.539	60.0	273	41.9
	2.006	80.4	161	94.7
	1.421	135	192	134
	1.194	158	189	159
9.01	1.167	146	170	163

^aCalculated using $k_1 = 190 M^{-1}min^{-1}$ and Equation 140.



were studied over the pH range 5 to 8. Known initial concentrations of PSSP and GSH were mixed and the reaction monitored by NMR either in situ in an NMR tube or by taking aliquots from the reaction vial as a function of time and quenching by lowering the pH.

Typical spectra obtained as a function of time are shown in Figure 50. Due to the slowness of the reaction, higher concentrations were necessary than used in the study of the kinetics of the reaction of PSH with GSSG. The resolution between the high field methyl resonances for PSH, PSSG and PSSP is sufficient for integration of the three resonances to obtain the concentrations of PSH, PSSG and PSSP. The time course curves for the formation of PSH and PSSG and the disappearance of PSSP for the data in Figure 50 are plotted in Figure 51. As expected, the concentrations of PSH and PSSG increase initially and that of PSSP decreases. After ~50 hours, however, the concentrations of PSSP and PSSG gradually increase whereas that of PSH decreases. These changes beyond 50 hours are probably due to air oxidation of PSH to PSSP and PSSG (Equations 48-49, Chapter II) and GSH to GSSG. Because of these interfering reactions, the rate constant, k_{4c} was

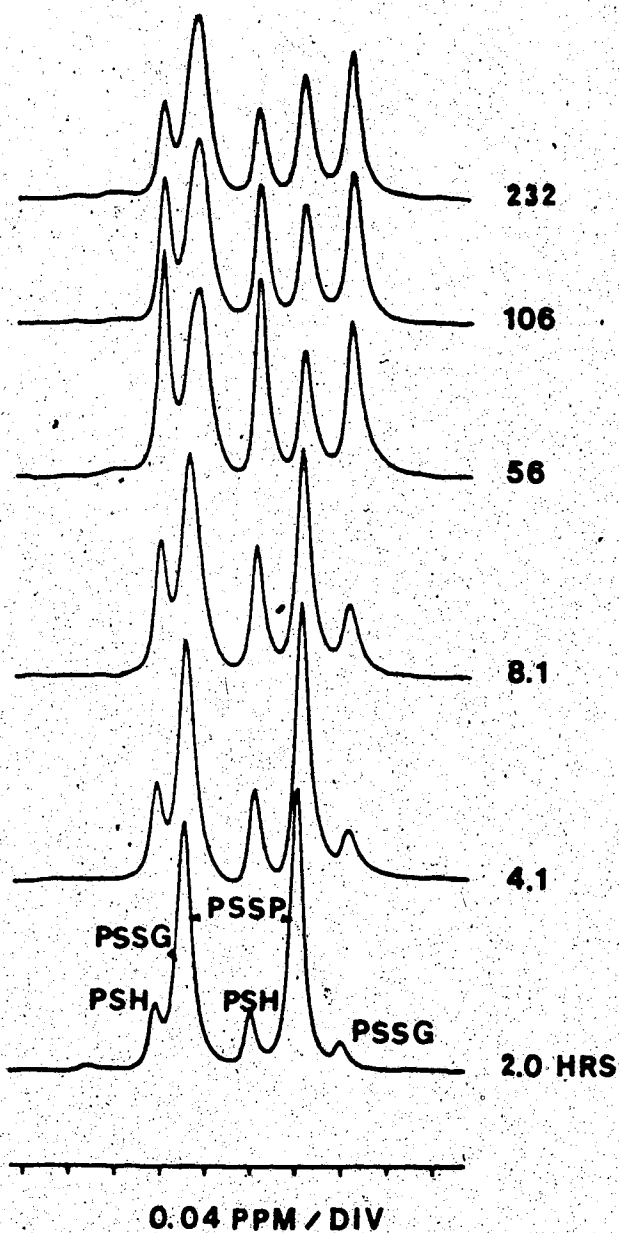


Figure 50. 200 MHz ^1H NMR time course spectra for the reaction of GSH with PSSP at pH 8.03. The initial concentrations were 0.108 M GSH and 0.100 M PSSP in 1 M KCl solution containing 0.003 M EDTA. Temperature of the water bath, 25°C. The extent of the reaction was monitored by quenching aliquots of the reaction mixture. The pH of the quenched aliquot was ~ 0.5 . Prior to the NMR measurement, each aliquot was adjusted to pH ~ 4 for better resolution of the methyl resonances.

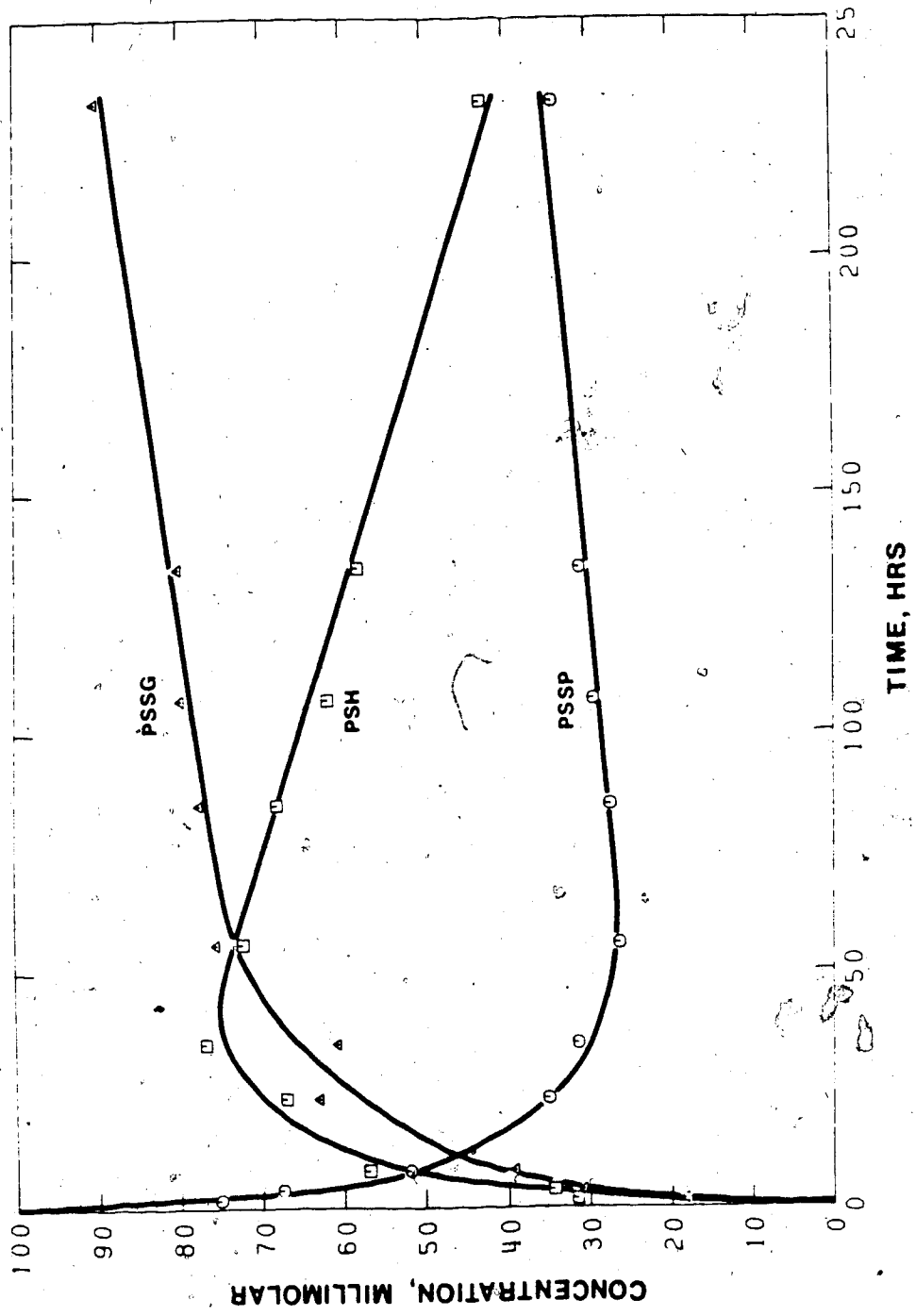


Figure 51. The concentrations of PSH; PSSG and PSSP obtained from the time course spectra in Figure 50.

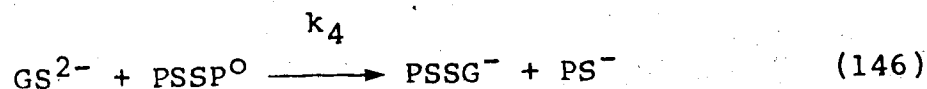
estimated by the initial slope method using an equation analogous to Equation 132. The reaction conditions and the values obtained for k_{4c} are summarized in Table 18. The values for k_{4c} vary from 0.00025 to 0.02 $M^{-1}min^{-1}$ in the pH range 5 to 8. These are ~1000 times smaller than the values of k_{1c} observed over the same pH range. The general pH dependence of k_{4c} is similar to that observed for k_{1c} in Figure 49, indicating the reactive glutathione species to be the thiol deprotonated form. As with penicillamine, there are two possible thiol deprotonated glutathione species, GS^{2-} and GS^{3-} , with the amino group protonated and deprotonated, respectively. However the slopes of plots of the log of the fractional concentration of these two forms versus pH are different, i.e. 1 and 2, respectively. The slope of a plot of $\log k_{4c}$ versus pH is approximately 1, indicating GS^{2-} to be the reactive species. Over the experimental pH range 5-6.5, the species $PSSP^0$, i.e. species H_2A in Figure 26 in Chapter III, is the predominant form of oxidized penicillamine. At $pH > 7$, a significant fraction is present as $PSSP^-$ and $PSSP^{2-}$ (Figure 27). A kinetic model that deals with these three species of PSSP simultaneously is quite complex and the k_{4c} data in Table 18 are too few and scattered for the calculation of specific rate constants for $PSSP^-$ and $PSSP^{2-}$. Therefore, the pH dependence is analyzed using

Table 18. Conditional rate constants for the reaction of GSH with PSSP.

pH	[GSH] ₀ mM	[PSSP] ₀ mM	k_{4c}^a M ⁻¹ min ⁻¹
5.11	100	99.9	0.00025
5.74	100	100	0.00094
6.54	31.9	33.4	0.0040
7.03	31.9	33.4	0.0052
7.35	31.9	33.4	0.012
8.03	108	100	0.021

^aReactions were monitored at 25°C either in situ or by the quenching method, in 1 M aqueous KCl solution containing 0.003 M EDTA under a blanket of argon gas. Average values were calculated from the initial slopes of the concentration of PSH and PSSP vs time curves with an average standard deviation of ±10%.

data over the pH range 5-6.5 in terms of a model involving only the reaction of GS^{2-} with $PSSP^{\circ}$.



In the pH range 5-6.5, $PSSG^{-}$ is the predominant species (Figure 33, Chapter III). Equation 147 gives the relationship between k_{4c} and k_4 .

$$k_{4c} = k_4 \left(\frac{k_{a123} a_H}{a_H^2 + K_{A3} a_H + K_{A3} K_{A4}} \right) \quad (147)$$

where k_{a123} is the microscopic acid dissociation constant for GSH and K_{A3} and K_{A4} are macroscopic constants as defined in Chapter III. The quantity in parenthesis is the fraction α of glutathione in the GS^{2-} form. Values for k_4 were calculated from the values of k_{4c} in Table 18 with Equation 147. The calculated values are (pH, k_4): 5.11, 1.6; 5.74, 1.4; 6.54, 0.94; 7.03, 0.40; 7.35, 0.46; 8.03, 0.20. The average of the first three values in the pH range 5-6.5 is $k_4 = 1.30 \pm 0.34$. At pH > 7, the negatively charged species $PSSP^{-}$ and $PSSP^{2-}$ are likely to be less reactive toward the doubly charged species GS^{2-} than the neutral species $PSSP^{\circ}$ used in the model.

This would result in lower k_{4c} values at $\text{pH} > 7$ and a smaller k_4 value, as is observed in the above results.

Using the average of k_4 , values of k_{4c} were predicted in the pH range 5-6.5. The values predicted are (pH, k_{4c} predicted in $\text{M}^{-1}\text{min}^{-1}$): 5.11, 0.00021; 5.74, 0.00088; 6.54, 0.0056. Although the scatter between the observed and calculated values for k_{4c} is relatively large due to problems in measuring k_{4c} , there is general agreement confirming the validity of this simple model in the pH range 5-6.5.

D. Reaction of N-Acetyl-D,L-Penicillamine with Oxidized Glutathione

The kinetics and equilibria of the N-acetyl penicillamine/GSSG exchange reaction were studied for comparison with the kinetics and equilibria of the penicillamine/GSSG system. Figure 52 shows the methyl region of ^1H NMR time course spectra for a solution containing N-PSH and GSSG at pH 6.58. Three pairs of methyl resonances are observed: one pair is for the two N-acetyl penicillamine methyl groups and the other two pairs are for the methyl groups in the mixed disulfides of N-PSH with GSSG: N-PSSG. Two pairs of resonances are observed for N-PSSG due to the two different

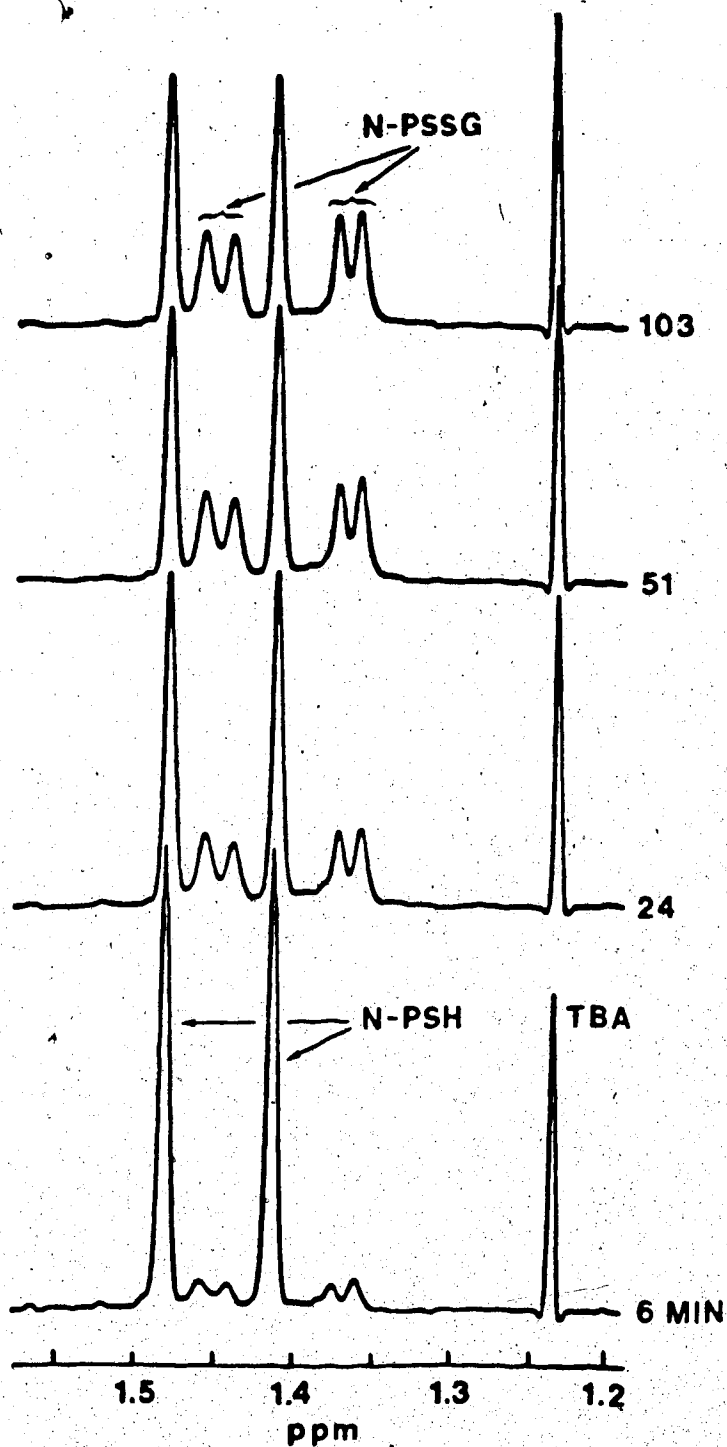


Figure 52. 200 MHz ^1H NMR time course spectra for the reaction of N-PSH with GSSG. The resonances are from the methyl groups on N-PSH. Initial concentrations were 0.00365 M and 0.0348 M for N-PSH and GSSG respectively. [TBA] = 0.004 M, pH 6.58 in 1 M KCl aqueous solution.

configurations: N-acetyl-D-penicillamine-glutathione mixed disulfide and N-acetyl-L-penicillamine-glutathione mixed disulfide. In these two configurations and in GSSG, glutathione is in the L-form. Since the reactant N-PSH is a racemic mixture, the two pairs of resonances from the N-PSSG have equal intensities. Throughout the time course study in Figure 52, these two pairs of resonances are of equal intensity indicating that the two configurations of N-PSH with GSSG have identical kinetic rates.

The equilibrium and rate constants for the N-PSH/GSSG exchange reaction were determined using procedures described above and in Chapter II. The values of K_{1c} , which is defined by an equation similar to Equation 108, were found to be (pH, K_{1c}): 6.95, 2.55 ± 0.15 ; 7.44, 2.60 ± 0.13 ; 8.02, 2.79 ± 0.13 . A value of 0.747 ± 0.012 $M^{-1}min^{-1}$ was measured for the forward conditional rate constant k_{1c} at pH 6.58. A pH independent forward rate constant of $3660 M^{-1}min^{-1}$ is calculated for k_1 from the k_{1c} value at pH 6.58 by assuming the reactive species in the N-PSH/GSSG exchange reaction at pH 6.58 to be the carboxyl and thiol-deprotonated form of N-PSH. $GSSG^{2-}$ is the reactive form of GSSG at this pH. In the above calculation, a pK_A of 10.27 was used for the thiol group of N-PSH [115]. Since the acid dissociation constants of the mixed disulfide are not known, a pH independent

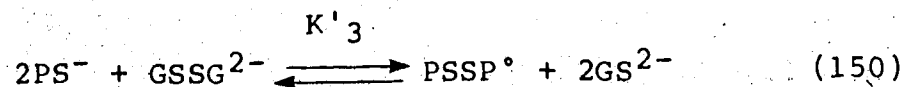
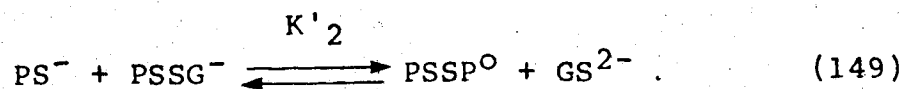
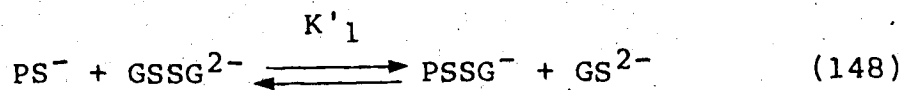
equilibrium constant for the reaction of the thiol-deprotonated form of N-PSH with GSSG^{2-} cannot be calculated.

As no oxidized N-PSH was detected, the equilibrium constant for the second N-PSH/GSSG thiol/disulfide exchange reaction could not be determined under the experimental conditions used in this study.

E. Discussion

It is well established that thiol/disulfide exchange reactions are mechanistically simple $\text{S}_{\text{N}}2$ displacement reactions [43,45], and that they proceed via the thiolate anion [21,34-38,43,45,49]. For both PSH and GSH, there are two thiolate species possible, PS^- and GS^{2-} , in which the thiol group is deprotonated and the amino group protonated, and PS^{2-} and GS^{3-} , in which both groups are deprotonated. The pH dependence of the conditional rate constants indicate that PS^- and GS^{2-} are the reactive species. The disulfide species involved in the oxidation of PS^- and GS^{2-} are GSSG^{2-} , PSSG^- and PSSP° . These are the predominant disulfide forms as shown in the various species distribution diagrams of Chapter III.

Equations 148 and 149 describe the two steps in the oxidation of PSH by GSSG in terms of the species involved and Equation 150 describes the overall reaction.



The two pH independent equilibrium constants, K'_1 and K'_2 can be determined from the values of K_1 and K_2 calculated earlier and the following relationships:

$$K_1 = K'_1 \frac{K_{A4} \text{PSSG} \quad K_{A5} \text{PSSG} \quad k_{a1234} \text{GSH}}{K_{A5} \text{GSSG} \quad K_{A6} \text{GSSG} \quad k_{a123} \text{PSH}} \quad (151)$$

$$K_2 = K'_2 \frac{K_{A3} \text{PSSP} \quad K_{A4} \text{PSSP} \quad k_{a1234} \text{GSH}}{K_{A4} \text{PSSG} \quad K_{A5} \text{PSSG} \quad k_{a123} \text{PSH}} \quad (152)$$

Equations 151 and 152 were derived from Equations 106 and 107. A value of 0.56 ± 0.02 was calculated for K'_1 and a value of 0.0143 ± 0.0014 for K'_2 . These values were calculated from K_1 and K_2 using literature values for the microscopic constants for PSH and GSH measured under ionic strength conditions different from those used in this

work. Using microscopic constants corrected to the ionic strength conditions used in this work, K'_1 and K'_2 were calculated to be 0.19 and 0.0049 respectively. This indicates that the actual values for K'_1 and K'_2 are very sensitive to the microscopic constants used in the calculations.

The rate constants k_1 and k_4 are for the forward and reverse reactions in Equations 148 and 149, respectively, i.e. $k_1 = 190 \text{ M}^{-1}\text{min}^{-1}$ and $k_4 = 1.30 \text{ M}^{-1}\text{min}^{-1}$. The reverse forward rate constants of Equations 148 and 149, k_2 and k_3 , respectively, are estimated from the pH independent equilibrium constants, K'_1 and K'_2 and the relationships: $K'_1 = k_1/k_2$ and $K'_2 = k_3/k_4$ to be $k_2 = 340 \pm 20 \text{ M}^{-1}\text{min}^{-1}$ and $k_3 = 0.019 \pm 0.005 \text{ M}^{-1}\text{min}^{-1}$.

At physiological pH, thiol groups are almost completely protonated and the reactive thiol-deprotonated species PS^- and GS^{2-} represent a minor fraction of the total PSH and GSH. Also, since the pK_A 's of the thiol groups of PSH and GSH are different, the fraction of PSH present as PS^- is different from the fraction of GSH present as GS^{2-} . Thus, at physiological pH, the conditional equilibrium and rate constants are different from the above values for K'_1 - K'_3 and k_1 - k_4 . The conditional equilibrium and rate constants calculated from these values for a pH of 7.4 are listed in Table 19.

Table 19. Conditional equilibrium and rate constants for the PSH/GSSG thiol/disulfide exchange reactions at pH 7.4.

Constant	Value
K_{1c}	1.36
K_{2c}	0.039
K_{3c}	0.053
k_{1c}	$36.6 \text{ M}^{-1}\text{min}^{-1}$
k_{2c}	$26.9 \text{ M}^{-1}\text{min}^{-1}$
k_{3c}	$0.00047 \text{ M}^{-1}\text{min}^{-1}$
k_{4c}	$0.012 \text{ M}^{-1}\text{min}^{-1}$

Conditional equilibrium constants were calculated from Equations 115 and 116 with the two pH independent equilibrium constants K_1 and K_2 . Similarly, the conditional rate constants k_{1c} and k_{4c} at pH 7.4 were calculated from Equations 140 and 147. From these conditional equilibrium and rate constants the conditional rate constants k_{2c} and k_{3c} were calculated from the following expressions: $K_{1c} = k_{1c}/k_{2c}$ and $K_{2c} = k_{3c}/k_{4c}$. The results are listed in Table 19. The values of k_{2c} and k_{3c} so obtained are in good agreement with the values estimated earlier from the concentration jump experiment and the equilibrium time course studies, respectively.

If the position of equilibrium in the two stepwise reactions was governed by random distribution, K_{1c} and K_{2c} would be 2 and 0.5 respectively, and K_{3c} would equal 1. The values obtained for K_{1c} and K_{2c} differ from these values by factors of 1.5 and 13 respectively. For comparison, Gorin and Doughty [38] reported values of $K_{1c} = 1.27$ and $K_{2c} = 0.27$ at pH 6.6 and 25°C for the reaction of cysteine with glutathione disulfide. Penicillamine differs from cysteine in that the thiol group of penicillamine is adjacent to two bulky methyl groups, which hinder its reactivity [28]. The large difference between k_{1c} and k_{3c} indicates this is particularly true in the reaction of PSH with PSSG, in which there also are two

methyl groups adjacent to the specific disulfide sulfur at which the reaction occurs. The large difference between k_{4C} and k_{2C} suggests that the methyl groups also hinder the access of thiolate groups to the disulfide group of *PSSP. Steric effects on thiol/disulfide exchange reactions have been observed previously for related systems. Equilibrium constants for thiol/disulfide exchange involving a series of alkyl thiols and disulfides differ from the statistically predicted values by a factor of 2 or less, except for the reaction of t-butyl thiol with n-butyl t-butyl mixed disulfide [39]. Also, exchange equilibrium constants for the reaction of a series of 2-aminoethane thiols with 4,4'-dithiobis(benzenesulfonate) are near statistical values except for those having two methyl groups next to the thiol [49]. Weber *et al.* found that the rate of reaction of GSH with RSSC, where R is an alkyl group and CS is cysteine, to form RSH and the cysteine-glutathione mixed disulfide is slowest when R is t-butyl and isopropyl [42]. The corresponding values for the reaction of N-PSH with GSSG at pH 7.4 are $K_{1C} = 2.6$, $k_{1C} = 4.9 \text{ M}^{-1}\text{min}^{-1}$ and $k_{2C} = 1.9 \text{ M}^{-1}\text{min}^{-1}$. This value for k_{1C} is less than that for PSH, even though k_1 is larger for N-PSH, because the fraction of the N-PSH in which the thiol group is deprotonated at pH 7.4 is less.

The small value for K_{2c} in Table 19 indicates that the tendency to form PSSP from the mixed disulfide is small. The small value for k_{3c} suggests that the PSSP found as a metabolite of penicillamine [116,117] is formed not by thiol/disulfide exchange but by other oxidation reactions. It has been proposed that, in cells, the nonenzymatic reduction of PSSP by GSH followed by the enzyme catalyzed reduction of GSSG to GSH is an efficient system for the reduction of PSSP [28]. However, the small value obtained for k_{4c} in this study suggests that, once formed, reduction of PSSP by other thiols, including GSH and protein thiols, will be of minor importance in the metabolism of penicillamine.

In biological systems, thiols undergo several oxidations via thiol/disulfide exchange reactions with disulfides [117-135]. The relative ease by which thiols are oxidized is measured by the overall conditional equilibrium constant, K_{3c} , i.e. $K_{3c} = K_{1c}K_{2c}$. From the values of K_{1c} and K_{2c} in Table 19, $K_{3c} = 0.053$. The overall conditional constant K_{3c} is related to the difference between the formal electrode potential of the GSSG/GSH and PSSP/PSH couples and gives the relative reducing power of thiols. This is discussed in more detail in Chapter V.

CHAPTER V

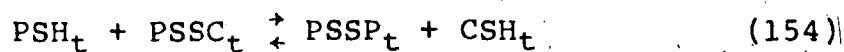
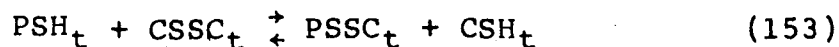
EQUILIBRIA AND KINETICS OF THIOL/DISULFIDE EXCHANGE REACTIONS OF PENICILLAMINE WITH CYSTINE AND RELATED DISULFIDES

A. Introduction

The thiol/disulfide exchange reactions of penicillamine with cystine are of interest because they form the basis for the treatment of cystinuria where a high plasma concentration of CSSC is found [17]; however the reactions have not been quantitatively characterized. The formation of cystine stones in the kidneys of cystinuric patients is reduced by treatment with PSH [22,117]; the mode of action is the reaction of PSH with the relatively insoluble cystine to form the more soluble penicillamine-cysteine mixed disulfide (PSSC, 8 in Figure 14). Other uses of penicillamine in medicine are for the treatment of heavy metal poisoning [136,137] and rheumatoid arthritis [138]. In these cases, the thiol/disulfide exchange reaction of PSH with extracellular cystine is a potential competing pathway by which PSH is metabolized. In extracellular fluids, CSSC predominates over cysteine [17] whereas in cellular

systems, absorbed CSSC is reduced to CSH via reaction with the predominant thiol GSH.

The thiol/disulfide exchange reactions involving PSH and CSSC are described by Equations 153 and 154.



Due to the acid/base properties of the five species involved, the characteristic behavior of the above reactions, as described by the equilibrium and rate constants, are expected to be pH dependent. Studies of these reactions in aqueous solution over the pH range 5-12 are described in this chapter.

Equilibrium and kinetic data for thiol/disulfide exchange reactions involving PSH and several other disulfides related to CSSC were also studied by ^1H NMR spectroscopy.

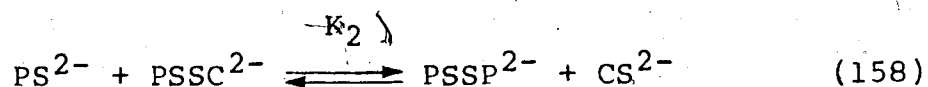
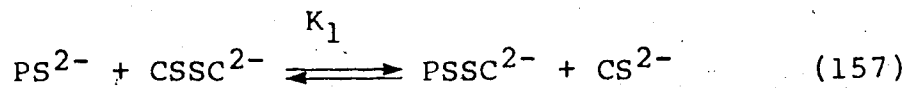
B. Determination of Equilibrium Constants for the PSH/CSSC System

The equilibria and kinetics of the thiol/disulfide exchange reactions for the PSH/CSSC system are pH dependent, as was also the case for the PSH/GSSG system in Chapter IV. The positions of the two thiol/disulfide equilibria in Equations 153 and 154 were measured experimentally over a wide pH range to give a series of conditional equilibrium constants, K_{1c} and K_{2c} defined as

$$K_{1c} = \frac{[\text{PSSC}]_t [\text{CSH}]_t}{[\text{PSH}]_t [\text{CSSC}]_t} \quad (155)$$

$$K_{2c} = \frac{[\text{PSSP}]_t [\text{CSH}]_t}{[\text{PSH}]_t [\text{PSSC}]_t} \quad (156)$$

The thiol/disulfide exchange reactions can be written in terms of the reactant and product species in their fully deprotonated forms:



The equilibrium constants for the two consecutive, reversible equilibria are defined as

$$K_1 = \frac{[\text{PSSC}^{2-}][\text{CS}^{2-}]}{[\text{PS}^{2-}][\text{CSSC}^{2-}]} \quad (159)$$

$$K_2 = \frac{[\text{PSSP}^{2-}][\text{CS}^{2-}]}{[\text{PSSC}^{2-}][\text{PS}^{2-}]} \quad (160)$$

where the various species are defined in Figures 21 and 26 in Chapter III. K_1 is related to K_{1c} by the acid dissociation constants of PSH, CSSC, PSSC and CSH. This can be done conveniently by using the fractional concentrations of PSSC^{2-} , CS^{2-} , PS^{2-} and CSSC^{2-} , i.e. α_1 , α_2 , α_3 and α_4 , respectively, where

$$\alpha_1 = \frac{[\text{PSSC}^{2-}]}{[\text{PSSC}]_t} = \frac{K_{A3}K_{A4}}{a_{\text{H}}^2 + a_{\text{H}}K_{A3} + K_{A3}K_{A4}} \quad (161)$$

In Equation 161, K_{A3} and K_{A4} are the third and fourth acid dissociation constants for the molecule PSSC. Similarly,

$$\alpha_2 = \frac{[\text{CS}^{2-}]}{[\text{CSH}]_t} \quad (162)$$

$$\alpha_3 = \frac{[\text{PS}^{2-}]}{[\text{PSH}]_t} \quad (163)$$

$$\alpha_4 = \frac{[\text{CSSC}^{2-}]}{[\text{CSSC}]_t} \quad (164)$$

$\alpha_2 - \alpha_4$ are defined in terms of acid dissociation constants and solution pH in a manner similar to Equation 161. Rearrangement and substitution of these equations into Equation 159 gives Equation 115 in Chapter IV for K_{1c} in terms of K_1 . Similarly, K_{2c} is given in terms of K_2 by Equation 116 with α_5 defined as in Equation 117 for the fractional concentration of PSSP^{2-} .

1. Experimental Data

The conditional equilibrium constants, K_{1c} and K_{2c} were determined over a range of pH values under reduced pressure and in sealed NMR tubes. The equilibrium concentrations of PSH, PSSC and PSSP were measured from the relative areas of their resonances. As shown in Chapter III, ^1H NMR spectra of the reaction mixture containing the five species (Figure 36 in Chapter III) shows overlapping methyl resonances for PSSC and PSSP for solutions at $\text{pH} < 8$.

Since the amount of PSSP produced by the reaction of PSH with the mixed disulfide PSSC is small, estimates of the conditional equilibrium constants were obtained at $\text{pH} < 8$ by neglecting the thiol/disulfide exchange reaction of PSH with PSSC. The error introduced by this approximation

was found to be negligible as the pH independent equilibrium constants calculated (pH \approx 8) were consistent, within the uncertainty of the experiment, with the range of equilibrium values calculated at pH $>$ 8 from data where the amount of PSSP produced was included in the equilibrium calculations. Well resolved methyl resonances are observed at pH $>$ 8 for the three species involved (Figure 36). The equilibrium concentrations of PSH, PSSC and PSSP were calculated from the areas of the methyl resonances as described in Chapter IV. The equilibrium concentrations of CSSC and CSH were then calculated by difference.

The conditions used and the values obtained for K_{1c} and K_{2c} are listed in Table 20. The extent of reaction in the sealed tubes was monitored by measuring ^1H NMR spectra every few days for a period of up to 15 days. As in the previous studies, NMR measurements were made over a long period of time to ensure that the second reaction (Equation 154), which is slow, had come to equilibrium. Extra resonances due to penicillamine-containing species were observed after long periods of time, e.g. \sim 6 days after mixing the reactants at pH 8. Collection of equilibrium data was stopped before significant amounts of these species had formed.

Table 20. Conditional equilibrium constants, K_{1c} and K_{2c} for the penicillamine-cystine thiol/disulfide exchange reaction as a function of pH.^a

pH	[PSH] ₀ ^b mM	[CSSC] ₀ ^b mM	K_{1c}	K_{2c}
5.96	1.01	1.02	4.48	-
7.95	1.01	1.02	4.78	-
8.77	3.55	4.49	3.70	0.0279
8.93	5.07	3.00	5.08	0.0470
9.07	3.55	4.49	5.40	0.0544
9.46	3.55	4.49	5.57	0.0427
10.00	5.07	3.00	5.48	-
10.02	3.55	4.49	6.19	0.0423

^aWater bath temperature, 25°C. Solutions prepared in 1 M aqueous KCl solution containing 0.003 M EDTA. Reactions studied in sealed NMR tubes.

^bInitial concentrations.

As shown in Table 20, the values of K_{1c} and K_{2c} are relatively pH independent. However, at higher pH, K_{1c} increases whereas K_{2c} stays relatively constant, e.g. at pH 11, K_{1c} and K_{2c} were estimated to be ~ 50 and ~ 0.06 , respectively.

2. Determination of the pH Independent Equilibrium Constants

The equilibrium constants, K_1 and K_2 , defined by Equations 159 and 160 respectively, were calculated from Equations 115 and 116 and the values listed in Table 20 using the two procedures described in Chapter IV. The results are listed in Table 21. The average of the eight K_1 values in Table 21 is 12.6 with a standard deviation of 2.2. A value of 12.0 with a linear estimate of the standard deviation of 1.5 was obtained by the second method using the non-linear least squares program KINET. Similarly, the average of the five K_2 values in Table 22, column 4, is 0.10 ± 0.03 . A value of $K_2 = 0.099 \pm 0.012$ was obtained with the second method of calculating K_2 . The last columns in Tables 21 and 22 show reasonable agreement between the observed and predicted values of K_{1c} and K_{2c} .

Table 21. Comparison between observed and predicted conditional equilibrium constant, K_{1c} .^a

pH	$\frac{\alpha_1 \alpha_2}{\alpha_3 \alpha_4}$ b.	K_{1c}	K_1	K_{1c} ^c predicted
5.96	2.06	4.48	9.24	5.82
7.95	2.78	4.78	13.3	4.32
8.77	3.10	3.70	11.5	3.88
8.93	2.99	5.08	15.2	4.02
9.07	2.86	5.40	15.4	4.21
9.46	2.44	5.57	13.6	4.92
10.00	1.92	5.48	10.5	6.27
10.02	1.90	6.19	11.7	6.34

^aConditions are those of Table 20.

^bDue to the large uncertainty in the value of pK_{A4} (CSSC) in Table 7, this constant was treated together with K_1 as an unknown in the non-linear least squares program KINET. The value obtained is 9.24 ± 0.10 .

^cCalculated using $K_1 = 12.0 \pm 1.5$ and Equation 115.

Table 22. Comparison between observed and predicted conditional equilibrium constant, K_{2c} .^a

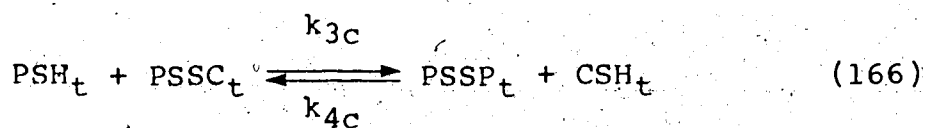
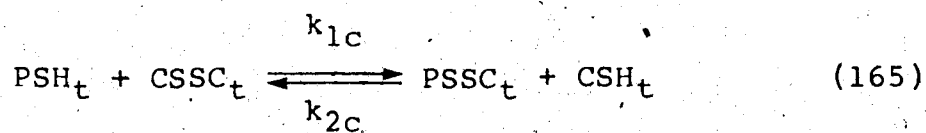
pH	$\frac{\alpha_2 \alpha_5}{\alpha_1 \alpha_3}$	K_{2c}	K_2	K_{2c} ^b predicted
8.77	2.79	0.028	0.078	0.035
8.93	2.64	0.047	0.12	0.037
9.07	2.52	0.054	0.14	0.039
9.46	2.22	0.043	0.095	0.044
10.02	1.83	0.042	0.077	0.054

^aConditions are those in Table 20.

^bCalculated using $K_2 = 0.099 \pm 0.012$, and Equation 116.

C. Determination of Rate Constants for the PSH/CSSC System

The kinetics of the thiol/disulfide reaction for the penicillamine/cystine system were characterized in aqueous solution over a range of pH. The conditional rate constants k_{1c} , k_{2c} , k_{3c} and k_{4c} are defined as



As discussed in Chapter IV, the rate of the second reaction is much slower than the first, and the kinetics of these two reactions can be determined separately. The kinetics of the reaction of PSH with CSSC were characterized over the pH range 5-8 whereas those of CSH with PSSP were studied at pH > 10.

1. The Reaction of PSH with CSSC

The conditional rate constants for the PSH/CSSC system were determined over the pH range 5-8 with concentrations of reactants ranging from 0.001 M to 0.005 M. The kinetics were followed either in situ or by quenching aliquots as a function of time.

Figure 53 shows time course spectra for the reaction of 0.005 M PSH with 0.003 M CSSC at pH 6. The bottom spectrum, taken 5 minutes after mixing the reactants, shows two major methyl resonances. These were assigned to the two non-equivalent methyl groups of PSH. The smaller resonances, assigned to the two methyl groups of PSSC, progressively increase in intensity thereafter, whereas those of PSH decrease. The equilibrium position is reached in ~100 minutes after mixing the reactants. The overlapping resonances of PSSC and PSSP at pH < 8 (Figure 36, Chapter III) prevents direct detection of PSSP which is likely to become significant with long reaction times due to aerial oxidation of PSH and CSH. For example, a spectrum taken 53 hours after mixing the reactants shows a relative increase in PSSC resonance intensities above those at 130 minutes. This indicates oxidation of PSH and CSH to PSSP and PSSC (Equations 48 and 49). At 130 minutes, no significant amount of PSSP was found. This indicates that the reaction of PSH with PSSC to give PSSP

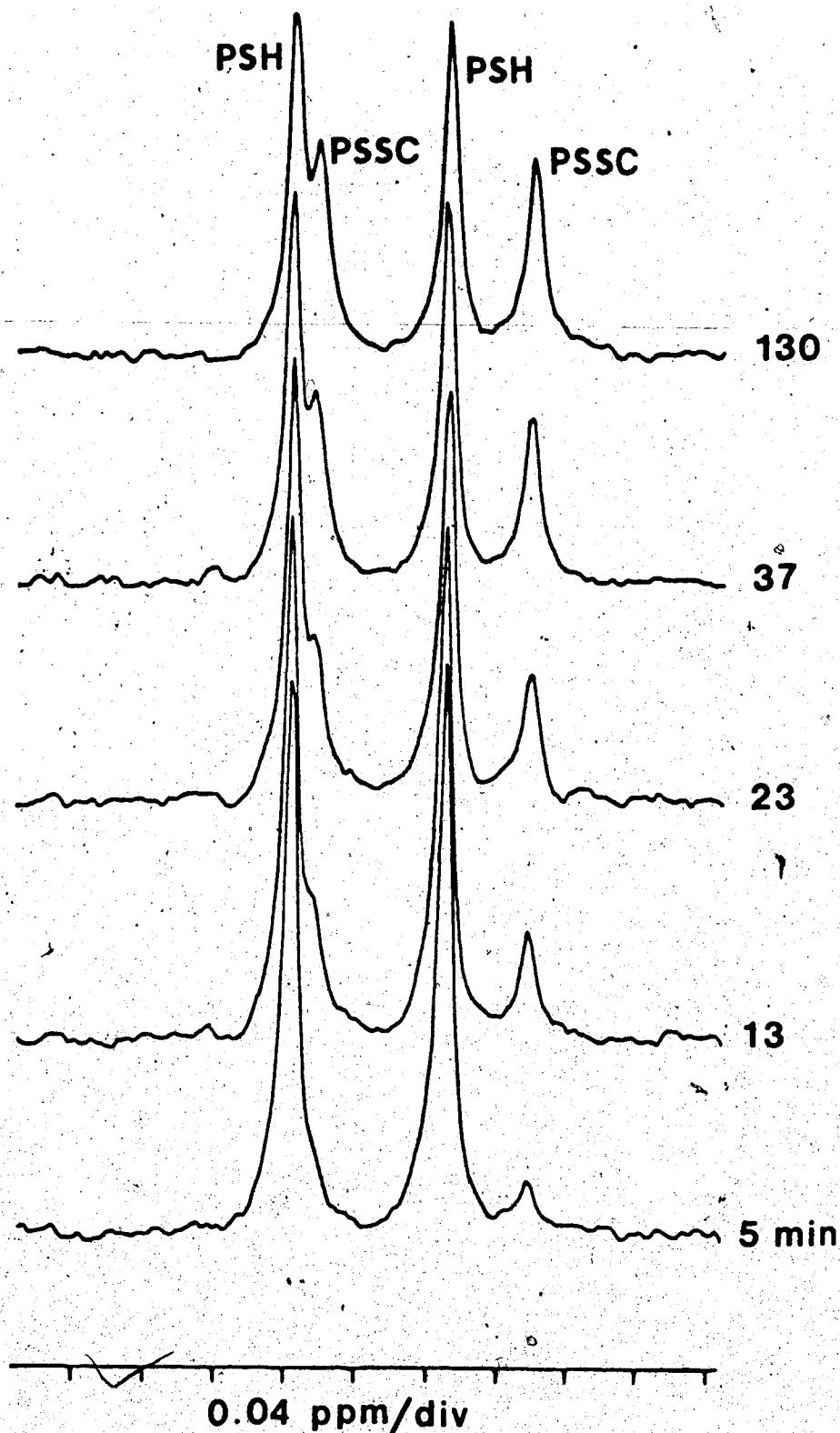


Figure 53. 200 MHz time course spectra for the reaction of PSH with PSSC. Solution pH, 5.94. Initial concentration, 0.00504 M PSH and 0.00297 M PSSC. Reaction was carried out at 24°C in situ, inside a 5 mm NMR tube in 1 M aqueous KCl solution containing 0.009 M EDTA.

and CSH is slower than the reaction of PSH with CSSC and consequently, k_{1c} values were determined separately from the other conditional rate constants.

The reaction time course curves for PSH and PSSC derived from Figure 53 by integration of both sets of resonances and conversion of areas to PSH and PSSC concentrations as described in the previous chapter are shown in Figure 54. The data in Figure 54 were treated by Equation 136 in Chapter IV for an overall second order reversible reaction. The values obtained are $k_{1c} = 8.35 \text{ M}^{-1}\text{min}^{-1}$ and $X_e = 0.00214 \text{ M}$. The two solid curves in Figure 54 are the predicted curves for these values. The good fit between the experimental points and the calculated curves suggests that the first reaction for the PSH/CSSC system is a second order reversible reaction with reaction 166 being negligible.

Time course data from six experiments, covering the pH range 5-8, were treated by Equation 136 to obtain values of k_{1c} and X_e as a function of pH. The results for k_{1c} are listed in Table 23. The magnitude of k_{1c} varies from $1.22 \text{ M}^{-1}\text{min}^{-1}$ at pH 5 to $465 \text{ M}^{-1}\text{min}^{-1}$ at pH 8. In these studies, reactant concentrations were restricted to the range 0.0001 M to 0.005 M due to the low solubility of cystine.

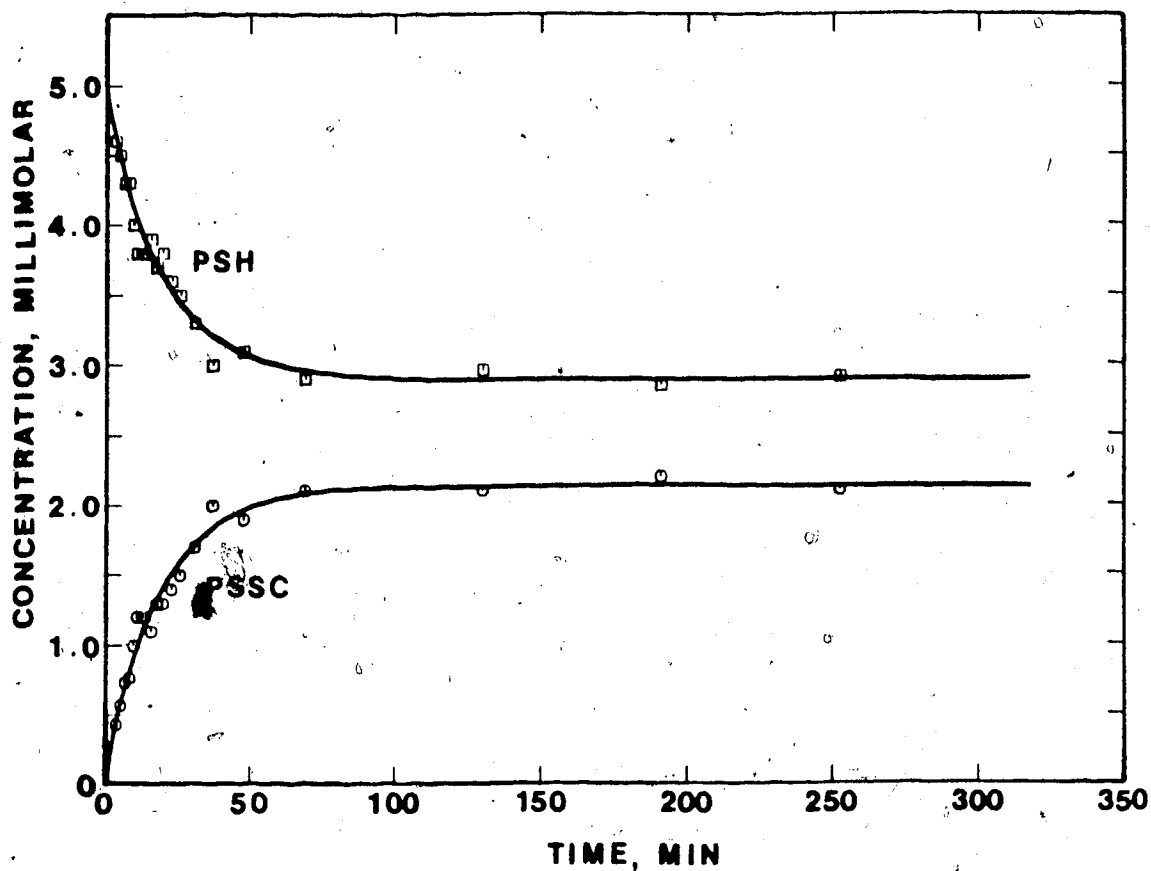


Figure 54. The concentrations of PSH and PSSC as a function of time for the experiment described in Figure 53. The solid lines are theoretical for a second order reaction with $k_{1c} = 8.35 \text{ M}^{-1}\text{min}^{-1}$ and $X_e = 0.00214 \text{ M}$ in Equation 136.

Table 23. Forward conditional rate constants, k_{1c} for the reaction of PSH with CSSC as a function of pH.^a

pH	[PSH] ₀ mM	[CSSC] ₀ mM	k_{1c} M ⁻¹ min ⁻¹	STD ^b M ⁻¹ min ⁻¹
5.07	3.02	1.98	1.22	0.16
5.89	5.04	1.12	7.75	0.37
5.94	5.04	2.97	8.35	0.33
6.72	5.04	1.12	46.2	3.7
6.93	3.02	1.98	97.2	4.6
8.05	2.00	2.00	465	130

^aSolutions in aqueous 1 M KCl containing 0.003 M EDTA. Temperature, 25°C. The extent of the reaction was followed in situ or by quenching.

^bLinear standard deviation from the non-linear least squares fit.

The solubility of CSSC at $\text{pH} < 8$ is $\sim 0.0005 \text{ M}$ [21,139]. Therefore, the solutions at $\text{pH} < 8$ in Table 23 are all saturated initially with CSSC. Usually, no precipitate was observed initially. As the reaction progresses, CSSC is being consumed by the reaction and its concentration decreases. The amount of CSSC remaining is sometimes less than its solubility of $\sim 0.0005 \text{ M}$, in which case the concentration of CSSC remaining is below the saturation level. For others, the amount of CSSC remaining at equilibrium is greater than its solubility. In this case, a precipitate forms slowly and becomes visible after a few days, i.e. well after the completion of the reaction.

At $\text{pH} 4$, CSSC precipitated before the equilibrium position was reached and the experiment was stopped. It is assumed that the saturation phenomenon does not affect significantly the rate of the reaction and, hence, the magnitude of k_{1c} .

The logarithm of the k_{1c} values listed in Table 23 is plotted versus pH in Figure 55. The slope of the plot up to $\text{pH} 7$ is 1. Beyond $\text{pH} 7$, the plot levels off gradually. This pH dependence is consistent with a model in which the reactive thiol species is in the thiol-deprotonated form. The pH dependence of the two possible thiolate anions, PS^- , in which the thiol group is

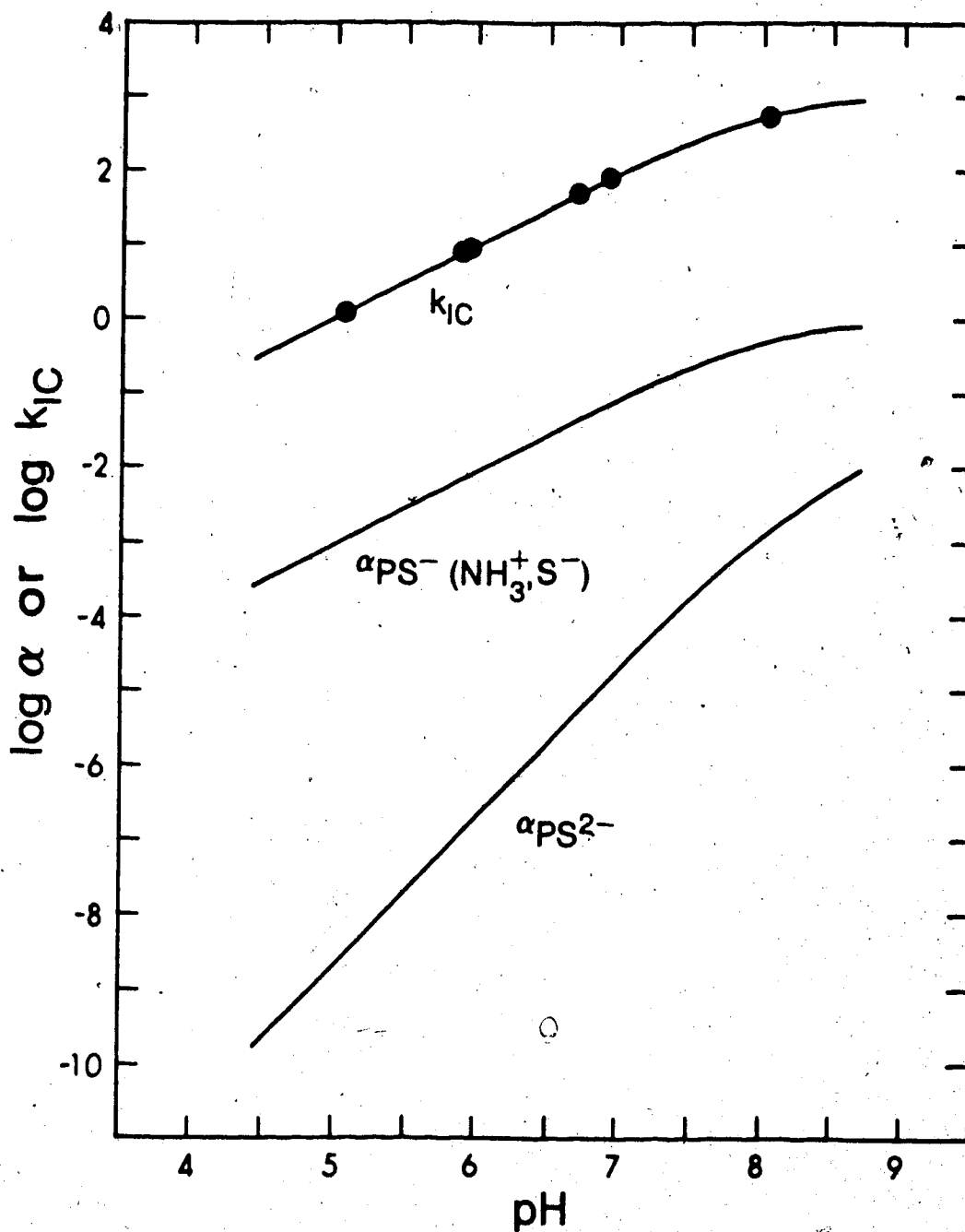


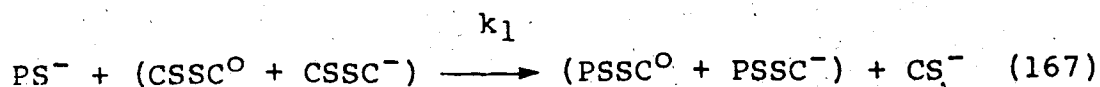
Figure 55. The logarithm of the fractional concentration α of PSH in the amino-protonated, thiol-deprotonated (PS^-) and amino-deprotonated, thiol-deprotonated (PS^{2-}) forms and of the forward rate constant k_{1C} for the reaction of PSH with CSSC versus pH. The solid curve through the experimental points is the theoretical curve predicted by Equation 140 and $k_1 = 1091 \text{ M}^{-1}\text{min}^{-1}$.

deprotonated and the ammonium group protonated and PS^{2-} are plotted as a function of pH in Figure 55 over the pH range 5-8. The slope of the $\log \alpha_{PS^-}$ vs pH plot is one over the pH range 5-7, while that in which both groups are deprotonated, $\log \alpha_{PS^{2-}}$, is two. Since the pH dependent behavior of $\log k_{1C}$ parallels the pH dependence of the PS^- form over the pH range studied, $\log \alpha_{PS^-}$, the reactive thiol-deprotonated species is concluded to be PS^- .

There is also the possibility that the rate constant depends on the protonation state of CSSC. However, the theoretical curve predicted by the model having a single rate constant, k_1 , is in excellent agreement with the experimental data (Figure 55). This indicates that either there is no dependence of k_{1C} on the protonation state of CSSC over the pH range 5-8 or the fractional concentration of the reactive form of CSSC is constant over this pH range. The various curves in Figure 38 show that the fractional concentration of the carboxylate-deprotonated, amino-protonated form, $CSSC^0$, varies from 1 to 0.4 over the pH range 5-8, while that of $CSSC^-$ (one amino group protonated) varies from 0.001 to 0.6. The results in Figure 55 suggest that the rate constants for the reaction of PS^- with $CSSC^0$ and $CSSC^-$ are similar as seen by the good fit of the experimental data to a model having a single rate constant. At $pH > 8$, the conditional rate

constant was found to be smaller, due possibly to the less favorable reaction between PS^- and the highly charged species $CSSC^{2-}$. Also, the fraction of PSH as PS^{2-} is increasing.

From the above results, the kinetic expression for the forward reaction in terms of the molecular species present in the pH range 5-8 is



The relationship between k_1 and k_{1c} is given by Equation 140 in Chapter IV. The pH independent rate constant, k_1 , was evaluated from the conditional rate constants in Table 23 by fitting them to Equation 140 with the non-linear least squares program KINET. The value obtained is $1091 \pm 53 \text{ M}^{-1}\text{min}^{-1}$. The fit of the data to the model can be seen by comparison of the solid curve in Figure 55 with the plotted experimental values or by comparison of the predicted k_{1c} values in Table 24 (column 5) with the observed values (column 3). The value for the pH independent rate constant k_1 was also obtained by calculating a value for α in Equation 141 in Chapter IV at each pH value. The results are also presented in Table 24 for α (column 2) and for k_1 (column 4). The average of k_1 from the 6 values is $1065 \pm 135 \text{ M}^{-1}\text{min}^{-1}$.

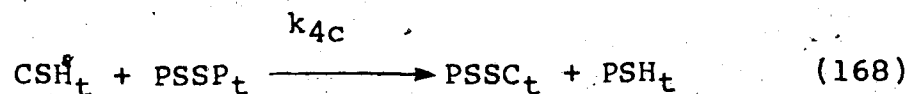
Table 24. Comparison between observed and predicted conditional forward rate constants as a function of pH.

pH	α	k_{lc} $M^{-1}min^{-1}$	k_1 $M^{-1}min^{-1}$	k_{lc}^a predicted $M^{-1}min^{-1}$
5.07	903	1.22	1100	1.21
5.89	137	7.55	1060	7.95
5.94	122	8.35	1020	8.91
6.72	21.2	46.2	978	51.5
6.93	13.5	97.2	1310	81.1
8.05	1.98	465	922	550

^aCalculated using $k_1 = 1091 M^{-1}min^{-1}$ and Equation 140. For the conditions used, see Table 23.

2. The Reaction of CSH with PSSP

The kinetics of the reaction of CSH with PSSP



were studied over the pH range 10-12. The rate of this reaction was so slow that a combination of high known initial concentrations of reactants, CSH and PSSP, and high solution pH were used to collect enough data within a reasonable period of time. At pH < 8, CSSC precipitates out due to its low solubility, and low initial concentrations of CSH and PSSP were used. However, under these conditions, i.e. ~0.001 M each of CSH and PSSP, the forward rate of the reaction was too slow to be conveniently studied. For example, at pH 7.25, the amount of PSSC produced was ~3% of the initial PSSP concentration after a period of 24 hours for a solution containing 0.005 M reactants. The estimated value for k_{4c} from these data is ~0.008 M⁻¹min⁻¹. At solution pH ~ 8, CSSC is much more soluble and higher known initial concentrations of CSH and PSSP were used so that within a few hours, enough kinetic points could be collected to determine k_{4c} more accurately. The reactions at pH > 10 were monitored by taking aliquots from the reaction vessel as a function of

time and quenching by lowering the pH to about 1. Prior to NMR measurement, each aliquot was adjusted to pH ~9, frozen solid and kept at -2°C in the freezer until its use on the same day. At pH 9, three of the six methyl resonances of the penicillamine-containing species are well resolved from each other as shown in Figure 36 of Chapter III. With this method, further reaction between CSH and PSSP in each aliquot after the second pH adjustment from pH 1 to 9 is kept to a minimum.

The reaction between CSH and PSSP at these high pH values is slow, e.g. 2 hours after mixing the reactants, only 5% of the initial PSSP concentration has been consumed by the reaction. Since each spectrum requires less than 10 minutes for temperature equilibration and data collection, the errors due to the further reaction of CSH with PSSP are therefore small. Figure 56 shows the methyl and methine resonances in typical time course spectra. The various resonances were assigned to the individual thiols and disulfides by comparison of their chemical shifts with those of Chapter III. The resonances for PSSC and PSSP in Figure 56 are not sufficiently well resolved for accurate integration when the relative area of PSSC is small. Therefore, methine resonances were also used to measure the extent of reaction. The fractions of PSH and PSSC were calculated from the methyl and methine

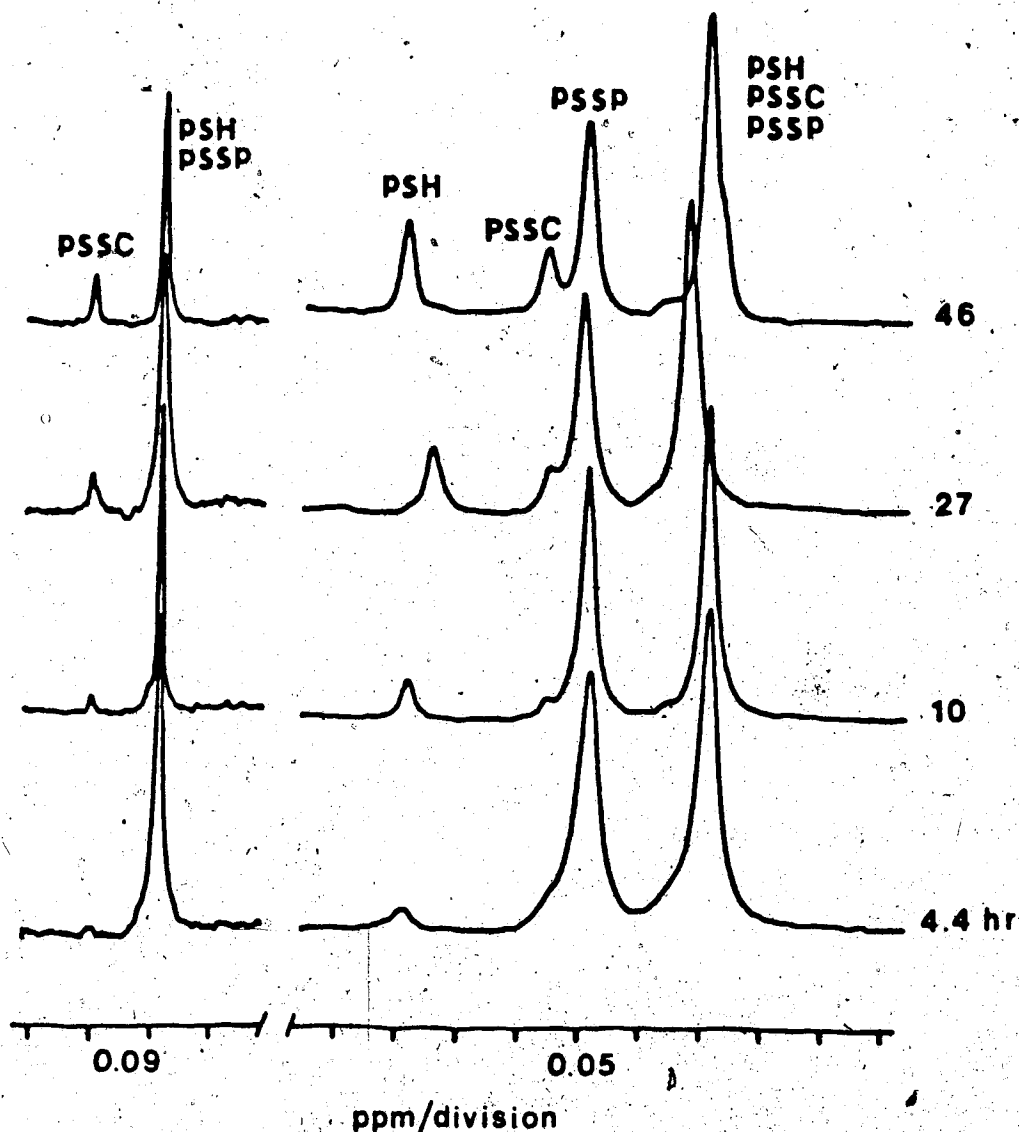


Figure 56. 200 MHz ¹H NMR time course spectra of the methyl and methine groups of PSH, PSSP and PSSC in a solution containing initially 0.102 M CSH and 0.100 M PSSP. The reaction was carried out at pH 12.44, aliquots were quenched as a function of time by lowering the pH to ~0.5, and then the pH was raised to pH 9 when NMR spectra were run so that resolved resonances would be obtained for the various species. The pH was not identical for each aliquot.

region, respectively and the fraction of PSSP calculated by difference. As expected, the intensities for PSH and PSSC resonances increase and that of PSSP decreases. The reaction between CSH and PSSP is slow as evidenced by the bottom spectrum; after 4.4 hours, only 8% of the initial PSSP has been used by the reaction. 340 hours after mixing the reactants, extra small resonances appeared (results not shown) indicating that additional penicillamine-containing species are being produced at a rate approximately 300 times slower than that of the CSH/PSSP forward reaction. Because of this interfering reaction, the rate constant, k_{4c} , was estimated by the initial slope method. The time course curves for PSH, PSSC and PSSP calculated from Figure 56 are shown in Figure 57. Values calculated for k_{4c} from the initial slope are (pH, k_{4c}): 10.39, $0.0052 \text{ M}^{-1}\text{min}^{-1}$; 10.73, $0.0037 \text{ M}^{-1}\text{min}^{-1}$; 11.95, $0.0033 \text{ M}^{-1}\text{min}^{-1}$; 12.44, $0.0029 \text{ M}^{-1}\text{min}^{-1}$. The initial concentrations of CSH and PSSP in the four experiments were 0.102 M and 0.100 M respectively in aqueous 1 M KCl/ 0.003 M EDTA solution.

For the thiol/disulfide exchange reactions involving PSH with GSSG and PSH with CSSC, k_{1c} is found to decrease as solution pH increases at $\text{pH} > 9$, possibly as a result of electrostatic effects when the species are highly

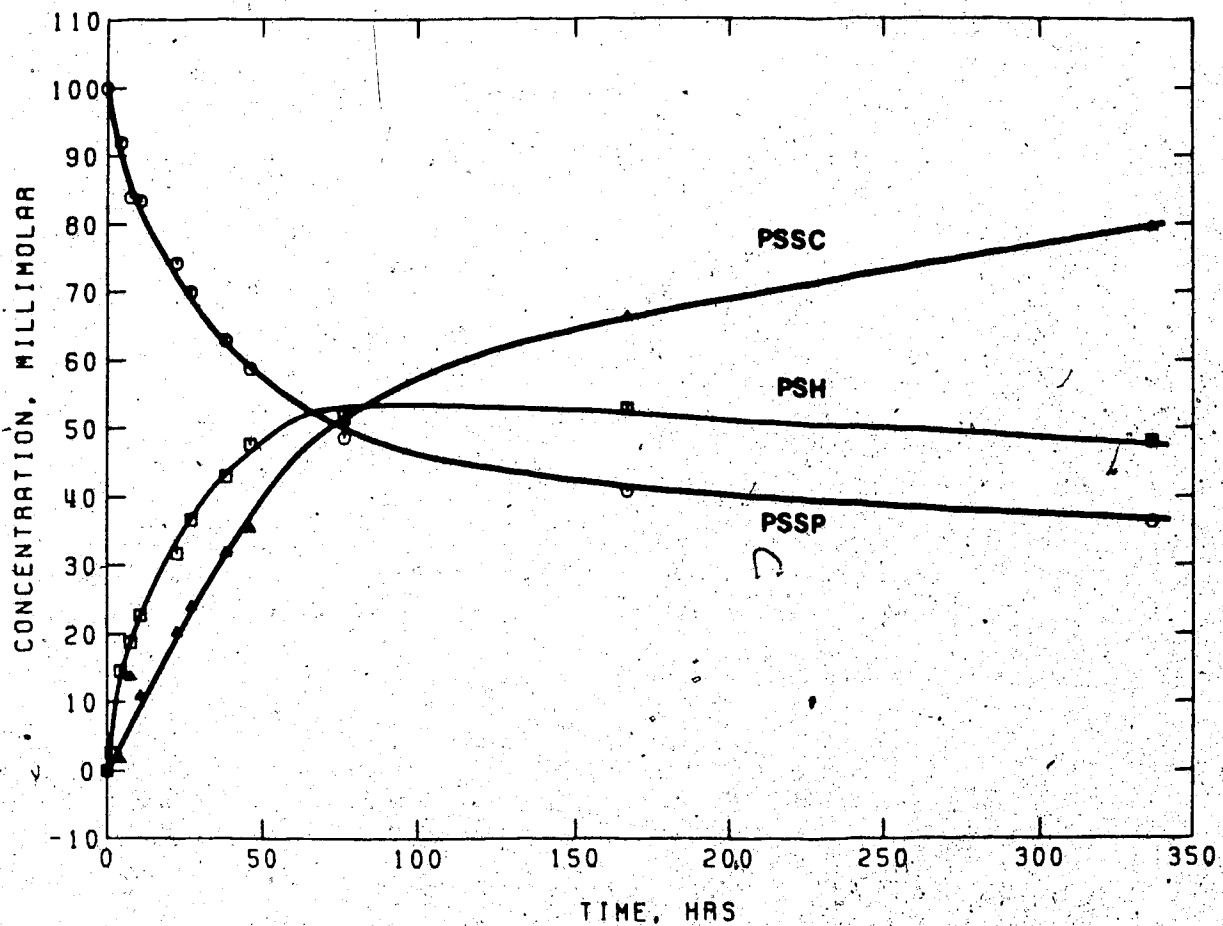


Figure 57. Progress curves for PSH, PSSC and PSSP as obtained from data of the type shown in Figure 56.

charged, e.g. CSSC^{2-} . Therefore, a direct extrapolation of k_{4c} values at high pH to lower pH, e.g. pH 7.4, is not feasible. However, it was observed that the ratio between k_{1c} at pH 9 and k_{1c} at pH 7.4 for PSH/CSSC and PSH/GSSG systems is 1.4 and 2.4 respectively. Assuming that the values of k_{4c} behave similarly, a rough estimate can be extrapolated from the k_{4c} value at pH 10. The result thus obtained is k_{4c} (pH 7.4) $\sim 0.003 \text{ M}^{-1}\text{min}^{-1}$ which is in reasonable agreement with the estimate of $\sim 0.008 \text{ M}^{-1}\text{min}^{-1}$ at pH 7.25.

D. Reaction of Penicillamine with Other Disulfides

The reaction of penicillamine with other disulfides of biological interest, including cystamine and homocystine, and with non-biological disulfides was investigated for comparison with the results obtained for CSSC and GSSG. The conditional equilibrium constants, K_{1c} and K_{2c} for the thiol/disulfide exchange reactions of PSH with the disulfides (structures shown in Figure 58) of cysteamine (CySSCy), homocysteine (HSSH), 2-mercaptoethanol (ESSE), mercaptoacetic acid (MSSM), 3-mercaptopropionic acid (PrSSPr) and mercaptosuccinic acid (SuSSSu) were measured in aqueous solution at pH between 7 and 8. Solutions used were degassed in the NMR tube by

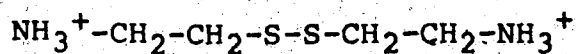
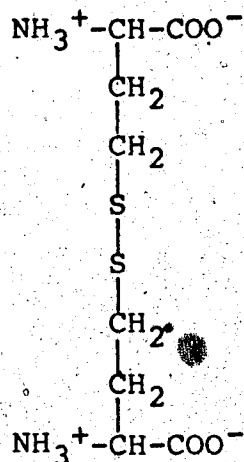
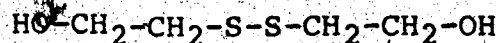
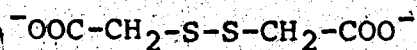
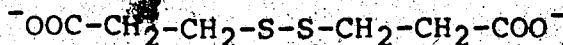
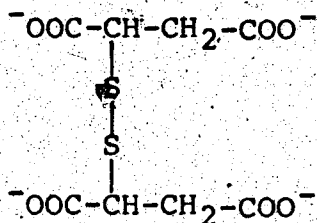
A) Cystamine (CySSCy)B) Homocystine (HSSH)C) 2-Hydroethyl Disulfide (ESSE)D) Dithiodiglycolic Acid (MSSM)E) 3,3'-Dithiodipropionic Acid, (PrSSPr)F) Mercaptosuccinic Acid Disulfide (SuSSSu)

Figure 58. Structural formulae of selected disulfides.

the freeze-pump-thaw method and the NMR tube sealed. Spectra were measured at times up to 200 hours after mixing the reactants to ensure that the equilibrium position had been reached. The conditional equilibrium constants were then calculated from the intensities of the methyl resonances by the methods described in Chapter IV. The results obtained for K_{1c} and K_{2c} at physiological pH are listed in Table 25^a together with the initial concentrations of PSH and disulfides used. The values of the pH independent equilibrium constants K_1 and K_2 for the reactions written in terms of the fully deprotonated species cannot be calculated from the conditional equilibrium constants in Table 25 since the acid dissociation constants of these various mixed disulfides are not known.

Conditional rate constant k_{1c} was also determined for the thiol/disulfide systems listed in Table 25. The kinetic data were collected either in situ or by the quenching method. One or two kinetic experiments were carried out in the pH range 5.5-7.6. Time course spectra were collected and the concentrations of the mixed disulfide, PSSR determined from the relative intensities of the methyl resonances for PSH and PSSR. Then, k_{1c} was calculated by fitting the concentration of PSSR as a function of time to Equation 136. As before, the reaction

Table 25. Conditional equilibrium constants for the reaction of penicillamine with selected disulfides (RSSR) in the pH range 7-8.^a

RSSR	[PSH] ₀ mM	[RSSR] ₀ mM	pH	K _{1c}	K _{2c}
CySSCy	49.1	53.8	6.95	1.64±0.11	0.029±0.006
	49.1	53.8	7.38	1.78±0.02	0.031±0.008
	49.1	53.8	7.93	1.96±0.19	0.034±0.003
HSSH	0.988	1.05	6.96	1.24	0.033
ESSE	57.3	51.7	7.16	1.81±0.05	0.022±0.001
	57.3	51.7	7.49	1.86±0.16	0.027±0.002
	57.3	51.7	8.13	1.40	0.022
MSSM	63.7	69.2	7.40	2.54	--
	54.9	86.7	7.41	2.44	--
PrSSPr	49.1	50.1	7.01	1.40±0.24	--
	49.1	50.1	7.43	1.40±0.32	0.027±0.003
	49.1	50.1	7.93	1.09±0.01	--
SuSSSu	54.5	61.9	7.01	2.08±0.31	0.015
	54.5	61.9	7.42	2.04±0.23	0.025±0.004
	54.5	61.9	7.97	1.45±0.14	--

^a25°C, 1 M aqueous KCl solution containing 0.003 M EDTA.

of PSH with PSSR was observed to be much slower than its reaction with RSSR and the kinetic experiments were stopped before significant amounts of PSSP were detected. The values obtained for k_{1c} together with the conditions used are listed in Table 26.

Assuming the reactive PSH species to be PS^- , pH independent rate constants can be calculated from the data in Table 26 using Equation 140. The results are (RSSR, k_1 in $M^{-1}min^{-1}$): CySSCy, 797 ± 316 ; ESSE, 63.4 ± 3.1 ; MSSM, 229 ± 27 ; PrSSPr, 92 ± 6 ; SuSSSu, 0.95 ± 0.23 . By comparison, the values for CSSC and GSSG are $k_1 = 1091 \pm 53 M^{-1}min^{-1}$ and $k_1 = 190 \pm 7 M^{-1}min^{-1}$ respectively.

Of practical interest is the relative rate for the reaction of PSH with different optical isomers of symmetrical disulfides. The results obtained for the reaction of the disulfide (GSSG) with the D and the L isomers of N-acetylpenicillamine were discussed earlier and can be referred to for comparison. Time course spectra for the reaction of PSH with the various optical isomers of SuSSSu are shown in Figure 59. At time $t = 7.5$ min, only the two methyl resonances of PSH are present. Two new sets of resonances appear at $t = 17$ min and these were assigned to the mixed disulfide of PSH with SuSSSu (PSSSu). The methyl resonances for PSSSu at high field show a doublet whereas those at low field overlap. The

Table 26. Conditional forward rate constants for the reaction of penicillamine with selected disulfides (RSSR).^a

RSSR	[PSH] ₀ mM	[RSSR] ₀ mM	pH	k _{1c} M ⁻¹ min ⁻¹	STD ^b M ⁻¹ min ⁻¹
CySSCy	34.5	37.8	5.65	2.43	0.02
	34.5	35.1	5.56	3.52	0.13
ESSE	31.3	39.0	5.49	0.187	0.009
	33.7	35.1	5.58	0.228	0.007
MSSM	35.0	35.1	5.49	0.688	0.018
	34.5	35.0	5.57	0.787	0.094
PrSSPr	32.8	33.7	5.50	0.276	0.018
SuSSSu	48.4	49.4	7.58	0.208	0.008
	32.8	33.1	7.61	0.309	0.017

^a1 M KCl aqueous solution containing 0.003 M EDTA.

^bLinear standard deviation from the non-linear least squares program.

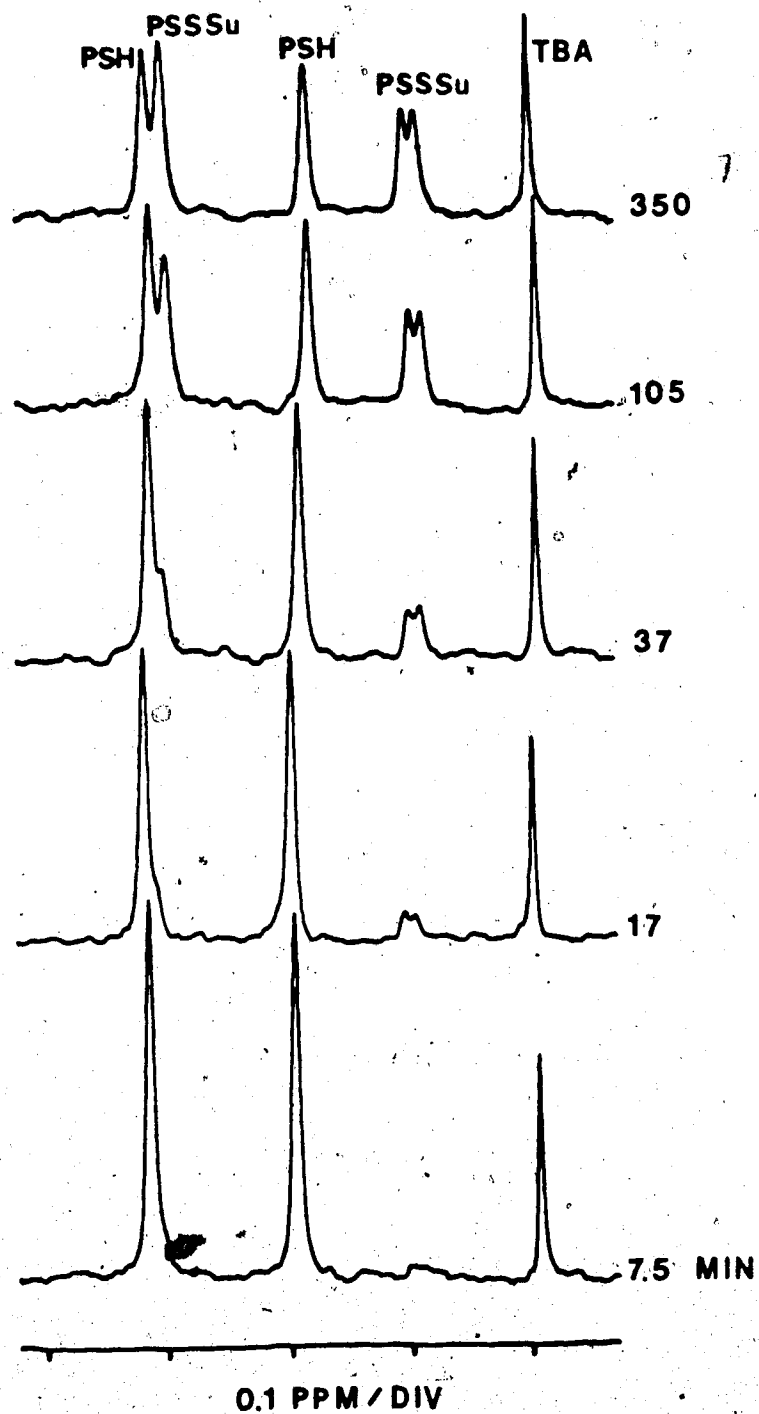
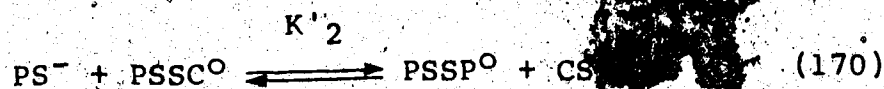
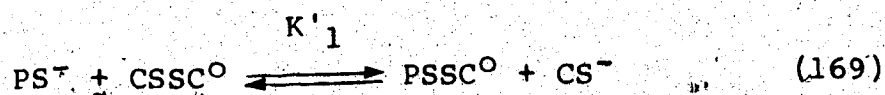


Figure 59. 200 MHz ^1H spectra of the methyl groups in a solution which contained initially 0.0328 M PSH and 0.0331 M SuSSu as a function of time. 1 M KCl, 0.003 M EDTA, pH 7.61, 25°C.

result of random reaction between PSH and the three pairs of optical isomers for SuSSSu (1:2:1) is that the extent of the three thiol/disulfide exchange reactions is similar. This is supported by the equal intensities for the two methyl resonances of PSSu at high field. Furthermore, from the behavior of these two methyl resonances as a function of time, the rate is essentially identical, as was also found to be the case for the N-acetylpenicillamine/GSSG system.

E. Discussion

The equilibrium constants for the PSH/CSSC system in Table 20 are pH dependent conditional equilibrium constants in terms of all the species existing at the particular solution pH. In terms of the reactive species present in the pH range 5-8 which includes the physiological pH, the thiol/disulfide exchange reactions taking place are:



PS⁻ and CS⁻ are the carboxylate-deprotonated and amino-protonated forms of PSH and CSH. The pH independent equilibrium constants, K'₁ and K'₂, are related to the values for K₁ and K₂ by equations similar to Equations 151 and 152. Values obtained are K'₁ = 5.36 ± 0.67 and K'₂ = 0.0198 ± 0.0023.

The pH independent rate constants for Equation 169 are k₁ = 1091 M⁻¹min⁻¹ as determined from rate data obtained over the pH range 5-8 and k₂ = k₁/K'₁ = 204 M⁻¹min⁻¹. Similarly, k₄ ~ 0.2 M⁻¹min⁻¹ and k₃ = K'₂ × k₄ ~ 0.004 M⁻¹min⁻¹ for Equation 170.

Equations for the thiol/disulfide exchange reactions of PSH with the other disulfides studied cannot be written in terms of the reactive species present at pH 7 because the fractional concentrations of the mixed disulfides cannot be calculated as their acid dissociation constants are not known. Consequently, the pH independent equilibrium constants for the reactions in terms of the reactive species cannot be determined.

Conditional equilibrium and rate constants for the reaction of PSH with CSSC at physiological pH are of practical interest in medicine because the reaction is the basis for the treatment of cystinuria. Using pH independent equilibrium and rate constants determined

earlier, the values of K_{1c} , K_{2c} and k_{1c} were calculated from Equations 115, 116 and 141 respectively. Others were calculated as shown previously for the PSH/GSSG system. The results are listed in Table 27. These results suggest that the mechanism of action in the treatment of cystinuria would be due mainly to the thiol/disulfide exchange of PSH with relatively insoluble CSSC to form the more soluble mixed disulfide PSSC. The second reaction involving PSH with PSSC would be a negligible pathway in the metabolism of PSH. Since the equilibrium constant K_{1c} is of intermediate value and K_{2c} exceptionally low, penicillamine has a large tendency to form PSSC.

Reactions with CSSC are fast and equilibrium is reached in ~10 minutes.

Conditional equilibrium and rate constants at physiological pH for the reaction of PSH with other disulfides (RSSR) studied are summarized in Table 28 together with the results obtained with GSSG and CSSC. Also listed is the conditional equilibrium constant, K_{3c} for the overall reaction of PSH with RSSR,

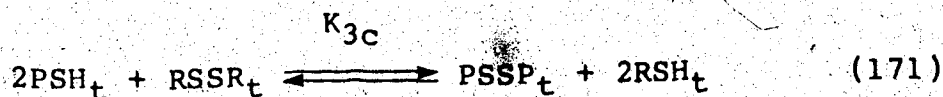


Table 27. Conditional equilibrium and rate constants for the PSH/CSSC thiol/disulfide exchange reaction at pH 7.4.

Constant	Value
K_{1c}	5.13
K_{2c}	0.0238
K_{3c}^a	0.123
k_{1c}	$210 \text{ M}^{-1}\text{min}^{-1}$
k_{2c}^b	$40.9 \text{ M}^{-1}\text{min}^{-1}$
k_{3c}^c	$\sim 0.0003 \text{ M}^{-1}\text{min}^{-1}$
k_{4c}^d	$\sim 0.01 \text{ M}^{-1}\text{min}^{-1}$

$$^a K_{3c} = K_{1c} K_{2c}$$

$$^b k_{2c} = k_{1c} / K_{1c}$$

$$^c k_{3c} = k_{4c} K_{2c}$$

^dEstimated from the data at pH 7.25 and Equation 147.

Table 28. Conditional equilibrium constants for the reaction of penicillamine with selected disulfides (RSSR) at pH 7.4.

RSSR	pH	K_{1c}^a	K_{2c}^a	K_{3c}^b	$\Delta E^{\circ\prime c}$ volt	k_{1c}^d $M^{-1}min^{-1}$	k_{2c}^e $M^{-1}min^{-1}$
Cysteamine disulfide (CySSCy)	7.4	1.78	0.031	0.0552±0.014	-0.0372±0.0033	153±61	86.2
Homocysteine disulfide (HSSSH)	7.0	1.24	0.033	0.0409	-0.0411	-	-
2-Mercaptoethanol disulfide (ESSE)	7.5	1.86	0.027	0.0502±0.0057	-0.0385±0.0015	12.2±0.6	6.56
Mercaptoacetic acid disulfide (MSSM)	7.4	2.49	-	-	-	44.0±5.3	17.3
3-Mercaptopropionic acid disulfide (PSSPr)	7.4	1.40	0.027	0.0378±0.0096	-0.0421±0.0033	17.7±1.1	12.6
Mercaptosuccinic acid disulfide (SuSSSu)	7.4	2.04	0.025	0.051±0.010	-0.0383±0.0025	0.18±0.044	0.0895
Cystine (CSSC) ^f	7.4	5.13	0.024	0.123±0.021	-0.0269±0.0022	210±10	40.9
Glutathione disulfide (GSSG) ^f	7.4	1.36	0.039	0.0530±0.0054	-0.0378±0.0013	36.6±1.3	26.9

^aData are those from Table 25. Uncertainties for K_{1c} and K_{2c} are listed in Table 25.

^b $K_{3c} = K_{1c}K_{2c}$.

^cCalculated with Equation 173 and with respect to the PSSP/PSH couple. The values of $\Delta E^{\circ\prime}$ for the various disulfides are the same within the experimental uncertainty except for that of cystine.

^dCalculated from pH independent rate constants derived from data in Table 26 and Equation 140.

^eCalculated from K_{1c} and k_{1c} : $k_{2c} = k_{1c}/K_{1c}$.

^fValues listed for K_{1c} , K_{2c} and k_{1c} are conditional constants given in Tables 19 and 27. Uncertainties in K_{1c} and K_{2c} are ± 0.64 and ± 0.003 respectively for the PSH/CSSC system and ± 0.04 and ± 0.004 respectively for the PSH/GSSG system.

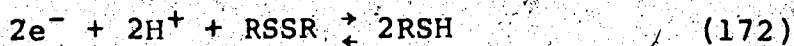
and $K_{3c} = K_{1c} \cdot K_{2c}$. The values for K_{1c} and K_{2c} for the reaction of PSH with the eight disulfides are quite similar. If the distribution of PSH and RSH groups were governed by random probability, a mixture originally containing 2 moles PSH and 1 mole RSSR for example, would give, at equilibrium, the following amounts: RSSR and PSSP, 1/4 mole each; PSSR, 1/2 mole; PSH and RSH, 1/2 mole each, i.e. K_{1c} and K_{2c} would be 2 and 0.5 respectively, and K_{3c} would be 1. The values obtained for K_{1c} range from 1.24 to 2.49 except for the reaction of PSH with CSSC whose value ($K_{1c} = 5.13$) differs from the random distribution value of 2 by a factor ~ 3 . In contrast, the seven values of K_{2c} (~ 0.03) differ from the random distribution value by a factor of ~ 20 . These results indicate that, even though the reaction of PSH with RSSR is random, in the reaction of PSH with its mixed disulfide PSSR, PSH has considerably less tendency to react with PSSC to form PSSP than predicted by random probability. That is, the equilibrium constants are not sensitive to structural changes in the groups attached to the sulfur atom except when steric factors are involved. The thiol/disulfide exchange reactions involving a series of alkyl thiols and disulfides [39], a series of substituted 2-aminoethane thiol and 4,4'-dithiobis (benzene sulfonate) [49] and glutathione reacting with a series of

mercaptoalkane-cysteine mixed disulfides [42] have been reported to have such steric factors.

The values listed in Table 28 for the conditional rate constant, k_{1c} cover a wide range in contrast to those for K_{1c} . The conditional rate constant for mercaptosuccinic acid disulfide is a factor of ~1000 less than those for cystine and cysteamine disulfide. These results do not identify the factors which govern the rate of reaction, however they do suggest that the total electrostatic charge on the disulfide is important. For example, mercaptosuccinic acid disulfide has a charge of -4 at pH 7.4, whereas the disulfides with a total charge of 0 or -2 have k_{1c} value in the intermediate range.

Cystine and cysteamine disulfide, which have total charges of 0 and +2 respectively, have the largest value for the rate constant because their reaction with the PSH reactive species is electrostatically more favorable. The reactive penicillamine species in each reaction is presumably the same with a charge of -1.

The RSSR/RSH pair of molecules forms the redox couple



with a formal electrode potential $E_{\text{RSSR/RSH}}^{\circ}$. The differences between the formal electrode potential for the various RSSR/RSH redox couples and that of PSSP/PSH couple are related to the values for the overall equilibrium constant K_{3c} (Table 28) by Equation 173 [21].

$$\Delta E^{\circ} = E_{\text{RSSR/RSH}}^{\circ} - E_{\text{PSSP/PSH}}^{\circ} = \frac{RT}{nF} \ln K_{3c} \quad (173)$$

The differences, ΔE° , listed in Table 28, are all negative. This indicates that the thiol form, RSH, of all seven disulfide molecules studied has greater reducing power (is more easily oxidized) than PSH at physiological pH. This smaller reducing power of PSH is due to its smaller tendency to form its symmetrical disulfide PSSP. As mentioned earlier, this is due to steric effects of the two methyl groups in PSH.

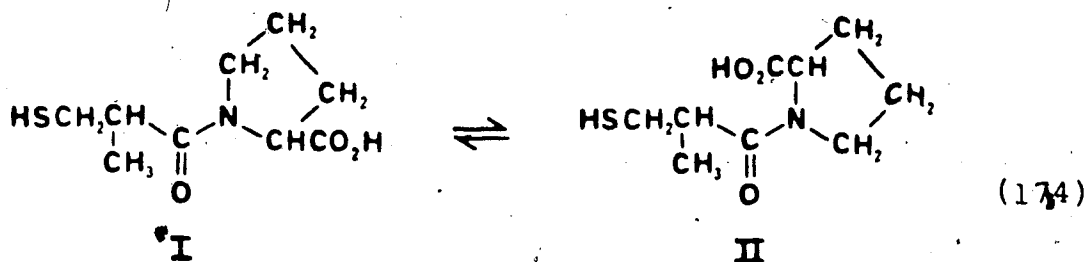
CHAPTER VI

A STUDY OF THE FORMATION AND CONFORMATIONAL EQUILIBRIA OF SYMMETRICAL AND MIXED DISULFIDES OF CAPTOPRIL

A. Introduction

Captopril, 1-(D-3-mercapto-2-methylpropanoyl)-L-proline (CpSH), is a recently developed drug for the treatment of high blood pressure [29-31]. The thiol group is the key functional group in the metabolism of captopril, undergoing oxidation and thiol/disulfide exchange reactions with disulfide molecules to form various captopril-containing metabolites. The major metabolites are captopril disulfide (CpSSCp) and mixed disulfides with thiol-containing amino acids, peptides and proteins [140-143]. These are thought to play a role in determining the nature and time course of adverse reactions to captopril in biological systems [144]. In order to understand these side-reactions, it is necessary to study both the formation and the chemistry of these captopril-containing metabolites and their chemistry in aqueous solutions.

Captopril exists in solution as an equilibrium mixture of cis (II) and trans (I) isomers with respect to the conformation across the peptide bond involving the proline amino group.



The relative populations of the cis and trans forms are dependent on the protonation states of the two functional groups of captopril [145]. Captopril disulfide and captopril-containing species are also expected to be present in aqueous solution as the cis and trans forms since cis-trans isomerism is a characteristic feature of proline-containing peptides [145-148].

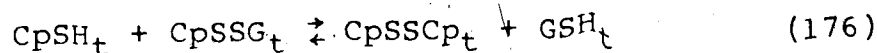
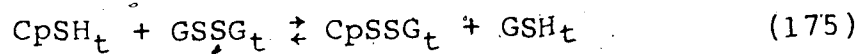
The conformational equilibria of captopril have previously been characterized in detail [145]. However, the conformational equilibria of captopril-containing disulfides have not been studied yet.

Since the rate of interchange between the cis and trans conformations by rotation around the C-N bond of the peptide linkage is slow on the NMR time scale [147-153], NMR is a convenient method for detecting the presence of cis/trans isomers and for studying simultaneously the equilibrium distribution of the isomers [145,148].

In this chapter, the results of ^1H NMR studies of the conformational equilibria of captopril and captopril-glutathione mixed disulfide (CpSSG) in aqueous (D_2O)

solutions are described. ^1H NMR titration curves were analyzed to obtain conformational equilibrium constants over a wide range of pH.

The oxidation of CpSH by GSSG via thiol/disulfide exchange is of interest since this type of reaction plays a key role in the formation of captopril-containing metabolites. Equations 175 and 176 describe the formation of symmetrical and mixed disulfides of CpSH by reaction with GSSG.



The results of ^1H NMR studies of these two thiol/disulfide exchange reactions between captopril and glutathione disulfide are also reported in this chapter. The equilibrium constants were determined with the aid of the conformational equilibrium constants mentioned above. Glutathione disulfide was chosen because of its natural occurrence [17], captopril-glutathione mixed disulfide has been detected as a metabolite of captopril [140,141] and, to a first approximation, GSSG serves as a model for disulfide bonds in proteins because its cystine is between

two amino acid residues.

B. Conformational Equilibria of Captopril and Captopril-Containing Species

CpSH, CpSSG and CpSSCp exist as equilibrium mixtures of cis and trans isomers with respect to the conformation across the peptide bonds involving the proline amino group. The cis/trans equilibria for each of these systems will now be characterized individually. This is necessary in order to characterize quantitatively the thiol/disulfide exchange reactions of captopril with GSSG.

1. Conformational Equilibria of Captopril

Although the conformational equilibrium of captopril has already been characterized in detail [145], the study was repeated under the present experimental conditions.

Figure 60 shows the 360 MHz ^1H NMR spectrum of CpSH in D_2O solution containing 1 M KCl at a pH meter reading (pH^*) of 6. The ^1H spectrum consists of two highly coupled spin systems: the $-\text{CH}_2\text{CH}_2\text{CH}_2\text{CH}-$ spin system of the proline moiety and the $-\text{CH}_2\text{CHCH}_3$ spin system from the 3-mercapto-2-methyl-1-oxopropyl group. The presence of two sets of resonances for each type of hydrogen due to the existence of both cis and trans isomers further complicates the spectra. For example, the spectrum shows

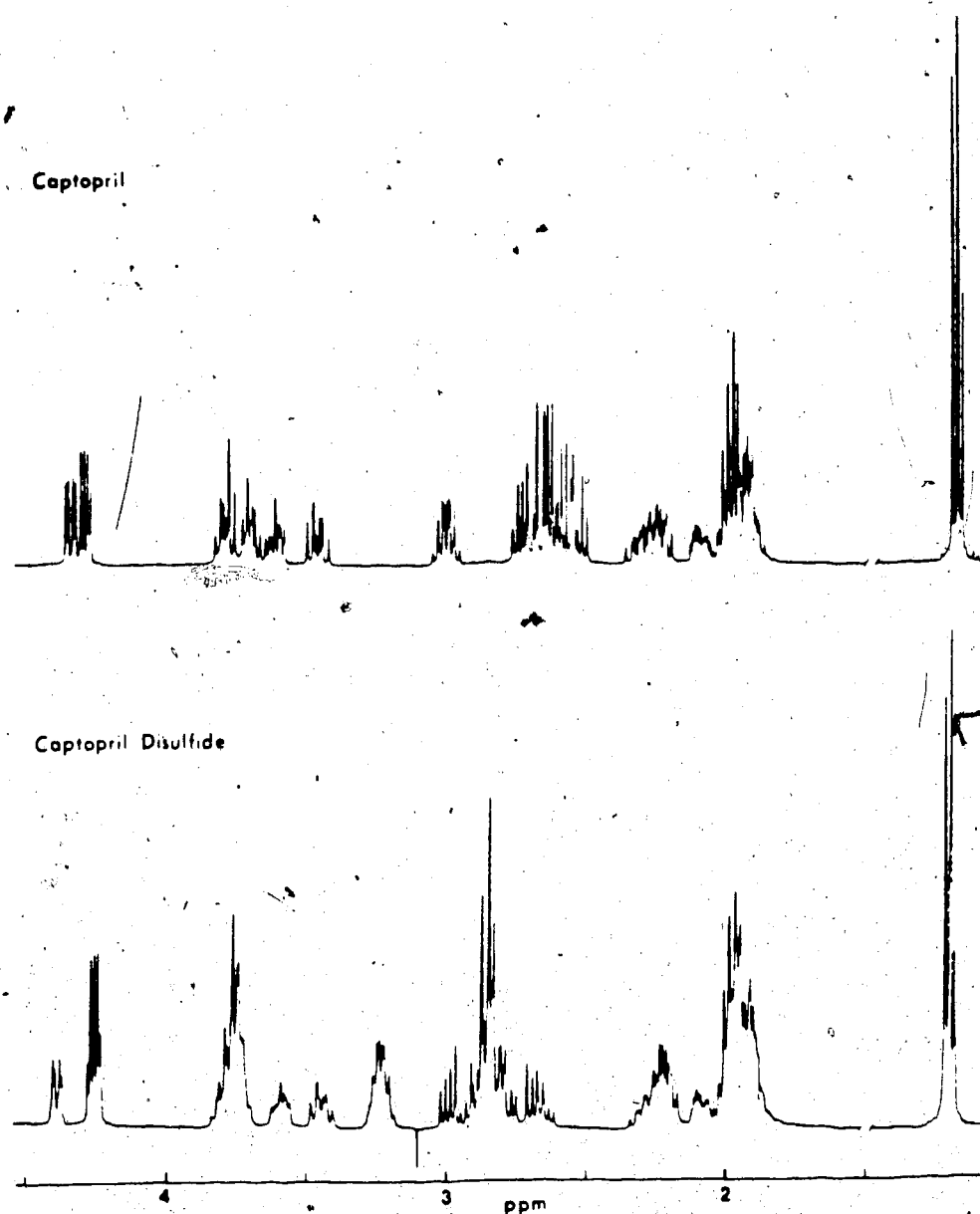


Figure 60. 360 MHz ^1H NMR spectra of 0.062 M captopril ($\text{pH}^* = 6.0$) and 0.042 M captopril disulfide ($\text{pH}^* = 6.0$). In the 1-1.5 ppm region, the gain was reduced by a factor of 2.

clearly the doubling of several resonance patterns, including the methyl resonances at 1.1-1.2 ppm and the multiplet patterns at 3.4-3.9 and 4.3-4.4 ppm which are for hydrogens on the proline residue. Resonances in the ^1H spectrum were assigned on the basis of previously published results on captopril [145]. The assignments are as follows: 1.1-1.2 ppm, the methyl hydrogens of the 3-mercapto-2-methyl-1-oxopropyl group (the methyl region is expanded in Figure 61 and the resonances are assigned to the cis and trans isomers in Table 29); 1.8-2.4 ppm, the hydrogens on C_γ and C_β of the proline residue; 2.5-3.1 ppm, the two hydrogens on C_3 and one hydrogen on C_2 of the 3-mercapto-2-methyl-1-oxopropyl group; and 3.4-3.9 ppm and 4.3-4.4 ppm, the two hydrogens on C_δ and the one hydrogen on C_α , respectively, of the proline residue. In the 3.4-3.9 ppm region, the resonances at 3.4-3.7 and 3.7-3.9 ppm are from cis and trans isomers respectively. Due to the complexity of the multiplet patterns and the extensive overlap of resonances, no attempt has been made to extract the chemical shift for the various resonances of the two forms.

The trans conformation of captopril has been assigned as the more abundant isomer [145] on the basis that it is the most abundant isomer for other proline-containing peptides, e.g. glycyl-L-proline, glycyl-L-hydroxyproline,

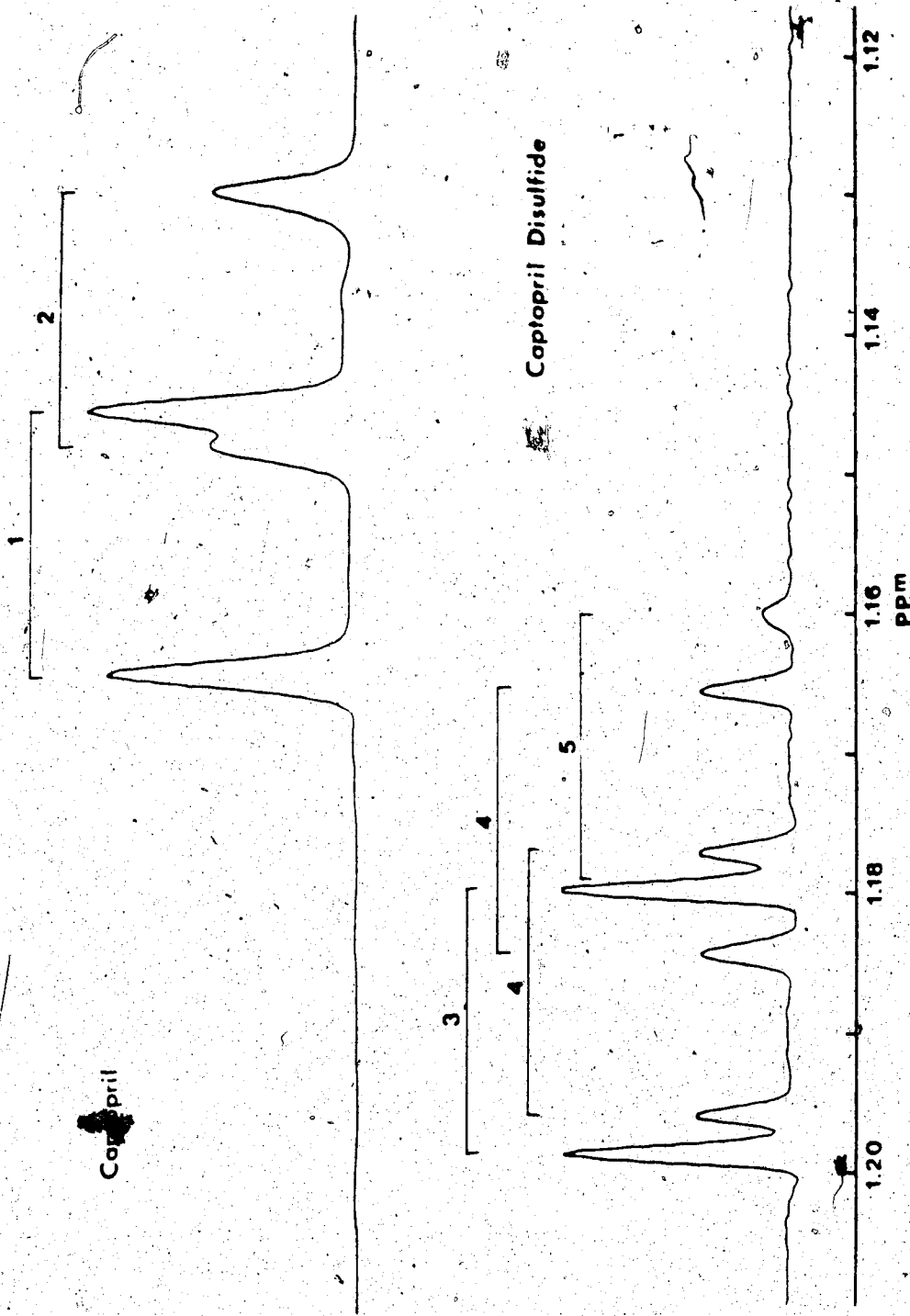


Figure 61. Expansion of the methyl resonances in Figure 60 (1.11-1.21 ppm). Resolution was enhanced by doing a Gaussian multiplication with the Bruker Aspect 2000 software. Resonance assignments are given in Table 29.

Table 29. Identification of captopril-containing species.

<u>Species</u>	<u>Conformation of the Captopril Amide Bond(s)</u>	<u>Species Number</u>
CpSH(t)	trans	1
CpSH(c)	cis	2
CpSSCp(tt)	trans, trans	3
CpSSCp(tc)	trans, cis	4
CpSSCp(cc)	cis, cis	5
CpSSG(t)	trans	6
CpSSG(c)	cis	7

L-alanyl-L-proline, and for the related peptides N-acetylsarcosine and glycylsarcosine.

As mentioned earlier, the relative populations of the cis and trans forms are dependent on the protonation state of the molecule. The fractional concentrations of the two isomers were determined as a function of pH* under the present experimental conditions by using the relative areas of the multiplet patterns in the 3.4-3.9 ppm region ($\text{CH}_2 \delta$). The results are summarized in Figure 62. The fractional concentrations for the fully protonated (at low pH), monoprotinated (at neutral pH) and fully deprotonated (at high pH) forms of the trans isomer (f_{I}) are 0.87, 0.63 and 0.71. The corresponding fractional concentrations for the cis isomer (f_{II}) are 0.13, 0.37 and 0.29 respectively. These forms correspond to CpSH^+ , CpSH^- and CpS^{2-} respectively. The protonation states were assigned to the various forms of CpSH using the acid dissociation constants for the thiol and carboxyl groups. The pK_A values for the carboxylic acid groups are 2.86 and 3.52 for the trans and cis isomers, respectively, and the pK_A values for the sulfhydryl groups are 9.71 and 9.99 for the trans and cis forms [145].

The fractional concentrations of the cis and trans isomers calculated from the relative areas of the methyl resonances (Figure 61) are in good agreement with the

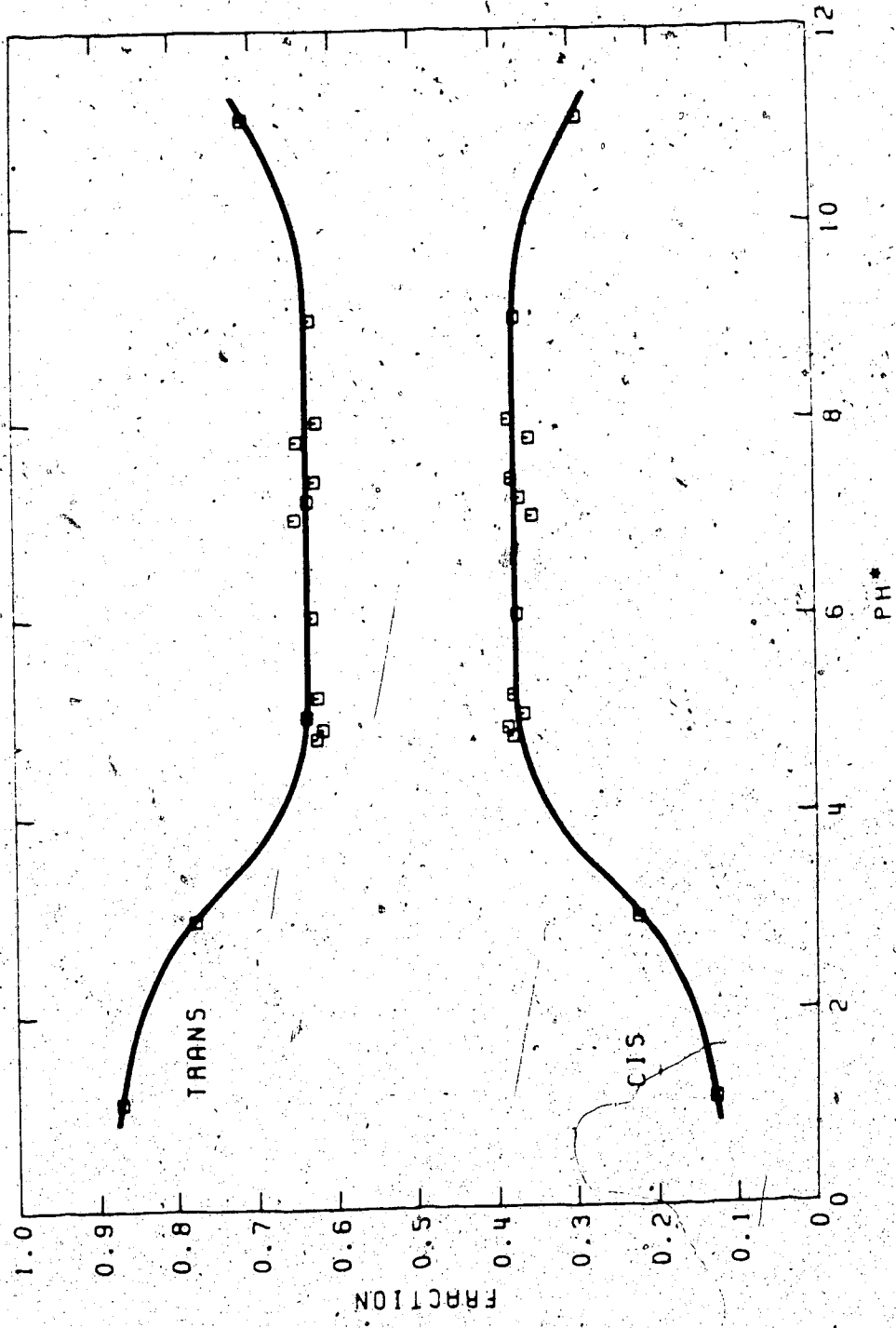


Figure 62. The fractional concentrations of the cis and trans forms of captopril as a function of pH*.

above results which were obtained from the CH_2 resonance intensities (Figure 62). For example, the fractional concentration (f_I) calculated for the trans isomer of CpSH at $\text{pH}^* 6$ using the methyl resonance intensity is 0.61.

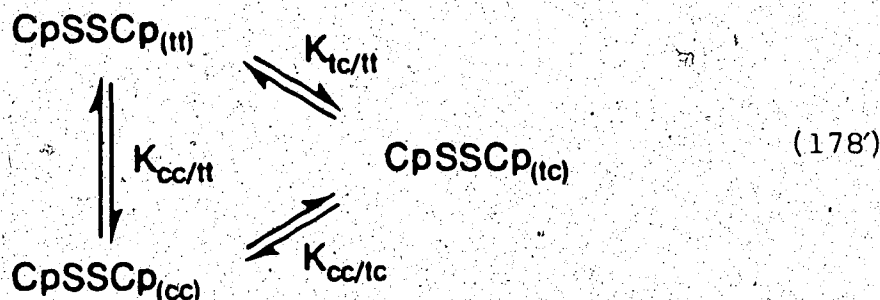
The equilibrium constant, $K_{c/t}$, for the cis/trans equilibrium in Equation 174 is given by Equation 177.

$$K_{c/t} = \frac{[\text{cis}]}{[\text{trans}]} = \frac{f_{II}}{f_I} \quad (177)$$

From the fractional concentrations determined above for the various protonated forms of CpSH, i.e. at low, neutral and high pH, the equilibrium constants are calculated to be 0.15, 0.59 ± 0.03 and 0.41 respectively.

2. Conformational Equilibria of Captopril Disulfide

Captopril disulfide exists as an equilibrium mixture of cis and trans isomers with respect to the peptide bonds of both captopril residues. The result is three isomers as described by the following equilibria:



$K_{tc/tt}$, $K_{cc/tt}$ and $K_{cc/tc}$ are equilibrium constants defined as

$$K_{cc/tt} = \frac{[\text{CpSSCp}_{(cc)}]}{[\text{CpSSCp}_{(tt)}]} \quad (179)$$

$$K_{tc/tt} = \frac{[\text{CpSSCp}_{(tc)}]}{[\text{CpSSCp}_{(tt)}]} \quad (180)$$

$$K_{cc/tc} = \frac{[\text{CpSSCp}_{(cc)}]}{[\text{CpSSCp}_{(tc)}]} \quad (181)$$

where $\text{CpSSCp}_{(tt)}$ stands for the equilibrium concentration of CpSSCp in which both captopril residues have the trans conformation.

The 360 MHz ^1H NMR spectrum of captopril disulfide is shown in Figure 60. The assignment is basically the same as that for reduced captopril. The spectrum comprises the spectra of captopril residues in four different environments due to the cis/trans isomerization (Equation 178). Only the methyl region shows well-resolved resonances for the four environments; four doublets from the four environments are clearly observed (Figure 61). The assignments are given in Table 29.

As was the case for reduced captopril, the resonances for the CH_2 δ hydrogens (3.4-3.8 ppm in Figure 60) consist of two sets of multiplet patterns corresponding to the trans and cis environments of CpSSCp. From these, the conformational equilibrium was characterized as a function of pH. However, the relative areas of these resonances give total fractional concentrations for the cis (f_{IItotal}) and trans (f_{Itotal}) environments, i.e.

$$f_{\text{Itotal}} = \frac{(2[\text{CpSSCp}_{(tt)}] + [\text{CpSSCp}_{(tc)}])}{2[\text{CpSSCp}]_{\text{total}}} \quad (182)$$

$$f_{\text{IItotal}} = \frac{(2[\text{CpSSCp}_{(cc)}] + [\text{CpSSCp}_{(tc)}^{\text{O}}])}{2[\text{CpSSCp}]_{\text{total}}} \quad (183)$$

The values of f_{Itotal} and f_{IItotal} , as calculated from the CH_2 δ relative areas, were found to be relatively independent of pH. For example, the total fractional concentration (f_{Itotal}) for the trans conformation is 0.83 at $\text{pH}^* 0.75$ and 0.72 ± 0.03 over the pH^* range 3.75-11.02. The fractional concentration could not be determined over the pH^* range 1-3 due to precipitation of CpSSCp.

The equilibrium constant, $K_{\text{c/t}}$, between the cis and trans CpSSCp environments (Equation 184)

$$K_{c/t} = \frac{[\text{cis}]_{\text{total}}}{[\text{trans}]_{\text{total}}} = \frac{f_{II\text{total}}}{f_{I\text{total}}} \quad (184)$$

is calculated to be 0.38 ± 0.04 for the pH* range 3.75-11.02. As the pH is decreased and the carboxylate groups are protonated, the total fractional concentration of the trans isomer increases and the equilibrium constant decreases to 0.20.

The characterization of the cis/trans equilibria of CpSSCp from the methyl resonance intensities is necessary in order to study the thiol/disulfide exchange reaction of CpSH with GSSG which involved quantifying overlapping methyl resonances.

The methyl region in Figure 61 shows four doublets from the four different environments (Equation 178). A Gaussian resolution enhancement routine was used to resolve the various methyl resonances. Six of the eight methyl resonances are well-resolved whereas two overlap at 1.18 ppm vs DSS. These methyl resonances were assigned (Table 29) to the various CpSSCp isomers (Equation 178). By analogy with reduced captopril, the most abundant resonances at 1.18 ppm and 1.20 ppm (pair no. 3) were assigned to the isomer in which both amide bonds are trans (CpSSCp_(tt)). The least intense pair of methyl resonances

at 1.18 ppm and 1.16 ppm (pair no. 5) was assigned to the two methyl resonances of CpSSCp(cc). The remaining two doublets (pair no. 4) of equal and intermediate intensity were assigned to CpSSCp(tc).

The fractional concentrations of the three CpSSCp isomers (Equation 178) were determined at pH* 5.90, 5.99 and 6.10 from the relative intensities of the four methyl doublets. From these, the three equilibrium constants $K_{cc/tc}$, $K_{tc/tt}$ and $K_{cc/tc}$ (Equations 179-181) were calculated. The results are listed in Table 30. The average equilibrium constants are: $K_{cc/tt} = 0.144 \pm 0.005$, $K_{tc/tt} = 0.84 \pm 0.01$ and $K_{cc/tc} = 0.171 \pm 0.006$.

The overall equilibrium constant, $K_{c/t}$ (Equation 184), was also determined using the results obtained from the methyl region for comparison with the value calculated from CH₂ δ resonances. $K_{c/t}$ is related to the various equilibrium constants by Equation 185.

$$K_{c/t} = \frac{(2K_{cc/tt} + K_{tc/tt})}{(2 + K_{tc/tt})} \quad (185)$$

$K_{c/t}$ was calculated at three pH* values using the results in Table 30. The average of the three values is 0.397 ± 0.006 which is in excellent agreement with the value obtained above using the relative intensities of the cis

Table 30. The conformational equilibrium constants of CpSSCp at pH* 6.^a

pH*	$K_{cc/tt}$	$K_{tc/tt}$	$K_{cc/tc}$
5.90	0.143	0.855	0.167
5.99	0.139	0.826	0.168
6.10	0.149	0.846	0.177
average	0.144 ± 0.005	0.84 ± 0.01	0.171 ± 0.006

^a0.044 M CpSSCp in D₂O containing 1 M KCl, 0.003 M EDTA and 0.05 M imidazole.

and trans CH_2 δ resonances. This excellent agreement indicates that the resolution enhancement method used for resolving the methyl resonances does not distort the methyl areas significantly and therefore can be used, under these experimental conditions to resolve resonances so that the various equilibria can be quantified.

Equation 185 suggests that, since the values of $K_{C/t}$ are pH independent, the various equilibria and equilibrium constants of CpSSCp in Equation 178 are also pH independent over the same pH range.

3. Conformational Equilibria of the Mixed Disulfide of Captopril with Glutathione

Figure 63 shows the 360 MHz ^1H NMR spectrum of the methyl region for the mixed disulfide of captopril with glutathione (CpSSG). The mixed disulfide was formed by reacting 0.009 M CpSH with 0.018 M GSSG in 1 M KCl solution (in D_2O) at pH* 7.1. CpSSG, GSH and CpSSCp were formed by thiol/disulfide exchange (Equations 175 and 176). After reaction for 15 min, the solution was stirred in air for 18 days to oxidize CpSH to CpSSCp and GSH to GSSG in order to simplify the NMR spectrum. Under these conditions, less than 10% of the total captopril is present as CpSSCp and no CpSH was detected. The two sets of methyl doublets (pairs no. 6 and 7) in Figure 63 are

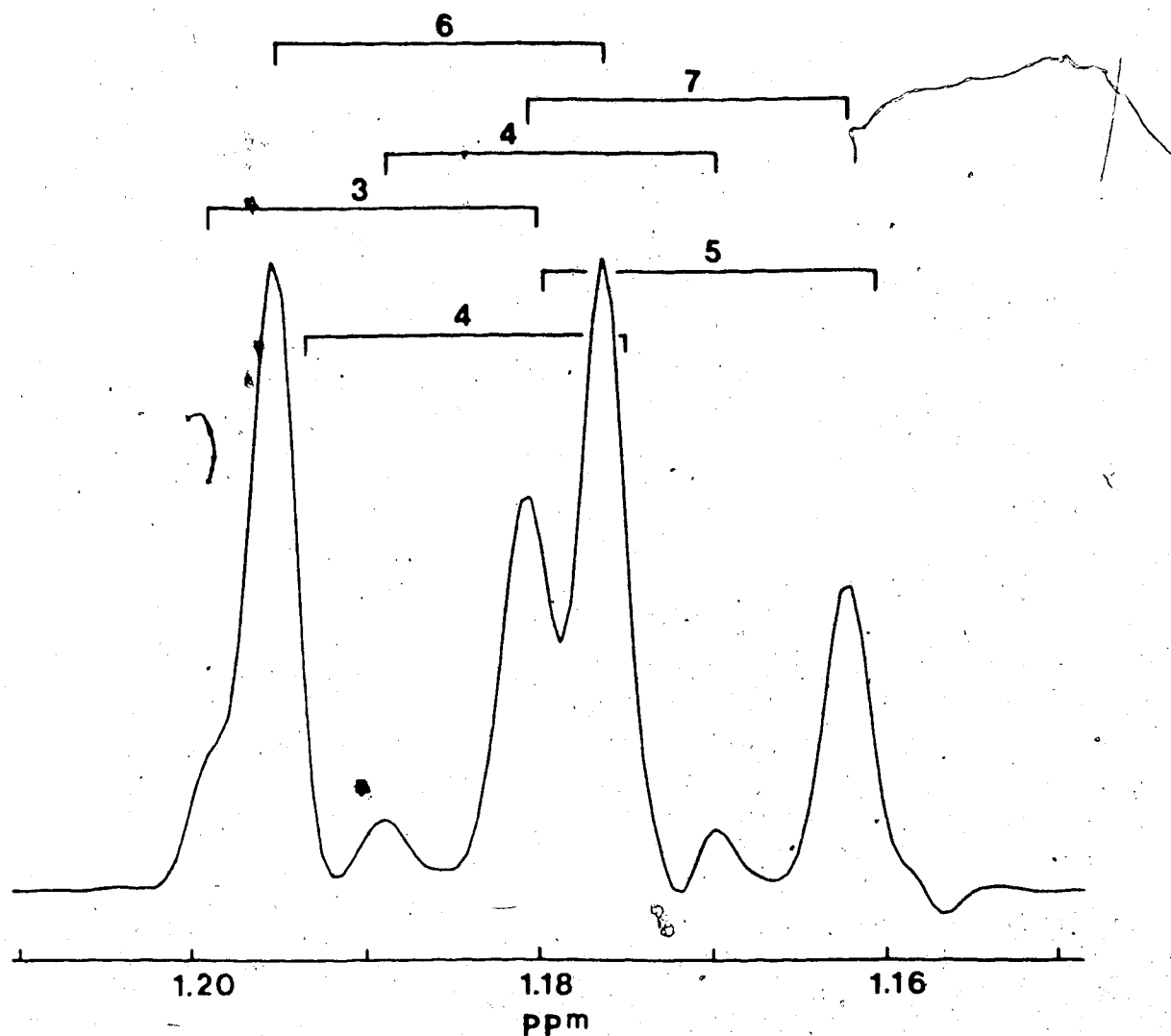
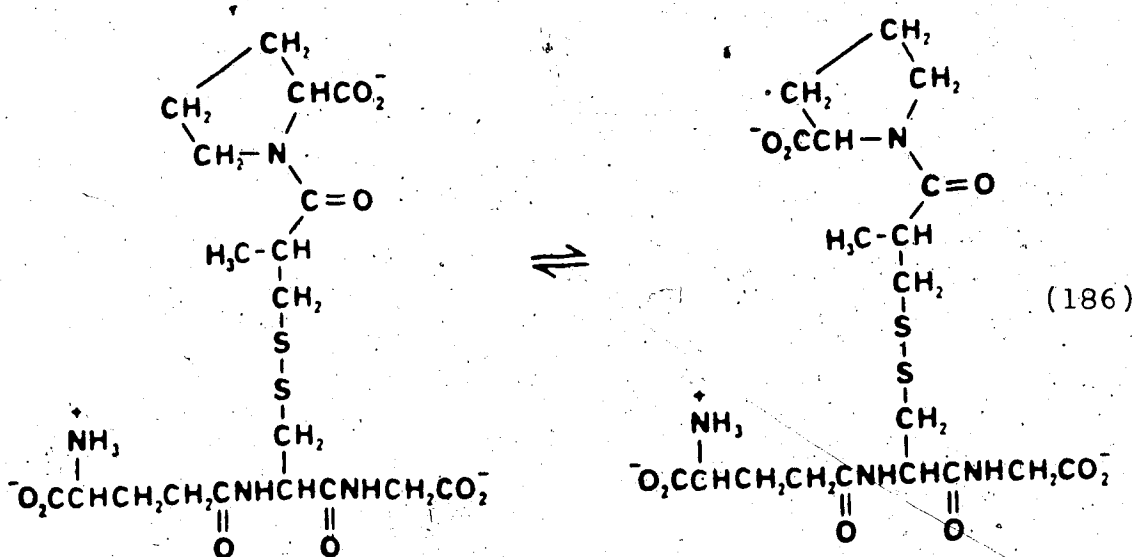


Figure 63. ^1H NMR spectrum of the methyl region of a pH* 7.0 solution containing captopril-glutathione mixed disulfide and captopril disulfide. Details of the preparation of the mixed disulfide, are given in the text. Gaussian multiplication was used to enhance the resolution.

due to the cis and trans isomers of the captopril residue in CpSSG. As before, the most abundant resonances have been assigned to the trans isomer. Using the relative intensities of the methyl doublets, the conformational equilibrium (Equation 186) was studied.



At low pH, the methyl resonances of the cis form are both less intense and less well resolved from those of the trans form than at high pH. However, in contrast to results observed at higher pH, the $\text{CH}_2 \delta$ multiplet patterns at low pH were sufficiently well-resolved from the glycine resonances of glutathione residues in GSSG and CpSSG for direct integration and calculation of fractional concentrations. Consequently, at $\text{pH}^* < 3$, the fractional concentrations of the cis and trans isomers of CpSSG were determined from the relative intensities of the $\text{CH}_2 \delta$

multiplet patterns whereas at higher pH they were determined from the relative intensities of the methyl resonances. When using the methyl resonances, peak heights were used instead of areas in order to minimize the contribution from the residual methyl resonances of CpSSCp (resonances 3, 4 and 5 in Figure 63).

The fractional concentrations of the trans and cis forms of CpSSG were determined as a function of pH over the pH* range 0.92-10.98 and the results are presented in Figure 64. The fractional concentration of the trans conformation is 0.67 ± 0.01 and independent of pH over the pH* range 4-8.5, corresponding to an equilibrium constant, $K_{c/t}$, of 0.49 ± 0.02 . As the pH is decreased, the carboxylate group becomes protonated and the fractional concentration of the trans isomer increases to 0.86 ± 0.02 at $\text{pH}^* < 2$ ($K_{c/t} = 0.16 \pm 0.02$). At $\text{pH} > 9$ where the CpSSG species becomes fully deprotonated, the fractional concentration of the trans isomer also increases (to 0.740 ± 0.003) (and $K_{c/t}$ decreases to 0.351 ± 0.005).

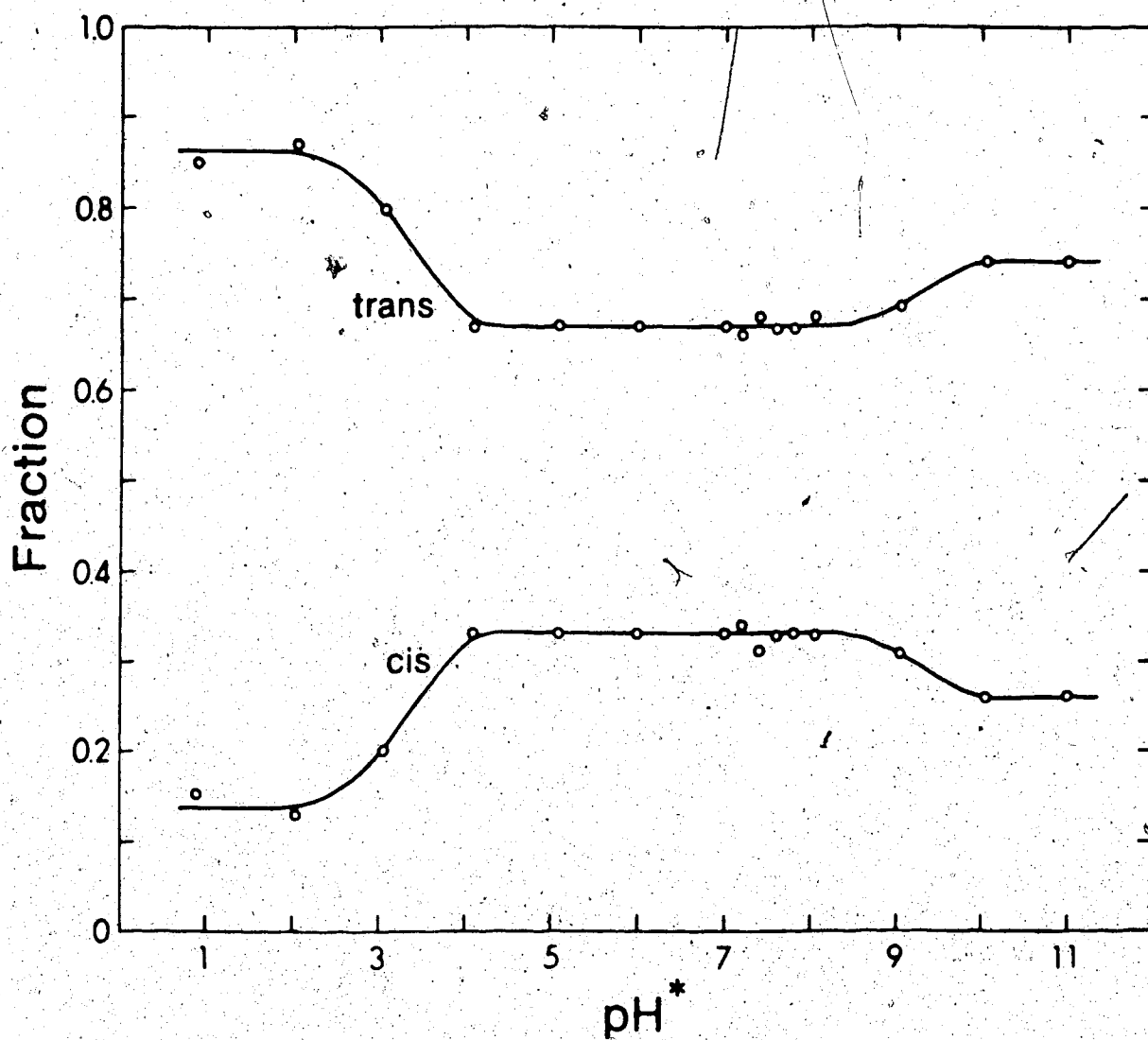


Figure 64. The fractional concentrations of the cis and trans forms of captopril-glutathione mixed disulfide as a function of pH*.

C. Equilibrium Constants for the Thiol/Disulfide Exchange Reactions Between Captopril and Oxidized Glutathione

The conditional equilibrium constants K_{1c} and K_{2c} for the oxidation of CpSH by GSSG described by Equations 175 and 176 were determined at pH* 6. K_{1c} and K_{2c} are defined as

$$K_{1c} = \frac{[\text{CpSSG}]_t [\text{GSH}]_t}{[\text{CpSH}]_t [\text{GSSG}]_t} \quad (187)$$

$$K_{2c} = \frac{[\text{CpSSCp}]_t [\text{GSH}]_t}{[\text{CpSH}]_t [\text{CpSSG}]_t} \quad (188)$$

where $[\text{CpSSG}]_t$ is the total concentration (cis + trans) of CpSSG, etc. Equilibrium concentrations were calculated from the intensities of the methyl resonances for the various captopril-containing species.

Figure 65 shows the methyl region of the NMR spectrum for a pH* 6.0 solution prepared by reacting CpSH with GSSG. The spectrum was obtained 341 hours after mixing the reactants to ensure that equilibrium had been reached. The reaction was carried out in a sealed NMR tube in order to minimize air oxidation of thiols to disulfides. The spectrum shows several well-resolved methyl resonances for the cis and trans forms of CpSH,

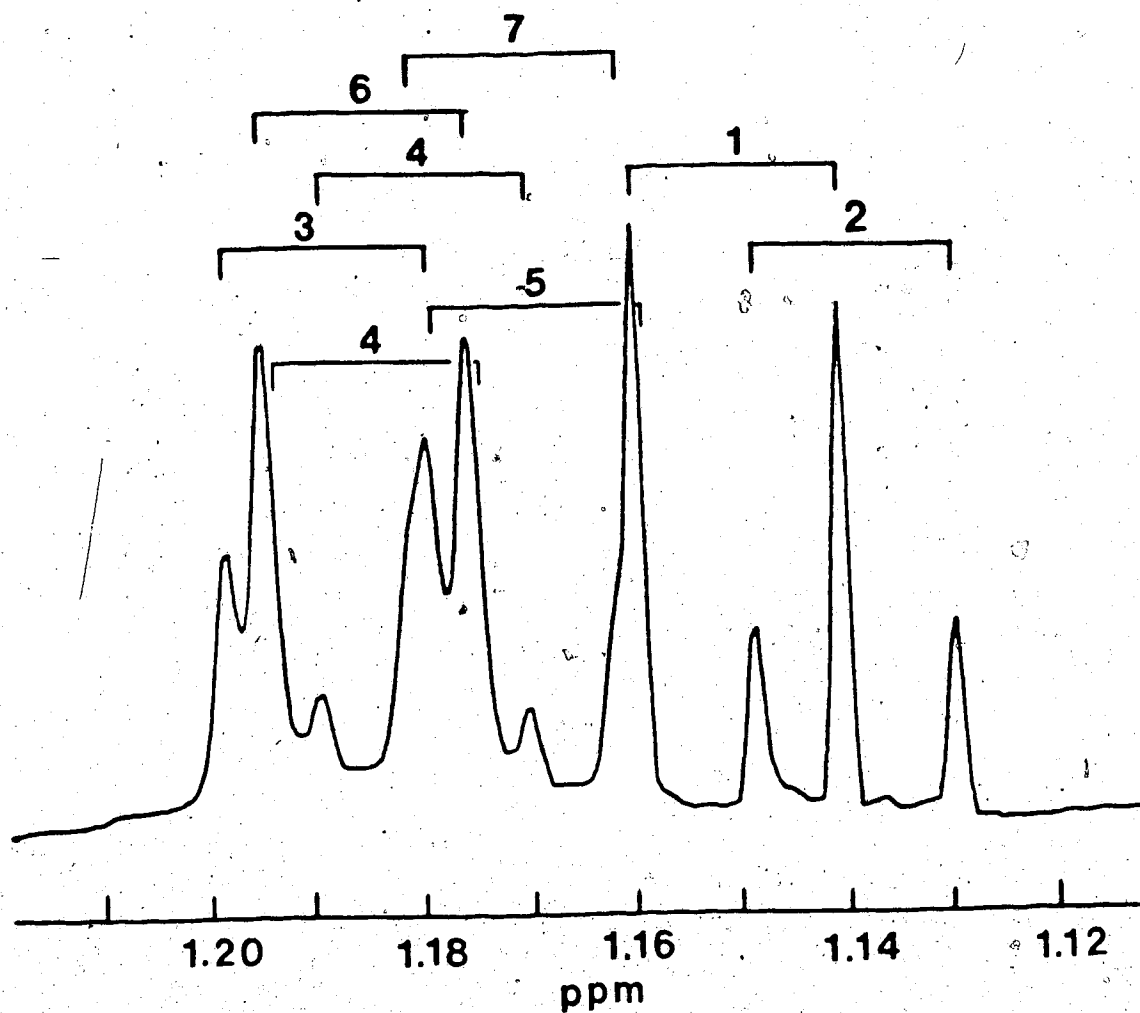


Figure 65. The methyl region of the ^1H NMR spectrum of a solution prepared by reacting 0.045 M CpSH with 0.041 M GSSG at pH* 6.0 for 341 hours in a degassed, sealed NMR tube. Resolution was enhanced by Gaussian multiplication. Resonance assignments are given in Table 29.

CpSSCp and CpSSG. The fractional concentrations were calculated from the relative areas of these resonances as described in Chapters II and IV.

The equilibrium concentrations of the various species in Equations 187 and 188 were determined from the relative intensities of the methyl resonances and the initial reactant concentrations, as follows. The total area of the methyl resonances for CpSH was obtained by doubling the sum of the areas of its resonances at 1.13 and 1.14 ppm. The total area of the methyl resonances for CpSSCp was calculated from the area of its resonances at 1.17 and 1.19 ppm (sum of areas = A) and the values determined above for the two conformational equilibrium constants of CpSSCp, $K_{tc/tt}$ and $K_{cc/tc}$, using Equation 189.

$$\text{total area} = 2A \left(1 + K_{cc/tc} + \frac{1}{K_{tc/tt}} \right) \quad (189)$$

The difference between the total methyl resonance area and the areas for the CpSH and CpSSCp resonances gives the total area of the methyl resonances for CpSSG. Next, fractional concentrations were calculated from the relative areas of CpSH, CpSSCp and CpSSG and the total methyl resonance area. Equilibrium concentrations of CpSH, CpSSG and CpSSCp were then calculated using these

fractional concentrations and the initial concentration of CpSH. The equilibrium concentrations of GSSG and GSH were calculated by difference using these concentrations and the initial concentration of GSSG as shown in Chapter IV.

The values calculated for K_{1c} and K_{2c} (Equations 187 and 188) from three separate experiments in the pH* range 5.9-6.1 are 2.1 ± 0.1 and 1.5 ± 0.6 respectively. The large uncertainties reflect the accumulation of errors that result from obtaining concentrations by difference.

D. Discussion

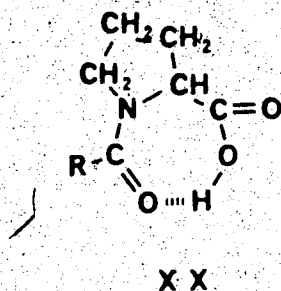
1. Cis/Trans Conformational Equilibria of CpSH, CpSSCp and CpSSG

The more abundant isomers of CpSSCp and CpSSG were assigned the trans conformation based on previous findings that the more abundant conformation for proline-containing dipeptides such as glycyl-L-proline, glycyl-L-hydroxyproline, L-alanyl-L-proline [148] and captopril [145] is the trans conformation.

The fractional concentration of the trans conformation of these dipeptides increases when the carboxylate group is protonated. For example, the fractional concentration of the trans conformation of glycyl-L-proline increases from 0.65 to 0.84 when the

carboxylate group is protonated [148]. This behaviour is very similar to that observed in this study for the more abundant isomers of CpSH, CpSSCp and CpSSG.

The cis/trans equilibrium constants for CpSH, CpSSCp, CpSSG and the proline-containing dipeptides are summarized in Table 31. The equilibrium constants for the carboxyl-protonated (low pH) forms of CpSH, CpSSCp and CpSSG are quite similar to each other and to those for the proline-containing dipeptides. The enhanced stability of the trans isomer at low pH (see footnote b, p. 280) probably results from intramolecular hydrogen bonding between the protonated carboxylate group and the carbonyl oxygen of the peptide bond. This is shown schematically in XX. Molecular models indicate that such hydrogen bonding is not possible in the cis isomer.



The enhanced stability of the trans conformation of proline-containing dipeptides at low pH was found to be due to such hydrogen bonding [147,148,154].

At high pH (see footnote d, p. 280), the

Table 31. Cis/trans conformational equilibrium constants for proline-containing molecules.^a

<u>Molecule</u>	<u>Low pH^b</u>	<u>Neutral pH^c</u>	<u>High pH^d</u>
glycyl-L-proline ^e	0.19	0.54	0.72
glycyl-L-hydroxyproline ^e	0.14	0.52	0.59
L-alanyl-L-proline ^e	0.12	0.54	0.89
captopril	0.15	0.59	0.41
captopril disulfide	0.20 ^f	0.38 ^f	0.38 ^f
captopril-glutathione mixed disulfide	0.16	0.49	0.35

^aDefined as $K_{C/t} = [\text{cis}]/[\text{trans}]$ where cis and trans refer to the conformation across the proline amide bond.

^bCarboxyl, thiol and amino groups, if present, are protonated.

^cCarboxyl groups deprotonated; thiol and amino groups, if present, protonated.

^dCarboxyl, thiol and amino groups, if present, deprotonated.

^eReference 148.

^f $K_{C/t} = [\text{cis}]_{\text{total}}/[\text{trans}]_{\text{total}}$.

conformational equilibrium constants for CpSH, CpSSCp and CpSSG are approximately the same, but are less than for the proline-containing dipeptides. The enhanced stability of the trans conformation of the fully deprotonated (high pH) form of CpSH is presumably due to the increased-charge repulsion between the deprotonated carboxylic acid and thiol groups [145] in the cis isomer. In CpSSG and the proline-containing dipeptides, the origin of the enhanced stability at high pH is not so obvious.

The magnitude of the cis/trans equilibrium constants in Table 31 for the neutral pH forms of CpSH, CpSSCp and CpSSG suggests that approximately two thirds of the captopril, both in the reduced and in the oxidized state, has the trans conformation at physiological pH.

2. CpSH/GSSG Thiol/Disulfide Exchange Reaction

The thiol/disulfide exchange equilibria between CpSH and GSSG (Equations 175-176) and the conformational equilibria of CpSH, CpSSCp and CpSSG are summarized in Figure 66. The nine equilibrium constants were determined at pH* 6. Since the conditional equilibrium constants in the related systems PSH/GSSG and PSH/CSSC are essentially pH independent up to pH values at which deprotonation of the thiol group begins to occur, the conditional equilibrium constants obtained for the reaction of CpSH

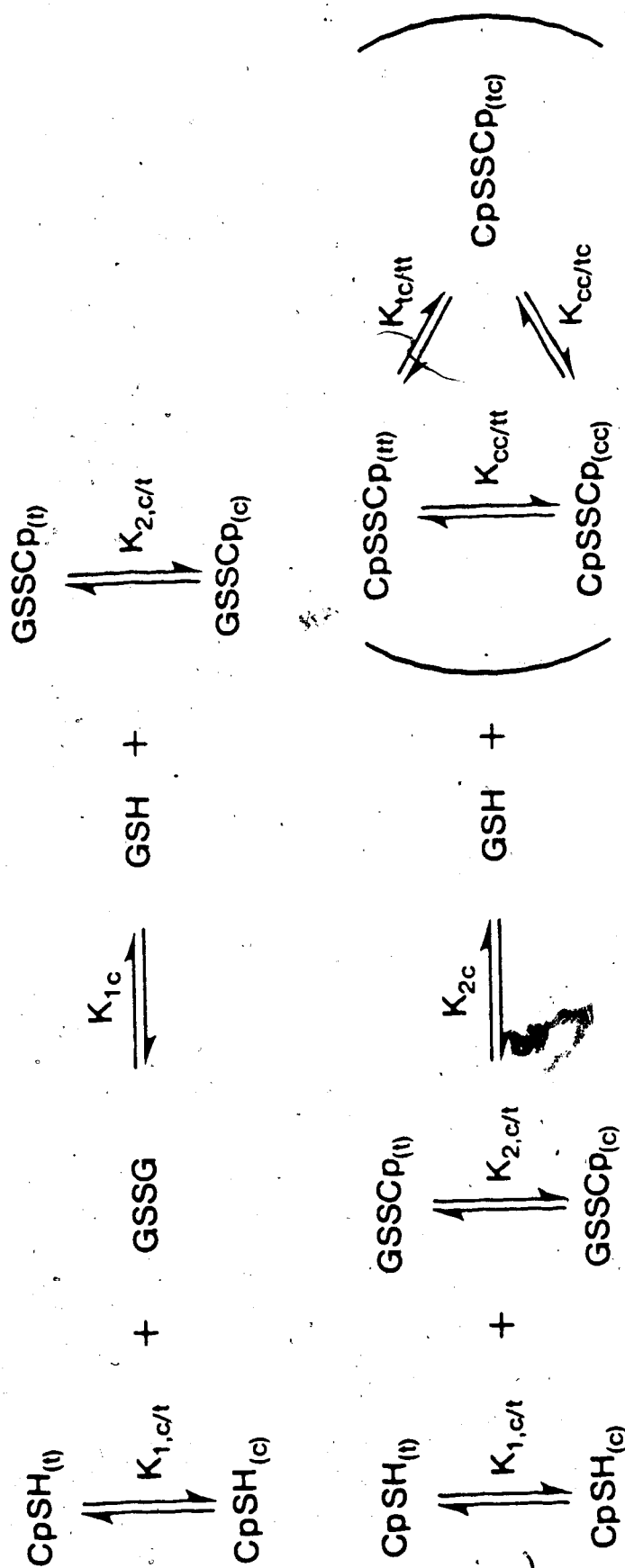
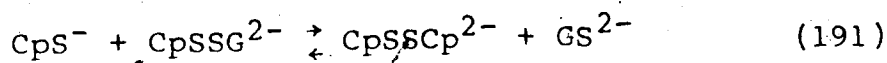
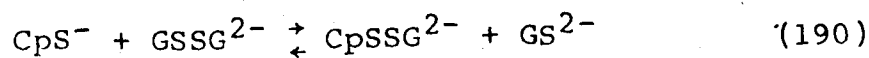


Figure 66. The thiol/disulfide exchange equilibria and CpSH, CpSSCP, and CpSSG conformational equilibria occurring in a solution prepared by reacting CpSH and GSSG. The subscripts t and c indicate trans and cis conformations across the amide bond(s) of the captopril in CpSH and CpSSCP or the captopril part of CpSSG.

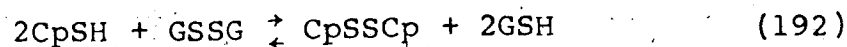
with GSSG at pH* 6 probably describe the reaction up to pH ~8 as well.

The reactive species in the oxidation of CpSH by GSSG is presumably the thiol-deprotonated species, CpS⁻. The thiol/disulfide exchange reactions written in terms of the reactive species are



The equilibrium constants for Equations 190 and 191 cannot be calculated from the values determined for K_{1c} and K_{2c} at pH* 6 since not all the acid dissociation constants are known.

The overall thiol/disulfide exchange reaction between CpSH and GSSG is given by Equation 192



The overall conditional equilibrium constant, K_{3c} , is calculated to be 3.2 ± 1.2 using the relation $K_{3c} = K_{1c}K_{2c}$. If the thiol/disulfide reaction was governed by random distribution, K_{1c} and K_{2c} would be 2 and 0.5

respectively and K_{3C} would be 1. The corresponding values for the reaction of cysteine (CSH) with GSSG and for PSH with GSSG can be used for comparison. At pH 6.6 and 25°C, the equilibrium constants for the reaction of CSH with GSSG [38] are $K_{1C} = 1.27$, $K_{2C} = 0.27$ and $K_{3C} = 0.34$. For the reaction of PSH with GSSG at pH 7.4 and 25°C (Chapter IV), these values are $K_{1C} = 1.36$, $K_{2C} = 0.039$ and $K_{3C} = 0.053$. The values for K_{3C} for the reactions involving both CpSH and CSH with GSSG are within a factor of 3 of the random distribution. The value for the reaction of PSH with GSSG is much smaller due probably to its two bulky methyl groups adjacent to the thiol group, which hinder the reaction of PSH with penicillamine-glutathione mixed disulfide in the second step (Equation 103).

The difference between the formal electrode potentials ($\Delta E^{\circ'}$) of the GSSG/GSH and CpSSCp/CpSH couples is 0.015 V as calculated from Equation 173 (where $\Delta E^{\circ'} = E_{GSSG/GSH}^{\circ'} - E_{CpSSCp/CpSH}^{\circ'}$) and the value of K_{3C} for CpSH. By comparison, the $\Delta E^{\circ'}$ value in Table 28 is -0.0378 V at pH 7.4 for the reaction of PSH with GSSG.

The $\Delta E^{\circ'}$ value for the reaction of CSH with GSSG ($\Delta E_{CSH}^{\circ'}$) at pH 6.6-7.0 [21,37,38] is reported to be in the range -0.013 to -0.018 V. These results indicate that $\Delta E^{\circ'}(\text{CpSH}) > \Delta E^{\circ'}(\text{CSH}) > \Delta E^{\circ'}(\text{PSH})$, i.e. CpSH has a greater tendency to reduce disulfide bonds by

thiol/disulfide exchange reaction than do thiol groups in amino acids such as CSH and PSH. The value of ΔE° (CSH) is greater than ΔE° (PSH) due to bulky methyl groups in PSH as mentioned earlier. The origin of the greater value of ΔE° (CpSH) over ΔE° (CSH) is not so obvious.

These results further indicate that, if the disulfide bond in GSSG is a good model for those in proteins, CpSH is more capable of reducing protein disulfide bonds than CSH. This conclusion is supported by the finding that CpSH is more effective for the activation of papain by reduction of a disulfide bond at its active site than is cysteine [155].

CHAPTER VII

CONCLUSION

The objective of the research presented in this thesis has been to characterize the tendency of thiol groups of penicillamine and captopril to react with disulfide groups in amino acids and peptides. The reactions between thiol and disulfide groups are thiol/disulfide exchange reactions, and the overall reaction results in the oxidation of the thiol to its disulfide form while the disulfide is reduced to its thiol form. The overall reaction takes place in two steps; one product of the first step is a mixed disulfide which then reacts with another thiol molecule to form the symmetrical disulfide. These reactions were studied in this thesis because they are thought to be the most important reactions in the metabolism of penicillamine and captopril [9,140-143]. Even though these reactions have been thought to be important in the metabolism of penicillamine for some time, and more recently for captopril, they have not been characterized in detail, presumably due to the difficulty of monitoring these types of reactions.

To characterize the tendency of the thiol group of penicillamine to react with disulfides, the kinetics and equilibria of its reaction with the disulfide groups in oxidized glutathione, cystine and related disulfides were studied. The reactions with the disulfide group of oxidized glutathione were studied for several reasons, the most important being that oxidized glutathione is present in intact cells and biological fluids and also its disulfide group serves as a convenient model for disulfide groups in proteins. The reactions with the disulfide group of cystine were studied because this reaction is thought to be the most important pathway for the metabolism of penicillamine, regardless of the disease being treated [9], as well as being the basis for the treatment of cystinuria with penicillamine [23]. To characterize the tendency of the thiol group of captopril to react with disulfide groups, the equilibria for the reaction of captopril with oxidized glutathione were studied.

The kinetics and equilibria of the reaction of penicillamine with oxidized glutathione and with cystine were characterized by ^1H NMR. From the pH dependence of the observed rate constant for the reaction of penicillamine with both disulfides, the reactive penicillamine species at physiological pH was identified

as the amino-protonated, thiol-deprotonated form of penicillamine while the reactive disulfide species are the amino-protonated, carboxyl-deprotonated forms of oxidized glutathione and cystine. To be able to calculate the rate and equilibrium constants for the specific reactions which occur at physiological pH, it was necessary to determine acid dissociation constants for the penicillamine-glutathione and penicillamine-cysteine mixed disulfides formed in the two reactions. Prior to this work, no acid dissociation constants had been determined for mixed disulfides such as these, presumably due to the necessity of having the compound in pure form for conventional methods of measuring acid dissociation constants. This is not a requirement of the NMR method for measuring acid dissociation constants since information is obtained at the molecular level. In this work, the acid/base chemistry of the mixed disulfides was conveniently studied by NMR by reacting thiol with disulfide to form the mixed disulfide in solution and then making NMR measurements on the equilibrium mixture. Both macroscopic and microscopic acid dissociation constants were obtained from chemical shift data for the mixed disulfides PSSG and PSSC. The chemical shift data indicate that the two ammonium groups in each mixed disulfide are of similar acidity. Thus the monoprotinated form of each molecule exists as a mixture

of protonation isomers. For PSSG, the ammonium group of the penicillamine part of the molecule is 4.4 times as acidic as that of the glutathione part, while for PSSC the ammonium group of the penicillamine part is 1.7 times as acidic as that of the cysteine part. This work demonstrates that new and important information about the solution chemistry of mixed disulfides can be obtained by NMR.

Using these acid dissociation constants for the mixed disulfides and acid dissociation constants for the thiols and disulfides, equilibrium constants for the two steps in the oxidation of amino-protonated, thiol-deprotonated penicillamine by amino-protonated, carboxyl-deprotonated GSSG and cystine were calculated from the pH dependent equilibrium constants. Similarly, both forward and reverse rate constants for both steps in the thiol/disulfide reaction were calculated from the observed pH dependent rate constants. These pH independent rate and equilibrium constants for the reaction of penicillamine with GSSG are discussed on pages 206-208 while those for the reaction of penicillamine with CSSC are discussed on pages 246-247. This is the first time that the reactive species in thiol/disulfide exchange reactions of penicillamine have been identified and that the kinetics and equilibria of the reactions have been

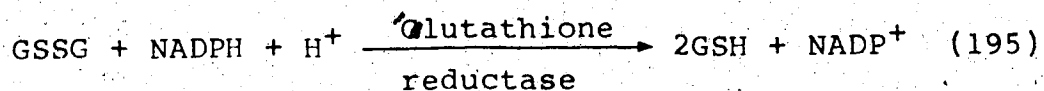
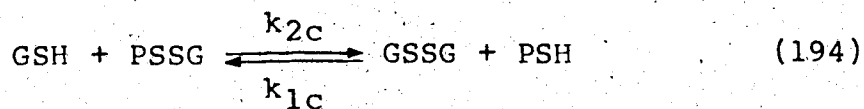
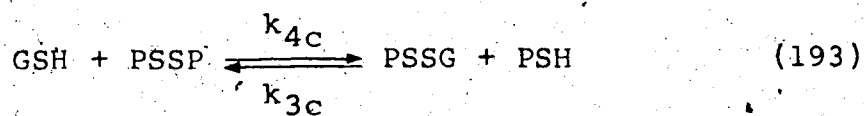
quantitatively characterized. This research has shown that NMR is a convenient and powerful technique for studying thiol/disulfide exchange reactions since all the species involved in the two steps of the reaction can be observed with the chemical shift dispersion of high field NMR spectrometers.

The study of the reaction of the thiol group of captopril with the disulfide group of oxidized glutathione was restricted to characterizing the equilibria for the two steps of the reaction over a narrow pH range near physiological pH. The equilibria involved are more complex than those for the analogous reactions of penicillamine due to the existence of appreciable concentrations of both cis and trans isomers with respect to the conformation across the captopril amide bond. To be able to describe the thiol/disulfide exchange equilibria, it was necessary to characterize first the conformational equilibria of captopril, captopril disulfide and captopril-glutathione mixed disulfide. The results obtained from the conformation equilibrium study are discussed on pages 278-281. Using these conformational equilibrium constants, equilibrium constants were calculated for the two steps in the reaction of captopril with GSSG to form CpSSCp and GSH.

To relate the findings to the physiological situation, conditional rate and equilibrium constants for pH 7.4 were calculated from the pH independent constants for the reaction of PSH with GSSG and CSSC. The pH 7.4 conditional constants differ from the pH independent constants because the reactive thiol-deprotonated species are a minor fraction of the total thiol at pH 7.4 and the fractional concentrations of the deprotonated thiol species are not the same for the various thiols since their pK_A 's are different. The conditional rate and equilibrium constants are summarized in Table 28 on page 250. Also listed are conditional constants which were determined for the reaction of penicillamine with several other disulfides. These results are discussed in detail on pages 248-252. Conditional equilibrium constants were also estimated for the two steps in the reaction of captopril with GSSG at pH 7.4, the values being $K_{1c} = 2.1$ and $K_{2c} = 1.5$. Of particular significance is the finding that K_{1c} for the reaction of penicillamine with the disulfides studied as well as K_{1c} for the reaction of CpSH with GSSG are all within a factor of ~ 2 of the random distribution value of 2 whereas the values for K_{2c} for all seven penicillamine/disulfide systems studied are considerably less than the random distribution value of 0.5 and considerably less than K_{2c} for the reaction of

captopril with CpSSG. These results are interpreted to indicate that the reaction of penicillamine with penicillamine mixed disulfide is hindered by the bulky methyl groups adjacent to the reacting centers. This suggests that the PSSP found as a metabolite of PSH [116,117] is not formed by thiol/disulfide exchange reactions but by other oxidation reactions. This is further supported by the magnitude of the rate constant for the reaction of PSH with PSSG at pH 7.4, and is discussed on page 212. However, the value of K_{2c} for the reaction of captopril with CpSSG indicates that the CpSSCp found as a metabolite of captopril [140-143] could be formed by thiol/disulfide exchange.

The rate constant for the reduction of PSSP by GSH was found to be very small relative to the rate constant for the reduction of PSSG by GSH, and this also was interpreted to be due to steric hindrance of the reactive center in PSSP. This is a significant finding because Jellum et al. [28] have proposed that oxidized penicillamine in cells will be converted to the reduced form by the nonenzymatic reduction of PSSP by GSH followed by the enzyme catalyzed reduction of GSSG to GSH, as summarized by Equations 193-195.



However, the small value determined in this work for k_{4c} suggests that reaction 193 is too slow to provide an important pathway for the reduction of PSSP.

As discussed on pages 252-253, the overall conditional equilibrium constant, K_{3c} , for the reaction of PSH with R'SSR' to form RSSR and R'SH is determined by the difference between the formal electrode potentials, ΔE° , of the two redox couples. The ΔE° values obtained from K_{3c} for the reaction of PSH with seven disulfides (Table 28, page 250) range from -0.0269 to -0.0421 V. The ΔE° value calculated from K_{3c} for the reaction of captopril with GSSG is +0.015 V. Comparison of the ΔE° values calculated from K_{3c} for the reaction of PSH with GSSG and captopril with GSSG indicate that the thiol group of captopril has a greater tendency to reduce disulfide bonds

by thiol/disulfide exchange than do the thiol groups of penicillamine and cysteine, which has a greater reducing strength than penicillamine. As discussed on pages 284-285, this conclusion is supported by the independent finding that captopril is more efficient for the activation of papain by reduction of a disulfide bond at its active site than is cysteine [155], and suggests that thiol/disulfide exchange reactions may be even more important in the metabolism of captopril than in the metabolism of penicillamine.

REFERENCES

1. E.S.G. Barron, "Thiol Groups of Biological Importance", in F. Ford, Ed., Advances in Enzymology, Vol. XI, Interscience, New York (1951).
2. R. Cecil and J.R. McPhee, "The Sulfur Chemistry of Proteins", in C.P. Anfinsen, Jr., K. Bailey, M. Anson and J.T. Edsall, Eds., Advances in Protein Chemistry, Vol. XIV, Academic Press, New York (1959).
3. C.F. Cullis, J.D. Hopton and D.L. Trimm, J. Appl. Chem., 18, 330 (1968).
4. T.J. Wallace and A. Schriesheim, J. Org. Chem., 27, 1514 (1962).
5. C.F. Cullis, J.D. Hopton, C.J. Swan and D.L. Trimm, J. Appl. Chem., 18, 335 (1968).
6. G.W. Frimpter, J. Biol. Chem., 236, PC 51 (1961).
7. G.W. Frimpter, J. Clin. Invest., 42, 1956 (1963).
8. J.A. Schneider, K.H. Bradley and J.E. Seegmiller, J. Lab. Clin. Med., 71, 122 (1968).
9. L. Eldjarn and L. Hambræus, Scand. J. Clin. Lab. Invest., 16, 153 (1964).
10. W.J.P. Neish and A. Rylett, Biochem. Pharmacol., 12, 913 (1963).

11. D.H. Calam and S.G. Waley, *Biochem. J.*, 93, 526 (1964).
12. R.N. Ondarza, *Biochim. Biophys. Acta*, 107, 112 (1965).
13. S.H. Chang and D.R. Wilken, *J. Biol. Chem.*, 240, 3136 (1965).
14. T.P. King, *J. Biol. Chem.*, 236, PC 5 (1961).
15. G.L. Ellman, *Archs. Biochem. Biophys.*, 82, 70 (1959).
16. D.R. Grassetti, J.F. Murray, *Archs. Biochem. Biophys.*, 119, 41 (1967).
17. P.C. Jocelyn, "Biochemistry of the SH Group", Academic Press Inc., London (1972).
18. J.M. Walshe, *Quart. J. Med.*, 22, 483 (1953).
19. J.M. Walshe, *Amer. J. Med.*, 21, 487 (1956).
20. J.E. Boulding and R.A. Baker, *Lancet*, 2, 985 (1957).
21. I.M. Kolthoff, W. Stricks and R.C. Kapoor, *J. Am. Chem. Soc.*, 77, 4733 (1955).
22. J.C. Crawhall, E.F. Scowen and R.W.E. Watts, *Brit. Med. J.*, 1, 588 (1963).
23. M. Tabachnik, H.N. Eisen and B. Levine, *Nature*, 174, 701 (1954).
24. B.S. Hartley and J.M. Walshe, *Lancet*, 2, 434 (1963).
25. I.A. Jaffe, "Penicillamine at 21: Its Place in Therapeutics Now", *Proceedings of the Royal Society of Medicine*, 70 (3), p. 130 (1977).

26. J.R. Golding, A.T. Day, M.R. Tomlinson, R.M. Brown, M.O. Hassan and S.R. Langstaff, in "Penicillamine at 21: Its Place in Therapeutics Now", Proceedings of Royal Society of Medicine, 70(3), pp. 131-135 (1977).
27. I.A. Jaffe, in "Penicillamine Research in Rheumatoid Disease", E. Munthe, Ed., Fabritius and Sonner, Oslo, pp. 11-24 (1976).
28. E. Jellum and S. Skrede, in "Penicillamine Research in Rheumatoid Disease", E. Munthe, Ed., Fabritius and Sonner, Oslo, pp. 68-79 (1976).
29. M.A. Ondetti, B. Rubin and D.W. Cushman, Science, 196, 441 (1977).
30. D.W. Cushman, H.S. Cheung, E.F. Sabo and M.A. Ondetti, Prog. Cardiovasc. Disg., 21, 176 (1978).
31. D.W. Cushman, H.S. Cheung, E.F. Sabo and M.A. Ondetti, Biochemistry, 16, 5484 (1977).
32. F. Quioco and W.N. Lipscomb, Adv. Protein Chem., 25, 1 (1971).
33. D.T. McAllan, T.V. Cullum, R.A. Dean and F.A. Fidler, J. Am. Chem. Soc., 73, 3627 (1951).
34. L. Eldjarn and A. Pihl, J. Am. Chem. Soc., 79, 4589 (1957).
35. A. Pihl, L. Eldjarn and K. Nakken, Acta Chem. Scand., 12, 1357 (1958).

36. L. Eldjarn and A. Pihl, *J. Biol. Chem.*, 225, 499 (1957).
37. P. Jocelyn, *Eur. J. Biochem.*, 2, 327 (1967).
38. G. Gorin and G. Doughty, *Arch. Biochem. Biophys.*, 126, 547 (1968).
39. G. Dalman, J. McDermed and G. Gorin, *J. Org. Chem.*, 29, 1480 (1964).
40. H.A. Smith, G. Doughty and G. Gorin, *J. Org. Chem.*, 29, 1484 (1964).
41. J.R. Roesler, J. Leslie and G. Gorin, *J. Org. Chem.*, 29, 1488 (1964).
42. U. Weber, P. Hartter and L. Flohé, *Hoppe-Seyler's Z. Physiol. Chem.*, 351, 1389 (1970).
43. R.P. Szajewski and G.M Whitesides, *J. Am. Chem. Soc.*, 102, 2011 (1980).
44. G.M. Whitesides, J.E. Lilburn and R.P. Szajewski, *J. Org. Chem.*, 42, 332 (1977).
45. J.M. Wilson, R.J. Bayer and D.J. Hupe, *J. Am. Chem. Soc.*, 99, 7922 (1977).
46. J.M. Wilson, D. Wu, R. Motiu-DeGrood and D.J. Hupe, *J. Am. Chem. Soc.*, 102, 359 (1980).
47. R. Freter, E.R. Pohl, J.M. Wilson and D.J. Hupe, *J. Org. Chem.*, 44, 1771 (1979).
48. C.E. Grimshaw, R.L. Whistler and W.W. Cleland, *J. Am. Chem. Soc.*, 101, 1521 (1979).

49. G. Gorin, G. Doughty and R. Gideon, *J. Chem. Soc. (B)*, 729 (1967).
50. G.M. Whitesides, J. Houk and M.A.K. Patterson, *J. Org. Chem.*, 48, 112 (1983).
51. T. Ozawa and A. Hanaki, *Chem. Pharm. Bull.*, 29, 1101 (1981).
52. K. Brockelhurst and G. Little, *Biochem. J.*, 128, 471 (1972).
53. M. Shipton and K. Brocklehurst, *Biochem. J.*, 171, 385 (1978).
54. S.A. Eriksson and B. Mannervik, *Biochim. Biophys. Acta*, 212, 518 (1970).
55. J. Rost and S. Rapoport, *Nature (London)*, 201, 185 (1964).
56. E.M. Scott, I.W. Duncan and V. Ekstrand, *J. Biol. Chem.*, 238, 3928 (1963).
57. C. Voegtlin, J.M. Johnson and S.M. Rosenthal, *J. Biol. Chem.*, 93, 435 (1931).
58. N.W. Pirie and K.G. Pinhey, *J. Biol. Chem.*, 84, 321 (1929).
59. R. Benesch and R.E. Benesch, *Biochim. and Biophys. Acta*, 23, 643 (1957).
60. H.A. Laitinen and W.E. Harris, "Chemical Analysis", 2nd Edition, McGraw-Hill, 1975.

61. P.W. Riddles, R.L. Blakeley and B. Zermer, *Anal. Biochem.*, 94, 75 (1979).
62. R. Saetre and D.L. Rabenstein, *Anal. Chem.*, 50, 276 (1978).
63. R.G. Bates, "Determination of pH; Theory and Practice", Wiley, New York (1964).
64. J. Schaefaer, *J. Mag. Res.*, 6, 670 (1972).
65. M.L. Martin, J.J. Delpuech and G.J. Martin, "Practical NMR Spectroscopy", Heyden and Sons Ltd., Philadelphia (1980).
66. Ref. 65, p. 108.
67. J.B. Stothers, "Carbon-13 NMR Spectroscopy", Vol. 24, Academic Press, New York, London (1972).
68. R.L. Vold, J.S. Waugh, M.P. Klein and D.E. Phelps, *J. Chem. Phys.*, 48, 3831 (1968).
69. H. Hanssum, *J. Mag. Res.*, 45, 461 (1981).
70. D.L. Dye and V.A. Nicely, *J. Chem. Ed.*, 48, 443 (1971).
71. D.E. Leyden and R.H. Cox, "Analytical Application of NMR", in *Chemical Analysis*, Vol. 48, John Wiley & Sons, New York/London/Sydney/Toronto (1977).
72. E.J. King, "Acid-Base Equilibria", Pergamon Press, Oxford, 1965.
73. C.W. Davies, *J. Chem. Soc.*, 2093 (1938).

74. R.A. Robinson and R.H. Stokes, "Electrolyte Solutions", 2nd Ed., Butterworths, London, 1959.
75. Ref. 63, p. 145.
76. Ref. 65, p. 45.
77. E.S.G. Barron, Archs. Biochem. Biophys., 59, 502 (1955).
78. R. Saetre, Ph.D. Thesis, University of Alberta, 1978.
79. M. Dixon and H.E. Tunnicliffe, Proc. R. Soc., [B], 94, 266 (1923).
80. I.G. Dance, R.C. Conrad and J.E. Clive, J. Chem. Soc., Chem. Commun., 13 (1974).
81. A.P. Mathews and S. Walker; J. Biol. Chem., 6, 21 (1909).
82. A.K. Ahmed, S.W. Schaffer and D.B. Wetlaufer, J. Biol. Chem., 250, 8477 (1975).
83. E.G. Rippie and T. Higuchi, J. Pharm. Sci., 51, 776 (1962).
84. J.W. Emsley, J. Feeney and L.H. Sutcliffe, "High Resolution Nuclear Magnetic Resonance", Vol. 1, New York, N.Y., Pergamon (1965).
85. Ref. 17, p. 53.
86. D.L. Rabenstein and T.L. Sayer, Anal. Chem., 48, 1141 (1976).
87. Ref. 71, p. 98.

88. M.T. Fairhurst, Ph.D. Thesis, University of Alberta (1975).
89. F.W. Wehrli and T. Wirthlin, "Interpretation of Carbon-13 NMR Spectra", Heyden & Son Ltd. (1978).
90. E.W. Wilson, Jr., and R.B. Martin, Arch. Biochem. Biophys., 142, 445 (1971).
91. D.L. Rabenstein, J. Am. Chem. Soc., 95, 2797 (1973).
92. R.B. Martin and J.T. Edsall, Bull. Soc. Chim. Biol., 40, 1763 (1958).
93. N.C. Li, O. Gawron and G. Bascuas, J. Am. Chem. Soc., 76, 225 (1954).
94. D.L. Rabenstein, R. Guevremont and C.A. Evans, in "Metal Ions in Biological Systems", H. Sigel, Ed., Marcell Dekker, Inc., New York, Vol. 9, p. 103 (1979).
95. M.M. Shoukry, unpublished results.
96. D.D. Perrin and R.P. Agarwal, in "Metal Ions in Biological Systems", H. Sigel, Ed., Marcell Dekker, Inc., New York, Vol. 2, p. 167 (1973).
97. M.A. Grafius and J.B. Neilands, J. Am. Chem. Soc., 77, 3389 (1955).
98. D.P. Wrathall, R.M. Izatt and J.J. Christensen, J. Am. Chem. Soc., 86, 4779 (1964).
99. E.L. Elson and J.T. Edsall, Biochemistry, 1, 1 (1962).

100. E. Coates, C.G. Marsden and B. Rigg, *Trans. Faraday Soc.*, 65, 3032 (1969).
101. A.H.M. Kirby and A. Neuberger, *Biochemistry J.*, 32, 1146 (1938).
102. C. Tanford and M.L. Wagner, *J. Am. Chem. Soc.*, 75, 434 (1953).
103. E.J. Kuchinskas and Y. Rosen, *Arch. Biochem. Biophys.*, 97, 370 (1962).
104. G.R. Lenz and A.E. Martell, *Biochemistry*, 3, 745 (1964).
105. D.D. Perrin and I.G. Sayer, *J. Chem. Soc. (A)*, 53 (1968).
106. H. Borsook, E.L. Ellis and H.M. Huffman, *J. Biol. Chem.*, 117, 281 (1937).
107. J.P. Casey and R.B. Martin, *J. Am. Chem. Soc.*, 94, 6141 (1972).
108. D.L. Rabenstein and R. Saetre, *Clin. Chem.*, 24, 1140 (1978).
109. J.C. Banford, D.H. Brown, A.A. McConnell, C.J. McNeil, W.E. Smith, R.A. Hazelton and R.D. Sturrock, *Analyst*, 107, 195 (1982).
110. S.K. Srivastava and E. Beutler, *Anal. Biochem.*, 25, 70 (1968).
111. H. McIlwain, "Glutathione", *Biochemistry Society Symposia*, No. 17, p. 76, E.M. Crook, Ed., Cambridge University Press (1959).

112. H. Guntherberg and J. Rost, *Anal. Biochem.*, 15, 205 (1966).
113. A.A. Frost and R.G. Pearson, "Kinetics and Mechanism", 2nd Ed., John Wiley & Sons, Inc., New York, London and Sydney (1961).
114. C. Capellos and B.H.J. Bielski, "Kinetic Systems", Wiley-Interscience, John Wiley & Sons Inc. (1972).
115. S.J. Backs and D.L. Rabenstein, *Inorg. Chem.*, 20, 410 (1981).
116. D. Perrett, "Penicillamine at 21: Its Place in Therapeutics Now", *Proceeding of the Royal Society of Medicine*, 70(3), pp. 61-64 (1977).
117. J.C. Crawhall, D. Lecavalier and P. Ryan, *Pharm. Drug Dispos.*, 1, 73 (1979).
118. L. Eldjarn, J. Bremer and H.C. Borresen, *Biochem. J.*, 82, 192 (1962).
119. S. Skrede, *Biochem. J.*, 108, 693 (1968).
120. F.J.R. Hird, *Biochem. J.*, 85, 320 (1962).
121. B. Mannervik and K. Axelsson, *Biochem. J.*, 190, 125 (1980).
122. N.S. Kosower and E.M. Kosower, *Int. Rev. Cytol.*, 54, 109 (1978).
123. B. States and S. Segal, *Biochem. J.*, 113, 443 (1969).

124. L. Libenson and M. Jena, *Archs. Biochem. Biophys.*, 100, 441 (1963).
125. B. Mannervik and K. Axelsson, *Biochem. J.*, 149, 785 (1975).
126. B.B. Levine, *Nature, Lond.*, 187, 940 (1960).
127. R.B. Freedman, *FEBS. Lett.*, 97, 201 (1979).
128. P.L. Wendell, *Biochem. Biophys. Acta*, 159, 179 (1968).
129. T.H.J. Huisman and A.M. Dozy, *J. Lab. Clin. Med.*, 60, 302 (1962).
130. E.R. Stadtman and A. Kurnberg, *J. Biol. Chem.*, 203, 47 (1953).
131. K. Wallevik, *Biochem. Biophys. Acta*, 420, 42 (1976).
132. S. Eriksson, P. Askelof, K. Axelsson, I. Carlberg, C. Guthenberg and B. Mannervik, *Acta Chem. Scand.*, B28, 922 (1974).
133. K. Brockelhurst and M.P.J. Kierstan, *Nature New Biol.*, 242, 167 (1973).
134. T.E. Creighton, *J. Mol. Biol.*, 87, 603 (1974).
135. J.M. Rodriguez and H.C. Pitot, *Arch. Biochem. Biophys.*, 177, 185 (1976).
136. A. Goldberg, J.A. Smith and A. Lockhead, *Br. J. Med.*, 1, 1270 (1963).
137. J.T. MacGregor and T.W. Clarkson, *Adv. Exp. Med. Biol.*, 48, 463 (1974).

- 138.. F.M. Andrews, A.J. Camp, A.T. Day, A.M. Freeman, D.N. Golding, J.R. Golding, A.G.S. Hill, E. Lewis-Fanning and W.H. Lyle, *Lancet*, 1, 275 (1973).
139. Merck Index, 9th Edition, Merck & Co., Inc. (1976).
140. S.-J. Lan, S.H. Weinstein and B.H. Migdalof, *Drug Metab. Dispos*, 10, 306 (1982).
141. B.K. Park, P.S. Grabowski, J.H.K. Yeung and A.M. Breckenridge, *Biochem. Pharmacol.*, 31, 1755 (1982).
142. O.H. Drummer, P.J. Worland and B. Jarrott, *Biochem. Pharmacol.*, 32, 1563 (1983).
143. J.H.K. Yeung, A.M. Breckenridge and B.K. Park, *Biochem. Pharmacol.*, 32, 2467 (1983).
144. S.J. Hoorntje, C.S. Kallenberg, J.J. Weening, A.J.M. Donken, T.H. The and P.J. Hoedemaeker, *Lancet*, 1212 (1980).
145. D.L. Rabenstein and A.A. Isab, *Anal. Chem.*, 54, 526 (1982).
146. V. Madison and J. Schellman, *Biopolymers*, 9, 511 (1970).
147. J.T. Gerig, *Biopolymers*, 10, 2435 (1971).
148. C.A. Evans and D.L. Rabenstein, *J. Am. Chem. Soc.*, 96, 7312 (1974).
149. W.E. Stewart and T.H. Siddal III, *Chem. Rev.*, 70, 517 (1970).

150. Bovey, J.J. Ryan and F.B. Hood, *Macromolecules*,
(1968).
151. Deber, F.A. Bovey, J.P. Carver and E.R. Blout,
Am. Chem. Soc., 92, 6191 (1970).
152. W.A. Thomas and M.K. Williams, *J. Chem. Soc.*, *Chem.*
Commun., 994 (1972).
153. D.E. Dorman, D.A. Torchia and F.A. Bovey,
Macromolecules, 6, 80 (1973).
154. S. Mizushima, *Adv. Protein Chem.*, 9, 299 (1954).
155. R.P. Igic, J.T. Gafford and E.G. Erdos, *Biochem.*
Pharmacol., 30, 683 (1981).

150. F.A. Bovey, J.J. Ryan and F.B. Hood, *Macromolecules*, 1, 305 (1968).
151. C.M. Deber, F.A. Bovey, J.P. Carver and E.R. Blout, *J. Am. Chem. Soc.*, 92, 6191 (1970).
152. W.A. Thomas and M.K. Williams, *J. Chem. Soc., Chem. Commun.*, 994 (1972).
153. D.E. Dorman, D.A. Torchia and F.A. Bovey, *Macromolecules*, 6, 80 (1973).
154. S. Mizushima, *Adv. Protein Chem.*, 9, 299 (1954).
155. R.P. Igic, J.T. Gafford and E.G. Erdos, *Biochem. Pharmacol.*, 30, 683 (1981).